THE RIBOSOMAL PROTEIN L23a FAMILY OF *ARABIDOPSIS THALIANA*

A Thesis Submitted to the College of

Graduate Studies and Research

In Partial Fulfillment of the Requirements

For the Degree of Doctor of Philosophy

In the Department of Biology

University of Saskatchewan

Saskatoon

By

Rory Frank Degenhardt

PERMISSION TO USE

In presenting this thesis in partial fulfilment of the requirements for a Postgraduate degree from the University of Saskatchewan, I agree that the Libraries of this University may make it freely available for inspection. I further agree that permission for copying of this thesis in any manner, in whole or in part, for scholarly purposes may be granted by the professor or professors who supervised my thesis work or, in their absence, by the Head of the Department or the Dean of the College in which my thesis work was done. It is understood that any copying or publication or use of this thesis or parts thereof for financial gain shall not be allowed without my written permission. It is also understood that due recognition shall be given to me and to the University of Saskatchewan in any scholarly use which may be made of any material in my thesis.

Requests for permission to copy or to make other use of material in this thesis in whole or part should be addressed to:

Head of the Department of Biology

University of Saskatchewan

Saskatoon, Saskatchewan S7N 5E2

ABSTRACT

The 80 S cytoplasmic ribosome is the largest of three populations of ribosomes responsible for protein synthesis in plants. It is comprised of two RNA/protein subunits of unequal size: the small (40 S) subunit selects messages to be translated and performs proofreading, while the large (60 S) subunit has peptidyl transferase acitivity, adding new amino acids to the growing polypeptide. In the model flowering plant *Arabidopsis thaliana* (hereafter Arabidopsis), four ribosomal RNAs and 81 ribosomal proteins (r-proteins) assemble to form the 80 S ribosome. Although the Arabidopsis ribosome contains only a single copy of each of the 81 r-proteins (with the exception of small number of acidic phophoproteins), all r-proteins are encoded from multi-gene families containing two or more expressed members. Herein, I investigated r-protein paralogy in Arabidopsis via specific examination of a two member gene family, *RPL23a*. By analyzing patterns of reporter gene expression driven by full-length and truncated regulatory regions, I was able to identify a core promoter that is largely conserved between paralogs. Regulation was found to be complex, involving transcriptional, post-transcriptional and translational components. The effects of knocking-out a single *RPL23a* paralog (*RPL23aB*) were determined. Results indicated that this paralog is broadly dispensable, and Arabidopsis does not compensate for its loss at the transcriptional level. Subcellular localization was investigated by tagging RPL23aA/B with fluorescent proteins, demonstrating that RPL23aA is targeted to nucleolus more efficiently than RPL23aB, possibly due to a stronger nucleolar localization signal. RNA-interference was used to individually silence *RPL23a* paralogs to characterize functional overlap. Results showed that *RPL23aA*, and not *RPL23aB*, is required for normal development. Mutants with reduced levels of *RPL23aA* develop a *pointed first leaf* phenotype that I postulate may be due to disruption of miRNA-mediated degradation of specific auxin response genes. Lastly, the 26 S proteasome was inhibited to determine the importance of protein turnover in regulating RPL23a levels. Findings suggest that proteasome-mediated degradation of RPL23a is essential for preventing accumulation of unincorporated r-proteins. Overall, results indicate that the Arabidopsis *RPL23a* paralogs have diverged from each other: RPL23aA has become the predominant paralog, while RPL23aB functions in an anciliary capacity and/or is undergoing neofunctionalization.

ACKNOWLEDGEMENTS

I thank Dr. Peta Bonham-Smith for her support and guidance throughout my PhD. Her commitment to science and constant enthusiasm was both inspiring and motivating.

Many thanks to Drs. Larry Fowke, Ken Wilson, and Gordon Gray for their contributions to this project, and to Dr. Thomas Berleth for serving as my external examinator. Thank you also to Drs. Federica Brandizzi, Chris Todd, Pierre Fobert, and Troy Harkness for providing me access to equipment and expertise.

I thank Drs. Kerri McIntosh, Jacqueline Hulm, Donna Lindsay, Loren Matheson, Sally Hanton, and Ms. Heather Wakely for their technical assistance and friendship. I would also like to thank future Drs. Robin Kusch and Remko Verspuy for keeping me grounded and for their contagious perseverance.

I would like to thank the faculty, staff, and graduate students of the Department of Biology for helping me through this process. I am especially grateful for the assistance of Dennis Dyck, Marlynn Mierau, Jeaniene Smith, Joan Virgl, Diedre Wasyliw, Shirley Hleck, Dr. Doug Chivers, and Dr. Francois Messier.

I thank Dr. Bill McGregor for his insight, mentorship and guidance. Also thanks to Dr. Jeff Nelson for his commitment to my personal development.

Utmost thanks goes out to my family and friends, especially Keith, Terry Lee, Richard, Fran, Kerry, Naomi, Josie, Heather, Kevin, Mike, Shannon, Blake, Reid, Owen, Grandma D, and Dani. This would not have been possible without their unconditional love and support. Special thanks to Grandma B for inspiring me and showing me how to avoid boredom.

I graciously acknowledge the financial contributions of the Natural Sciences and Engineering Research Council and the University of Saskatchewan College of Graduate Studies and Research.

DEDICATION

I dedicate this thesis to my parents, Keith and Terry Lee, and my wife, Dani. I am thankful for the sacrifices they have made during this project, and for their unwavering encouragement, support, optimism and love.

TABLE OF CONTENTS

LIST OF TABLES

LIST OF FIGURES

LIST OF ABBREVIATIONS

Abbreviation	
A site	aminoacyl site
ABA	abscisic acid
ABRC	Arabidopsis Biological Resource Center
bp	base pair
cDNA	complementary DNA
CLSM	confocal laser scanning microscope
E site	exit site
EF	elongation factor
EJC	exon junction complex
EM	electron microscope/electron microscopy
ETS	external transcribed spacer
fl	full-length
FR	flanking region
GUS	β-glucuronidase
IF	translation initiation factor
ITS	internal transcribed spacer
LSU	large subunit
mRNA	messenger RNA
NLS	nuclear localization signal
NoLS	nucleolar localization signal
NOR	nucleolar organizing region
nt	nucleotide
P site	peptidyl site
pI	isoelectric point
PCNA	PROLIFERATING CELL NUCLEAR ANTIGEN
pfl	pointed first leaf
qRT-PCR	real-time quantitative RT-PCR
RACE	rapid amplification of cDNA ends
RACK	receptor of activated C-kinase

RNAi	RNA interference
RNP	ribonucleoprotein
r-protein	ribosomal protein
RR	regulatory region
rRNA	ribosomal RNA
RT-PCR	reverse transcription polymerase chain reaction
snRNA	small nuclear RNA
snRNP	small nuclear RNP
snoRNA	small nucleolar RNA
snoRNP	small nucleolar RNP
SRL	sarcin-ricin loop
SRP	signal recognition particle
SSU	small subunit
TCP	TEOSINTE BRANCHED1, CYCLOIDEA, PCF
TF	trigger factor
TOP	terminal oligopyrimidine tract
TOR	target of rapamycin
tRNA	transfer RNA
TSS	transcription start site
UTR	untranslated region
wt/WT	wild type

1 CHAPTER 1. LITERATURE REVIEW

1.1 Introduction

Ribosomes are large enzymatic complexes that synthesize proteins in all organisms. They are comprised of two ribonucleoprotein (RNP) subunits of unequal size (one large subunit [LSU] and one small subunit [SSU]), which exist as free entities in cytoplasm but assemble on mRNA to become translationally competent. The SSU recruits mRNA templates and performs decoding, while the LSU catalyzes the addition of amino acids to the nascent peptide. Although the peptidyl transferase active center of the LSU is comprised entirely of ribosomal RNA (rRNA, Nissen et al., 2000), ribosomal proteins (r-proteins) perform essential roles in ribosome function.

Plants are unique from other eukaryotes in having three distinct ribosome populations: 80 S cytoplasmic ribosomes and 70 S mitochondrial and plastid ribosomes. Mitochondrial and plastid ribosomes have endosymbiont origin and are bacterial-like, whereas cytoplasmic ribosomes are more complex and synthesize proteins from nuclear-encoded mRNAs (Bailey-Serres, 1998; Bogorad, 1975). The 80 S ribosome of the model flowering plant, *Arabidopsis thaliana*, (hereafter Arabidopsis), contains four rRNA species (SSU 18 S and LSU 26 S, 5.8 S and 5 S) and 81 r-proteins (33 SSU, 48 LSU). With the exception of a small number of acidic r-proteins that assemble as a multimeric lateral stalk, ribosomes contain only a single copy of each r-protein, yet all r-proteins are encoded by multi-gene families with more than one transcribed member (Barakat et al., 2001). Proteomic analyses of the ribosome have determined that in many cases multiple paralogs are translated and incorporated, contributing to ribosome heterogeneity (Carroll et al., 2008; Chang et al., 2005; Guarinos et al., 2003). Further, unlike prokaryotes where r-proteins are clustered in a small number of operons, enabling feedback regulation of expression, plant r-proteins are dispersed as single genes throughout the genome (Barakat et al., 2001; Matsumoto et al., 2005b; Merchant et al., 2007). Plants must therefore have a system for coordinately regulating the synthesis and assembly of r-proteins.

To investigate the requirement for r-protein paralogs in Arabidopsis, I conducted experiments on a single r-protein gene family, *RPL23a*. The two members of this family, designated *RPL23aA* and *RPL23aB*, are located on chromosomes 2 and 3, respectively, and encode proteins with 95% amino acid sequence identity (146 of 154 residues). Herein, 5' regulatory regions (5' RRs) of paralogs were cloned upstream of a reporter gene to identify important *cis*-acting

elements governing their expression. Transcript levels of paralogs were quantified in wildtype and *RPL23aB* knockout plants under non-stressed and stressed conditions to determine the extent to which paralogs are coordinately regulated. Subcellular localization was investigated by tagging *RPL23aA* and *RPL23aB* with fluorescent proteins. RNA-interference was used to individually and coordinately silence *RPL23a* paralogs to characterize functional overlap. Lastly, the 26 S proteasome was inhibited to determine the importance of protein turnover in regulating r-protein levels.

1.2 Composition and Structure of the Ribosome

1.2.1 The prokaryotic ribosome

The most well characterized prokaryotic ribosome is that of *Escherichia coli*, where the 30 S SSU is comprised of a 16 S rRNA and 22 r-proteins, and the 50 S LSU contains 23 S and 5 S rRNAs and 34 r-proteins. Comparative analysis of 66 fully sequenced genomes (45 eubacterial, 14 archaeal, and 7 eukaryotic) has identified that of 56 conserved eubacterial r-protein families, 34 (15 SSU and 19 LSU) are shared among all three major Domains of life, Bacteria, Archaea and Eucarya (Lecompte et al., 2002). The molecular masses of the SSU and LSU are approximately 0.9 and 1.6 MDa, respectively, with more than half of the mass arising from rRNAs and the remainder from r-proteins that range in mass from ca. 4–61 kDa (Arnold and Reilly, 1999; Boublik et al., 1990; Moore and Steitz, 2003).

The crystal structure of the prokaryotic ribosome has been solved in several species, revealing that the ribosome is ~21–25 nm in size and its shape is largely determined by rRNA tertiary structure (Ban et al., 2000; Cate et al., 1999; Moore and Steitz, 2003; Pioletti et al., 2001; Schuwirth et al., 2005; Wimberly et al., 2000; Yusupov et al., 2001). Moreover, it has been reported that synthetic oligoribonucleotides with sequences identical to that of three 23 S rRNA domains (I, IV and VI) were capable of assuming near-native secondary and tertiary conformations in isolation (Egebjerg et al., 1987; Leffers et al., 1988). Further, when reconstituted with total proteins of the 50 S subunit *in vitro*, synthetic 23 S rRNA domains I–VI were capable of forming some native r-protein associations (Ostergaard et al., 1998). Small subunit 16 S rRNA folds and packs into a tertiary structure with three compact domains (5', central, and 3' major) and one extended domain (3' minor) (Wimberly et al., 2000). The 3' minor domain contains the decoding region and, consistent with findings of *in vitro* experiments

on synthetic 23 S rRNA domains, a synthetic oligoribonucleotide of the decoding region alone was capable of adopting a conformation that interacted with ligands of the 30 S subunit (tRNA and mRNA), and bound antibiotics whose target site is the decoding region (Purohit and Stern, 1994).

At low resolution (~40 Å) the LSU has a hemispherical structure with three projections radiating outwards from its interfacial surface: one positioned centrally (the central protuberance) that includes the 5 S rRNA, one positioned approximately 60° to the left of the central protuberance that includes r-protein L1 (denoted the L1 arm; L1 is the prokaryotic ortholog to eukaryotic RPL10a), and one positioned approximately 60° to the right of the central protuberance that is referred to as the L7/L12 lateral stalk (Figure 1.1a, actually a heterodimer of L12, the prokaryotic ortholog to eukaryotic RPP1/RPP2, composed of one acetylated and one non-acetylated copy of L12, Stark et al., 1995). Higher resolution reconstruction reveals the presence of a polypeptide exit tunnel, composed largely of rRNA, which begins immediately below the peptidyl transferase active center and exits through the bottom of the LSU at an opening surrounded by r-proteins, including L23 (Figure 1.1a, Ban et al., 2000; Beckmann et al., 1997). The tunnel is approximately 100 Å in length and can accommodate 30–50 amino acids of the nascent polypeptide chain (Ban et al., 2000; Wilson and Nierhaus, 2003).

The structure of the SSU has been described anthropomorphically, with a large head and laterally projecting beak that comprise approximately one-third of the subunit's total mass and rest on top of the body, separated by a shoulder, platform, and thin neck region (Figure 1.1a, Stark et al., 1995). At the bottom of the SSU is a spur formed from a variable-length region (helix 6) of 16 S rRNA (Gabashvili et al., 2000; Wimberly et al., 2000).

1.2.2 The eukaryotic ribosome

The cytoplasmic ribosome of eukaryotes is larger than, but structurally and functionally similar to, its prokaryotic counterpart. Its greater complexity is believed to reflect the requirement for increased translational accuracy and regulation (Nygard and Nilsson, 1990; Verschoor et al., 1996). It is comprised of a 40 S SSU and 60 S LSU that assemble into the 80 S cytoplasmic ribosome. The 40 S subunit contains 18 S rRNA and ~33 r-proteins that are conserved among most eukaryotes (Bielka, 1982; Chandramouli et al., 2008; Lecompte et al., 2002; Sengupta et al., 2004). It has a relatively constant molecular mass of approximately 1.2–

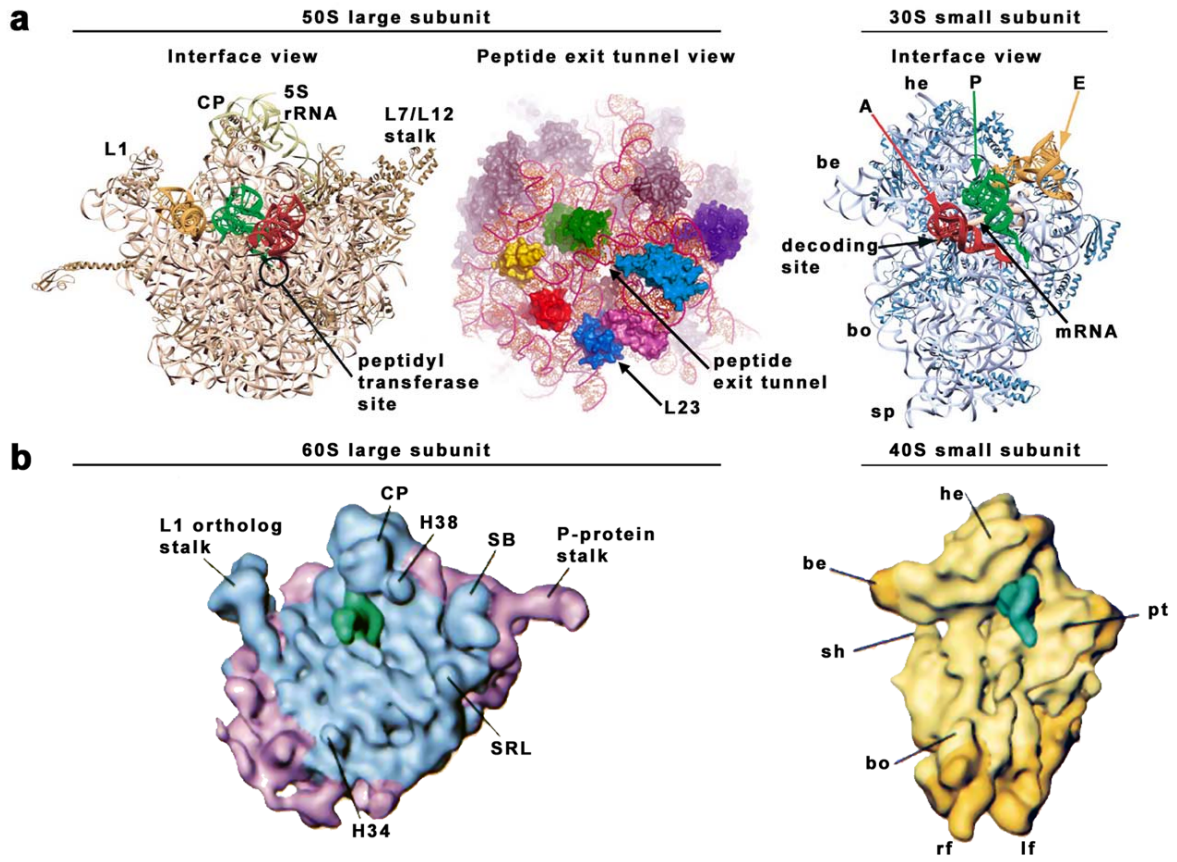

Figure 1.1 Structure of the ribosome. **a** Crystal structure of the 70 S ribosome. The interfacial sides of the *Thermus thermophilus* SSU and LSU are shown, along with the bottom view of LSU from *Haloarcula marismortui* looking down the exit tunnel towards the peptidyl transferase active site. The position of L23, the prokaryotic ortholog to RPL23a, is shown relative to the peptide exit tunnel. Transfer RNAs are shown in the aminoacyl-(A), peptidyl-(P), and exit (E)-sites of each subunit. Important structural and functional features are denoted on the figure. The shoulder, neck and platform regions of the SSU are hidden by tRNAs. **b** Cryo-electron micrograph reconstruction of the *Saccharomyces cerevisiae* 80 S ribosome. Additional mass not observed in equivalent reconstructions of the 70 S ribosome are indicated by purple (LSU) and gold (SSU). A P-site tRNA is shown in green. Two important helices involved in intersubunit bridge formation (H34 and H38) are shown. Abbreviations: CP, central protuberance; he, head; be, beak; bo, body; sp, spur; H38, helix 38; SB, stalk-base; H34, helix 34; SRL, sarcin-ricin loop; sh, shoulder; pt, platform; rf, right foot; lf, left foot. Interfacial and bottom views of the 70 S ribosome are adapted from Ramakrishnan (2002) and Brodersen and Nissen (2005), respectively. Cryo-EM structure of 80 S ribosomal subunits adapted from Spahn et al. (2001).

1.5 MDa, and structural studies have observed only minor differences in size between 40 S subunits of different species (Manuell et al., 2005; Verschoor et al., 1996; Verschoor et al., 1998). This finding is consistent with the low degree of variability of 18 S rRNA between eukaryotes, with the exception that mammalian 18 S rRNA sequences are ~10% larger than those of yeast and plants (Van de Peer et al., 2000; Van de Peer et al., 1997). The 60 S subunit contains 5 S, 5.8 S and 23 S-like (25–28 S) rRNAs and ~47 r-proteins that are conserved among most eukaryotes (Lecompte et al., 2002). All three rRNA species of the LSU have prokaryotic equivalents: the eukaryotic 5 S, 5.8 S and 25–28S rRNAs are equivalent to the 5 S, 23 S 5' end and 23 S rRNAs of prokaryotes, respectively (Bailey-Serres, 1998; Raue et al., 1988; Schnare et al., 1996). The mass of the 60 S subunit is variable among eukaryotes, ranging from ~2.0–2.5 MDa in some plants and fungi to ~3 MDa in mammals (Bielka, 1982; Chang et al., 2005). This difference is primarily attributed to divergence in the size of 23 S-like rRNA, which contains >30% more sequence in mammals than in yeast or plants, and ranges in mass from ~1.1–1.7 MDa (Bielka, 1982; Chang et al., 2005; De Rijk et al., 1998). Most 23 S-like rRNA variation arises from insertions at variable loop regions, termed expansion sequences, which increase the size of the mammalian sequence to ~5,000 bp, while that of fungi and plants is approximately 3300–3500 bp (Ben Ali et al., 1999; De Rijk et al., 1998; Schnare et al., 1996). In comparison with its prokaryotic counterpart, the 80 S ribosome has a lower ratio of RNA:protein (Verschoor et al., 1996). Consistent with its presumed evolution from an archaebacterial ancestor, the cytoplasmic 80 S ribosome resembles an upscaled version of the archaeal ribosome (Lecompte et al., 2002).

Three-dimensional structures of 80 S ribosomes from a number of species have been obtained at resolutions of 8.7–55 Å by cryo-electron microscopy, including wheat (*Triticum aestivum*, Verschoor et al., 1996), green algae (*Chlamydomonas reinhardtii*, Manuell et al., 2005), rabbit (40 S subunit only, Srivastava et al., 1995), human (Spahn et al., 2004), dog (Chandramouli et al., 2008), *S. cerevisiae* (Verschoor et al., 1998), and a thermophilic fungus (*Thermomyces lanuginosus*, Nilsson et al., 2007). Generally, all structural features of the 70 S ribosome are present on the 80 S ribosome, although in the former they tend to exist in a more discrete and compact manner due to the presence of rRNA expansion segments and additional r-proteins in the 80 S ribosome that contribute extra peripheral mass. The 80 S ribosome is ~20–30 nm in

size, and occupies a volume approximately 30% larger than that of its prokaryotic counterpart (Verschoor et al., 1996; Verschoor et al., 1998).

When viewed separately, the 60 S subunit has a less compact, more elliptical shape than its globular prokaryotic counterpart (Figure 1.1b, Spahn et al., 2004; Verschoor et al., 1998). The three main projections of the LSU, the central protuberance, P-protein-stalk (eukaryotic equivalent of the L7/L12 stalk) and the L1 ortholog-stalk, are well conserved. In agreement with the high degree of core functional conservation, features of the interface region of the 60 S subunit, such as the interface channel, are near-identical with those of the 50 S subunit, while those at the periphery tend to exhibit a higher degree of divergence (Verschoor et al., 1998).

The eukaryotic 40 S subunit retains all the characteristic features of the prokaryotic SSU, although many take on an exaggerated appearance. For example, the beak of the eukaryotic SSU protrudes to a much greater extent than its prokaryotic equivalent (Figure 1.1b, Verschoor et al., 1996; Verschoor et al., 1998). Similarly, the crest that extends off the back of the head of the 40 S subunit has a prokaryotic equivalent that extends to a lesser degree from the neck region (Srivastava et al., 1995). The spur of the 30 S subunit is replaced by feet that protrude from the base of the 40 S subunit, and vary in size due to the length of 18 S rRNA expansion segments (Figure 1.1b, Spahn et al., 2004; Srivastava et al., 1995; Verschoor et al., 1998). As with the LSU, the greatest region of similarity between the 40 S and 30 S subunits is in the morphology of the interface regions of the head, neck and mRNA channel that have critical importance for ribosome function (Srivastava et al., 1995; Stark et al., 1995; Verschoor et al., 1998).

1.3 Ribosome Function

Ribosomes synthesize proteins for all living organisms. The process uses mRNA as a template, transfer RNAs (tRNAs) charged with amino acids as the substrate, and produces polypeptides. The LSU and SSU of the ribosome interact with two distinct domains of tRNA: the LSU primarily with the $^{5'}$CCA$^{3'}$ termini of the acceptor stem, and the SSU with the anticodon loop. During translation, both subunits are highly dynamic, undergoing conformational changes as the ribosome translocates along mRNA and interacts with translation factors. For example, in the LSU the L7/L12 stalk, and its eukaryotic equivalent the P-protein-stalk, undergo positional changes when the GTP-bound form of elongation factor G (EF-G, or its eukaryotic equivalent eEF-2) binds the ribosome (Agrawal et al., 1999; Bargis-Surgey et al., 1999; Gomez-Lorenzo et

al., 2000). Similarly, the L1-stalk is also flexible and pivots away from the P-site of the ribosome following the hydrolysis of GTP on EF-G bound to the L7/L12 stalk, mediating the exit of E-site tRNAs and the movement of discharged P-site tRNAs to the E-site (Chandramouli et al., 2008; Gomez-Lorenzo et al., 2000; Valle et al., 2003). Concomitant with the interaction of GTP-bound EF-G with the lateral stalk, the entire SSU rotates counterclockwise relative to the LSU, widening the mRNA channel and, following GTP hydrolysis, enabling translocation of the ribosome and subsequent return to pre-translocation conformation by clockwise rotation of the SSU (Chandramouli et al., 2008; Frank and Agrawal, 2000; Valle et al., 2003). These and other experiments (as examples Agrawal et al., 2000; Stark et al., 2000; Stark et al., 2002) highlight both the dynamic nature of the ribosome and the complex interactions that occur between rRNAs, r-protein, mRNA and tRNAs, and the large array of factors responsible for facilitating initiation, elongation and termination of translation (reviewed in Kozak, 1999; Ramakrishnan, 2002; Sachs et al., 1997).

1.4 The Central Role of rRNA

1.4.1 Synthesis of rRNA

The four eukaryotic rRNA species, 23 S-like, 18 S, 5.8 S and 5 S, and the three prokaryotic rRNA species, 16 S, 23 S and 5 S, are transcribed from genes that are repeated multiple times within the genome, and which have undergone purifying selection such that there are virtually no differences between copies within a species (Hadjiolov, 1985). It is currently believed that unequal cross-over and/or gene conversion events are responsible for the within-species homogenization of rRNA genes (Dover, 1982; Klein and Petes, 1981; Petes, 1980; Petes and Hill, 1988; Szostak and Wu, 1980).

In *E. coli*, all three rRNA genes are present in tandem repeats, and each repeat forms a single transcription unit (reviewed in Srivastava and Schlessinger, 1990). Most eukaryotes have clusters of transcriptional units consisting of the three largest rRNA species (23 S-like, 18 S, 5.8 S), present in head-to-tail repeats separated by an intergenic spacer, at chromosomal loci known as nucleolar organizer regions (NORs) (Brown and Dawid, 1969). These transcriptional units are transcribed by their own polymerase, RNA polymerase I (RNA pol I), forming a polycistronic pre-rRNA transcript. From the 5' end, the transcriptional unit repeated within NORs consists of a 5' external transcribed spacer (ETS), 18 S rDNA, internal transcribed spacer

(ITS) 1, 5.8 S rDNA, ITS2, 23 S-like rDNA, and a 3' ETS. Generally, the genes for 5 S rRNA are present in arrays of multiple repeats found outside the NOR. For example, in Arabidopsis 5 S rDNA repeats are found proximal to centromeres of chromosomes 3, 4 and 5 (AGI, 2000). However, in some fungi including *S. cerevisiae*, *Mucor racemosus*, and *Candida utilis*, and the slime mold *Dictyostelium discoideum*, the 5 S rDNA repeats are found in reverse orientation within the intergenic spacer of the 18 S–5.8 S–25 S transcriptional unit (Hadjiolov, 1985; Philippsen et al., 1978; Warner, 1989). Nevertheless, 5 S rDNA in all eukaryotes is transcribed separately by RNA pol III (Warner, 1989).

The number of tandem 18 S–5.8 S–23 S-like rDNA repeats within each NOR is highly variable between and within species, and can even differ between cells or cell types of the same strain or individual (Hadjiolov, 1985). Humans have ~160–200 tandem repeats of their rDNA cluster spread over five NORs located on chromosomes 13, 14, 15, 21 and 22 (Raška, 2003). Similarly, mammals *Rattus norvegicus* and *Mus musculus* have copy numbers of ~150–170 and ~100, respectively, per haploid genome (Long and Dawid, 1980). In general, plants have a much higher copy number per haploid genome, possibly reflecting the high ploidy number of some species. For example, copy number, estimated by modified Southern blots, ranges from ~600 to ~9500 in angiosperms and ~1,250 to ~13,400 in gymnosperms (Long and Dawid, 1980; Pruitt and Meyerowitz, 1986). These values may be slightly exaggerated given that the actual number of rDNA repeats in Arabidopsis (~350–400, AGI, 2000), is less than estimated number (~570, Pruitt and Meyerowitz, 1986). In *S. cerevisiae*, the lone NOR occurs on chromosome 7, and contains a strain-dependent copy number of 100–220 tandem repeats, encompassing as much as two-thirds of the chromosome's DNA (Kobayashi et al., 1998; Warner, 1989). Interestingly, substantial clonal variation in copy number within strains has also been reported in *S. cerevisiae*, with some colonies having less than 40 tandem repeats with no substantial reduction in growth rate (Kobayashi et al., 1998; Warner, 1989).

In higher eukaryotes, where the RNA pol III-transcribed 5 S rDNA repeats are dispersed at non-NOR locations of the genome, their copy number is also highly variable. For example, Drosophila (*Drosophila melanogaster*) has ~100–200 5 S rDNA repeats per haploid genome, which is approximately a 1:1 ratio with the other rDNA species (Tartof and Perry, 1970). In contrast, 5 S rDNA of Arabidopsis, *R. norvegicus*, *Homo sapiens, Xenopus laevis* and *Notophtalmus viridescens* is present in copy numbers of ~1000, 830, 2,000, 9,000–24,000, and

300,000, respectively, which is >2-fold more than for the remaining 18 S–5.8 S–23 S-like rDNAs (Campell et al., 1992; Long and Dawid, 1980). Apparent from investigations into rDNA copy number in eukaryotes is that they tend to occur at levels greater than strictly required for viability (Bailey-Serres, 1998; Hadjiolov, 1985).

Although the RNA pol I-transcribed rDNA sequences of eukaryotes are highly conserved, the total length of the tandem repeat varies substantially, predominantly due to differences in the intergenic region (De Rijk et al., 1998). This region contains important *cis*-acting elements necessary for rDNA transcription. In higher eukaryotes, such as Arabidopsis, *X. laevis*, *Mus spp.* and *D. melanogaster*, organization of the intergenic region is similar, consisting of transcription terminators at its 5' end, a promoter that initiates transcription at its 3' end, duplications of the promoter sequence (spacer promoters) and direct sequence repeats that can function as enhancer elements (i.e. 60/81-bp repeats of *X. laevis*) interspersed throughout the central portion (Pikaard, 2002). The sequence of the promoter directing transcription by RNA pol I is not highly conserved. In higher plants, a consensus initiator sequence has been identified ($^{-5}$TATATARGGG^{+5}, transcription start site underlined) that, when altered by point mutation in Arabidopsis, results in diminished or abolished transcription (Doelling and Pikaard, 1995). In Arabidopsis, the core promoter necessary and sufficient for accurate initiation of transcription by RNA pol I appears to be monopartite, extending from -55 to +6 (transcription start site at +1, Doelling et al., 1993; Doelling and Pikaard, 1995). Similar monopartite promoters of ~40–50 bp length have been identified in other plants and the soil amoeba *Acanthamoeba castellanii* (Pikaard, 2002; Radebaugh et al., 1997), but in other eukaryotes such as yeast, *Neurospora spp.*, *D. melangaster*, *X. laevis* and mammals, the promoter is bipartite consisting of a central core from approximately -40 to +15 that directs weak transcription, and an upstream sequence, required for normal transcriptional activity, that extends from ~-150 to 100 (Grummt, 1999; Hannan et al., 1998; Russell and Zomerdijk, 2005). In *S. cerevisiae*, the core extends from -1 to ~-192, while the upstream sequence is a 190 bp fragment located ~2 kb upstream of the transcription initiation site, but is equally effective when moved closer to or downstream of the transcription initiation site, or when inverted (Warner, 1989).

RNA pol I-transcribed RNAs are generally the most actively transcribed genes within the genome, with RNA pol I performing up to 80% of total transcription in rapidly growing cells (Jacob, 1995; Li et al., 1999). In hypoosmotic spreads of amphibian nuclei, single rDNA repeats

undergoing transcription are referred to as Christmas trees (CTs) because of their appearance, having multiple engaged RNA polymerases producing transcripts of increasing length (the branches), dangling from either side of the rDNA (the trunk) (Miller and Beatty, 1969). Branches (pre-rRNA) each have a RNP knob on their free 5' end (terminal knob), corresponding to the U3 snoRNP processing complex (see below), suggesting a tight temporal relationship between rRNA transcription and pre-rRNA processing (Dragon et al., 2002; Mougey et al., 1993). While CTs are less easily visualized in somatic cells, they have been observed in mammalian, yeast and plant spreads (González-Melendi et al., 2001; Puvion-Dutilleul et al., 1997; Scheer and Benavente, 1990; Trendelenburg et al., 1974).

1.4.2 Biogenesis of ribosomes in eukaryotes occurs in the nucleolus

During interphase, the NORs of eukaryotes participate in the formation of non-membrane bound, subnuclear domains, known as the nucleoli. A nucleolus is the location of rDNA transcription, pre-rRNA transcript processing (including cleavage and post-transcriptional methylation and pseudouridylation), r-protein aggregation, and ribosomal subunit biogenesis (Scheer and Weisenberger, 1994). Nucleoli are also the location for maturation of several types of cellular RNAs, including tRNAs, small nuclear RNAs (snRNAs), small nucleolar RNAs (snoRNAs), signal recognition particle (SRP) RNA, telomerase RNA and even some mRNAs (reviewed in Carmo-Fonseca et al., 2000; Pederson, 1998; Thiry and Lafontaine, 2005). Indeed evidence indicates that nucleoli are involved in the biogenesis of most RNP (i.e. ribosomes, telomerase RNPs, SRPs, snRNPs, snoRNPs, Carmo-Fonseca et al., 2000; Pederson, 1998; Thiry and Lafontaine, 2005). During late prophase of mitosis, the nucleoli are disassembled, ceasing nucleolar processes, and are subsequently reassembled following telophase (Hernandez-Verdun et al., 2002).

Ultrastructural analysis of sectioned nucleoli from eukaryotes shows the presence of three (or two, see discussion below) morphologically distinct regions: dense fibrillar components (DFCs), fibrillar centers (FCs), and granular components (GCs) (Figure 1.2, Shaw and Jordan, 1995). FCs appear translucent in electron micrographs (EMs) and often have a circular shape. They are abutted by electron dense DFCs that can form invaginations into the FC, and both are surrounded by an agglomeration of circular GCs. The composition of nucleoli is highly variable between species and throughout the cell cycle, but generally animal nucleoli that are actively synthesizing

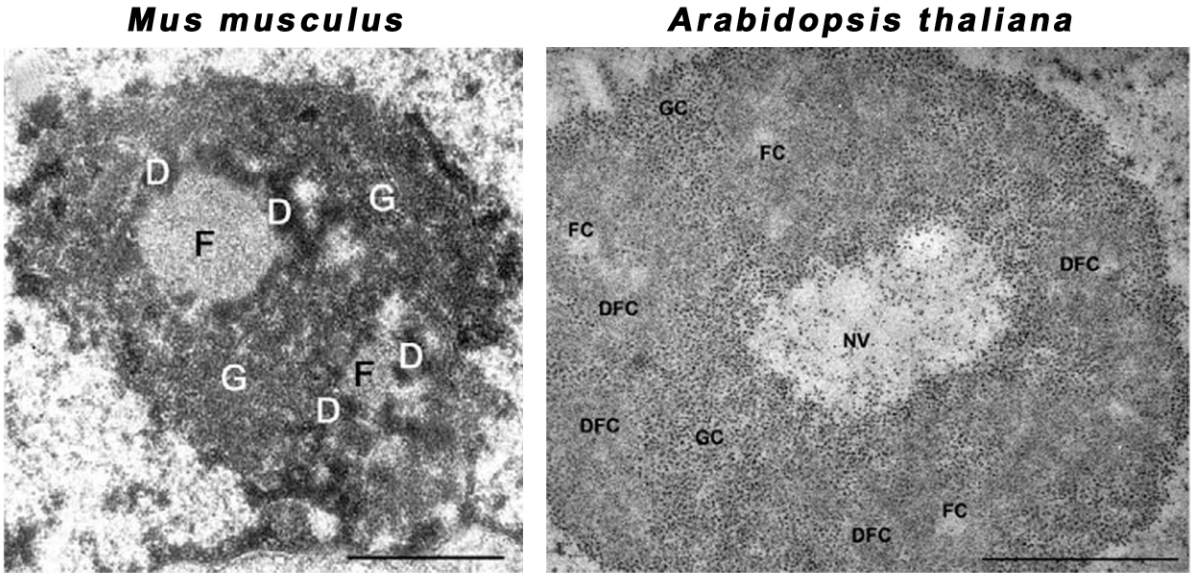

Figure 1.2 Electron micrographs of a thin-sectioned nucleolus from mouse (*Mus musculus*) and Arabidopsis (*Arabidopsis thaliana*). The tricompartmentalization (FC, DFC, GC) of the representative amniote (mouse) is very distinctive relative to that of the representative anamniote (Arabidopsis). Abbreviations: F or FC, fibrillar centers; D or DFC, dense fibrillar centers; G or GC, granular components. Scale bars are 1 μm. The mouse and Arabidopsis EM images are adapted from Raska et al. (2006) and Pontvianne et al. (2007), respectively.

ribosomes are comprised predominantly of GCs (~75%), with DFCs and FCs accounting for a smaller proportion of volume (cf. Figure 1.2, Jordan and McGovern, 1981). Higher plant nucleoli appear morphologically similar, although they have a lower proportion of FCs, and a much higher proportion of DFCs (~50%), which are less electron dense than their animal counterparts (cf. Figure 1.2, Shaw et al., 2002).

Fibrillar centers contain rDNA, but very little rRNA, and are believed to be interphasic equivalent of metaphase NORs (Carmo-Fonseca et al., 2000; Huang, 2002; Olson et al., 2002). Support comes from EM studies showing that the secondary constrictions formed by NORs during metaphase resemble FCs, and that components of the rDNA transcriptional machinery (i.e. RNA pol I, topoisomerase I) remain associated with the metaphase NORs, which never fully condense (Shaw and Jordan, 1995). It is postulated that a single NOR must be capable of forming several FCs because the number of FCs greatly exceeds the number of NORs in an active nucleolus (Raška, 2003). Although still contentious, the finding that FCs, and not DFCs, contain RNA pol I suggests that transcription occurs in FCs, and evidence points to this happening at the transition zone between FCs and DFCs, with nascent transcripts extending into the DFCs (Thiry and Lafontaine, 2005 and references therein). An alternate model suggests that the FCs are a reservoir for inactive RNA pol I (and rDNA), which relocate to DFCs upon initiating rDNA transcription (Raška et al., 2006 and references therein).

DFCs are rich in rRNA and are unequivocally believed to be the sites of nascent pre-rRNA accumulation, and of the initial steps of pre-rRNA processing (Granboulan and Granboulan, 1965; Raška, 2003). This is supported by studies where nascent RNAs, visualized both by incorporation of tritiated uridine followed by autoradiography (Granboulan and Granboulan, 1965), or by nonisotopic EM where a modified ribonucleoside triphosphate is briefly incorporated and detected by an electron-dense antibody (Dundr and Raska, 1993), are observed in DFCs and the DFC/FC border. Essential pre-rRNA processing machinery (e.g. fibrillarin, nucleolin) is localized to DFCs (reviewed in Shaw and Jordan, 1995; Thiry and Lafontaine, 2005), and it is believed that maturation occurs vectorially as the pre-ribosomal particles progress towards GCs. That CTs, which are observed only in EMs of loosened chromatin spreads from specific cell types (i.e. yeast, maturing amphibian oocytes, Raška et al., 2006), have not yet been identified *in situ* in ultrathin sections of somatic cells is likely because they are electron dense structures themselves, due to their high concentration of RNA, varying degrees of

compaction, and association with proteins/RNPs, which makes them indistinguishable within electron-dense DFCs (Biggiogera et al., 2001; Raška, 2003).

Granular components are ~15 nm in size and are the sites of later stages of pre-rRNA processing and subunit assembly (Raška, 2003). Here the maturing RNA pol I-transcribed rRNAs associate with 5 S rRNA and r-proteins, in a process facilitated by snoRNAs, nucleases and non-r-proteins (Carmo-Fonseca et al., 2000).

On the basis of the lack of RNA Pol I in the electron lucid FCs of plants (González-Melendi et al., 2001; Serganov et al., 2003) and other anamniotes (reviewed in Thiry and Lafontaine, 2005), it has been postulated that only amniotes have truly tricompartmentalized nucleoli, with remaining eukaryotes having bicompartmentalized nucleoli, containing only fibrillar strands and GCs (Thiry and Lafontaine, 2005). Under this model, the structures previously denoted as FCs in anamniotes are considered to be nucleolar interstices, which in amniotes are loci of inactive rDNA transcriptional units, or rDNA lacking transcription machinery. It is believed that the large intergenic spacers between rDNA transcription units in amniotes enables the spatial separation of active and inactive transcription units and facilitates establishment of FCs (Thiry and Lafontaine, 2005). Under the bipartite model, the fibrillar strand component would be the site of rRNA transcription, with processing and maturation occurring as preribosomal subunits progress toward the GC.

The existence of nucleoli as discrete structures appears to predominantly be due to the stable association of a few core nucleolar proteins with rDNA, and the increased residence time of nucleolar components due to ligand binding (Raška et al., 2006 and references therein). Nonnucleolar proteins can diffuse into the nucleolus (Handwerger and Gall, 2006), while nucleolar components are in a constant flux between the nucleolus and the surrounding nucleoplasm (Andersen et al., 2005; Chen and Huang, 2001; Lam et al., 2007; Olson and Dundr, 2005). Moreover, unlike the defined signals required for nuclear import, protein entering the non-membrane bound nucleolus do not require a targeting sequence (Andersen et al., 2002; Scherl et al., 2002), but rather a binding sequence that allows for interaction with other nucleolar components and hence increases retention time (Carmo-Fonseca et al., 2000; Kundu-Michalik et al., 2008; Misteli, 2005; Raška et al., 2006).

1.4.3 Pre-rRNA processing in eukaryotes

In eukaryotes, immunocytochemical studies have identified that snoRNP complexes begin to associate with pre-rRNA transcripts during their transcription by RNA pol I (Puvion-Dutilleul et al., 1997; Scheer and Benavente, 1990). These complexes are involved in splicing and modification of the primary transcript (5'ETS–18 S–ITS1–5.8 S–ITS2–23 S-like–3'ETS) into mature rRNA species that are distinct, methylated and pseudouridylated. In eukaryotes, ca. 60–120 distinct snoRNAs have been identified, ranging in size from ca. 67–280 nt (Brown et al., 2003; Chen et al., 2003; Maxwell and Fournier, 1995). Generally, snoRNAs function by base-pairing with pre-rRNA sequences that are consequently targeted for modifications. All snoRNAs are divided into one of two classes defined by conserved RNA sequence and associated proteins: box C/D and box H/ACA snoRNAs (Granneman and Baserga, 2004). Box C/D snoRNAs guide ribose 2'-*O*-methylation and interact with a methylase snoRNP complex containing Nop1/fibrillarin, whereas box H/ACA snoRNAs direct the conversion of uridine to pseudouridine and interact with a pseudouridine synthase snoRNP complex containing Cbf5/Nap57 (Brown et al., 2003; Granneman and Baserga, 2004; Kiss, 2001). Some snoRNAs have other distinctive roles, such as the box C/D snoRNAs U3 and U14, and the RNase MRP snoRNA that guide cleavage of the polycistronic pre-rRNA transcript releasing 18 S rRNA and 23 S-like rRNA, respectively (Brown et al., 2003; Granneman and Baserga, 2004). The function of snoRNA-mediated rRNA base modifications remains unclear, although it is known that they can promote base-pairing interactions and affect ribosome activity (Granneman and Baserga, 2004 and references therein). Only a small number of snoRNAs that are involved in facilitating cleavage events, such as U3 and U14, are reported to be essential for the viability of yeast and vertebrate cell cultures (Venema and Tollervey, 1999), although many snoRNAs have multiple isoforms (Brown et al., 2001; Chen et al., 2003; Huang et al., 2004; Weber, 2006), and thus the lack of an abnormal phenotype in mutants may be due to functional redundancy between snoRNA copies.

During the production of mature rRNAs, the polycistronic pre-rRNA undergoes sequential endo and exonucleolytic cleavage events that remove the two ETSs and ITSs (reviewed in Granneman and Baserga, 2004; Nazar, 2004; Nissan et al., 2002). The primary rRNA, assembled co-transcriptionally into a massive 80–90 S pre-ribosome is initially cleaved at two

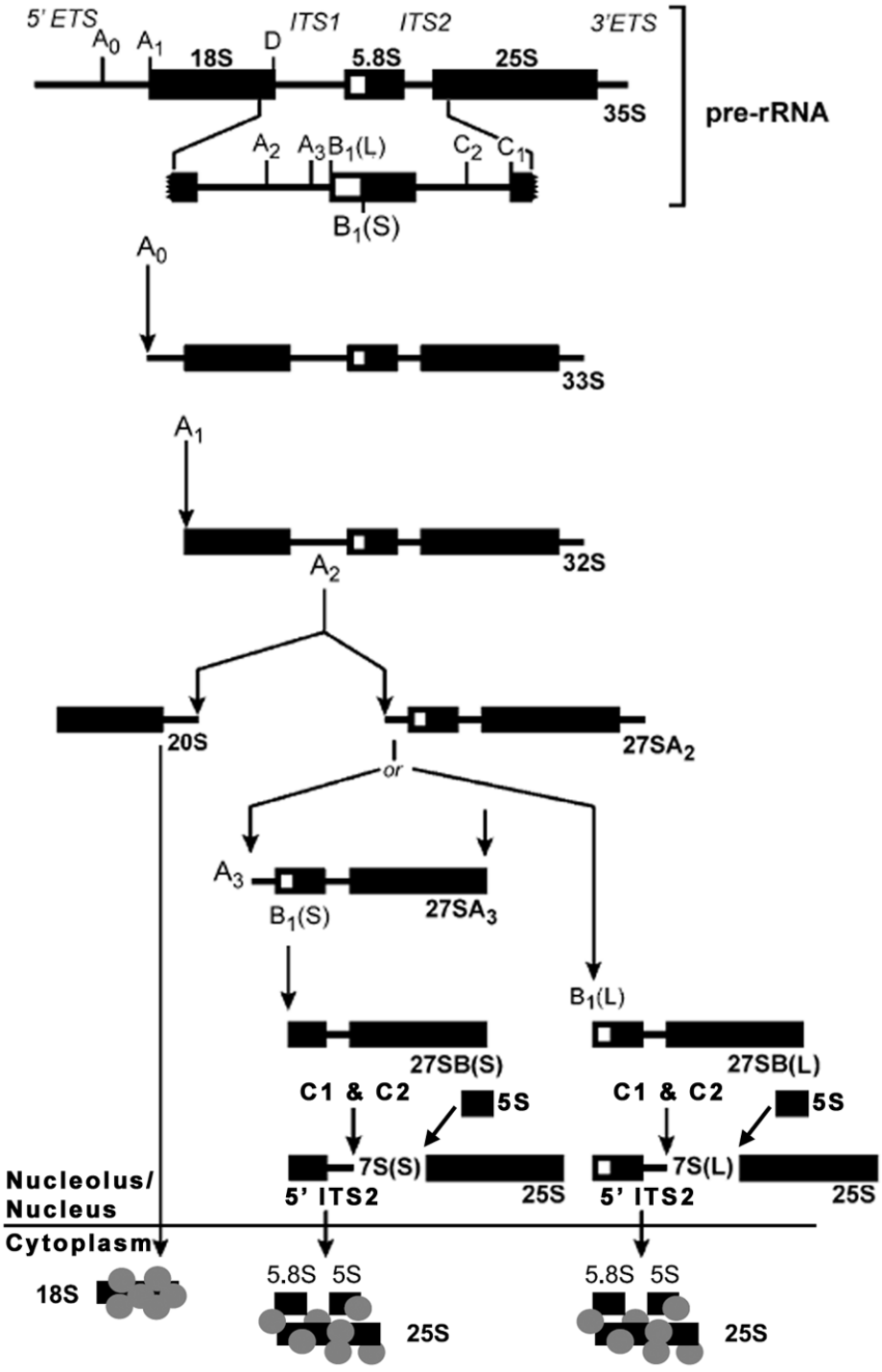

Figure 1.3 Processing of pre-rRNA in eukaryotes. Schematic of the processing steps that occur during maturation of the primary 35S pre-rRNA transcript in *S. cerevisiae*. Processing steps are indicated at the top of arrows. Gray circles represent associations with multiple r-proteins. Details provided in text. Adapted from Granneman and Baserga (2004).

sites within the 5' ETS (A_0, A_1) and one site within ITS1 (A_2), which cleaves the 5' ETS and separates the 18 S precursor from the 5.8 S–23 S-like precursor (Figure 1.3). The 18 S precursor, assembled into a 43S pre-SSU, is subsequently exported to the cytoplasm, through the nuclear pore complex (NPC), where its ITS1 tail is cleaved (at site D), producing a mature SSU. The precursor for 5.8 S–23 S-like rRNAs undergoes further cleavage events to remove ITS1 attached to its 5' end (sites A_3 then B_1[S], or B_1[L]), followed by cleavage at two locations in ITS2 (C_1 and C_2) to produce the mature 5.8 S and 23 S-like rRNAs that assemble with 5 S rRNA into 60 S pre-LSU particles that are exported to the cytoplasm for final maturation. The transcription and maturation of pre-rRNA that occurs within the nucleolus is highly dynamic, insomuch as the polycistronic pre-rRNA is processed during and after transcription by the association and dissociation of a huge array of non-ribosomal processing factors (~150 in yeast) and r-proteins (Brown et al., 2003; Granneman and Baserga, 2004). The latter group contains members that associate with cognate rRNAs both cotransciptionally and concomitantly with cleavage events (Granneman and Baserga, 2004; Hadjiolov, 1985). In yeast and *Dictyostelium*, the pre-rRNA transcript can also undergo cleavage events during transcription, as cotranscriptional removal of both the 5' ETS and ITS1 have been observed (Grainger and Maizels, 1980; Raška, 2003). Hence, rRNAs have assembled into "pre-ribosomes" prior to their export to the cytoplasm where the final processing and assembly of r-proteins occurs, forming the mature ribosomal subunits competent for assembly on mRNA.

1.4.4 Catalytic rRNA

Early evidence that rRNA could perform the peptidyl transferase function of the ribosome came from the observation that an aminoacyl tRNA could be cross-linked to the central loop of domain V of 23 S rRNA at near-identical locations to point mutations conferring resistance to antibiotics that specifically interfere with peptidyl transferase activity (Barta and Kuechler, 1983; Barta et al., 1984). Later, ribosomes of the eubacterial thermophile *Thermus aquaticus* were observed to retain peptidyl transferase activity after phenol extraction, and treatment with proteinase K (Noller et al., 1992). While these studies suggested that peptidyl transferase activity was a property exclusive to LSU rRNA, they could not definitively draw this conclusion because some r-proteins were resistant to protein removal treatments (Noller, 1993). Confirmation that the ribosome is actually a ribozyme came from structural studies of the archaeal *Haloarcula marismortui* ribosome with and without tRNAs bound in the A- and P-sites

(Ban et al., 2000; Nissen et al., 2000). Here it was determined that the peptidyl transferase active site is entirely rRNA, located within the central loop of domain V of 23 S rRNA. No r-proteins are closer than ~18 Å from the peptide bond being synthesized.

The central role of the SSU during translation is decoding/proofreading, wherein base-pairing between the tRNA anticodon and mRNA is monitored to prevent erroneous incorporation of a noncognate tRNA into the A-site (Carter et al., 2000; Moore and Steitz, 2002). This function is an exclusive property of SSU rRNA, performed by the top portion of helix 44 (H44, located at the bottom of the head; cf. Figure 1.1) within the 3' minor domain that runs along the interface of the subunit (Clemons et al., 1999; Wimberly et al., 2000). The 690 and 790 hairpin loops (so called because they span residues 690 and 790 of 16 S rRNA, respectively) of H23B and H24A of the central domain are also functionally important, as they form the binding site for P-site tRNA and are critical for large and small subunit association (Merryman et al., 1999; Moazed and Noller, 1990). The H27 hairpin loop functions as a conformational switch that maintains translational accuracy by altering the conformation of the decoding site, presumably in response to correct codon-anticodon interaction (Clemons et al., 1999; Lodmell and Dahlberg, 1997). The findings that both central components of translation, namely mRNA decoding and peptidyl transferase, are all-rRNA functions provides support for the hypothesis that ancestral ribosomes consisted of RNA alone, with r-proteins being recruited gradually as the ribosome evolved into its current RNP structure (Joyce and Orgel, 1993; Wool, 1996).

1.5 Ribosomal Proteins

1.5.1 Conservation of r-proteins

Although the critical roles of peptidyl transferase and decoding are performed exclusively by rRNA, r-proteins are required for ribosome biogenesis and function. The necessity for r-proteins for survival is exemplified by their high degree of conservation across all Domains of life. Comparison of r-protein genes from 66 different species (45 Bacteria, 14 Archaea, 7 Eucarya) whose complete genomes are sequenced identified the existence of 102 unique r-protein families, of which 34 (15 SSU and 19 LSU) are represented across all Domains, and 32 (15 SSU and 17 LSU) are strictly conserved in every species examined (Lecompte et al., 2002). Ribosomal proteins involved in early assembly events (including prokaryotic S4, S7, S8, S15, S17, L2, L3, L4, L5, L15, L18, L23), those involved in the formation of r-protein–r-protein or r-protein–

rRNA bridges between the subunits (including prokaryotic S15, S13, S19, L2, L5, L14), those near the polypeptide exit tunnel (including prokaryotic L22, L23, L24, L29), and those that make tRNA contacts (including prokaryotic S7, S9, S12, S15, L1, L5) are among the 32 strictly conserved r-proteins (El-Baradi et al., 1984; Held et al., 1974; Rohl and Nierhaus, 1982; Yusupov et al., 2001).

Eukarya and Archaea exhibit the highest degree of r-protein conservation, as all but one of the 68 archaeal r-proteins (LXa) has a eukaryotic equivalent (Lecompte et al., 2002). Eukaryotes also have 11 exclusive r-proteins (4 SSU and 7 LSU). In contrast, Bacteria have 23 exclusive r-proteins (8 SSU and 15 LSU), which is consistent with the major evolutionary division between Bacteria and Archaea/Eucarya; no proteins are shared exclusively between Bacteria and Eucarya, or between Bacteria and Archaea (Lecompte et al., 2002). It has been postulated that r-proteins unique to Bacteria or Eucarya/Archaea function as chaperones for Domain-specific rRNA extensions that are identified when comparing Bacteria rRNA with that of Eukarya/Archaea rRNA. (Lecompte et al., 2002; Wuyts et al., 2001). Another possibility is that these proteins have Domain-specific extra-ribosomal functions, or interact with specific translation factors (Sengupta et al., 2004; Wool, 1996).

Within each Domain, reductive evolution is believed to be responsible for disparity between the r-protein composition of some groups (Lecompte et al., 2002). Bacteria contain four r-protein families that are heterogeneously distributed (not found in all bacterial species), of which three are specific to eubacteria and one (prokaryotic L30) is universally conserved among the three Domains of life. Eucarya exhibit a very high degree of intra-Domain r-protein conservation, as all but two r-protein families appear conserved across the animal, plant and fungal kingdoms. Exceptions include the acidic P3 protein that is plant-specific, and L28e that is absent from *S. cerevisiae*, but not other fungi (de Souza et al., 2005; Lecompte et al., 2002). This high degree of homogeneity is also reflected in the deduced primary sequence identity between rat and yeast r-proteins (range of 40–88%, average of 60%), and rat and Arabidopsis r-proteins (range of 35–96%, average of 66%) (Barakat et al., 2001; Wool et al., 1995). Interestingly, the lowest sequence identity between rat and Arabidopsis was L28e, for which there is no yeast ortholog, possibly suggesting that this protein is highly divergent (Barakat et al., 2001). Early-branching eukaryotes exhibit a lower degree of r-protein conservation. For example, the genome of the microsporidian *Encephalitozoon cuniculi* lacks four eukaryotic r-

proteins, including the strictly Eukarya S21e and L28e, and the Archaea/Eukarya L14e and L38e (Lecompte et al., 2002). Greatest intra-Domain heterogeneity is found in the Archaea Domain, where 10 r-protein families are disparately conserved, including the strictly archaean LXa. Interestingly, the pattern of r-protein reduction follows the phylogenic branching order, with representatives of the more primitive Crenarchaeota having all 10 of the heterogeneous r-proteins that are absent from the most recently diverged members of Euryarchaeota (Lecompte et al., 2002).

1.5.2 Properties of r-proteins

Most r-proteins are small (~3–50 kDa), and consistent with their requirement for rRNA binding, basic with a high concentration of lysine and arginine and a low concentration of aspartic acid and glutamic acid (Arnold and Reilly, 1999; Barakat et al., 2001; Warner, 1999; Wool et al., 1995). Barakat et al. (2001) deduced the primary amino acid sequence of members from 79 Arabidopsis r-protein gene families and calculated their isoelectric points (pI); the basic r-proteins (73 of 79 families) have a predicted pI range from 8.1 (RPS27) to 12.8 (RPS30 and RPL39), which is in agreement with the average pI of 11 determined for rat r-proteins (Wool et al., 1995).

In eukaryotes, most r-proteins are single-copy within the ribosome and assemble with rRNA in the nucleolus. However, a small group of acidic (pI 4–5) r-proteins are present in multiple copy and form the P-protein stalk of the LSU. In prokaryotes, the stalk is formed by two heterodimers of L12 (containing one acetylated [designated L7] and one non-acetylated copy [designated L12]) that interact with 23S rRNA-bound L10 protein, generating the stalk pentamer (Gudkov et al., 1978; Stark et al., 1995). In eukaryotes, the stalk forms from the interaction of 12 kDa, acidic P1 and P2 proteins with the acidic P0 protein; plants are unique in having a third acidic r-protein, P3 (Szick et al., 1998). In *S. cerevisiae*, two forms of P1 and P2 r-proteins exist (P1α/β, P2 α/β), and the stalk generally is comprised of two heterodimers (one P1α–P2β, one P1β–P2α) (Guarinos et al., 2003; Hanson et al., 2004). Animals have only one form of P1 and P2, and their stalk forms from two P1/P2 dimers (Tsurugi and Ogata, 1985). The exact composition of the plant P-protein stalk is unknown, but experimental evidence suggests that it may exhibit spatiotemporal variability. Maize contains 2 types of P2 (P2a and P2b), and they are differentially expressed during development (Szick-Miranda and Bailey-Serres, 2001).

Arabidopsis P2 is encoded from a five member gene family that exhibits phylogenetic divergence, dividing the genes into two groups: type I (*RPP2A*, *RPP2B* and *RPP2D*) and type 2 (*RPP2C* and *RPP2E*, Barakat et al., 2001; Chang et al., 2005). Analysis of the Arabidopsis ribosomal protein complement by mass spectrometry (MS) has determined that both type I and type II P2 r-proteins are incorporated into the ribosome, conferring variability in stalk composition (Chang et al., 2005). Acidic lateral stalk r-proteins of eukaryotes do not assemble onto pre-ribosomes in the nucleolus, but rather cycle between active ribosomes and a cytoplasmic pool (Elkon et al., 1986; Sanchez-Madrid et al., 1981).

Several r-proteins are modified post-translationally, although the significance of some of these changes remains unclear (Niedhardt et al., 1990). In prokaryotes, the most common modification is loss of the N-terminal methionine, which occurs in nearly all cases where the amino acid in position two has a short enough side-chain to allow aminopeptidase access (Arnold and Reilly, 1999); large side-chains sterically block the methionine aminopeptidase cleavage site (Sherman et al., 1985). Other *E. coli* modifications detected by MS, include single methylation of S11, L3, L12 and L33, methylation of L11 at nine positions, acetylation of S5, S18 and L7, thiomethylation of S12, and cleavage of eight amino acids from the C-terminus of L31 (Arnold and Reilly, 1999 and references therein). Examination of *S. cerevisiae* LSU r-protein modifications by MS determined that all but five of the 42 detected r-proteins had lost their N-terminal methionine (Lee et al., 2002a). Acetylation of the N-terminus, which similar to methionine removal occurs cotranslationally (Driessen et al., 1985), was observed for two isoforms of rpL1, rpL4, rpL11, rpL14 and rpL16. Other modifications included the mono-methylations of lysine/arginine residues of rpL1, rpL3, and rpL43, dimethylation of rpL42 and multiple methylations of rpL12 (ortholog of *E. coli* L11) and rpL23 (Lee et al., 2002a). The acidic r-proteins of yeast (P0, P1α/β, P2α/β) are post-translationally phosphorylated at serine residues (Lee et al., 2002a; Sanchez-Madrid et al., 1981). Similar modifications (removal of N-terminal methionine, N-terminal acetylation, and lysine/arginine methylation) occur in plants (Carroll et al., 2008; Chang et al., 2005) and animals (Louie et al., 1996; Odintsova et al., 2003; Yu et al., 2005), and in most cases ortholog modifications are conserved, especially the phosphorylation of the acidic proteins (P0, P1 and P2) and S6 (Bailey-Serres and Freeling, 1990; Carroll et al., 2008; Chang et al., 2005; Krieg et al., 1988; Scharf and Nover, 1982; Wool et al., 1995). In Arabidopsis, S6 is encoded by a two-member gene family, and their gene products can

be differentially phosphorylated at C-terminal serine residues producing at least four different forms of S6 (Carroll et al., 2008; Chang et al., 2005). Similar findings have been reported in maize, mammals and *D. melanogaster*, and it is believed that S6 phosphorylation has a role in regulation of ribosomal activity (Krieg et al., 1988; Radimerski et al., 2000; Williams et al., 2003).

1.5.3 Copy number and organization of r-protein genes

Prokaryotic r-protein genes are, with few exceptions, single copy (Makarova et al., 2001). These genes are generally clustered in a few operons (20 in *E. coli*), simplifying their coordinated regulation (Mager, 1988; Nomura et al., 1984). The prokaryotic r-protein superoperon, an array containing several operons and >20 r-protein genes, is the most highly conserved portion among prokaryotic genomes (Wolf et al., 2001). In *E. coli*, the *S10-spc-alpha* superoperon contains 22 of the 32 r-protein genes that are universal to all three Domains of life (Lecompte et al., 2002). The small number of paralogous r-protein genes, including genes for only four r-proteins (S14, L31, L33, L36) that are duplicated within more than one prokaryotic genome, are believed to have arisen predominantly from horizontal gene transfer (Makarova et al., 2001). Both of the duplicated genes are generally translated, and in nearly all cases one paralog contains a zinc-ribbon with putative metal-binding ability (believed to be important for ribosome stability at high temperatures), while the other has lost this attribute (Makarova et al., 2001).

Eukaryotic r-protein genes are monocistronic and dispersed throughout the genome (Barakat et al., 2001; Mager, 1988; Uechi et al., 2001). Duplication of r-protein genes as part of whole and partial genome duplications and retrotranspositions has resulted in the formation of multi-gene families for most eukaryotic r-proteins (Barakat et al., 2001; Maere et al., 2005; Planta and Mager, ; Wool et al., 1995; Zhang et al., 2002). In yeast, 59 of 79 r-protein genes are duplicated; in all cases both copies are expressed, albeit often at divergent levels (reviewed in Planta, 1997; Warner, 1989). This contrasts the situation in mammals, where r-protein genes generally have a high copy number, but only one copy is expressed and the remainder are inactive pseudogenes (Wool et al., 1995). For example, the human genome reportedly contains 1,756 processed r-protein pseudogenes (those introduced by retroposition), representing almost one-quarter of all

human processed pseudogenes (Zhang et al., 2003). This is consistent with the findings of Wool et al. (1995), who reported an average of 12 pseudogenes for each of 59 rat r-proteins.

In plants, r-protein genes are found in multi-gene families, and more than one family member is usually transcribed, resulting in overlapping and/or differential patterns of transcript abundance (Barakat et al., 2001; Hulm et al., 2005; McIntosh and Bonham-Smith, 2005; Wu et al., 1995). For example, *Z. mays* has two genes encoding the acidic RPP2 (*RPP2a* and *RPP2b*), and transcripts of both accumulate to their highest levels in coleoptiles and immature ears (Szick-Miranda and Bailey-Serres, 2001). However, *RPP2a* transcripts were less abundant than those of *RPP2b* in leaf, silk and pollen, whereas *RPP2a* transcripts predominated in all tissues of the kernel. In Arabidopsis, the 81 r-proteins are encoded by 254 genes, with gene families ranging in size from two to seven members (Barakat et al., 2001; Chang et al., 2005). Plant r-protein gene families are believed to have arisen from ancestral polyploidisation events that have played a major role in plant evolution, especially that of angiosperms (Cannon et al., 2004; Maere et al., 2005; Simillion et al., 2002). Since those events, r-protein genes may have undergone specialization/neofunctionalization to confer greater plasticity to environmental conditions (Barakat et al., 2001). For example, one copy may be constitutively expressed, while others are developmentally or environmentally regulated to accommodate increased demands for ribosome biogenesis and protein synthesis (McIntosh and Bonham-Smith, 2006; Van Lijsebettens et al., 1994).

1.5.4 Function of r-proteins

Although the ribosome is a ribozyme (Nissen et al., 2000), r-proteins have a number of critical roles, both within and outside the ribosome. A large number of r-proteins have structural roles and are necessary to stabilize the tertiary structure of both LSU and SSU rRNAs (Ban et al., 2000; Brodersen et al., 2002; Klein et al., 2004; Wimberly et al., 2000). This is necessary because the negatively charged rRNA folds into a compact, convoluted structure that would be electrostatically unfavorable if not for the charge buffering of positively charged r-proteins (Steitz and Moore, 2003).

In addition to structural roles, resolution of the structure of the prokaryotic ribosome has identified and confirmed a number of direct roles for r-proteins within the ribosome. For example, S12 is positioned close to the rRNA active site for decoding of A-site tRNA, and

contains residues that are involved in recognizing correct binding in the third (wobble) base pair between the codon and anticodon (Ogle et al., 2001). The eubacteria-specific S1 protein, is positioned on the solvent side of the head portion of the SSU and is believed to be important for non-sequence specific binding of mRNA, mediated by its six repeats of the oligonulceotide-binding fold (OB-fold) (Brodersen and Nissen, 2005). In its role in tethering mRNA to the ribosome, S1 works cooperatively with both S7 and S11, positioned near the E-site of the SSU, and most importantly with the 3' end of 16 S rRNA that is complementary to the mRNA Shine-Dalgarno sequence required for translation initiation (Shine and Dalgarno, 1974).

A number of r-proteins are positioned near the polypeptide exit tunnel of the LSU: L4 and L22 have loops that form a constriction on the interior of the tunnel, L39e (Archaea and Eucarya only) also has residues that line the tunnel, and L22, L23, L24 and L29 are positioned immediately surrounding the exit site of the tunnel (Nissen et al., 2000). The constriction formed by L4 and L22 is believed to be involved in perceiving nascent chain sequence and/or structure, and inducing conformational changes that modulate translation (Woolhead et al., 2006; Woolhead et al., 2004). Residues of L22 and L39e that are exposed to the interior of the tunnel add to its hydrophilic nature to prevent energetically unfavorable interactions with nascent peptides (Nissen et al., 2000). In prokaryotes, r-proteins L23, L24 and L29, that surround the tunnel exit, interact with Ffh (Fifty-four homolog; the protein component of prokaryotic SRP), trigger factor chaperone, and the membrane-embedded SecYEG (translocon) complex to mediate cotranslational folding/translocation/secretion processes (Ferbitz et al., 2004; Gu et al., 2003; Kramer et al., 2002; Maier et al., 2005; Mitra et al., 2005). Similarly, nascent chain targeting is accomplished by the eukaryotic r-protein counterparts L23a/L25, L26 and L35, which interact with SRP and the membrane embedded Sec61 translocon (Beckmann et al., 1997; Halic et al., 2004; Menetret et al., 2005; Morgan et al., 2002; Pool et al., 2002).

In addition to the r-protein-rich region surrounding the exit tunnel that interacts with external factors relating to the nascent polypeptide, a second r-protein-rich, factor-interacting, region exists on the LSU. The L7/L12 lateral stalk is composed of r-proteins the L10, L11 and L7/L12 (eukaryotic P0, L12 and P1/P2/P3, respectively). The r-proteins L10 and L11 are bound to LSU rRNA through specific helices of domain 2, while r-protein–r-protein interactions connect the C-terminal domain of L10 with the N-terminal domains of 2–3 copies (species-dependent) of L7/12 dimers (Ban et al., 2000; Diaconu et al., 2005; Kavran and Steitz, 2007). The flexible C-terminal

domains of L7/L12 function to recruit GTPase translation factors (initiation, elongation and release), which upon binding induce a conformational change, mediated by flexibility of L10 and L11, in the entire L7/12 stalk (Diaconu et al., 2005; Helgstrand et al., 2007; Kavran and Steitz, 2007). Hydrolysis of translation factor-bound GTP is facilitated by both L7/12 and the sarcin-ricin loop of LSU rRNA (Figure 1.1b), which becomes proximal to translation factors following factor-binding induced conformational change. GTP-hydrolysis results in further changes to ribosome conformation that direct different stages of translation (initiation, elongation, release) in a factor-dependent manner (Frank and Agrawal, 2000; Stark et al., 2000; Stark et al., 2002; Valle et al., 2003; Wahl and Moller, 2002).

Several r-proteins have been ascribed functions outside their role within the ribosome. Extra-ribosomal functions of prokaryotic r-proteins include roles in transcription, DNA repair, DNA replication, and RNA processing (reviewed in Wool, 1996). In eukaryotes, r-proteins have been implicated in nuclear export, transcriptional regulation, autogenous translational regulation and DNA repair (Brodersen and Nissen, 2005; Wool, 1996). Additionally, a large number of eukaryotic r-proteins have roles in cell-cycle regulation and development (reviewed in Kaeberlein et al., 2007; Lai and Xu, 2007; Marygold et al., 2007; McIntosh and Bonham-Smith, 2006; Uechi et al., 2001). The identification of extra-ribosomal functions for some r-proteins supports the hypothesis that r-proteins were recruited to the ribosome, adding to its rRNA core over time (Wool, 1996).

1.5.5 Regulation of r-protein expression

1.5.5.1 Operons and feedback regulation in prokaryotes

All r-proteins, except the acidic L7/L12 (eukaryotic P-proteins) that form the stalk, are present in unimolar quantities in an assembled ribosome. Consequently, mechanisms must exist to ensure that all r-proteins are produced in sufficient quantity to support ribosome biogenesis, and not overproduced leading to the potentially deleterious accumulation of unincorporated r-proteins (Nomura, 1999; Warner, 1999). In prokaryotes, r-proteins are clustered into species-specific operons, facilitating the expression of equimolar amounts of transcript. The level of r-proteins is regulated by post-transcriptional feedback mechanisms, whereby one of the r-proteins encoded by the operon binds to a location on its own polycistronic transcript, the operator, which "mimics" the rRNA binding site for that r-protein (Mager, 1988; Nomura et al., 1980). For

instance, r-protein L1 of *E. coli* reduces expression of both itself and L11 by binding to the operator site of the *L11-L1* dicistronic transcript (Nomura et al., 1984; Zengel and Lindahl, 1994). This operator site is structurally similar to the binding site for L1 on 23 S rRNA, and mutations to either have effects consistent with their competitive interaction (Cole and Nomura, 1986; Said et al., 1988). Similar findings have been reported for other operons including the *spc* (Wu et al., 1994), *IF3* (Guillier et al., 2002) and *S15* operons (Philippe et al., 1993). This mechanism requires that the regulatory r-protein has a greater affinity for its rRNA binding site than for its operator, and this has been confirmed both by dissociation constants (for example Kohrer et al., 1998) and by structural analysis of molecular contacts (for example Nevskaya et al., 2005; Nikulin et al., 2003).

1.5.5.2 Transcriptional regulation of eukaryotic r-proteins

In contrast to prokaryotes, eukaryotic r-protein genes are monocistronic and dispersed throughout the genome. Further complicating coordinated regulation is the existence of multiple expressed paralogs for each r-protein in most eukaryotes (Barakat et al., 2001; Barthelemy et al., 2007; Berriman et al., 2005; Ivens et al., 2005; Marygold et al., 2007; Planta and Mager, 1998), the exception being vertebrates that generally have only one expressed gene for each r-protein (Uechi et al., 2001; Wool et al., 1995). Several possible control points exist for regulation of eukaryotic r-proteins. Genes for r-proteins are transcribed in the nucleus, with resultant mRNAs transported to the cytosol through NPCs. Transcripts are translated in the cytoplasm and most r-proteins are subsequently imported into the nucleus through NPCs where they are retained by the nucleolus and assembled into immature ribosomal subunits. Lastly, these subunits are exported from the nucleus to the cytoplasm, where the final processing steps and subunit assembly on mRNA occur.

In yeast, r-proteins are regulated predominantly at the level of transcription, with transcript abundance reflecting nutritional status and growth rate (Planta, 1997; Warner, 1989; Warner, 1999). This is achieved by the presence of conserved *cis*-elements in the upstream RR of most r-protein genes, the majority of which contain two binding sites for the Rap1 (repressor/activator protein 1) transcription factor; a smaller number contain binding sites for Abf1 (autonomously replicating sequence [Ars] binding factor 1) instead of the two Rap1 sites (reviewed in Planta, 1997; Planta et al., 1995). In all cases, a T-rich stretch is found downstream of the transcription

factor binding site. Binding of Rap1 or Abf1, in conjunction with the T-rich region, mediates nucleosome-displacement and chromatin reorganization, enabling binding of other regulatory proteins to the core promoter (Lascaris et al., 2000; Vignais and Sentenac, 1989) . Rap1 and Abf1 are not specific for r-proteins, but rather are involved in the transcription of genes involved in a variety of cellular processes (Lieb et al., 2001; Planta, 1997). Further work showed that displacement of nucleosomes by Rap1/Abf1 leads to recruitment of a histone acetylase, Esa1, and the acetylation of r-protein gene histones (Reid et al., 2000). Concomitantly, the transcription factor Fhl1 (forkheadlike 1) associates with the core r-protein promoter (Lee et al., 2002b), and its coactivator Ifh1 (interacting with forkhead 1) binds to Fhl1 (Rudra et al., 2005; Wade et al., 2004), activating transcription. In response to conditions that repress growth (nutrient starvation, heat stress, osmotic shock), Ifh1 releases from Fhl1 and is replaced by Crf1 (corepressor with Fhl1) (Martin et al., 2004), Esa1 is replaced by the histone deacetylase complex, Rpd3–Sin3 (Rohde and Cardenas, 2003), and transcription is repressed.

Transcription of yeast r-protein genes in response to nutritional status is under the control of the TOR (target of rapamycin) pathway, which is mediated by two serine/threonine kinases, TOR1 and TOR2 (Mayer and Grummt, 2006; Powers and Walter, 1999; Warner, 1999). During nutritional downshift, TOR repression activates a protein kinase A-regulated kinase, YAK, which phosphorylates Crf1 (Martin et al., 2004). Crf1 is retained in a cytoplasmic pool when nonphosphorylated, but upon phosphorylation accumulates in the nucleus and competes with Ifh1 for their mutually exclusive binding site on Fhl1, leading to repression of r-protein gene transcription. Further, TOR activity is required for the occupation of r-protein promoters by Esa1 (Rohde and Cardenas, 2003), and TOR repression by rapamycin treatment or nutritional deprivation results in the recruitment of the Rpd3–Sin3 deacetylase complex to r-protein promoters and downregulation of expression (Humphrey et al., 2004; Rohde and Cardenas, 2003).

The mechanisms that control coordinated expression of plant cytosolic r-proteins have been less well characterized, although it appears that transcriptional regulation is an important component. Transcripts of most r-protein genes accumulate to the greatest extent in tissues undergoing active cell division and are least abundant in mitotically-inactive tissues (Bonham-Smith et al., 1992; Hulm et al., 2005; McIntosh and Bonham-Smith, 2005; Van Lijsebettens et al., 1994; Williams and Sussex, 1995). Transcript levels for many r-protein genes increase in

response to treatment with growth stimulating phytohormones such as auxins (Gantt and Key, 1983, 1985; Gao et al., 1994) and cytokinins (Cherepneva et al., 2003; Dai et al., 1995; Hulm et al., 2005; McIntosh and Bonham-Smith, 2005; Sakakibara et al., 2006). Conversely, many r-protein genes are coordinately downregulated by treatment with abscisic acid (Cherepneva et al., 2003; Hoth et al., 2002; Hulm et al., 2005; McIntosh and Bonham-Smith, 2005). Similarly, global repression of r-protein gene expression was observed following sucrose starvation of Arabidopsis cell cultures (Contento et al., 2004), while global induction of r-protein gene transcription has been reported following transfer of Arabidopsis from sugar-restrictive to sugar-repletive conditions (Li et al., 2006).

Three plant *cis*-acting motifs responsible for the coupled regulation of r-proteins and the cell cycle have been identified in upstream RRs. These include the *PROLIFERATING CELL NUCLEAR ANTIGEN* (*PCNA*) site II motif ($^{5'}$TGGGCY$^{3'}$, Kosugi and Ohashi, 1997; Tatematsu et al., 2005; Tremousaygue et al., 2003), the interstitial telomeric repeat, *telo*-box ($^{5'}$AAACCCTA$^{3'}$, Li et al., 2006; Tatematsu et al., 2005; Tremousaygue et al., 2003; Tremousaygue et al., 1999), and the translation elongation factor *eEF1A* box or *tef*-box ($^{5'}$ARGGRYAnnnnnGTM$^{3'}$, Curie et al., 1991; Manevski et al., 1999; Regad et al., 1995). The *telo*-box and site II motifs function synergistically and have been identified in combination in the RRs of 153 Arabidopsis r-protein genes (Tremousaygue et al., 2003). AtPurα binds *telo*-boxes in Arabidopsis (Tremousaygue et al., 1999), and the TEOSINTE BRANCHED1, CYCLOIDEA, PCF (TCP) domain transcription factor, TCP20 binds to both Arabidopsis and rice site II motifs (Kosugi and Ohashi, 2002; Li et al., 2005a; Tremousaygue et al., 2003). The finding that DNase I hypersensitivity maps proximal to the *telo*-box of Arabidopsis *PCNA1* (Kodama et al., 2007), and that the human homolog of AtPurα has DNA helix destabilizing properties (Darbinian et al., 2001), suggests that AtPurα and TCP-domain transcription factors might function in chromatin remodeling of plant r-protein genes and mediate binding of additional transcription factors and/or the TATA box-binding protein–RNA pol II complex (Li et al., 2005a; Tatematsu et al., 2005; Tremousaygue et al., 2003).

1.5.5.3 Post-transcriptional regulation of eukaryotic r-proteins

In vertebrates, primary regulation of r-protein expression occurs at the level of translation, mediated by long mRNA half-lives and a common r-protein architecture that enables

synchronous translational response to growth and nutrition (Hamilton et al., 2006; Meyuhas, 2000). In active cells, or in response to mitogens, r-protein mRNAs are found in polysomes, whereas they are shifted to the RNP (subpolysomal fraction) in quiescent cells or following treatment with agents that lead to growth arrest (reviewed in Meyuhas, 2000). The key architectural feature of vertebrate r-protein mRNAs is a 5' terminal oligopyrmidine tract (5'TOP) in the 5' untranslated region (5' UTR), consisting of a C-residue at the extreme 5' terminus, followed by 4–14 consecutive pyrimidines (Amaldi et al., 1995; Meyuhas, 2000). The rate of translation of 5'TOP transcripts is controlled at the level of initiation by the binding of specific *trans*-acting factors (Meyuhas, 2000). Specifically, it is believed that positive growth signals are integrated by the phosphoinositide 3-kinase (PI3K) pathway, which activates the downstream mammalian TOR (mTOR) pathway, resulting in the displacement of repressors bound to 5'TOPs (Hamilton et al., 2006). Conversely, growth dormancy results in the sequestration of 5'TOP mRNAs in the RNP fraction via binding of repressors, possibly including the La autoantigen, cellular nucleic acid binding protein (CNBP), and A+U-rich element-binding factor AUF1, to the 5'TOP (Cardinali et al., 2003; Kakegawa et al., 2007; Pellizzoni et al., 1997).

Post-transcriptional regulation of plant r-protein genes has also been reported. For example, stored, unprocessed transcripts of *RPL3* and *RPL6* have been detected by Northern analysis in dry embryonic axes of maize (Beltran-Pena et al., 1995). In Arabidopsis, recent evidence suggests that regulation of r-protein levels in response to stress may occur predominantly post-transcriptionally. In response to sucrose starvation (Nicolai et al., 2006), dehydration stress (Kawaguchi et al., 2004), or hypoxia (Branco-Price et al., 2005), r-protein transcripts exhibit a coordinated decrease in polysomal loading and corresponding shift to the RNP fraction, without significant change in transcript levels. As in animals, AtTOR, the Arabidopsis TOR kinase homolog, may be involved in this translational response (Menand et al., 2002). RNA interference- (RNAi-) mediated silencing of *AtTOR* resulted in a decrease in r-protein transcript polysome formation, concomitantly conferring hypersensitivity to osmotic stress (Deprost et al., 2007). The finding that *EBP1*, a protein involved in regulation of cell proliferation, cell expansion and possibly ribosome biogenesis (Horvath et al., 2006), was induced by *AtTOR* silencing suggests that it may be a downstream integrator of AtTOR signaling that regulates translation.

1.5.5.4 Post-transcriptional regulation of eukaryotic r-proteins

In mammalian HeLa cells, a combination of quantitative MS and bioimaging has been used to investigate the synthesis, nucleocytoplasmic transport, mobility and degradation of nucleolar proteins (Andersen et al., 2005; Lam et al., 2007). These studies found that newly synthesized r-proteins are targeted to the nucleolus more rapidly than other nucleolar proteins, and far in excess of physiological demands (Lam et al., 2007). The r-proteins are in constant flux between the nucleolus, where they can be retained if nascent rRNAs are available for subunit assembly, and the surrounding nucleoplasm, where they are exposed to the 26 S proteasome and degraded (Lam et al., 2007; Matsumoto et al., 2005a). A similar mechanism is postulated to exist in yeast (Warner, 1989) given the short half-life of unused r-proteins (El-Baradi et al., 1986; Tsay et al., 1988; Warner, 1989), and the finding that ectopically expressed r-proteins are highly unstable (Gritz et al., 1985; Warner et al., 1985), but can be stabilized by depletion of the corresponding endogenous r-protein (Abovich et al., 1985). Under this model, the rate-limiting step governing production of ribosome subunits is the synthesis of rRNA (Lam et al., 2007). It is unknown whether the proteasome is involved in regulating plant r-proteins, although the finding that r-proteins were overrepresented in a global proteomic analysis of ubiquitylated Arabidopsis proteins suggests that a similar pathway may exist in all eukaryotes to prevent the over-accumulation of r-proteins (Maor et al., 2007).

1.6 The L23/L23a/L25 Ribosomal Protein Family

The L23/L23a/L25 family is universal to all three Domains of life (Lecompte et al., 2002). It has been demonstrated that this family of r-proteins binds directly to a conserved site (domain III) of the 23 S or 23 S-like rRNA (Buisson and Reboud, 1982; El-Baradi et al., 1987; El-Baradi et al., 1984; El-Baradi et al., 1985; Jeeninga et al., 1996; Rutgers et al., 1991; Vester and Garrett, 1984), and is required for LSU assembly within the nucleolus (Ross et al., 2007; Schaap et al., 1991; van Beekvelt et al., 2001; van Beekvelt et al., 2000). Structural studies have mapped its yeast, mammalian and prokaryotic counterparts (L25, L23a and L23, respectively), to the solvent-exposed side of the LSU, adjacent to the polypeptide exit tunnel (Figure 1.1a, Chandramouli et al., 2008; Nissen et al., 2000; Spahn et al., 2001; Spahn et al., 2004; Yusupov et al., 2001). This location suggests a role for RPL23a in nascent peptide folding and/or translocation, and these roles have been validated in both prokaryotes and eukaryotes. In the latter, concurrent with translation, the signal peptide of nascent chains is recognized by the SRP,

which via its SRP54 subunit binds RPL23a (and adjacent RPL35) to direct the ribosome/nascent chain complex to the translocon pore (Sec61 complex) of the endoplasmic reticulum, where RPL23a makes additional contacts directly with the Sec61 complex (Beckmann et al., 1997; Menetret et al., 2005; Morgan et al., 2002; Pool et al., 2002). The prokaryotic chaperone trigger factor also docks to the ribosome via L23, suggesting that this r-protein family is broadly involved in cotranslational processes (Ferbitz et al., 2004; Halic et al., 2004; Kramer et al., 2002; Maier et al., 2005).

The eukaryotic L23a/L25 r-proteins possess an N-terminal extension region that is absent from prokaryotic counterparts, and this region contains the nuclear localization signal (NLS, Jakel and Gorlich, 1998; Rutgers et al., 1990; Schaap et al., 1991). In both yeast and mammals, importin-β-like transport receptors mediate L25/L23a nuclear import through NPCs (Schlenstedt et al., 1997).

There are two members of the *RPL23a* family in Arabidopsis, *RPL23aA* and *RPL23aB*, encoding proteins with 74.8 and 74.1% amino acid identity to rat RPL23a, respectively (Barakat et al., 2001). Both paralogs of *RPL23a* are expressed (Barakat et al., 2001; McIntosh and Bonham-Smith, 2005), and incorporated into ribosomes (Carroll et al., 2008; Chang et al., 2005; Giavalisco et al., 2005). Functionality of RPL23aA was confirmed by its ability to complement a yeast *l25* mutant (McIntosh and Bonham-Smith, 2001). Transcript profiling by semi-quantitative RT-PCR determined that *RPL23aA* transcript abundance was greater than that of *RPL23aB* in all tissues of adult Arabidopsis plants. Paralogs responded coordinately to most developmental stimuli and exogenous phytohormones, but expression differed in response to cold-, wounding- and copper-stress (McIntosh and Bonham-Smith, 2005).

1.7 Objectives

In the experiments described in this thesis, I investigated the requirement for r-protein paralogy in plants by studying the two-member *RPL23a* family of the model flowering plant Arabidopsis. Specific objectives are listed below:

1) Identify specific regulatory elements necessary for expression of each *RPL23a* paralog.
2) Establish the requirement for *RPL23a* paralogs during development.

3) Determine whether Arabidopsis compensates for loss of a single paralog (*RPL23aB*) by upregulating transcription of the remaining paralog.
4) Characterize the subcellular localization of RPL23aA and RPL23aB.
5) Determine the involvement of protein turnover in regulating RPL23a accumulation.

2 CHAPTER 2. EXPRESSION OF ARABIDOPSIS RIBOSOMAL PROTEIN RPL23A IS REGULATED AT MULTIPLE LEVELS

This chapter contains work completed collaboratively. KB McIntosh conducted the 5' RACE experiments, analyzed GUS activity in seedlings and tissues of mature plants driven by the 5' deletion series constructs, identified leader intron splice-sites in the 5' deletion series constructs, designed the 3' deletion series, 2nd intron and intron-less constructs, and contributed portions of the relevant text sections and figures (McIntosh, 2005). I analyzed GUS activity in seedlings driven by the empty vector control, 3' deletion series, 2nd intron and intron-less constructs, identified leader intron splice-sites in the 3' deletion series constructs, analyzed transcriptional regulation in stressed Arabidopsis protoplasts, conducted the bioinformatic analyses, assembled all figures and tables, and wrote the final chapter.

The 80S cytoplasmic ribosome of Arabidopsis is responsible for producing most cellular proteins. Demand for ribosome production depends on growth rate, and both the ribosomal RNA (rRNA) and ribosomal protein (r-protein) components must respond coordinately and rapidly to positive and negative growth stimuli to prevent deleterious effects of excess or insufficient ribosomes. The 81 r-proteins of the Arabidopsis 80S ribosome are encoded by multi-gene families that often exhibit overlapping patterns of transcript accumulation, which further complicates regulation because only a single copy of each r-protein (with the exception the acidic r-proteins) can assemble into a single ribosome. Here we dissected the regulatory regions (RRs) of both members of the *RPL23a* family (*RPL23aA* and *RPL23aB*) to identify salient *cis*-acting elements involved in transcriptional, posttranscriptional and translational regulation of expression. Full length and truncated RRs of *RPL23a* paralogs were cloned upstream of reporter genes and expressed both stably in Arabidopsis transgenics, and transiently in stressed-Arabidopsis protoplasts. High level expression in mitotically active tissues, driven by *RPL23aA* and *RPL23aB* RRs, required *telo*-box, site II motif and TATA box elements. The site II motif, and especially the *telo*-box, were also shown to be involved in repressing transcription under certain stress conditions (i.e. hypoxia, sucrose-starvation). First and second introns were found to play a minor role in posttranscriptional regulation of paralogs, and conserved transcript features (e.g. UTR base composition) may be involved in enhancing translational efficiency.

Overall, our results indicate that RPL23a expression is governed by a complex network of multiple regulatory layers.

2.1 Introduction

Ribosomal proteins are integral to the assembly and functioning of the ribosome, a universally conserved, two-subunit, RNP enzyme responsible for polypeptide synthesis. Although r-proteins are non-catalytic (Nissen et al., 2000), the importance of their function is emphasized by the high degree of r-protein conservation. Of 105 known r-protein families, 35 (15 SSU and 20 LSU) are conserved among all three domains of life (Bacteria, Achaeae, and Eukarya), and only 13 (5 SSU, 8 LSU) are exclusive to eukaryotes (Lecompte et al., 2002; McIntosh and Bonham-Smith, 2006). In the model flowering plant Arabidopsis, the cytoplasmic ribosome contains one and three rRNAs) in the SSU and LSU, respectively, and 81 r-proteins (33 SSU and 48 LSU). All but one (RPP3) of these r-proteins has an ortholog in the animal kingdom, and the degree of primary sequence conservation with rat orthologs ranges from 44–85% and 35–96% amino acid identity for SSU and LSU r-proteins, respectively (Barakat et al., 2001).

The complete sequencing of a number of eukaryote genomes has verified earlier experimental findings that most r-proteins are not single copy, but rather exist as families owing to whole and partial duplication events and retrotranspositions (Barakat et al., 2001; Maere et al., 2005; Planta and Mager, 1998; Wool et al., 1995; Zhang et al., 2002). In vertebrates, generally only a single copy is functional and the remainder exist as processed pseudogenes (Wool et al., 1995; Zhang et al., 2002), however in invertebrates, protists, fungi, and plants more than one paralog can be functional (Barakat et al., 2001; Barthelemy et al., 2007; Berriman et al., 2005; Ivens et al., 2005; Marygold et al., 2007; Planta and Mager, 1998). In Arabidopsis, all r-proteins are encoded from multigene families containing two or more transcriptionally expressed members (Barakat et al., 2001; Hulm et al., 2005; McIntosh and Bonham-Smith, 2005) that can be translated and incorporated into ribosomes (Carroll et al., 2008; Chang et al., 2005; Giavalisco et al., 2005). The functional consequences of ribosome heterogeneity in plants due to r-protein isoforms is unknown. In budding yeast (*S. cerevisiae*), 59 of 79 yeast r-proteins are encoded by two genes (Planta and Mager, 1998) and recent studies indicate that many paralogs exhibit functional specialization (Baudin-Baillieu et al., 1997; Komili et al., 2007). For example, yeast ribosomal proteins RPL7A, RPL12B, RPL22A, and RPS18B have specialized roles in bud-site selection via involvement in the translational regulation of the *ASH1* transcript (Komili et al., 2007).

Single paralog knockouts of any of the four aforementioned r-protein genes result in defective yeast bud-site selection that cannot be complemented by ectopic expression of the corresponding r-protein paralogs (i.e. RPL7B, RPL23A, RPL22B, RPS18A). As growth rate of yeast can be restored by overexpression of paralogous genes (Abovich et al., 1985; Rotenberg et al., 1988), the findings of Komili et al. (2007) highlight the subtle functional differences that may have arisen through evolutionary divergence of paralogs.

Most Arabidopsis r-proteins show a degree of coordinated regulation at both the transcriptional and posttranscriptional level. Transcripts of most r-proteins accumulate to the greatest extent in tissues undergoing active cell division and are least abundant in mitotically-inactive tissues (Bonham-Smith et al., 1992; Hulm et al., 2005; McIntosh and Bonham-Smith, 2005; Van Lijsebettens et al., 1994; Williams and Sussex, 1995). Transcript expression of many r-proteins increases in response to treatment with mitogenic cytokinins (reviewed in Sakakibara et al., 2006), including both paralogs of the *RPL23a* family (McIntosh and Bonham-Smith, 2005) and all three members of the Type I *RPS15a* family (Hulm et al., 2005). Conversely, members of the *RPL23a* and Type I *RPS15a* families are coordinately downregulated by treatment with abscisic acid (Hulm et al., 2005; McIntosh and Bonham-Smith, 2005), which also causes a global decrease in the levels of several other r-protein transcripts (Hoth et al., 2002). Similar global repression of r-protein expression is observed following sucrose starvation of Arabidopsis cell cultures (Contento et al., 2004). A small number of *cis*-acting motifs responsible for the coupled regulation of r-proteins and the cell cycle have been identified in upstream regulatory regions (RRs). These include the *PCNA* site II motif, which is also known as Up1 or Frankiebox ($^{5'}$TGGGCY$^{3'}$, Ditt et al., 2006; Tatematsu et al., 2005; Tremousaygue et al., 2003), the interstitial telomeric repeat, known as a *telo*-box or Up2 ($^{5'}$AAACCCTA$^{3'}$, Li et al., 2006; Tatematsu et al., 2005; Tremousaygue et al., 2003; Tremousaygue et al., 1999), and the *translation elongation factor 1* box or *tef*-box ($^{5'}$ARGGRYAnnnnnGTM$^{3'}$, Curie et al., 1991; Manevski et al., 1999; Regad et al., 1995). The *telo*-box and site II motifs function synergistically and have been identified in the RRs of 153 r-protein genes (Tremousaygue et al., 2003). Although site II motifs, and not *telo*-box motifs, are sufficient to direct reporter gene expression to zones of active cell division (Tremousaygue et al., 2003), the two motifs act synergistically and deletion of either element in the 1 kb RR of Arabidopsis *RPL15B* disrupts the decapitation-induced expression of a GUS reporter gene (Tatematsu et al., 2005).

Plant mRNAs have half-lives comparable to that of other multicellular eukaryotes (Gutierrez et al., 1999), enabling translational regulation via recruitment of transcripts to translationally-active heavy (≥ 5 ribosomes per transcript) or light polysomes (< 5 ribosomes per transcript), or to the translational-inactive RNP fraction. Ribosome loading of r-protein transcripts was shown to be positively correlated with metabolic activity. For example, sucrose starvation (Nicolai et al., 2006), oxygen-deprivation (Branco-Price et al., 2005), and dehydration-stress (Kawaguchi et al., 2004) resulted in the coordinated translational repression of a large number of r-protein transcripts. In all cases the stress had little affect on r-protein transcript abundance, indicating that translational regulation is the predominant mechanism governing plant r-protein expression. Features of plant r-protein transcripts that allow for coordinate induction and repression are unknown. In animals, where primary regulation occurs at the translational level, r-protein transcripts have a common architecture that enables synchronous response to growth and nutrition (Hamilton et al., 2006; Meyuhas, 2000). The key architectural feature is a 5'TOP in the 5' UTR, consisting of a cytosine residue at the extreme 5' terminus, followed by 4–14 consecutive pyrimidines (Amaldi et al., 1995; Meyuhas, 2000). In this system, repressors that are bound to the 5' TOPs during growth dormancy, resulting in their sequestration in the RNP fraction, are displaced following receipt of positive growth stimuli, shifting the 5' TOP mRNAs to the polysomal fraction (Hamilton et al., 2006).

In the present study we investigated the *cis*-elements that transcriptionally, posttranscriptionally and translationally regulate expression of the RPL23a r-protein family of Arabidopsis. Orthologs to RPL23a in prokaryotes and eukaryotes are involved in maturation of LSU rRNA (El-Baradi et al., 1987; El-Baradi et al., 1984), ribosome biogenesis (Schaap et al., 1991), and cotranslational transport of membrane-bound polypeptides (Halic et al., 2004; Menetret et al., 2005; Pool et al., 2002). Both members of this family, *RPL23aA* and *RPL23aB*, are expressed and can be incorporated into ribosomes (Carroll et al., 2008). Our lab has previously shown that *RPL23aA* is the predominant paralog, as its transcript is more abundant in all tissues of wildtype plants (Degenhardt and Bonham-Smith, 2008c; McIntosh and Bonham-Smith, 2005), and its protein is targeted to the nucleolus more efficiently than that of RPL23aB when tagged with fluorescent proteins (Degenhardt and Bonham-Smith, 2008a). Further, knockdown/knockout of *RPL23aB* does not produce an abnormal phenotype, while knockdown of *RPL23aA* results in severe growth defects (Degenhardt and Bonham-Smith, 2008a, b).

Nevertheless, the RPL23a paralogs encode isoforms with 95% amino acid identity, suggesting that they have undergone purifying selection and that both are required. Transcriptional profiling of *RPL23aA* and *RPL23aB* during development and following exposure to abiotic stresses demonstrated that paralogs are generally up/downregulated in tandem, but exhibit some differential responses to specific stimuli (Degenhardt and Bonham-Smith, 2008c; McIntosh and Bonham-Smith, 2005). Here we fused whole or partial upstream RRs of RPL23a paralogs to a reporter gene construct to identify elements responsible for governing expression. We also conducted *in silico* analyses of RPL23a transcript assemblies from Arabidopsis and other eukaryotes to elucidate conserved motifs. We found that paralog expression is coordinated by a common architecture that is shared by many other flowering plants. We also show that specific *cis*-elements function in both induction and repression of RPL23a transcription.

2.2 Material and Methods

2.2.1 Plant material

Arabidopsis thaliana (cv. Columbia-0) was cultivated in soil (Redi-Earth, WR Grace & Co., Ajax, ON, Canada) or on solid media (2.2 g/L MS salts (PhytoTechnology Laboratories, Shawnee Mission, KS, or Sigma-Aldrich, St. Louis, MO), 1.5% sucrose, 0.8% phytagar (Invitrogen, Carlsbad, CA), pH 5.7) and grown with a 23/18 ºC temperature regime and a 16/8 h photoperiod of ~50–80 µmol photons m^{-2} s^{-1}. Seed plated on solid media was sterilized as previously described (Degenhardt and Bonham-Smith, 2008c). For RNA extractions, collected tissue was snap-frozen in $N_{2(l)}$.

2.2.2 Constructs

Molecular cloning was conducted following standard lab procedures (Sambrook et al., 1989). Cloning products were verified by automated sequencing (National Research Council – Plant Biotechnology Institute (NRC–PBI), Saskatoon, SK). *Escherichia coli* strains DH5α and MC1061 were used for all cloning. All RR constructs in pCAMBIA1381z, the *RPL23aA* and *RPL23aB* 2nd introns in pCAMBIA1381z, and a pCAMBIA1381z empty vector control, were used to transform *Agrobacterium tumefaciens* strain pC2760 (Hoekema et al., 1983). PCR primers and cloning details are provided in Appendix A.

2.2.2.1 Deletion constructs in pCAMBIA1381z

Full-length RRs were 1503 and 1061 bp for *RPL23aA* and *RPL23aB*, respectively, and were defined, off an earlier genome annotation, as the genomic region between the start/stop codon of the preceding gene and the respective ATG start codons of *RPL23aA* and *RPL23aB*. Current annotation of the Arabidopsis genome indicates that actual distances are 1313 bp for *RPL23aA* and 1258 bp for *RPL23aB* (Swarbreck et al., 2008). Full-length and truncated RR constructs were cloned upstream of the *β-glucuronidase* (*GUS*) gene in the pCAMBIA1381z (CAMBIA, Canberra, Australia) binary vector. 5' and 3' RR deletions were designed to remove specific motifs identified by the Plant *Cis*-acting Regulatory DNA Elements database (PLACE, Higo et al., 1999; Prestridge, 1991).

2.2.2.2 *RPL23aA* and *RPL23aB* intron-less fragments in pCAMBIA1381z

Complementary synthetic oligonucleotides consisting of the sequence extending from mapped transcription start sites (TSSs) to immediately 5' to ATG start codons were annealed and cloned into pCAMBIA1381z.

2.2.2.3 *RPL23aA* and *RPL23aB* 2nd introns in pCAMBIA1381z

Second introns of *RPL23aA* and *RPL23aB* were inserted upstream of the -60 *Cauliflower Mosaic Virus* (*CaMV*) minimal promoter within a pMECA derivative (Deyholos and Sieburth, 2000; Pylatuik et al., 2003). The second intron–*CaMV* minimal promoter fragments were subsequently cloned into pCAMBIA1381z.

2.2.2.4 Deletion constructs in pGREENII0000

The 5' RR deletion fragments of *RPL23aA* and *RPL23aB* were cloned into a modified pGREEN II0000 vector (Hellens et al., 2000), upstream of an intron-containing green fluorescent protein gene modified for expression in plants, *erGFP7int* (Mankin and Thompson, 2001). A positive control was created by cloning a tandem repeat of the (*CaMV*) *35S* promoter upstream of *erGFP7int*. The empty vector, lacking a promoter, served as a negative control.

2.2.3 Stable Transgenics

Transformation of Arabidopsis was carried out using a modified floral dip protocol (Clough and Bent, 1998). Selection of T_1 and T_2 plants was done by plating seed on solid media containing appropriate antibiotics and herbicides. Surviving T_2 plants were used for GUS assays

and tissue collections. Details of the transformation and selection procedures are available in Appendix A.

2.2.4 RNA extraction and RT-PCR

The methods used for total RNA extraction, quantitation of RNA and DNase I treatment were previously described (McIntosh and Bonham-Smith, 2005), with the modification that a Plant Total RNA Extraction Kit (Real Biotech Corporation, ChungHo, Taiwan) was also used. For examination of *RPL23A* and *RPL23aB* leader intron splicing, RNA extracted from 10–17 day-old wildtype and T_2 seedlings expressing the *RPL23aA* and *RPL23aB* 5'FR–GUS, 5'Δ4–GUS, 5'Δ5–GUS, 5'Δ6–GUS, 3'Δ2–GUS and 3'Δ5–GUS constructs (minimum of three lines per genotype), was subjected to two-step RT-PCR. The identity of the PCR product was determined via automated sequencing (NRC–PBI). The same method was used for identification of a transcript resulting from a reverse-oriented 35S *CaMV* promoter in T_2 seedlings carrying the pCAMBIA1381z empty vector control. Details of RT-PCR are available in Appendix A.

2.2.5 Transcription start site determination

Total RNA for 5' RACE (5' rapid amplification of cDNA ends) was isolated from ten day old seedlings, and bud and leaf tissues from 5 week-old plants. Poly(A)+ RNA was isolated from DNase-treated total RNA samples using the PolyAT Tract mRNA Isolation System (Promega, Madison, WI) according to manufacturer's instructions. Both total and poly(A)+ RNA were used for TSS mapping, yielding identical results (data not shown). To verify mapped TSSs in mature tissues, RT-PCR was conducted on total RNA from root, stem, leaf, bract, flower, bud, elongating carpel, and mature green siliques tissues using the OneStep RT-PCR kit (Qiagen) and previously described methods (McIntosh and Bonham-Smith, 2005). Details of 5' RACE are available in Appendix A.

2.2.6 Transient expression in Arabidopsis protoplasts

Arabidopsis protoplasts were prepared from 15–21 day-old wildtype seedlings, grown on solid media (4.4 g/L MS salts (PhytoTechnology Laboratories), 1.5% sucrose, 0.6% phytagar (Invitrogen), pH 5.7) under a 23/18 ºC temperature regime and a 12/12 h photoperiod of ~120 μmol photons m^{-2} s^{-1}. Isolated protoplasts were transformed via electroporation (350 V cm^{-1} and 200 μF) with 20 μg pGI0029 plasmid DNA (transformation control, Hellens et al., 2000) and 20 μg pGII000 plasmids containing *erGFP7int* reporter gene cassettes using a Gene Pulser II with

attached Capacitance Extender (Bio-Rad, Mississauga, ON, Canada). Electroporated protoplasts were allowed to rest for 20–30 min, diluted to 2 mL with culture media (0.4 M mannitol, 15 mM MgCl, 4 mM MES and 0.442% MS medium, pH 5.7) and placed in 1 mL aliquots into a 24-well tissue culture plate (BD Biosciences, San Jose, CA). Plates were incubated for 5 h in the dark at 20 °C, after which protoplasts were pelleted at 100 *g* for 2 min and flash frozen in $N_{2(l)}$. The entire experiment was repeated a minimum of four times. Details of protoplast isolation are available in Appendix A.

2.2.7 Quantitative RT-PCR and statistical analyses

The real-time quantitative RT-PCR (qRT-PCR) protocol was essentially as previously described (Degenhardt and Bonham-Smith). RNA extractions from protoplasts used the Plant Total RNA Extraction Kit (Real Biotech Corporation). All real-time reactions were performed in triplicate and a single amplicon (*erGFP7int* or *nptII*) was produced per reaction. A minimum of two technical replications (RNA extraction, DNase treatment, first strand synthesis, qRT-PCR) were conducted for each biological replicate. Optical data collection and Ct determination were done using the iQ5 Optical System software (Bio-Rad). Primer details are available in Appendix A.

Statistical analysis was conducted using the mixed model procedure of the SAS Statistical Analysis software (SAS Institute, Cary, NC). Construct effects were considered fixed and replicates were considered as a random effect. The test statistic adjustment of Kenward and Roger (1997) was used to correct for small sample size. Pairwise comparisons of least-squares means were considered significant when $P \leq 0.05$.

2.2.8 GUS Assays

GUS activity of 16–19 day old wild type and T_2 seedlings was determined as previously described (Sieburth and Meyerowitz, 1997). The same procedure was used to assay mature excised tissues from six to nine ~7–10 week-old wildtype plants, and T_2 plants carrying full-length or 5'Δ RRs (five independently transformed lines per genotype). Expression of GUS was evaluated qualitatively under a stereomicroscope (Wild M3Z, Leica Microsystems, Wetzlar, Germany).

2.2.9 Bioinformatics and alignments

Alignments of *RPL23a* paralog regulatory regions and introns were conducted using Clustal W2 (Larkin et al., 2007) with the IUB scoring matrix. To identify orthologous *RPL23a* transcript assemblies from other species, the full-length cDNAs (fl-cDNAs) of RPL23aA/B were used as queries to search the TIGR databases (Childs et al., 2007; Lee et al., 2005). Assemblies from each species were manually aligned with orthologs using Clustal W2 (Labarga et al., 2007; Larkin et al., 2007) to identify duplicates, possible paralogs and expressed pseudogenes. Expressed sequence tags (ESTs) used to build assemblies were analyzed and, based on the consensus overlap, used to trim assemblies at 5' and 3' ends. For comparison of Arabidopsis *RPL23a* paralogs against other Arabidopsis r-protein genes, fl-cDNAs for 217–220 Arabidopsis r-protein genes with annotated UTRs (min. 8 bp in length) were obtained from RIKEN and TAIR databases (Rhee et al., 2003; Seki et al., 2002). The 5' and 3' UTRs from unique, trimmed assemblies or from fl-cDNAs were analyzed (direct strand only) for conserved motifs using MEME (Bailey et al., 2006), and multiple sequence motif alignments were made using WebLogo 3 (Crooks et al., 2004). RNA secondary structure free energy calculations for 5' and 3' UTRs were made using DINAMelt (Markham and Zuker, 2005) with predictions made at a growth temperature of 22 °C (Kawaguchi and Bailey-Serres, 2005). Basic DNA statistics (length, base composition) were compiled from MEME output.

2.3 Results

2.3.1 The *RPL23a* paralogs have leader introns and multiple transcript start sites

Primer extension (5' RACE) analysis of total and poly-A enriched RNA from whole seedlings, and bud and leaf tissues from 5 week-old plants, identified multiple TSSs for *RPL23aA* and *RPL23aB* (Figure 2.1), but no tissue or age-specific differences. By comparing RACE-mapped TSSs to Arabidopsis fl-cDNAs (Seki et al., 2002; Swarbreck et al., 2008) and EST transcript assemblies (Childs et al., 2007), a predominant TSS, fitting the consensus for promoters of dicots containing TATA-boxes ($^{-2}$YBAN^{+2}, Shahmuradov et al., 2003), was identified for each paralog (Figure 2.1). 5' UTRs are 54 and 55–56 nt for *RPL23aA* and *RPL23aB*, respectively.

A leader intron was also identified in both *RPL23aA* and *RPL23aB*; canonical splice sites ($^{5'}$GU–AG$^{3'}$) border the 107 nt leader intron of *RPL23aA*, while for *RPL23aB* canonical splice sites border a 214 nt leader intron, and non-canonical splice sites ($^{5'}$GU–UC$^{3'}$) border a 215 nt

Figure 2.1 Alignment of upstream regulatory regions and transcription start sites for *RPL23aA* and *RPL23aB*. The region from the ATG start codons (highlighted gray) to 350 bp upstream of predominant TSSs was aligned using Clustal W2 (Larkin et al., 2007). Conserved bases are indicated by asterisks. RACE-mapped TSSs are indicated by black arrows, while the blue arrow shows the consensus TSS for *RPL23aA* based on annotated fl-cDNAs and transcript assemblies (Childs et al., 2007; Lee et al., 2005). Exons initiating from predominant TSSs are highlighted in yellow, and leader introns are indicated by red text. Alternate splice sites for *RPL23aB*, detected in only a single RACE clone isolated from seedlings, are underlined. Forward primers used for RT-PCR to confirm TSSs and splice sites in mature tissues are indicated by green text (L23aA–RTintF) for *RPL23aA* and by blue and green text (L23aB–RTintF1 and L23aB–RTintF2, respectively) for *RPL23aB*. Putative TATA-boxes are highlighted green. Two known regulatory elements, site II motifs and *telo*-boxes, are highlighted red and blue, respectively. An additional *telo*-box is located from positions +5 to +12 of *RPL23aB* exon 1. An Arabidopsis IME element, ($^{5'}$TYnGATYTGT/AT/G$^{3'}$, core sequence underlined, Rose et al., 2008) present in the leader intron of *RPL23aB*, is highlighted brown. Numbering is relative to the +1 TSS and assumes splicing of leader introns. Percent identity is for the entire 511 and 620 bp RRs of *RPL23aA* and *RPL23aB*, respectively.

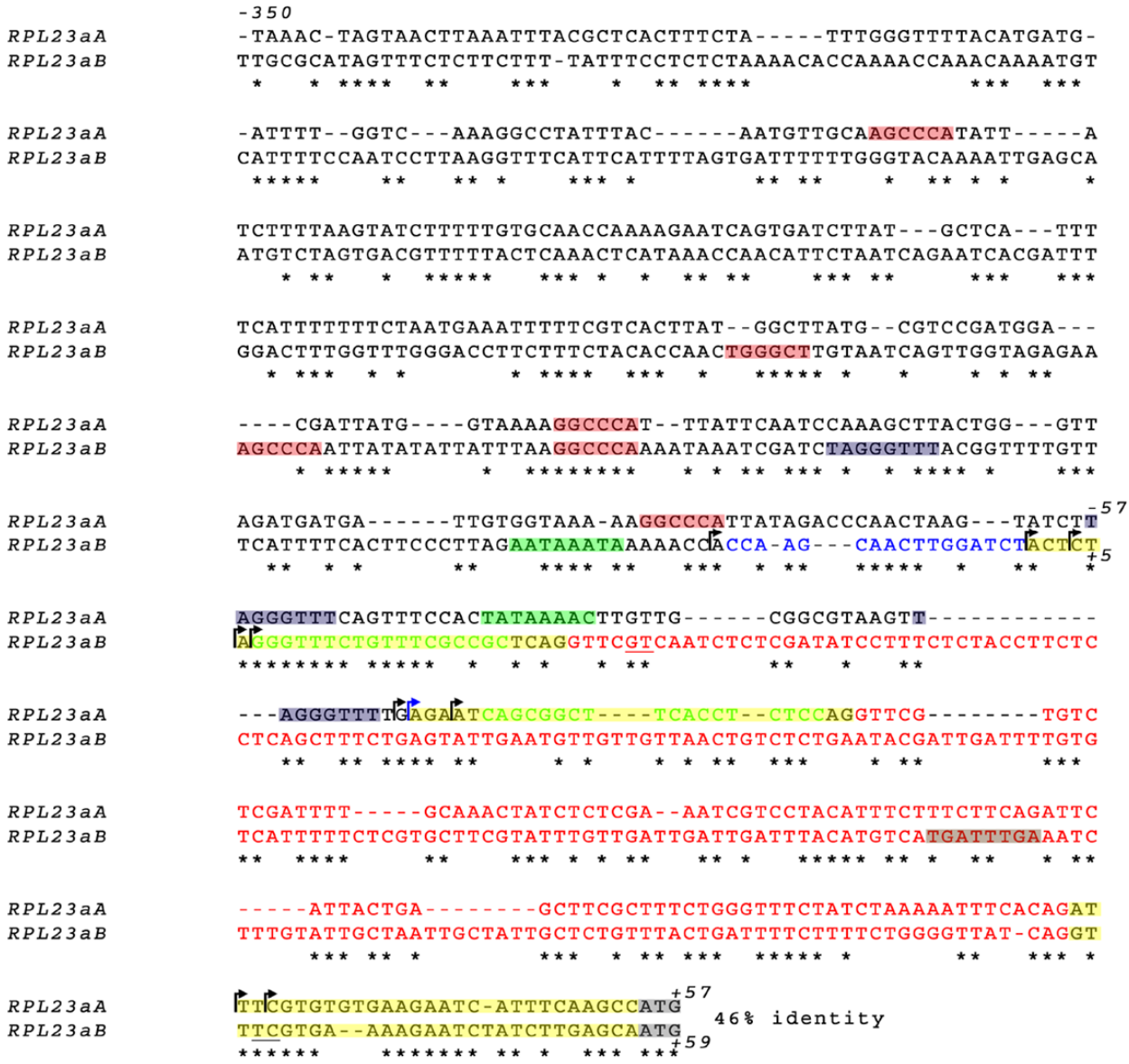
-350
RPL23aA -TAAAC-TAGTAACTTAAATTTACGCTCACTTTCTA-----TTTGGGTTTTACATGATG-
RPL23aB TTGCGCATAGTTTCTCTTCTTT-TATTTCCTCTCTAAAACACCAAAACCAAACAAAATGT
RPL23aA -ATTTT--GGTC---AAAGGCCTATTTAC------AATGTTGCAAGCCCATATT-----A
RPL23aB CATTTTCCAATCCTTAAGGTTTCATTCATTTTAGTGATTTTTTGGGTACAAAATTGAGCA
RPL23aA TCTTTTAAGTATCTTTTTGTGCAACCAAAAGAATCAGTGATCTTAT---GCTCA---TTT
RPL23aB ATGTCTAGTGACGTTTTTACTCAAACTCATAAACCAACATTCTAATCAGAATCACGATTT
RPL23aA TCATTTTTTTCTAATGAAATTTTTCGTCACTTAT--GGCTTATG--CGTCCGATGGA---
RPL23aB GGACTTTGGTTTGGGACCTTCTTTCTACACCAACTGGGCTTGTAATCAGTTGGTAGAGAA
RPL23aA ----CGATTATG----GTAAAAGGCCCAT--TTATTCAATCCAAAGCTTACTGG---GTT
RPL23aB AGCCCAATTATATATTATTTAAGGCCCAAAATAAATCGATCTAGGGTTTACGGTTTTGTT
RPL23aA AGATGATGA------TTGTGGTAAA-AAGGCCCATTATAGACCCAACTAAG---TATCTT
RPL23aB TCATTTTCACTTCCCTTAGAATAAATAAAAACGACCA-AG---CAACTTGGATCTACTCT
RPL23aA AGGGTTTCAGTTTCCACTATAAAACTTGTTG------CGGCGTAAGTT----------
RPL23aB AGGGTTTCTGTTTCGCCGCTCAGGTTCGTCAATCTCTCGATATCCTTTCTCTACCTTCTC
RPL23aA ---AGGGTTTTGAGAATCAGCGGCT----TCACCT--CTCCAGGTTCG--------TGTC
RPL23aB CTCAGCTTTCTGAGTATTGAATGTTGTTGTTAACTGTCTCTGAATACGATTGATTTTGTG
RPL23aA TCGATTTT-----GCAAACTATCTCTCGA--AATCGTCCTACATTTCTTTCTTCAGATTC
RPL23aB TCATTTTTCTCGTGCTTCGTATTTGTTGATTGATTGATTTACATGTCATGATTTGAAATC
RPL23aA -----ATTACTGA--------GCTTCGCTTTCTGGGTTTCTATCTAAAAATTTCACAGAT
RPL23aB TTTGTATTGCTAATTGCTATTGCTCTGTTTACTGATTTTCTTTTCTGGGGTTAT-CAGGT
RPL23aA TTCGTGTGTGAAGAATC-ATTTCAAGCCATG
RPL23aB TTCGTGA--AAAGAATCTATCTTGAGCAATG
46% identity

leader intron (Figure 2.1). The latter *RPL23aB* splice variant was only identified in seedling tissue and comparison to fl-cDNAs and ESTs confirms that it is a rarely used splice variant. Another leader intron splice variant for *RPL23aB* (*At3G55280.2*) is also annotated in the TAIR database. It uses the downstream GU splice donor and the canonical AG splice acceptor, resulting in a 59 nt 5' UTR. This splice variant was not detected in our primer extension analyses. A set of direct repeats, $^{5'}$UCAGGUU(U)CGU$^{3'}$, differing only by the presence of an extra U in the repeat surrounding the 3' splice site, surrounds the 5' and 3' splice sites of the *RPL23aB* leader intron. Similar but more degenerate direct repeats, $^{5'}$CAG(AU)UUCGUGU$^{3'}$ and $^{5'}$CAGGUUCGUGU$^{3'}$, surround the 5' and 3' splice sites, respectively, of the *RPL23aA* leader intron.

TSS and splice site selection was assessed in tissues of mature plants (root, stem, leaf, bract, flower, bud, elongating carpel, and mature green silique) using RT-PCR and primers designed immediately downstream of RACE mapped TSSs. Results confirmed the predominant TSSs and splice sites previously identified from seedlings and 5 week-old bud and leaf tissues (Figure 2.1). The *RPL23aB* transcript with the longer 5' UTR was not detected in any tissue (Figure 2.1, L23aB–RTintF1), whereas a single product with canonical leader intron splice sites was detected in all tissues using primers designed 3' to the shorter 5' UTR TSS (Figure 2.1, L23aB–RTintF2).

2.3.2 Minimum RRs required to direct GUS activity in seedlings differ between paralogs

The reverse-oriented, enhanced double *CaMV 35S* promoter, located 230 bp upstream of the multiple cloning site (MCS) in pCAMBIA1381z vector, reportedly directs a basal level of *GUS* expression (CAMBIA, http://www.cambia.org/daisy/cambia/materials/vectors/585.html). To determine if this expression would interfere with results, T_2 transgenic Arabidopsis seedlings transformed with the pCAMBIA1381z empty vector were assayed for assayed for transgene transcripts and GUS activity. Although a *GUS* transcript was detected in empty vector transgenic seedlings (data not shown), 14 of 18 independently transformed lines showed no GUS staining at all (Figure 2.3a), and only two showed consistent staining, presumably resulting from positional effects of the T-DNA insertion (data not shown). Therefore, some degree of transcriptional interference might be present using the pCAMBIA1381z vector, especially for small deletion constructs lacking sufficient insulation from the reverse oriented *35S* promoter,

but translation of *GUS* transcripts in sufficient quantities to confer GUS staining must require additional elements within RRs.

Full-length RRs (1.503 and 1.061 kb for *RPL23aA* and *RPL23aB*, respectively) or sequentially truncated fragments of RRs (Figure 2.2a) were analyzed for their ability to direct *GUS* reporter gene expression in transgenic plants. Between 7–14 independently transformed T_2 lines per RR construct were stained for GUS activity qualitatively using a three point scale (Figure 2.3; ++, +, -). The exception was *RPL23aB* 5'Δ1–GUS, where only a single line was obtained due to poor transformation efficiency. Wildtype seedlings showed no GUS staining (Figure 2.3a). For *RPL23aA* ΔRR seedlings showed consistent ++ staining down to 5'Δ5–GUS, which only stained faintly in meristematic regions, and 3'Δ5–GUS, which showed no staining (Figure 2.3). These results indicate that a 52 bp region of the *RPL23aA* RR, located between −57 to −6 relative to the +1 predominant TSS (Figure 2.1), is required for GUS expression in seedlings. However, staining was completely abolished in as 5'Δ6–GUS lines, therefore additional required elements must be present between +17 to +54 of exon 2, or within the leader intron (Figure 2.2a and 2.3a). All *RPL23aB* ΔRR lines showed GUS staining, indicating that multiple redundant elements control GUS expression in this paralog (Figure 2.3). Specifically, elements must be present between +28 to +56, including the latter 26 bp of the leader intron, and from between −293 to −33. The reduced staining in *RPL23aB* 3'Δ2–GUS seedlings, together with the inconsistent staining in 5'Δ5–GUS seedlings (2 of 9 lines 5'Δ5–GUS lines showed no staining while an additional 2 of 9 lines showed reduced GUS staining in seedlings, data not shown), suggest the presence of a negative regulatory element(s) between +95 to +206 of the leader intron.

2.3.3 RPL23a paralogs have different minimum RRs directing tissue-specific GUS expression in adult plants

Transgenics (T_2) carrying the pCAMBIA1381z empty vector control showed no GUS staining in any adult tissues (J. Hulm and P. Bonham-Smith, personal communication), and no GUS staining was observed in any adult tissue from wildtype plants (Table 2.1). Staining patterns in plant tissues carrying *RPL23aA* and *RPL23aB* whole and ΔRRs revealed a complex network of positive and negative regulatory elements controlling tissue-specific GUS expression (Table 2.1 and Figure 2.4). In general, full-length RRs from *RPL23aA* and *RPL23aB* conferred GUS expression in mitotically and developmentally active tissues such as root (especially in root vasculature and lateral root primordia), leaf margins and vasculature, developing tissues of the

	Tissue																									
RPL23aA					Unopened bud						0 DPA bud						Open flower						<6	6–10	>10	
RR							♂		♀				♂		♀				♂		♀		mm	mm	mm	Mat.
construct	Leaf	Bract	Stem	Root	Se	P	A	F	St	O	Se	P	A	F	St	O	Se	P	A	F	St	O	sil.	sil.	sil.	sil.
Wildtype	--	--	--	--	--	--	--	--	--	--	--	--	--	--	--	--	--	--	--	--	--	--	--	--	--	--
A5'FR	--	--	cut	++	--	+	++	+	++	++	--	+	++	+	+	++	--	--	++	--	--	++	+	+	+	--
A5'Δ1	++	+	cut	++	++	++	++	+	++	++	--	+	++	++	++	++	--	--	++	++	++	++	++	++	++	+
A5'Δ2	++	+	cut	++	++	+	++	+	++	++	++	+	++	++	++	++	+	+	++	++	++	++	++	++	++	+
A5'Δ3	+	+	cut	++	++	+	++	++	++	++	++	+	++	+	++	+	+	+	pol	++	++	+	++	++	+	++
A5'Δ4	+	+	cut	++	++	++	++	+	+	+	+	+	++	+	++	++	+	+	++	+	++	++	+	+	+	+
A5'Δ5	--	--	cut	+	--	--	+	--	+	+	--	+	+	--	+	+	--	--	pol	--	--	+	+	+	--	+
A5'Δ6	--	--	--	-	--	--	--	--	--	--	--	--	--	-	--	--	--	--	--	--	--	--	--	--	--	--
RPL23aB RR construct																										
B5'FR	--	+	cut	++	+	+	++	+	++	++	+	+	++	++	++	++	+	+	++	++	++	++	++	++	+	+
B5'Δ1	+	+	cut	++	++	+	++	++	++	++	++	++	++	++	++	++	+	+	++	++	++	++	++	++	n/a	++
B5'Δ2	+	+	cut	++	++	+	++	++	++	++	+	+	++	+	+	++	+	+	++	++	++	++	++	++	++	++
B5'Δ3	--	+	cut	++	++	+	++	+	++	++	++	+	+	++	+	++	+	+	++	++	++	++	++	++	+	+
B5'Δ4	--	cut	cut	++	+	+	--	+	+	++	+	+	--	+	+	+	+	+	--	+	+	+	+	+	+	+
B5'Δ5	+	+	+	++	+	+	--	++	+	++	+	+	--	+	+	+	+	+	--	+	+	+	++	++	+	+
B5'Δ6	--	+	+	++	++	++	--	+	+	++	+	+	--	+	+	+	+	+	--	+	+	+	++	++	+	+

Table 2.1 GUS activity in tissues of 5–7 week-old T_2 transgenics carrying full-length or 5' truncated regulatory regions of *RPL23aA* and *RPL23aB*. Results are representative of five independently transformed lines, except for *RPL23aB* 5'Δ1–GUS, where only a single line was available. GUS activity was evaluated qualitatively on a four point rating scale: ++, consistent dark staining throughout tissue; +, weak–moderate staining throughout some, but not all, of specified tissue; +/-, inconsistent and faint staining of tissue; --, no staining. Staining at cut/wound sites, or pollen only is indicated by 'cut' and 'pol', respectively. Cells with equivalent shading indicate comparisons discussed in text. Abbreviations: ♂, stamens; ♀, carpels; sil., silique; mat. sil., mature/drying silique; se, sepal; p, petal; a, anther; f, filament; st, stigma; o, ovary; n/a, tissue not available.

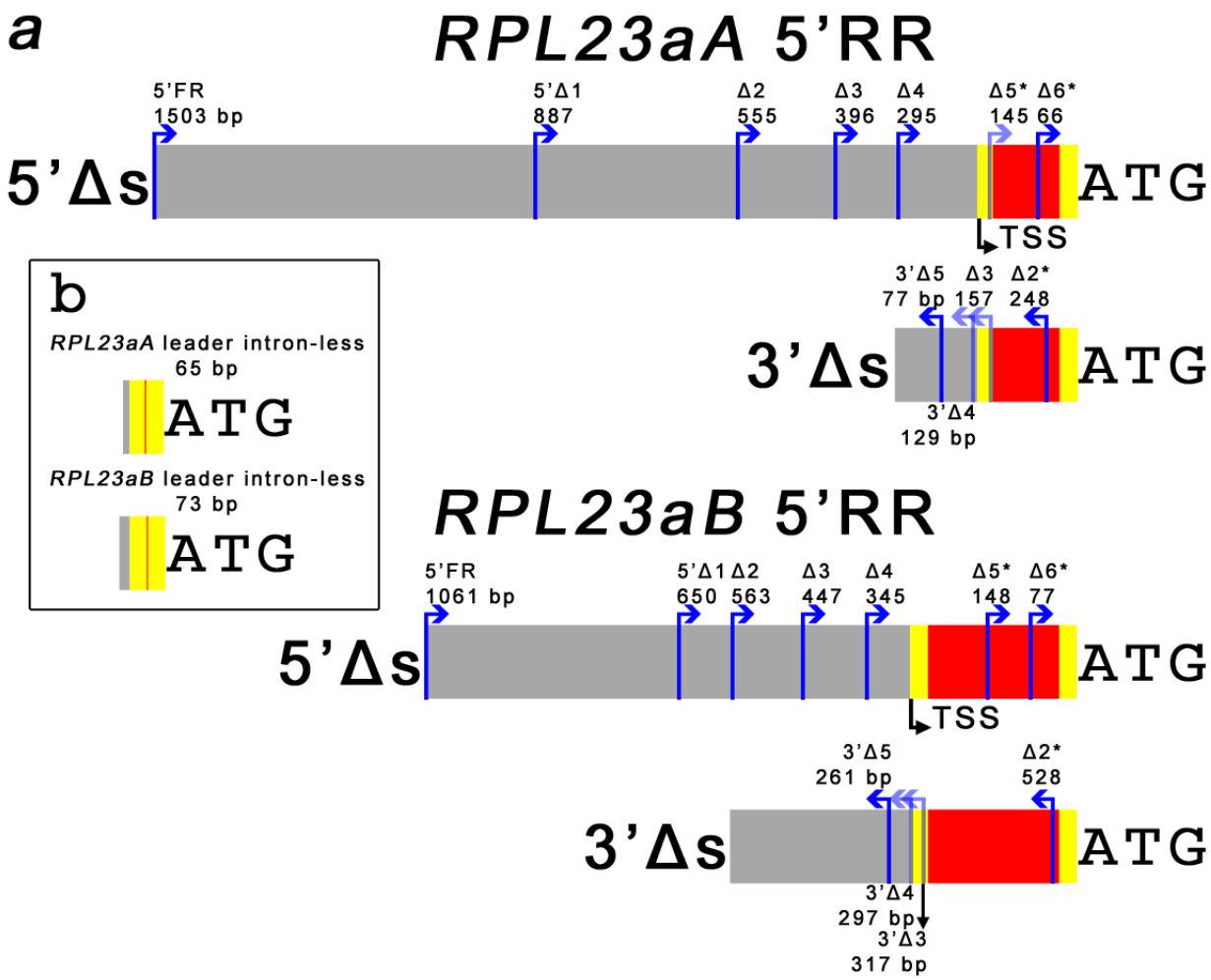

Figure 2.2 Upstream regulatory region deletion constructs of *RPL23aA* and *RPL23aB* used to drive *GUS* expression in Arabidopsis transgenics. **a** 5' and 3' RR full-length and deletion constructs of *RPL23aA* and *RPL23aB*. All 5' deletions terminated immediately 5' to the ATG start codon and initiated at the positions indicated by blue arrows. 3' deletions initiated at the 5'Δ4 or 5'Δ2 position for *RPL23aA* and *RPL23aB*, respectively, and terminated at the positions indicated by blue arrows. Asterisks (*) indicate deletions that removed single splice junctions of leader introns, or in the case of the *RPL23aA* 5'Δ5 construct, potentially interfered with leader intron splicing due to the length of upstream spliceosome recognition sequence. **b** (inset) *RPL23aA* and *RPL23aB* leader intron-less constructs. Gray bars indicate RR upstream of exons, which are denoted by yellow bars. The TSSs are indicated by arrows below bars. Red bars indicate leader introns (**a**), while a red line separates exon one and exon two in the leader intron-less constructs (**b**).

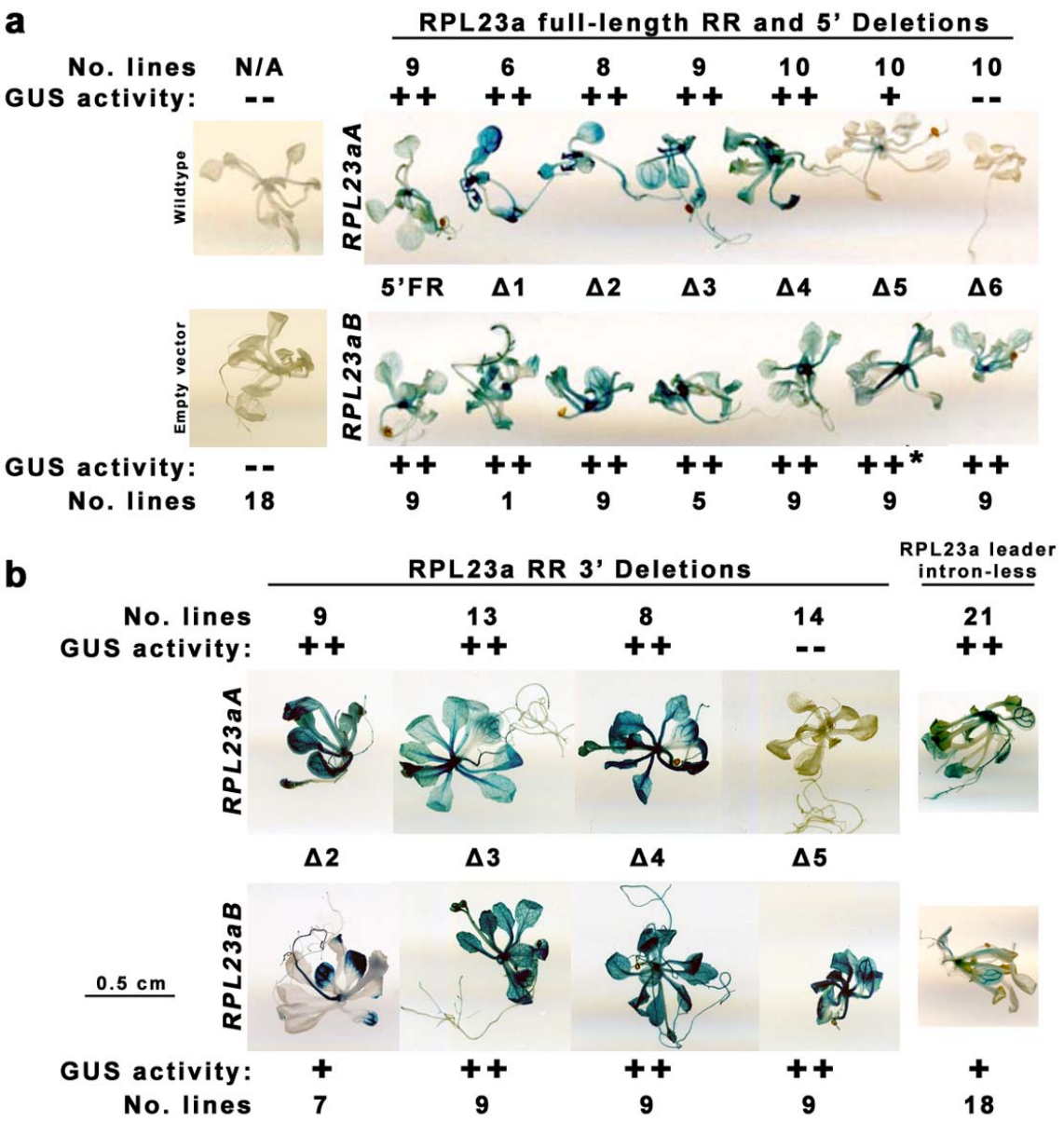

Figure 2.3 GUS activity in 16–19 day-old T_2 transgenic seedlings carrying full-length, 5' or 3' truncated regulatory regions of *RPL23aA* and *RPL23aB*. **a** Staining pattern in RR 5' deletions, the empty vector control and wildtype (non-transformed) plants. **b** Staining pattern in RR 3' deletions and the leader intron-less constructs. Images are representative of the pattern observed in the majority of independently transformed lines (total number of lines indicated by 'No. lines'). GUS activity was evaluated qualitatively on a four point rating scale: ++, consistent dark staining throughout tissues; +, consistent staining throughout most, but not all tissues; +/-, inconsistent and faint staining of tissues; --, no staining. An asterisk indicates that a minor proportion of seedlings did not show this staining pattern. Scale bar applies to all images.

androecium and gynoecium, and elongating carpels (Figure 2.4). GUS activity was also seen at excision sites (i.e. cut sites of stems, leaves and bracts) and mechanically damaged regions (Table 2.1 and Figure 2.4). Conversely, full-length RRs of *RPL23a* paralogs conferred little to no GUS expression in mature tissues, such as leaves, bracts, sepals and petals of open flowers, or drying siliques (Table 2.1, Figure 2.4).

Despite the overall similarity in GUS activity conferred seen from both *RPL23a* full-length RRs, there were some notable differences between genes. While *RPL23aB* 5'FR–GUS plants showed some GUS activity in all floral tissues, *RPL23aA* 5'FR–GUS plants consistently lacked GUS expression in sepals, and showed weak expression in petals (Table 2.1). Likewise, no GUS expression was seen in leaves or bracts from *RPL23aA* 5'FR–GUS plants, while *RPL23aB* 5'FR–GUS plants showed staining at the bract margins. Staining of carpels in *RPL23aB* 5'FR–GUS plants was also more persistent relative to *RPL23aA* 5'FR–GUS plants, continuing after carpels elongated into siliques following anthesis (Table 2.1). Further, in open flowers of *RPL23aA* 5'FR–GUS plants, staining was retained only in sporogenous tissues and was lost in stamen filaments and connective tissue of the anthers, while in *RPL23aB* 5'FR–GUS staining was maintained in both sporogenous and non-sporogenous stamenal tissues (Table 2.1, Figure 2.4).

Adult tissue staining in transgenics carrying the *RPL23aA* RR 5' deletion constructs followed the general patterns observed in seedlings. Constructs that lacked the core promoter (i.e. TATA-box, initiator elements), 5'Δ5–GUS and 5'Δ6–GUS, were largely unable to confer GUS expression. It would appear that 5'Δ5–GUS contains only sufficient positive regulatory elements to confer expression in the most mitotically active tissues, such as roots, young anthers and stamens, ovaries, and developing seed (Table 2.1, Figure 2.4). The exception was the faint staining of mature siliques in 5'Δ5–GUS transgenics, but this was reduced to terminal sites corresponding to the floral abscission zone and former stigmatic regions, and to seed pods. As 5'Δ4–GUS transgenics showed tissue staining fairly consistent with plants carrying the 5'FR–GUS, it would seem that the region from −134 (relative to the TSS) to the ATG start codon contains most of the elements required for tissue-specific expression of *RPL23aA*. Additional positive elements necessary for full-expression in carpels of unopened buds, and additional negative regulatory elements that inhibit expression in sepals, petals, stamen filaments and stigmatic tissue, are found upstream of the −134 position (Table 2.1).

Figure 2.4 Representative images of GUS activity in tissues of 5–7 week-old T_2 transgenics carrying full-length or 5' truncated regulatory regions of *RPL23aA* and *RPL23aB*. The qualitative rankings (++, +, +/-, --, cut) given to tissues with depicted amounts of GUS staining, summarized in Table 2.1, are adjacent to images. For buds and flowers, the top four panels show a group of unopened buds, zero days post-anthesis buds and open flowers (left to right) from representative wildtype or transgenic plants. Abbreviations: rp, root primordial; se, sepal; pe, petal; sta, stamen; c, carpel; r, receptacle; sp, stigmatic papillae; sty, style; rep, replum; ov, ovules; ct, connective tissue; m, microsporangia; v, vascular strand; p, pollen, sti, stigma; az, floral abscission zone; f, funiculus.

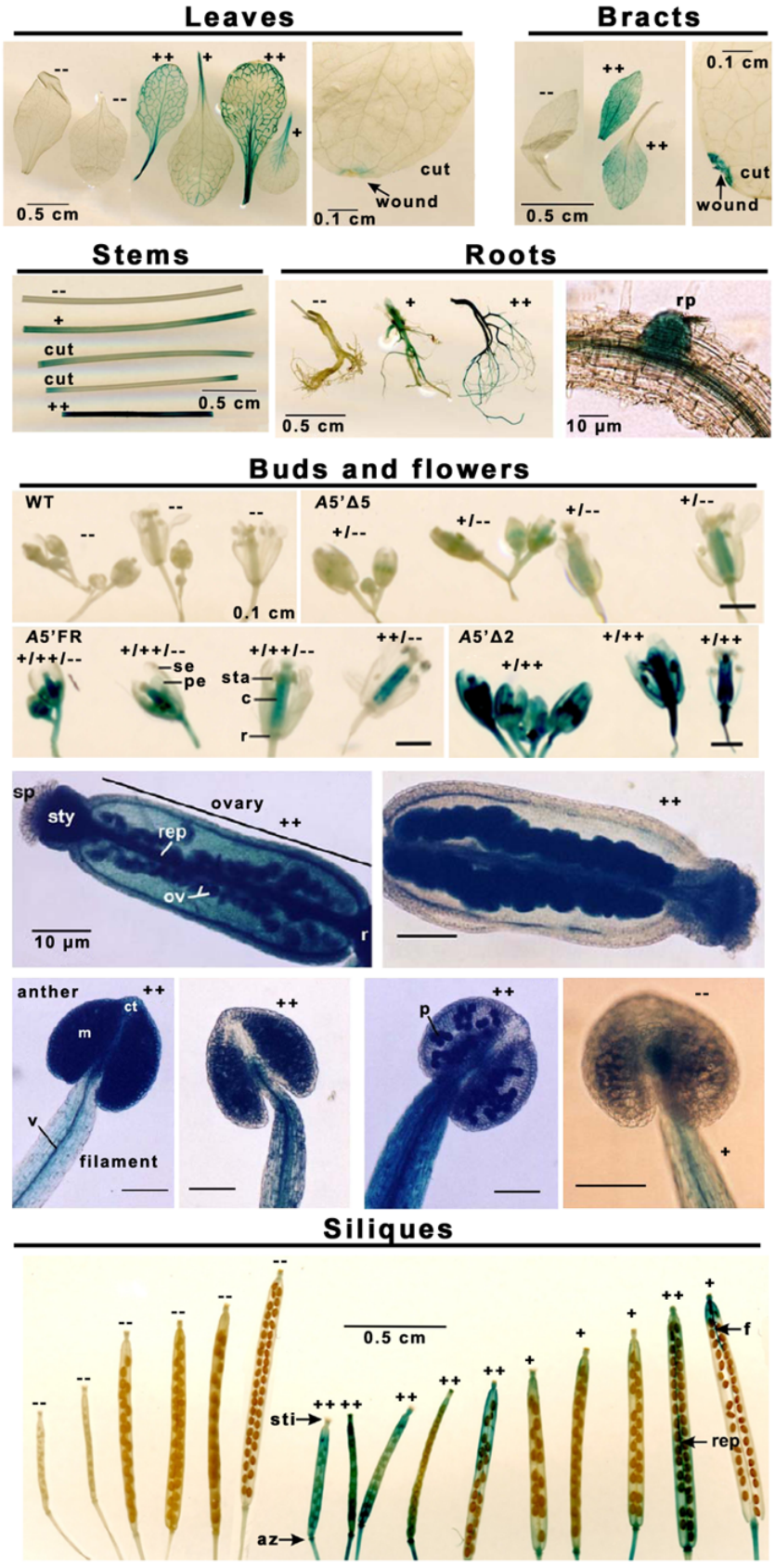
Leaves
Bracts
Stems
Roots
Buds and flowers
Siliques
WT
A5'Δ5
A5'FR
A5'Δ2
anther
filament
ovary
sty
rep
ov
sp
ct
m
v
p
sti
az
f
cut
wound
rp
se
pe
sta
c
r
0.5 cm
0.1 cm
10 µm

In agreement with results from seedlings, the *RPL23aB* 5' RR contains multiple elements for directing GUS activity in adult tissues. Plants carrying the *RPL23aB* 5'Δ6–GUS construct (+28 to +56 of exon 2 and the last 26 bp of the leader intron), possessed all elements necessary for directing GUS expression in all tissues except leaves and anthers (Table 2.1). Based on the reduced expression in reproductive tissues (stamens, carpels) of *RPL23aB* 5'Δ4–GUS plants, additional elements for positive regulation in reproductive organs must be present from −177 to −76 relative to the TSS, including an element essential for directing expression in anthers (Table 2.1 and Figure 2.4). However, despite the loss of staining in sporogenous tissues of anthers in RR 5' deletions lacking the −177 to −76 region, staining persisted in stamen filaments and anther connective tissue even in *RPL23aB* 5'Δ6–GUS plants (Table 2.1 and Figure 2.4). The −177 to −76 region may also contain a negative regulatory element for directing expression in receptacles, as plants carrying constructs without this region showed staining in receptacles of closed buds and flowers, while GUS staining in the receptacles of *RPL23aB* 5'FR–GUS to 5'Δ3–GUS plants did not appear strongly as a discrete region of activity until flowers were open and carpels began to elongate (data not shown).

2.3.4 RR sequence context is critical for correct splicing of leader introns

Six of the RR deletion constructs interfere, or due to length of upstream spliceosome recognition sequence, potentially interfere with splice sites for leader introns present in *RPL23aA* and *RPL23aB* primary transcripts (Figure 2.2a, see asterisks). To determine whether whole or partially truncated leader introns are spliced from plants carrying *RPL23aA* and *RPL23aB* 5'FR–GUS, 5'Δ4–GUS, 5'Δ5–GUS, 5'Δ6–GUS, 3'Δ2–GUS and 3'Δ5–GUS constructs (minimum of three lines per genotype), RT-PCR was conducted using a reverse primer specific to the *GUS* second exon and a forward primer specific to the deletion construct being analyzed (see Appendix A).

Transgenics carrying *RPL23aA* 5'FR–GUS and 5'Δ4–GUS constructs produced a single population of transcripts with *RPL23aA* leader introns spliced at canonical GU–AG splice sites (Figure 2.5). Conversely, sequence analysis determined that two different products were amplified from the *RPL23aA* 5'Δ5–GUS plants, which contains only 9 bp of exon 1 sequence (+17 to +25) upstream of canonical leader intron splice sites. Although both RT products show splicing of the leader intron, they each use different non-canonical splice sites, UU–AU (5'Δ5 RT #1, Figure 2.5) and CU–GU (5'Δ5 RT #2; Figure 2.5). The *RPL23aA* 5'Δ6–GUS transcript

Figure 2.5 Analysis of *RPL23aA* and *RPL23aB* leader intron splicing in Arabidopsis transgenics carrying whole and partial upstream regulatory regions. Full-length constructs showing the 5' or 3' ends of RR deletions are shown with symbols as in Figure 2.2, with the additions of the following features: a 195 bp intragenic spacer between the MCS and the *GUS* gene (light gray bar), the 15 bp *GUS* first exon (short green bar), the 184 bp *CATALASE* intron separating *GUS* exons (pink) and the 161 bp fragment of the *GUS* second exon (long green bar) terminating with the reverse primer used for RT-PCR (pC–GUS–R2). RT-PCR amplification products obtained for each genotype are shown below full-length constructs. Primers used for PCR amplification are indicated by blue arrows. Spliced regions are indicated by colored lines and 5' and 3' splice sites are located at the left and right ends of lines, respectively. Black lines indicate portions of the full-length RRs not present in specific 3' deletions.

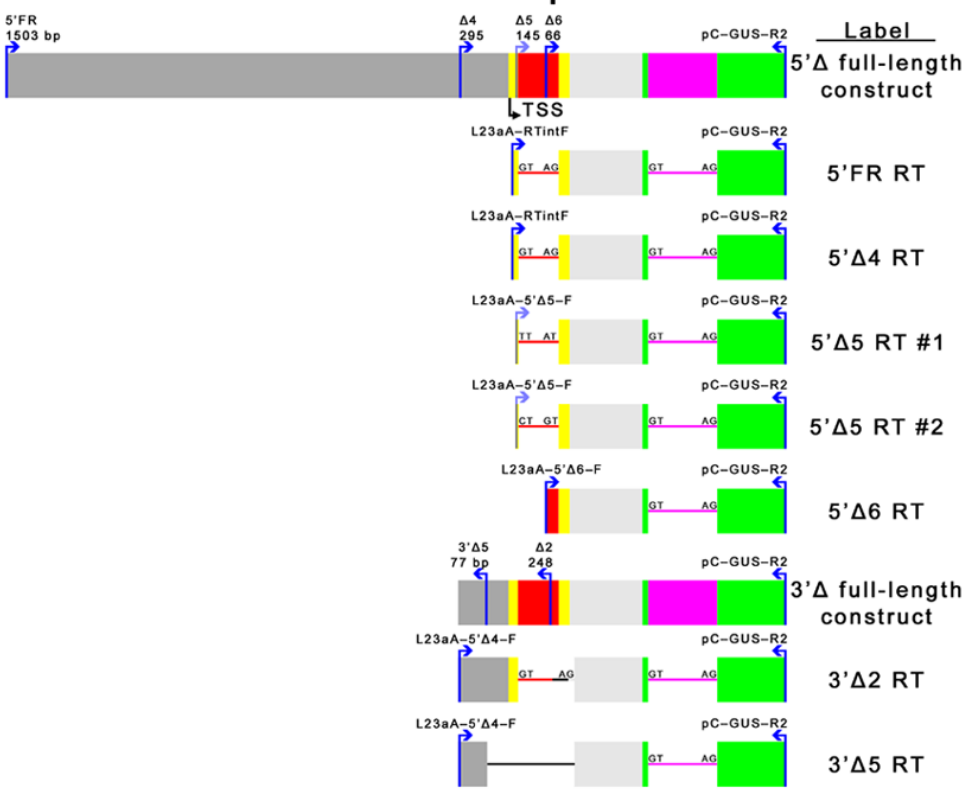
RPL23aA Δ RT products
5'FR
1503 bp
Δ4
295
Δ5
145
Δ6
66
pC–GUS–R2
Label
5'Δ full-length construct
TSS
L23aA–RTintF
5'FR RT
L23aA–RTintF
5'Δ4 RT
L23aA–5'Δ5–F
5'Δ5 RT #1
L23aA–5'Δ5–F
5'Δ5 RT #2
L23aA–5'Δ6–F
5'Δ6 RT
3'Δ5
77 bp
Δ2
248
3'Δ full-length construct
L23aA–5'Δ4–F
3'Δ2 RT
L23aA–5'Δ4–F
3'Δ5 RT

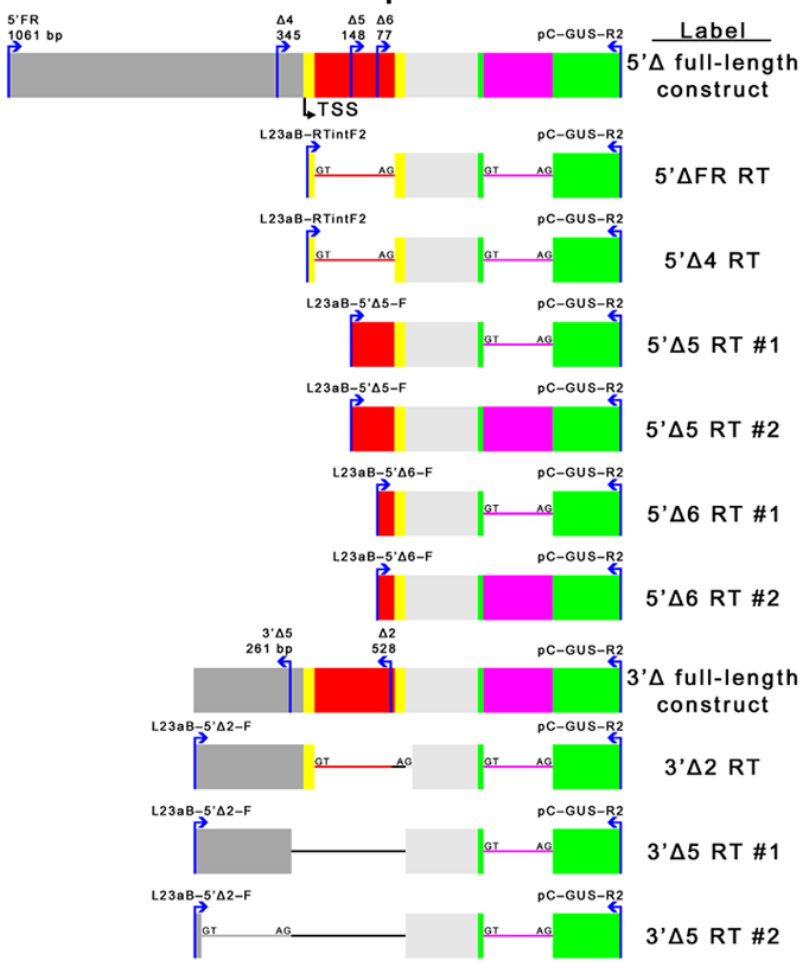
RPL23aB Δ RT products
5'FR
1061 bp
Δ4
345
Δ5
148
Δ6
77
pC–GUS–R2
Label
5'Δ full-length construct
TSS
L23aB–RTintF2
5'ΔFR RT
L23aB–RTintF2
5'Δ4 RT
L23aB–5'Δ5–F
5'Δ5 RT #1
L23aB–5'Δ5–F
5'Δ5 RT #2
L23aB–5'Δ6–F
5'Δ6 RT #1
L23aB–5'Δ6–F
5'Δ6 RT #2
3'Δ5
261 bp
Δ2
528
3'Δ full-length construct
L23aB–5'Δ2–F
3'Δ2 RT
L23aB–5'Δ2–F
3'Δ5 RT #1
L23aB–5'Δ2–F
3'Δ5 RT #2

displayed no splicing of the 5' truncated leader intron. However, the 3' truncated leader intron in *RPL23aA* 3'Δ2–GUS plants was spliced using the canonical GU splice donor at the 5' end of the leader intron and an AG splice acceptor found within an intragenic spacer of the T-DNA sequence located just downstream of the MCS (Figure 2.5). A single RT-PCR product was amplified from *RPL23aA* 3'Δ5–GUS transgenics, which lack the leader intron entirely, containing the entire unspliced 3'Δ5–GUS RR fragment (Figure 2.5). That transcripts were amplified from *RPL23aA* 5'Δ5–GUS, 5'Δ6–GUS and 3'Δ5–GUS plants, which showed little to no GUS staining, indicates that these transcripts lack elements necessary for efficient translation.

Consistent with results of *RPL23aA* RR deletions, plants carrying the *RPL23aB* 5'FR–GUS and 5'Δ4–GUS constructs produced single RT-PCR products with canonically spliced leader introns, and no splicing of 5' truncated leader introns was observed in *RPL23aB* 5'Δ5–GUS and 5'Δ6–GUS plants (Figure 2.5). However, a second population of higher molecular weight transcripts was detected by RT-PCR from both 5'Δ5–GUS (5'Δ5 RT #2) and 5'Δ6–GUS (5'Δ6 RT #2) transgenics. These products were not a result of DNA contamination or a single-primer artifact as no product was amplified in minus RT controls or in reactions conducted with single primers. Upon sequencing, it was determined that this product resulted from failure to splice the *CATALASE* intron located between the *GUS* first and second exons (Figure 2.5). As observed for the *RPL23aA* 3' RR deletions, the 3' truncated leader intron in *RPL23aB* 3'Δ2–GUS plants was spliced with the leader intron GU splice donor and the same intragenic AG splice acceptor used by *RPL23aA* 3'Δ2–GUS plants (Figure 2.5). Sequencing confirmed that the leader intron-lacking *RPL23aB* 3'Δ5–GUS transgenics produced transcripts containing the entire unspliced RR deletion fragment (3'Δ5 RT #1, Figure 2.5), however, these plants had an additional smaller product (3'Δ5 RT #2, Figure 2.5) that appeared predominant on an EtBr-stained gel (roughly twice the intensity, data not shown). Sequenced showed this product to be a splice variant that removes, at canonical splice sites, all but 20 bp of the RR (containing only −293 to −274 relative to the TSS). This splice variant predominated in all four *RPL23aB* 3'Δ5–GUS transgenic lines tested.

2.3.5 Leader intron splicing may be important for GUS expression

Findings from RT-PCR analyses suggested a correlation between GUS activity and splicing of the leader intron at canonical splice sites. Consistent GUS expression in seedling tissues was concomitant with leader intron splicing for all but three (*RPL23aB* 5'Δ6–GUS, 3'Δ2–GUS, and

3'Δ5–GUS) of the twelve transgenic genotypes tested for intron splicing. To determine if this relationship was causal or incidental, complementary oligonucleotides were synthesized containing the RR and exon sequence from −11 to +54 and −17 to +56 for *RPL23aA* (*RPL23aA*–INL–GUS) and *RPL23aB* (*RPL23aB*–INL–GUS), respectively, and lacking entire leader introns (Figure 2.2b). T_2 seedlings carrying the *RPL23aA*–INL–GUS construct showed GUS activity in seedlings, with consistent expression in meristems, roots, vasculature, and trichomes, and occasional expression in stems and interveinal leaf tissue (Figure 2.3b). GUS activity in *RPL23aB*–INL–GUS seedlings was weaker and more spatially restricted, with consistent expression in meristems, but irregular expression in roots, vasculature, stems and trichomes (Figure 2.3b). Together, these results indicate that leader intron splicing is not strictly required for high protein expression.

2.3.6 *RPL23aA* and *RPL23aB* second introns enhance expression

Introns can possess *cis*-elements necessary for directing expression of genes in plants, often in a tissue-specific manner (Pylatuik et al., 2003; Sieburth and Meyerowitz, 1997). The *RPL23a* paralogs both possess second introns that are substantially larger than the average intron size of ~173 bp in Arabidopsis (Wang and Brendel, 2006). To determine if the 303 and 317 bp second introns of *RPL23aA* and *RPL23aB*, respectively, contain *cis*-acting regulatory elements, the introns were cloned upstream of the −60 *CaMV* minimal promoter, which by itself is unable to direct reporter gene expression (Campisi et al., 1999). The second introns share 53% identity (Figure 2.6a) and directed similar GUS expression in T_2 seedlings, with faint staining consistently observed in meristems and vasculature of respective transgenics (Figure 2.6b), suggesting that the second introns possess conserved elements for enhancing basal expression in mitotically active tissues.

2.3.7 *RPL23a* paralogs possess elements that repress transcription in stressed protoplasts

The upstream RRs of *RPL23aA* and *RPL23aB* contain two *cis*-elements, site II motifs and *telo*-boxes (Figure 2.1; see discussion), that have been shown to be important for upregulating expression of an r-protein (*RPL15B*) in response to mitogenic signals (Tatematsu et al., 2005). To investigate whether these or other RR elements also possess negative regulatory functions, we analyzed transcript expression driven by *RPL23aA*/*B* RRs in protoplasts under stress conditions

Figure 2.6 Alignment and regulatory activity of *RPL23aA* and *RPL23aB* second introns. **a** Full-length second introns of *RPL23aA* and *RPL23aB* were aligned using Clustal W2 (Larkin et al., 2007). Arabidopsis IME elements (see Figure 2.1 legend for details) are highlighted yellow. **b** GUS activity driven by *RPL23a* paralog second introns upstream of a -60 *CaMV* minimal promoter. Staining was evaluated qualitatively as in Figure 2.3.

(mild hypoxia and sugar deprivation) that reportedly downregulate transcription of a subset of r-proteins (Contento et al., 2004; Klok et al., 2002; Liu et al., 2005), including *RPL23aA* and *RPL23aB* (Branco-Price et al., 2005). Accordingly, Arabidopsis protoplasts were cotransformed with a *CaMV 35S*-driven *nptII* construct (transformation control) and a green fluorescent protein reporter gene (*erGFP7int*) driven by full-length and 5' truncated *RPL23aA*/*B* RRs. To induce a stress response, transformed protoplasts were cultured for 5 h at a depth of 0.6 mm in an isotonic solution containing only salts, minerals and the non-metabolized sugar mannitol (Hwang et al., 1998; Yoo et al., 2007). Quantitative RT-PCR was used to measure *nptII* standardized *erGFP7int* expression driven by no promoter (negative control), *RPL23a* paralog RRs, or the *CaMV 35S* promoter (positive control). Transcript abundance for each construct was expressed relative to the positive control (set to a value of 1).

Expression driven by longer *RPL23aA* RR fragments (*RPL23aA* 5'FR–erGFP7int to 5'Δ4–erGFP7int) was low (26–42% of positive control levels) and did not differ significantly from negative control levels, which lacked a promoter but still directed a basal level of transcription (Figure 2.7). Conversely, the two shortest *RPL23aA* RR fragments, 5'Δ5–erGFP7int and 5'Δ6–erGFP7int, had transcript levels between 106–117% of positive control levels (Figure 2.7), indicating that the region between −134 to +16 relative to the +1 TSS is essential for downregulating transcript expression in response to hypoxia/sugar deprivation. Similarly, *erGFP7int* expression driven by *RPL23aB* RRs was only 17–65% of positive control levels in the longer fragments, but increased to 137–166% in protoplasts expressing 5'Δ5–erGFP7int and 5'Δ6–erGFP7int constructs (Figure 2.7). This suggests that the region between −75 to +32 and possibly including the first 90 bp of the leader intron, contains elements for downregulating transcriptional expression of *RPL23aB*. There was also a trend of lower transcript abundance with the *RPL23aB* 5'Δ2–erGFP7int fragment, relative to 5'Δ3–erGFP7int ($P < 0.06$) and 5'Δ4–erGFP7int ($P < 0.10$) fragments, indicating that the −293 to −178 region contains additional elements for regulating *RPL23aB* stress-induced repression.

2.3.8 Shared 5' and 3' UTR sequence motifs may coordinate r-protein expression

The *RPL23aA*/*B* 5' and 3' UTRs share a number of architectural features (length, base-composition, free energies) with other Arabidopsis r-proteins and orthologs of closely related species (see Table A.2, Figure A.1, and Appendix A). To identify whether *RPL23a* paralogs also

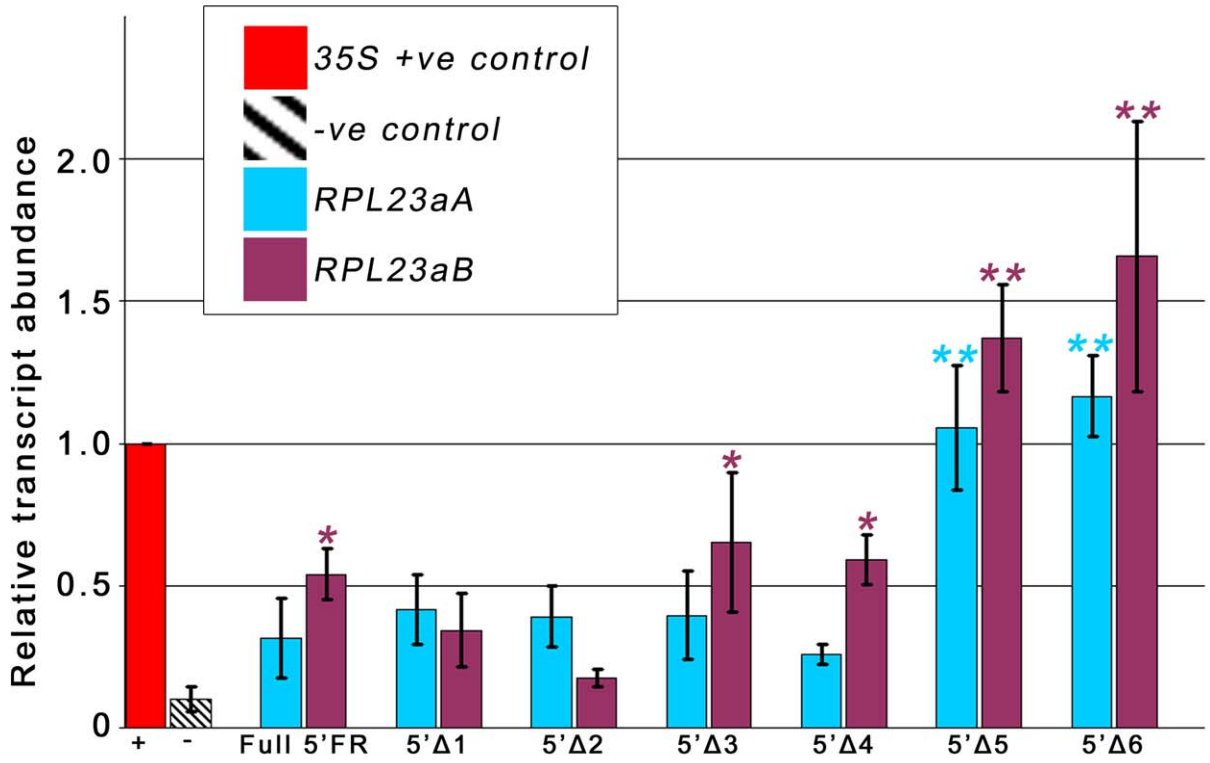

Figure 2.7 Quantification of *erGFP7int* reporter gene transcript expression driven by *RPL23aA* and *RPL23aB* upstream regulatory regions. Protoplasts were isolated from 15–21 day-old Arabidopsis seedlings and electroporated with 20 µg of pGI0029 (internal control containing *35S* driven *nptII*) and 20 µg of plasmids containing *RPL23aA* (blue columns) or *RPL23aB* (purple columns) RRs driving expression of the *erGFP7int* reporter gene. Transcript levels driven by RRs and the empty vector negative control (pGREEN–erGFP7int–nos, '-', diagonal-hatched column) were standardized against the *nptII* internal control transcript level and compared to the *nptII*-standardized *erGFP7int* transcript level driven by the *CaMV 35S* promoter (set to 1, '+', red column) using the comparative Ct method (Livak and Schmittgen, 2001). Black bars show SEM. Transcript levels that differ significantly at $P \leq 0.05$ and $P < 0.01$ from levels in the negative control are indicated by asterisks (* and **, respectively) above columns.

possess conserved motifs within 5' and 3' UTRs that may coordinate expression transcriptionally or posttranscriptionally, MEME (Bailey et al., 2006) was used to search for motifs in UTR sequences from Arabidopsis *RPL23a* paralogs and 101–103 *RPL23a* orthologs from 55 eukaryotic species, including 4 Brassicales, 21 Magnoliopsida plants (eudicots), 4 Liliopsida plants (monocots), 3 gymnosperms, 6 nonvascular plants, 5 vertebrates, 6 invertebrates, 4 fungi, and 2 protists. The most common 5' UTR motif was $^{5'}$AGGGUUUCAG$^{3'}$ (motif 1), which was identified in 90 and 65% of Brassicales and dicot transcripts, respectively, and was also found in a monocot and a gymnosperm (Figure 2.8). This element, which contains the core of the *telo*-box, was also identified in reverse orientation ($^{5'}$AAAACCCUA$^{3'}$) in the 5' UTRs of an additional 5 non-Brassicales dicots, suggesting that it may function bidirectionally. Motif 2 ($^{5'}$GGAAAGAAUC$^{3'}$), 4 ($^{5'}$AUUUUGAGYU/A$^{3'}$) and 5 ($^{5'}$CAGAG/TCA/T$^{3'}$) were predominantly Brassicales-specific and were generally proximal (<25 nt) to AUG start codons, suggesting that they may function in establishing the initiation context (Figure 2.8). Two pyrmidine-rich motifs were identified, including one Brassicales-specific (Figure 2.8; motif 3), and one found in *RPL23a* orthologs from four dicots and two nonvascular plants ($^{5'}$CUCUUCCUC$^{3'}$). It has been reported that wheat germ ribosomes specifically recognize 5' TOP mRNAs *in vitro* (Shama and Meyuhas, 1996), and thus these motifs may perform a similar function in plants, although we note that these elements are not at the extreme 5' terminus and the closest element in a monocot (*Triticum aestivum* L.) is less pyrimidine rich ($^{5'}$CA/UCGCGYCCG$^{3'}$). Moreover, a similar pyrimidine stretch exists in the +1 to +50 region of more than 4000 Arabidopsis fl-cDNAs (Molina and Grotewold, 2005), suggesting that this is a general transcript feature in Arabidopsis, and perhaps all plants (Yamamoto et al., 2007a). Motifs found in 3' UTRs of *RPL23a* orthologs were generally A/U rich and less Brassicales-specific (Figure 2.8). Motif 6 ($^{5'}$CAGUUUUGUU$^{3'}$) was identified in both Arabidopsis *RPL23a* paralogs and appears to be a conserved plant element located between 10 and 75 nt downstream of stop codons. Motif 8 ($^{5'}$ARA/CAAAR$^{3'}$) was often found adjacent or in close proximity to motif 6.

To investigate whether motifs found in *RPL23a* orthologs were also present in other Arabidopsis r-proteins, MEME analysis was conducted on all r-proteins with >8 nt of 5' or 3' UTR sequence (218 and 220, respectively). The top two most significant 5' UTR motifs (motif 11 and 12) were found to be *telo*-box elements in forward and reverse orientation, confirming

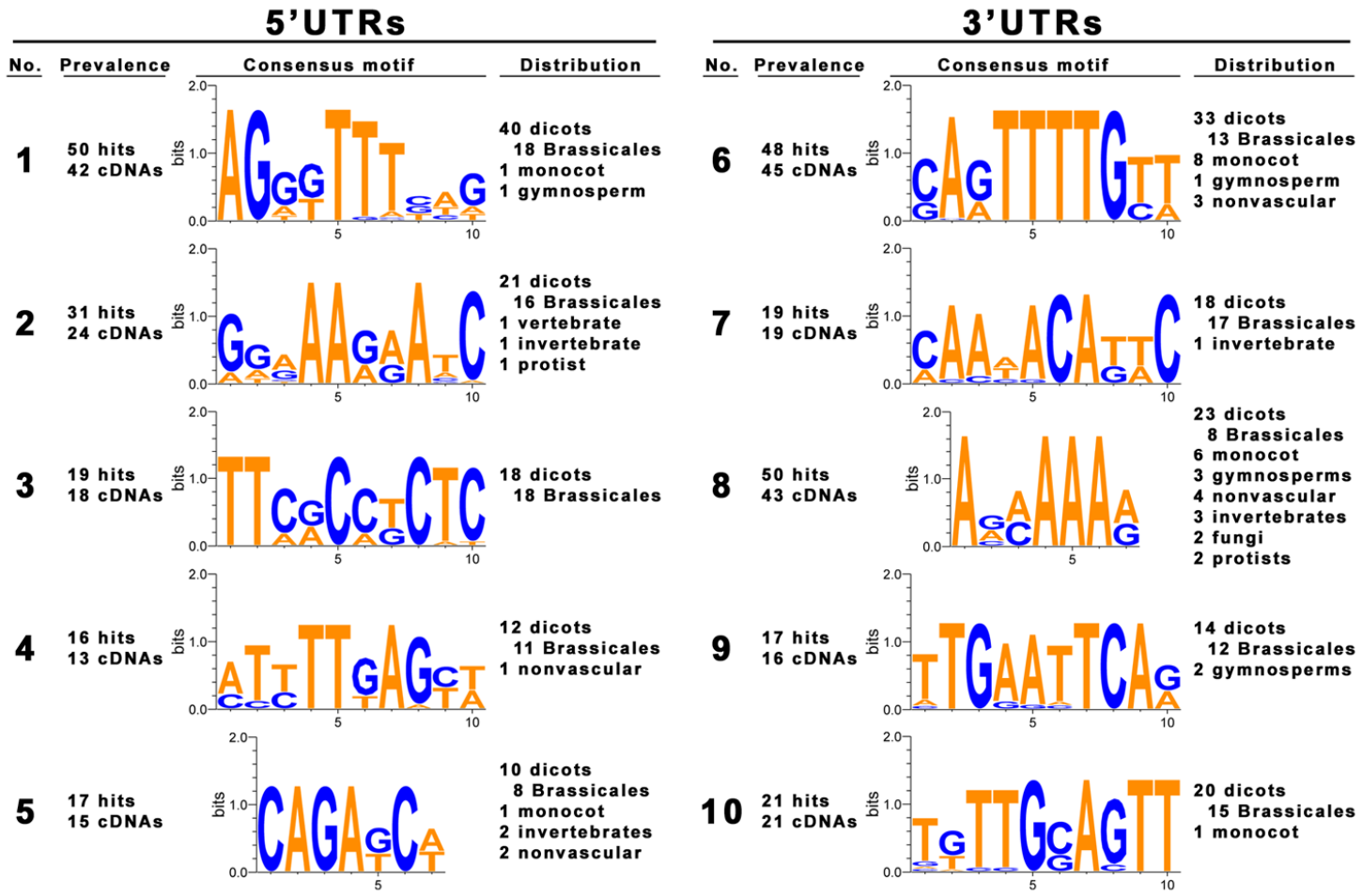

Figure 2.8 Sequence motifs present in 5' and 3' UTRs of *RPL23a* ortholog transcripts from 56 species. The top 5 most significant motifs from both 5' and 3' UTR sequences (direct strand only), as determined by MEME analysis (Bailey et al., 2006), are presented. Significant motifs not containing elements from at least two Brassicales species are not shown. The number of hits indicates the total number of times the motif was identified, including duplicate occurrences on the same transcript. Distribution indicates the total number of transcripts from each group containing the specified motif. Motif numbers (No.) are for reference only. Groups are as in Table A.2.

that this motif is broadly conserved among Arabidopsis r-proteins (Figure 2.9). These two motifs, which are generally single copy and rarely co-occur on the same transcript, are present in at least 36% of r-protein gene transcripts (79 of 218), representing at least one member of 57% (46 of 81) of r-protein families. Motif 13 ($^{5'}$GAGAAAGAAG$^{3'}$) is very similar to motif 2, identified in *RPL23a* orthologs, in terms of base composition (purine-rich) and proximity to AUG start codons (<25 nt, Figure 2.9). Motifs 14 and 15 were pyrimidine-rich and reminiscent of mammalian pyrimidine tracts, but were seldom located at the 5' terminus (only 10 of 79 were within 5 nt of the 5' end). Similar to 3' UTR elements found in *RPL23a* orthologs, Arabidopsis r-proteins primarily have A/U-rich 3' UTR motifs. The most abundant and widely distributed motif, (motif 17, $^{5'}$AAAG/AUUUUG$^{3'}$) resembles motif 6, but tended to be more highly dispersed along 3' UTRs than the latter. Further, while motif 6 tended to be clustered proximal to motif 8, motif 16, which contains the core consensus of motif 8, was seldom found on the same transcripts as motif 17. Generally, the position of motifs within 3' UTRs was not highly conserved between different r-proteins, and no motifs were consistently clustered at either the 5' or 3' ends of 3' UTRs.

2.4 Discussion

2.4.1 Promoter characterization of *RPL23a* paralogs

Regulation of RPL23a expression is complex and occurs at many levels. Investigation of promoter architecture of plant genes using 12,951 and 11,370 cap-trapper fl-cDNAs from Arabidopsis and rice, respectively, has shown that the generalized plant promoter contains elements from three groups: (1) a regulatory element group (REG) that contains a large number of non-directional motifs with a broad distribution centered around ~−80 relative to the TSS, (2) a TATA-box group that is directional with a narrow distribution around −35; and (3) a Y patch group containing pyrimidine-rich motifs that is directional with an intermediate distribution around −13 (Yamamoto et al., 2007a; Yamamoto et al., 2007b). Both *RPL23a* promoters largely fit this generalized architecture. The essential REG elements (1) of *RPL23aA* and *RPL23aB* appear to be site II motifs (TGGGCY or RGCCCA) and *telo*-boxes (AAACCCTA or TAGGGCCC; Figure 2.1). Analysis of a subset of 72 r-protein genes (−500 to −1 region),

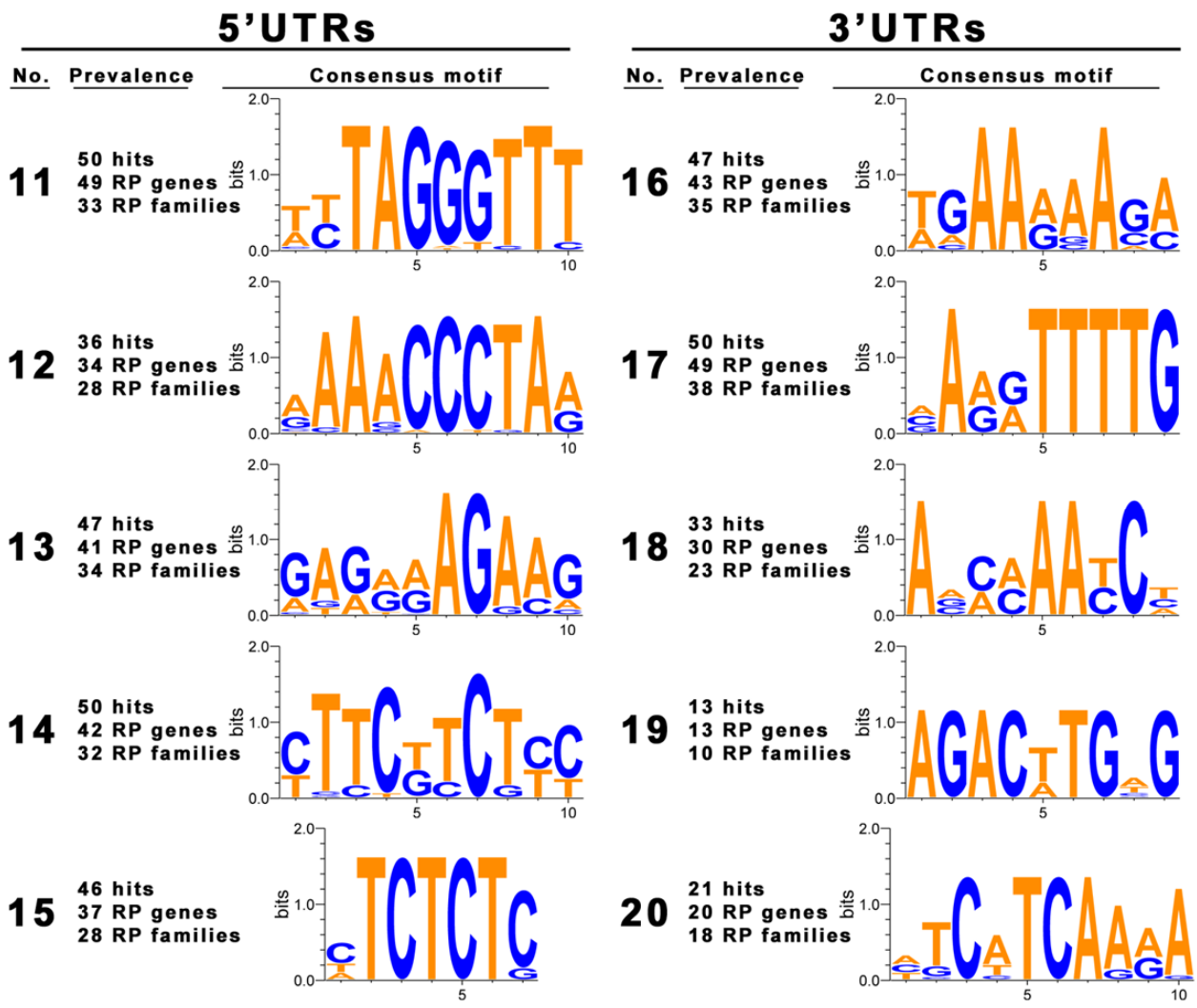

Figure 2.9 Sequence motifs present in 5' and 3' UTRs of 217 and 220 Arabidopsis r-protein transcripts, respectively. The top 5 most significant motifs from both 5' and 3' UTR sequences (direct strand only), as determined by MEME analysis (Bailey et al., 2006), are presented. The number of hits indicates the total number of times the motif was identified, including duplicate occurrences on the same transcript. The number of different r-protein gene transcripts (RP genes) containing each specified motif is indicated, as is the number of different r-protein families (RP families) represented. Motif numbers (No.) are for reference only. Groups are as in Table A.2.

representing 27 r-protein families, determined that 92% (66) contained at least one consensus site II motif, and 61% (44) contained at least one *telo*-box of the extended consensus AAACCCTAR (or YTAGGGCCC; data not shown). In agreement with previous reports (Tremousaygue et al., 2003) and their relative positions in *RPL23a* paralog RRs, site II motifs were clustered between −200 to −40, while *telo*-boxes were more proximal to TSSs, clustered between −60 to −1 (Figure 2.1; data not shown). These two elements are believed to be involved in coupling cell proliferation with high level gene expression and are found in only a small subset of Arabidopsis genes (Molina and Grotewold, 2005; Yamamoto et al., 2007b), including those encoding translational apparatus, some nuclear encoded mitochondrial genes, and cell-cycle genes (Li et al., 2005a; Tatematsu et al., 2005; Tremousaygue et al., 2003; Welchen and Gonzalez, 2005; Yamamoto et al., 2007b), suggesting that they are not general factors for mediating transcription in Arabidopsis. Site II motifs have also been identified in the RRs of a subset of circadian clock-regulated genes, however, *telo*-boxes are not found in conjunction with site II motif in these RRs (Janaki and Joshi, 2004; Schaffer et al., 2001), suggesting that the role of site II motifs in regulating transcription is mediated through heterogeneous transcription factor complexes.

Canonical TATA-boxes (2) of *RPL23aA* ($^{-34}$TATAAAAC^{-27}) and *RPL23aB* ($^{-32}$AATAAATA^{-25}), based on criterion outlined by Perry (2005), are potentially high-affinity binders of the TATA-binding protein (TBP), and with the exception of single nucleotide substitutions, they also fit the Arabidopsis TATA consensus (5'TATAT/AAT/AA3', Molina and Grotewold, 2005). Furthermore, 100% of the previously described subset of 72 r-protein genes contained a canonical high-affinity TATA-box between positions −45 to −31 (data not shown). This distribution contrasts with mammalian r-protein genes, where only ~35% contain a high-affinity TATA-box, with a further ~25% having an A/T rich-region predicted to bind TBP with low affinity (Perry, 2005). Given estimates that only 29% (Molina and Grotewold, 2005) to 37% (Shahmuradov et al., 2003) of Arabidopsis genes contain canonical TATA-boxes, our data suggests that the TATA-box element is overrepresented in Arabidopsis r-protein promoters. Even the minor TSS for *RPL23aB*, represented by ~1% of ESTs in the TIGR transcript assembly (Childs et al., 2007), is 42 nt downstream of a second high affinity TATA-box ($^{-103}$TATATATT^{-96}; numbering relative to the +1 predominant TSS), suggesting that TSSs for *RPL23a* paralogs are determined by conserved spacing requirements relative to TATA-boxes. This is in agreement with *in vitro* experiments on bean (*Phaseolus vulgaris* L.) *β-PHASEOLIN*,

which contains two consensus TATA-boxes within 12 bp of each other (Grace et al., 2004). The 3' TATA-box is predominant, however *β-PHASEOLIN* transcripts initiated approximately 32 bp downstream of each TATA-box, with the spacing maintained in base insertion of deletion mutants (Grace et al., 2004). Our results indicate that TATA-box mediated transcription may be an important, conserved feature for regulation of the *RPL23a* paralogs, and perhaps all Arabidopsis r-proteins.

The lone discrepancy between the generalized plant promoter architecture (Yamamoto et al., 2007b) and that of the *RPL23a* paralogs is the lack of a discernible Y-patch (3). Using MEME to analyze the −500 to −1 region of the 72 r-protein gene subset, we found that the Y-patch was not a general r-protein promoter element, but was present (consensus $^{5'}$CTTCTYCT/AYC$^{3'}$) in the −25 to −1 region of 14% (10) of analyzed r-protein promoters.

2.4.2 Full-length *RPL23aA/B* RRs direct overlapping and differential expression patterns

The most intense GUS staining driven by full-length RRs of *RPL23aA* and *RPL23aB* was observed in zones of active cell division such as young leaves, meristems, gametogenic tissues of the androecium and gynoecium, and roots, especially lateral root primordia (Figure 2.3 and 2.4). This is in agreement with the observed expression patterns of r-proteins from a number of dicot and monocot species (reviewed in McIntosh and Bonham-Smith, 2006), and the reported induction of r-protein expression following treatment with mitogens, such as synthetic cytokinins (Cherepneva et al., 2003; Hulm et al., 2005; Kiba et al., 2005; McIntosh and Bonham-Smith, 2005). Patterns of GUS expression were consistent with transcript abundance determined using semi-quantitative and quantitative RT-PCR (Degenhardt and Bonham-Smith, 2008c; McIntosh and Bonham-Smith, 2005), and this suggests that transcriptional regulation is a major component of RPL23a expression.

That both *RPL23aA* and *RPL23aB* full-length RRs directed strong GUS expression at wound/cut sites (Figure 2.4) indicates a very rapid induction of GUS activity mediated by *RPL23a* RRs. Expression was particularly strong at the cut ends of stems, and may explain our previous findings by semi-quantitative RT-PCR of relatively high *RPL23aA* and *RPL23aB* transcript levels in cut stem sections (roughly equivalent to seedling levels, McIntosh and Bonham-Smith, 2005). Subsequent analysis of rapid flash-frozen cut stem sections via real-time quantitative RT-PCR determined transcript levels to be ~14–20% of seedling levels (Degenhardt

and Bonham-Smith, 2008c). Wound inducibility of single or multiple r-proteins has been previously reported in several plants, including Arabidopsis (Van Lijsebettens et al., 1994), chestnut (Castanea sativa Mill., Schafleitner and Wilhelm, 2002), tobacco (Nicotiana tabacum L., Gao et al., 1994) and poplar (Populus trichocarpa Torr. and A. Gray, Lawrence et al., 2006; Major and Constabel, 2006). Whether this is a global r-protein-, or a subset specific-, response has yet to be determined, but the rapidness of the induction (~5–20 s from tissue harvesting until fixation in acetone) suggests that the response may be a consequence of both transcriptional and translational upregulation.

While full-length RRs of both *RPL23a* paralogs conferred largely overlapping patterns of GUS expression, *RPL23aB* consistently directed higher GUS activity in non-gametogenic reproductive tissues (i.e. sepals, petals, filaments, receptacles, seed pods). Spatial variation in expression of members of the same r-protein family has been previously reported (Dresselhaus et al., 1999; Weijers et al., 2001; Williams and Sussex, 1995), with Van Lijsebettens (1994) postulating that the requirement for r-proteins in plants is met by the constitutive expression of one or more r-protein family member, with additional demand met by the development/stress-induced synthesis of auxiliary family members. Our results support this hypothesis, with *RPL23aA* appearing to be the predominantly expressed paralog, especially in zones of active cell division, similar to the expression patterns of *RPS5B*, *RPS18A* and *RPL11C* (Van Lijsebettens et al., 1994; Weijers et al., 2001; Williams and Sussex, 1995), while *RPL23aB* shows expression overlap with *RPL23aA* (at lower levels, cf. Degenhardt and Bonham-Smith, 2008c; McIntosh and Bonham-Smith, 2005), and ancillary expression in non-meristematic zones of cell differentiation and elongation, and greater wound responsiveness.

2.4.3 *RPL23aA/B* RR deletions identify conserved *cis*-acting motifs

High level of expression of *RPL23aA* in meristematic zones is dependent on the −57 to −6 region (relative to the +1 TSS) of the RR that contains a canonical TATA-box and a *telo*-box, but no site II motifs. However, in the context of the deletion constructs used to identify this region, the minimum region necessary for GUS expression (the 3'Δ3–GUS fragment) extended from −134 to −6, and included two site II motifs. A search for additional motifs within this region identified two CAAT-boxes (consensus 5'CAAT3', Shahmuradov et al., 2003) at −122 and −93, and a GT element (consensus 5'GRA/TAAA/T3', Zhou, 1999) at −88. In conjunction with GT transcription factors, GT elements are necessary for light responsiveness of some genes (Le

Gourrierec et al., 1999; Villain et al., 1996). Only a single tissue specific element was identified in this region, a single pollen-specific element at +35 (5'GTGA3', Rogers et al., 2001), suggesting that elements for tissue specific expression of *RPL23aA*, especially in mitotically active tissues, may not be required. Moreover, our results indicate that negative regulatory elements, necessary for restricting expression to mitotically active regions, exist upstream of −134, particularly between −726 to −395. The −726 to −395 region contains two pollen-specific motifs at −606 and −471 (5'GTGA3' and 5'AGAAA3', respectively, Bate and Twell, 1998) and an abscissic acid response element (ABRE)-related motif at −419 (5'ACGTG3', Nakashima et al., 2006). It is unknown whether the ABRE of *RPL23aA* is functional, but the core palindromic tetramer (5'ACGT3', Zhang et al., 2005b) was found at least once in the −500 to −1 region of 65% (47) of the 72 r-protein gene subset, and ABA has been shown to downregulate r-protein gene expression (Cherepneva et al., 2003; Hoth et al., 2002; Hulm et al., 2005), including that of *RPL23aA* and *RPL23aB* (RPL23aB contains an ABRE tetramer at -221, McIntosh and Bonham-Smith, 2005).

As well as conferring GUS expression in mitotically active plant tissues, the same region of the *RPL23aA* RR repressed expression of the *erGFP7int* reporter gene in hypoxic, sucrose-starved Arabidopsis protoplasts, suggesting that the *telo*-box and/or site II motifs mediate binding of both transactivators and transcriptional repressors. It has previously been reported that site II motifs negatively regulate the Arabidopsis alternative oxidase gene, *AtOX1c* (Ho et al., 2007); specific deletion of one or both site II motifs present in the upstream RR of *AtOX1c* led to a 2–8 fold increase in reporter gene activity. Additionally, site II motifs in conjunction with *telo*-boxes are overrepresented among genes repressed by *A. tumefaciens* infection (Ditt et al., 2006). It is not presently known if or how the *telo*-box is involved in suppressing transcription, but a mechanism involving class II *TEOSINTE BRANCHED1*, *CYCLOIDEA*, *PCF* (TCP)-domain transcription factors has been postulated to downregulate genes containing its cognate binding site, the site II motif (see below).

GUS-activity driven by the RR of *RPL23aB* indicates a very high degree of redundancy of controlling elements. The 77 bp 5'Δ6–GUS fragment, consisting of the final 26 bp of the leader intron and the +28 to +56 region of exon 2, contains few recognized regulatory motifs other than two CAAT-boxes within the unspliced leader intron fragment, and showed GUS activity in seedlings and all tissues of adult plants except mature leaves and gametogenic tissue of anthers.

Moreover, this entire region is absent in the 3'Δ5–GUS construct, which also confers a high level of GUS activity in seedlings, indicating that elements between −293 to −33 are also sufficient to direct GUS expression. The −293 to −33 region, containing a TATA-box, three site II motifs and a *telo*-box (Figure 2.4), is compositionally equivalent to the core region required for expression of *RPL23aA*. Interestingly, high level GUS expression in carpels, and GUS expression generally in anthers and pollen, was found to be dependent on the −177 to −76 (102 bp) region, which is entirely encompassed by the larger −293 to −33 region. The 102 bp sequence contains all three site II motifs and the TATA-box of the larger region. Two pollen-specific motifs are also present at −150 and −115 ($^{5'}$AGAAA$^{3'}$), but at least in tomato, these motifs only function in concert with a $^{5'}$TCCACCATA$^{3'}$ motif not present within the *RPL23aB* RR (Bate and Twell, 1998). Taken together, these results suggest that for both *RPL23aA* and *RPL23aB*, consistent high levels of GUS expression in meristematic regions driven by RRs requires a *telo*-box, site II motif and TATA box. In contrast, GUS expression observed in transgenics carrying the *RPL23aB* 5'Δ6–GUS fragment, which lacks *telo*-box, site II motif and TATA box elements, may be a result of favorable base composition within the unspliced leader intron. The 5'Δ6–GUS construct contains both a pyrimidine stretch ($^{5'}$TTTTCTTTTCT$^{3'}$ within the leader intron) and a purine stretch ($^{5'}$GAAAAGAA$^{3'}$, within exon 2), both of which were identified as common 5' UTR elements of r-proteins (Figure 2.9). It is possible that GUS activity from this construct is a result of transcription driven by cryptic promoter elements and the subsequent recognition, by the ribosome, of conserved r-protein 5' UTR elements, leading to increased ribosome loading of the transcript.

In agreement with our *RPL23aA* RR findings, the full length RR of *RPL23aB* also suppressed *erGFP7int* reporter gene expression in hypoxic, sucrose-starved Arabidopsis protoplasts. Repression was relieved by removal of the −75 to +28 fragment that includes the TATA-box and both *telo*-boxes, however, removal of three site II motifs between −177 and −76, did not alleviate reporter gene suppression, indicating that either the *telo*-boxes alone are capable of impairing expression, or that additional elements, present between −75 to +28, function coordinately to negatively regulate expression. Analysis of the −75 to +28 region with PLACE led to the identification of a motif ($^{5'}$AAACAAA$^{3'}$) at position −57 that has previously been identified in the RRs of 9 of 13 fermentation-pathway genes analyzed from seven angiosperm species (including 2 of 2 genes from Arabidopsis, Mohanty et al., 2005). Also overrepresented in the

fermentation pathway genes (7 of 13, and 2 of 2 from Arabidopsis) was an $^{5'}$AAA(A/C)CCTC$^{3'}$ motif that differs from the consensus *telo*-box by a 3' C to A substitution. Thus it is possible that under the semi-anaerobic conditions used to culture protoplasts, the site II motif independent suppression we observed was due to binding of specific transcription repressors to the *telo*-box and $^{5'}$AAACAAA$^{3'}$ fermentation motif. It is clear nevertheless, that the *telo*-box plays an important role in both the positive and negative regulation of r-protein gene expression.

2.4.4 Posttranscriptional regulation via intron-mediated enhancement plays a small role in regulation of RPL23aA/B

RPL23aA and *RPL23aB* possess leader introns that were processed regardless of plant age or tissue type. Only 12 (17%) of our subset of 72 Arabidopsis r-protein genes have leader introns, and no leader intron is present in either rice *RPL23a* ortholog, suggesting that leader introns are not a highly conserved feature among plant r-proteins. This is further confirmed by the finding that of 18,812 annotated Arabidopsis genes with 5' UTR sequences, ~20% contain leader introns (Chung et al., 2006), roughly equivalent to the proportion of our r-protein subset. In contrast, it has been reported that most r-protein genes in vertebrates exhibit separation of transcript regulatory sequence from protein coding sequences via a leader intron or the clustering of AUG start codons to the extreme 3' end of exon 1 (Amaldi et al., 1995; Perry, 2005).

We observed that RR 3' deletions that removed canonical leader intron splice acceptor sites resulted in the utilization of an alternate AG acceptor site located within the T-DNA intragenic spacer, and showed high level GUS activity in seedlings. Conversely, RR 5' deletions that interfered with, or removed, the splice donor site of *RPL23aA* showed missplicing (5'Δ5–GUS) or a lack of splicing (5'Δ6–GUS), with the resultant transcripts either poorly translated or untranslatable (Figure 2.3). Impaired splicing of other plant introns have shown similar outcomes (Clancy and Hannah, 2002; Rose, 2002), however, in most cases it appears that the reduced gene expression resulted from the removal of *cis*- (or *trans*-) acting elements present within the intron, and not strictly impaired intron splicing (Fu et al., 1995; Jeong et al., 2007; Rose and Beliakoff, 2000; Vitale et al., 2003). Moreover, our results indicate that splicing of the leader intron is not necessary for directing a high level of reporter gene expression. The *RPL23aB* 5'Δ5–GUS and 5'Δ6–GUS constructs produced efficiently translated reporter gene transcripts despite containing unspliced 5' truncated leader introns. Additionally, several of our 3' deletion constructs (*RPL23aA* 3'Δ3–GUS and 3'Δ4–GUS, *RPL23aB* 3'Δ3–GUS, 3'Δ4–GUS,

and 3'Δ5–GUS) completely lacked the leader intron, but were still able to confer high-level GUS staining in seedlings. Furthermore, leader intron deletion constructs (intron-less) for both *RPL23aA* and *RPL23aB* RRs, possessing one and two *telo*-boxes, respectively, showed GUS activity in meristematic regions, indicating that *cis*-elements, especially *telo*-boxes, are more important for governing expression patterns than leader-intron splicing. Nevertheless, splicing may have minor additive effects mediated through the occupation of intron splice sites with small nuclear RNAs and spliceosomal small nuclear RNPs that can increase the efficiency of transcription, processing or translation (Bourdon et al., 2001; Le Hir et al., 2003; Rose, 2004; Rose and Beliakoff, 2000).

In mammals, *cis*-elements involved in transcriptional regulation are contained within the introns of some r-protein genes, such as the YY1 motif in introns of *RPL7* and *RPL32* (Chung and Perry, 1993; Meyuhas and Klein, 1990). A large number of plant introns are known to contain features that enhance gene expression (Fu et al., 1995; Jeong et al., 2007; Rose and Beliakoff, 2000; Vitale et al., 2003), including the large (3 kb) second intron of the Arabidopsis *AGAMOUS* gene, which contains all elements necessary for directing accurate spatiotemporal expression, including binding sites for two important transcription factors (Busch et al., 1999; Lohmann et al., 2001; Sieburth and Meyerowitz, 1997). The second introns of both *RPL23aA* and *RPL23aB* contain two copies of the Arabidopsis intron-mediated enhancement (IME) element, $^{5'}$TYnGATYTGT/AT/G$^{3'}$ (Rose et al., 2008), which is overrepresented in introns capable of enhancing expression (Rose et al., 2008). Both introns conferred low level GUS activity in meristems and venation (Figure 2.6). The mechanism by which the putative IME-elements operate is unknown, but they may function synergistically with other intron elements to recruit spliceosomal and/or exon junction complex RNPs, thereby enhancing transcription and improving efficiency of mRNA processing, nuclear export and polysome association (Meinhart et al., 2005; Nott et al., 2004; Rose et al., 2008). Interestingly, an IME-element is also found in the leader intron of *RPL23aB* (Figure 2.1). Our finding that the shortest 5' deletion construct still containing the IME-element (*RPL23aB* 5'Δ5–GUS) has reduced expression relative to the 5'Δ6–GUS construct lacking the IME element (Table 2.1), suggests that it is not functional in the context of an unspliced, 5' truncated intron, and thus may be involved more in posttranscriptional recruitment of exon junction complex components than in pre-transcriptional recruitment of spliceosomal components.

The only other known Arabidopsis *cis*-elements found within the *RPL23aA*/*B* second introns are putative CAAT-boxes (three per paralog). Within the *AGAMOUS* second intron, repeated, evolutionarily conserved CAAT-box motifs of the longer consensus $^{5'}$CCAATCA$^{3'}$ were shown to be important for maintaining gene expression (Hong et al., 2003). CAAT-boxes are binding sites for the trimeric nuclear factor Y (NF-Y) complex and, in Arabidopsis, each monomer is encoded by a family of 9–10 members (Gusmaroli et al., 2001, 2002). It is possible that the CAAT-boxes of the *RPL23aA* and *RPL23aB* second introns actively bind specific NF-Y complexes to enhance transcription.

2.4.5 Transcript properties of *RPL23aA*/*B* may enhance stability and translational efficiency

Features of *RPL23aA* and *RPL23aB* 3' UTRs were found to be conserved among other Arabidopsis r-protein genes and with Arabidopsis genes predominantly regulated at the translational level (Kawaguchi and Bailey-Serres, 2005). The 3' UTRs are generally A/U-rich and of moderate length (~200 nt, Table A.2), which is shorter than the reported optimal length for ribosome loading (280–320 nt, Kawaguchi and Bailey-Serres, 2005), but presumably long enough to allow for ribosome reinitiation (> 40–120 nt) and short enough to prevent triggering non-sense mediated decay (Kertesz et al., 2006). Both *RPL23a* paralogs possess 3' UTR motifs that are overrepresented slow turnover mRNAs, including $^{5'}$UCUCUU$^{3'}$ (+561 and +563 relative to AUG start codons of *RPL23aA* and *RPL23aB*, respectively), $^{5'}$AUCUCU$^{3'}$ (+528, *RPL23aA*; +614, *RPL23aB*), $^{5'}$UGCUUU$^{3'}$ (+580, *RPL23aA*; +626, *RPL23aB*), and $^{5'}$UUAUCU$^{3'}$ (+631, RPL23aB only, Narsai et al., 2007), but these were not detected as common motifs among all r-proteins (Figure 2.9). Neither *RPL23aA* or *RPL23aB* contain a consensus near upstream element ($^{5'}$AAUAAA$^{3'}$), or cleavage site ($^{5'}$YA$^{3'}$ dinucleotide within a U-rich stretch, Loke et al., 2005) but this is not unexpected given the variation among poly-A signals and the relatively poor consensus of 3' UTR motifs in plants (Ji et al., 2007; Loke et al., 2005; Narsai et al., 2007).

We found that the *telo*-box, an element with a defined role in transcriptional regulation that binds AtPurα (Tremousaygue et al., 1999; Welchen and Gonzalez, 2005) and maps adjacent to a DNase I hypersensitivity site in the Arabidopsis *PCNA1* gene (Kodama et al., 2007), was a common 5' UTR feature of *RPL23a* dicot orthologs, and most Arabidopsis r-proteins, including *RPL23aB* (Figure 2.8 and 2.9). It is tempting to speculate that it may additionally function

posttranscriptionally to mediate polysome formation on r-protein transcripts, but our finding that it is present in both orientations seems to argue against this notion.

2.4.6 Summary

How do *telo*-box and site II motifs regulate Arabidopsis *RPL23a* paralogs and other coordinately regulated genes? Li et al. (2005a) postulated that in actively dividing cells, class I TCP-domain transcription factors, such as TCP6, TCP11 (Li et al., 2005a), and TCP20 (Li et al., 2005a; Tremousaygue et al., 2003; Welchen and Gonzalez, 2005) bind specifically to site II motifs and function as transactivators, possibly as hetero- or homodimers (Kosugi and Ohashi, 1997, 2002). One known TCP binding partner, AtPurα (Tremousaygue et al., 2003), binds specifically to the *telo*-box (Tremousaygue et al., 1999; Welchen and Gonzalez, 2005) and given that the human homolog to AtPurα has DNA helix destabilizing properties (Darbinian et al.) and that DNase I hypersensitivity has been mapped next to the *telo*-box of Arabidopsis *PCNA1* (Kodama et al., 2007), AtPurα and class I TCPs might function coordinately to displace nucleosomes and facilitate the binding of TFIID or additional transcription factors. As cells exit the meristematic region, or in response to negative growth stimuli, class II TCPs, such as TCP2 and TCP4, which are negative regulators of cell division (Crawford et al., 2004; Nath et al., 2003; Palatnik et al., 2003), may displace class I TCPs on site II motifs and concomitantly downregulate gene expression (Li et al., 2005a). In Arabidopsis, for example, *TCP4* was found to be miRNA-regulated and expression of a *TCP4* variant (*mTCP4*), with point mutations preventing miRNA-guided *TCP4* degradation, led to growth arrest (Palatnik et al., 2003). Interestingly, the seedling-arrested phenotype identified by Palatnik et al. (2003) strongly resembles that produced by silencing both *RPL23a* paralogs (Degenhardt and Bonham-Smith, 2008a), suggesting that the observed *mTCP4* phenotype may indeed result from the negative regulation of site II-motif containing genes, such as r-proteins including *RPL23aA* and *RPL23aB*.

Expression of RPL23a in Arabidopsis is the result of complex network of regulatory controls operating at multiple levels. Transcription depends on a core promoter architecture that is largely conserved between paralogs, and includes TSS-distal site II motifs, downstream *telo*-boxes and a TATA-box with a highly conserved spacing requirement (~30–40 bp upstream of the TSS). These core promoter elements couple *RPL23aA*/*B* expression to the physiological status of the cell, and hence are sufficient for inducing expression in mitotically active tissues and repressing expression in response to negative growth stimuli. The leader and second introns

of *RPL23a* paralogs function posttranscriptionally to enhance transcription, possibly mediated through recruitment/occupation of introns with spliceosomal and/or exon junction complex RNPs. Translational regulation appears to be mediated through both conserved transcript *cis*-elements (e.g. similar initiator; Figure A.1) that may enhance ribosome loading, and transcript properties (i.e. 3' UTR length and sequence) that increase *RPL23aA*/*B* mRNA half-life. Future work will be required to (1) quantify the relative importance of each level of regulation, (2) determine the role of post-translational regulation (protein turnover) in RPL23a expression, and (3) to identify the precise elements and/or positional information responsible for the observed differences in spatiotemporal regulation of RPL23a.

3 CHAPTER 3. TRANSCRIPT PROFILING DEMONSTRATES ABSENCE OF DOSAGE COMPENSATION IN ARABIDOPSIS FOLLOWING LOSS OF A SINGLE *RPL23a* PARALOG

A version of this chapter has been accepted for publication in Planta. Under the supervision of PC Bonham-Smith, I designed and conducted all experiments and wrote the manuscript. Permission to use was obtained from the publisher and is contingent on the following citation.

Degenhardt, R.F. and Bonham-Smith, P.C. (2008) Transcript profiling demonstrates absence of dosage compensation in Arabidopsis following loss of a single RPL23a paralog. *Planta*, DOI: 10.1007/s00425-008-0765-6.

The original publication is available at www.springerlink.com

Mechanisms involved in coordinating expression of r-proteins must be dynamic, allowing for adjustments to fulfill biological requirements for protein synthesis during development, and following stress induction of global changes in gene expression. In this study, I investigated whether r-protein paralogs are feedback regulated at the transcript level by obtaining a T-DNA knockout of one member, *RPL23aB*, from the two-member *RPL23a* family. Expression of the lone functional paralog, *RPL23aA*, in this line was compared to the expression of both paralogs in wildtype plants under non-stressed, low-temperature-, and high-light stresses. *RPL23aA* expression was not upregulated in *RPL23aB* knockouts to compensate for paralog-loss, and consequently knockouts showed reduced total abundance of *RPL23a* transcripts. However, no abnormal phenotype developed in *RPL23aB* knockouts, suggesting that this paralog is dispensable under experimental conditions examined, or that compensation by *RPL23aA* may occur post-transcriptionally. Patterns of *RPL23aA* and *RPL23aB* transcript accumulation in wildtype plants suggest that paralogs respond coordinately to developmental and stress stimuli.

3.1 Introduction

The plant cytoplasmic ribosome is a RNP enzyme that catalyzes peptidyl transferase activity. In the flowering plant Arabidopsis, it is comprised of two subunits of unequal size: a LSU (60 S) with a core of three rRNAs (5 S, 5.8 S, 26 S) and 48 associated r-proteins, and a SSU (40 S) with a single core rRNA (18 S) and 33 associated r-proteins (Barakat et al., 2001; Chang et al., 2005). The subunits form within the nucleolus, a non-membrane bound substructure of the nucleus, and are subsequently exported to the cytoplasm where they assemble on messenger RNA (mRNA).

Regulation of ribosome biogenesis in plants is complicated by the existence of one or more paralogs for every r-protein gene. For example, recent annotation suggests that there are approximately 259 (152 LSU and 107 SSU) and 228 (139 LSU and 89 SSU) r-protein genes for the 81 r-proteins in Arabidopsis and rice (*Oryza sativa*), respectively (Barakat et al., 2001; Chang et al., 2005, and unpublished observations). As the translating ribosome contains only a single molecule of each r-protein, with the exception of the acidic P-proteins (RPP1 to RPP3, Ban et al., 2000; Guarinos et al., 2003; Hanson et al., 2004; Schuwirth et al., 2005; Wimberly et al., 2000), plants must possess mechanisms to govern both the coordinated production and equimolar accumulation of r-proteins. In budding yeast, regulation of r-protein paralogs occurs predominantly at the transcriptional level. Each r-protein transcript accumulates to roughly stoichiometric amounts (Kim and Warner, 1983). In families with more than one expressed paralog (59 of 79 yeast r-proteins are encoded by two genes, Planta and Mager, 1998), transcription rates of family members are modulated to ensure equimolar accumulation. For example, the two RPS10 paralogs of yeast are reportedly each transcribed at approximately half the rate of single-copy r-protein genes (Warner et al., 1985). In plants, evidence suggests that r-protein regulation occurs predominantly post-transcriptionally, via partitioning of r-protein transcripts in either the polysomal (actively translated) or RNP (inactive) fractions. For example, in response to sucrose starvation (Nicolai et al., 2006), drought (Kawaguchi et al., 2004), or hypoxia (Branco-Price et al., 2005), r-protein transcripts exhibit a coordinated decrease in polysomal loading. Nevertheless, transcriptional regulation is also important given findings that r-protein transcripts from a number of plant species show their greatest accumulation in mitotically active tissues and are coordinated upregulated following wounding and phytohormone treatments (reviewed in McIntosh and Bonham-Smith, 2006).

Several studies have investigated the functional consequence of absent/reduced expression of a single r-protein paralog. The findings that loss of single paralogs from the RPS5 (Weijers et al., 2001), RPS13 (Ito et al., 2000), RPS18 (Van Lijsebettens et al., 1994), RACK1 (Chen et al., 2006), RPL23a (Degenhardt and Bonham-Smith, 2008a), and RPL24 (Nishimura et al., 2004) families affects development suggests that compensation from other paralogs is either absent or insufficient. Support for absence of compensation comes from analysis of a RPS18A knockdown (Van Lijsebettens et al., 1994), which reportedly resulted in a 10-fold reduction in *RPS18A* transcript accumulation, but caused no compensatory increase in levels of *RPS18B* or *-C*

transcripts relative to wild-type plants (Vanderhaeghen et al., 2006). However, in tobacco, RNAi-mediated silencing of the predominantly expressed paralog of the two member RPL3 family, *RPL3A*, caused a substantial increase in *RPL3B* transcript levels, suggesting that the RPL3A protein might negatively regulate expression of *RPL3B* (Popescu and Tumer, 2004). The extent to which plants transcriptionally compensate for up/down regulation of a single paralog from an r-protein family remains to be determined.

Arabidopsis RPL23a is the plant ortholog of the L23/L25 family that is found in all domains of life (Lecompte et al., 2002). Structural studies on its yeast and bacterial counterparts (L25 and L23, respectively), have shown direct binding to LSU rRNA and mapped this r-protein to the bottom of the LSU, adjacent to the polypeptide exit tunnel (Nissen et al., 2000; Spahn et al., 2001). It functions in the cotranslational-targeting of nascent polypeptides through its association with both the RNP SRP subunit, SRP54, and the translocon pore of the endoplasmic reticulum (Beckmann et al., 1997; Menetret et al., 2005; Morgan et al., 2002; Pool et al., 2002). In Arabidopsis the RPL23a family contains two members (*RPL23aA* and *RPL23aB*), which encode proteins differing by only 8 amino-acids. Both members are transcribed and translated, and either can be incorporated into the ribosome (Carroll et al., 2008; McIntosh and Bonham-Smith, 2005). RPL23a is essential in Arabidopsis, as loss-of-function of both members is lethal (Degenhardt and Bonham-Smith, 2008a). While no abnormal phenotype develops following downregulation of *RPL23aB* via RNAi, a reduction in transcript level of *RPL23aA* leads to development of a severe *pointed first leaf* (*pfl*) phenotype (Degenhardt and Bonham-Smith, 2008a), similar to that produced by other r-protein single-paralog mutants (Ito et al., 2000; Nishimura et al., 2005; Van Lijsebettens et al., 1994; Weijers et al., 2001).

In plants, exposure to stress, such as low temperature or high light, evokes short and long-term responses causing global changes in the cellular proteome (Kultz, 2005), which in turn presumably requires modulation of ribosome biogenesis mediated through changes in expression levels of structural components. Here I have investigated whether Arabidopsis, under both non-stessed and stressed conditions, alters regulation of r-protein transcript levels following loss of a single paralog from a two-member family. Accordingly, a T-DNA insertional knockout line of *RPL23aB* (hereafter *B*KO) was obtained and the levels of *RPL23aA* transcript were profiled and compared to corresponding levels of *RPL23aA* and *RPL23aB* transcripts in wildtype (WT) plants

during development and in response to light and temperature stresses. Results suggest that paralog expression is regulated independently at the level of transcription.

3.2 Materials and Methods

3.2.1 Plant material

Arabidopsis (cv. Columbia-0) WT or transgenic seed was bleach-sterilized (2.625% sodium hypochlorite, 0.5% Tween 20 [Calbiochem]) for 5 min followed by sequential washes with water, or vapor-phase sterilized for 16–20 h (Clough and Bent, 1998), and sown in a vermiculite/peat soil (Redi-Earth, WR Grace & Co.) or, as indicated, on basal media (2.17 g/L MS salts [PhytoTechnology Laboratories], 1.5% sucrose, 0.8% phytagar [Invitrogen], pH 5.7). Prior to stress treatments, plants were grown with a 23/18 ºC temperature regime and a 16/8 h photoperiod of ~120 µmol photons m^{-2} s^{-1}. All collected material was flash frozen in $N_{2(l)}$ and ground with a mortar and pestle prior to RNA extraction.

3.2.2 T-DNA lines

Arabidopsis T-DNA insertion lines were obtained from the ABRC (Alonso et al., 2003; Sessions et al., 2002). Four hemizygous lines with putative insertions in or near *RPL23aA* (SAIL-258-C12 and SALK-091329.46.50) or *RPL23aB* (SAIL-597-B08 and SAIL-444-A06) were made homozygous by successive inbreeding. Zygosity was confirmed by conducting PCR on genomic DNA isolated from ABRC lines using two sets of primers: one set designed to flank the T-DNA insert, producing an amplicon only from WT and heterozygous plants (Table B.1, left primers [LPs] and right primers [RPs]), and one set designed to produce an amplicon extending into the genome from the left border of a T-DNA insert, producing an amplicon only from plants heterozygous or homozygous for the insert (Table B.1, left border primers [LBs] and RPs). Genomic DNA was isolated using the DNeasy Plant Mini kit (Qiagen), following the manufacturer's instructions. For PCRs, each reaction was set up to produce a single amplicon following 30 cycles amplification (2 cycles of 3 min at 94 °C, 30 s at 50 °C and 2 min at 72 °C, followed by 28 cycles of 30 s at 94 °C, 30s at 53 °C and 1.5 min at 72 °C) from 100 ng genomic DNA template using either LP + RP primers, or LB + RP primers (200 pM each). Homozygous lines (T_6 to T_7) were screened for the presence of *RPL23aA* or *RPL23aB* transcripts by RT-PCR using previously described methods (McIntosh and Bonham-Smith, 2005) and gene-specific primers (Figure B.1). RT-PCR results were verified by conducting qRT-PCR on homozygous T-

DNA lines as described below. I attempted to obtain another line with a putative T-DNA insertion in the 3rd exon of *RPL23aA*, GABI_531C01, but seed was unavailable (GABI-KAT, personal communication) and I suspect this may be due to embryo lethality of heterozygous/homozygous *RPL23aA* knockouts (cf. Degenhardt and Bonham-Smith, 2008a).

3.2.3 Knockout verification by *RPL23aA*-silencing

*B*KOs (T_6 to T_7) were infiltrated with a previously described estrogen-inducible *RPL23aA*-silencing cassette (RPL23aA–ihp, Degenhardt and Bonham-Smith, 2008a) via the floral dip protocol (Clough and Bent, 1998), generating *B*KO–*A*ihp transgenics. Stable transformants were selected on basal media supplemented with 25 μg ml^{-1} hygromycin (InvivoGen) and 200 μg ml^{-1} cefotaxime (Sanofi-Aventis). Silencing of *RPL23aA* was induced in T_2 transgenics by plating seed on basal media supplemented with 10 μM estradiol (Sigma-Aldrich) and grown as described above.

3.2.4 Seedling and mature tissue analysis

Wildtype and *B*KO seed were sown in soil as described above. Whole seedlings were collected at 15–19 days old. Six tissues were collected from 35 day-old plants: mature leaf, internodal stem sections, closed buds, open flowers, small green siliques (< 1 cm) with petioles and large green siliques (>1 cm) with petioles. A minimum of three biological replicates (batches of seedlings or separate plants for tissues) were analyzed.

3.2.5 Photoinhibition treatment

Photoinhibition was conducted essentially as described by Gray et al. (2003), with minor modifications. Wildtype and *B*KO seedlings (15–19 day-old) were thinned to 2–3 per pot and four pots per genotype were treated in each experiment. Pots were moved to 4 °C and continuously exposed to 1150–2400 μmol photons m^{-2} s^{-1}, generated by a 400 W metal halide lamp (Philips, Scarborough, ON, Canada). Pots were rotated every 1 h to minimize the effects of spatial variation in temperature/light. After 5 h photoinhibition, plants were placed at 20 °C under continuous light (<3 μmol photons m^{-2} s^{-1}) for recovery. Whole seedlings with roots removed were collected after 0 (pre-treatment), 1, 3 and 5 h exposure, and following 24 and 48 h recovery. The entire experiment was repeated four times.

3.2.6 Low temperature stress treatment

Nineteen day-old WT and *B*KO seedlings were thinned to three per pot and moved to one of three trays in a growth chamber with a 4 °C constant temperature and a 16/8 h photoperiod of 90–100 μmol photons m^{-2} s^{-1}. Trays were rotated within the chamber 2–3 times per week. Whole seedlings with roots removed were collected after 0 (pre-treatment), 1, 4, 8, 24, 48, 168 (7 d), and 336 h (14 d) treatment. At the 14 d sampling, leaves that had emerged prior to cold-treatment were collected separately from leaves that had emerged subsequent to cold-treatment. Seedlings were incubated for an additional 14 d at 4 °C to allow for growth of leaves that had emerged in the cold and then were returned to pre-treatment growing conditions and sampled following 15 min, 1 and 24 h recovery. Plants from each of three trays were harvested and processed separately to provide biological replication.

3.2.7 High light stress treatment

Nineteen day-old WT and *B*KO seedlings were thinned to three per pot and moved to one of three trays in a growth chamber with a 23/17 °C temperature regime and a 16 h/8 h photoperiod of 200–250 μmol photons m^{-2} s^{-1} for 1 h, followed by 300–330 μmol photons m^{-2} s^{-1}. Whole seedlings with roots removed were collected after 0 (pre-treatment), 1, 4, 8, 24, 48, 168, and 336 h treatment. At the 7 and 14 d samplings, rosette and bud tissues were collected separately. Plants from each of three trays were harvested and processed separately to provide biological replication.

3.2.8 Quantitative RT-PCR and statistical analyses

Techniques for extraction of total RNA, RNA quantitation, DNase I treatment, first-strand synthesis and qRT-PCR were previously described (Degenhardt and Bonham-Smith, 2008a). Primers for amplification of *RPL23aA*, *RPL23aB* and *ACTIN7* (*ACT7*), the internal control, were designed to produce amplicons of ~200 bp and have a uniform Tm of ~60 °C (Table B.1). A minimum of three biological replicates were analyzed for each treatment. Optical data collection and C_t determination were done using the iQ5 Optical System software (Bio-Rad). Data from each treatment were analyzed within separate mixed models using the SAS Statistical Analysis software (SAS Institute). Treatment level (time period or tissue type) and genotype effects were considered fixed and replicates were considered as a random effect. Gene effects were originally included in the model as a fixed effect, but were ultimately analyzed in separate models due to

heterogeneous error variances. To correct for small sample size, the denominator degrees of freedom was adjusted using the method outlined by Kenward and Roger (1997). Pairwise comparisons of least-squares means were considered significant when $P \leq 0.05$. Trends are discussed at $P < 0.10$.

3.2.9 Detection of a stress-induced transcript

To verify that the imposed photoinhibition, low temperature and high light-regimes induced stress responses, RT-PCR was conducted to detect the presence of *COR15A*, a cold-, dehydration-, abscisic acid- and high light-responsive gene (Kimura et al., 2003; Lin and Thomashow, 1992; Seki et al., 2002; Wilkosz and Schlappi, 2000). Total RNA was extracted from seedlings pre-treatment, and following 1 and 3–4 h of stress treatments. For first-strand synthesis, 100 ng of DNase-treated RNA was combined with 5 pmoles of *COR15A* and *ACT7* reverse primers and 200 units of RevertAid H- RT (Fermentas) as per manufacturer's instructions. PCR amplifications were set up to produce single amplicons following 1 cycle of 1 min at 94 °C, 30 s at 52 °C and 30 s at 72 °C, and 27 cycles of 30 s at 94 °C, 30 s at 55 °C and 30 s at 72 °C using Taq polymerase and 10% of the first-strand product as template. Amplification products were resolved on a 1.5% agarose gel stained with EtBr. Primers for amplification of *COR15A* were previously described (McIntosh and Bonham-Smith, 2005). For each stress treatment, RT-PCR analysis was conducted on RNA from a single biological replicate.

3.2.10 Microscopy

Digital images of *B*KO, *B*KO–*A*ihp transgenics and WT plants were taken with a Zeiss Stemi 2000-C stereomicroscope (Jena, Germany). Vasculature was examined as previously described (Degenhardt and Bonham-Smith, 2008a). Approximately 8–10 cleared seedlings were analyzed for each genotype (WT and *B*KO).

3.3 Results

Four lines with putative T-DNA insertions in or near *RPL23aA* or *RPL23aB* genes were obtained from ABRC. Lines were selfed and T_5–T_6 progeny homozygous for the T-DNA insertions were screened for the presence of *RPL23aA* and *RPL23aB* transcripts by RT-PCR. Line SAIL-444-A06 was found to have no T-DNA insert proximal to *RPL23aB* (data not shown). All remaining lines except SAIL-597-B08 (*B*KO), which produced no *RPL23aB* transcript, were

found to have wild-type transcript levels as determined by RT-PCR (Figure B.1) and qRT-PCR (data not shown). T_6 and T_7 *B*KOs were used for all experiments.

To functionally verify the *RPL23aB* knockout, I introduced an estrogen-inducible cassette into *B*KOs that specifically targets *RPL23aA* for RNAi-mediated silencing (Degenhardt and Bonham-Smith, 2008a). Seventeen stably transformed lines were obtained (*B*KO–*A*ihp–1 to *B*KO–*A*ihp–17). Eight of these lines were non-viable when plated on inductive media and an additional seven showed a severe pleiotropic phenotype consistent with that produced by silencing both *RPL23aA* and *RPL23aB* (e.g. BKO–Aihp–2 and –7, Figure 3.1a, cf. Degenhardt and Bonham-Smith, 2008a). These results confirm that *RPL23aB* expression is lost in *B*KOs. *B*KO–*A*ihp lines provide a robust system for the inducible analysis of *RPL23a* loss-of-function mutants.

3.3.1 *RPL23aB* knockouts produce no abnormal phenotype

Previous work has shown that RNAi-mediated silencing of *RPL23aB* does not affect growth or development of Arabidopsis (Degenhardt and Bonham-Smith, 2008a). However, this technique conferred a maximum 45% decrease in *RPL23aB* transcript levels. To determine if an *RPL23aB* null mutant affects development, I compared the growth of WT and *B*KO plants, in soil and on basal media, under normal growing conditions. No appreciable differences were observed in rate of development, morphology, flowering or fecundity of *B*KOs (Figure 3.1b). Several r-protein mutants have abnormal vasculature (Degenhardt and Bonham-Smith, 2008a; Ito et al., 2000; Nishimura et al., 2005), characterized by a reduction in higher order venation and loss of closed, reticulate patterning. Leaves of the *B*KO were cleared and the venation examined by dark-field microscopy. Vascular patterning was found to be consistent with that of WT plants (Figure 3.1c). Together, these results suggest that *RPL23aB* is not required under normal growing conditions.

3.3.2 RPL23aA and *RPL23aB* transcript profiling

Prior work in our lab investigated the relative transcript abundance of *RPL23aA* and *RPL23aB* in WT plants using a semi-quantitative RT-PCR approach (McIntosh and Bonham-Smith, 2005). This study showed that *RPL23aA* and *RPL23aB* are predominantly coordinately regulated, but

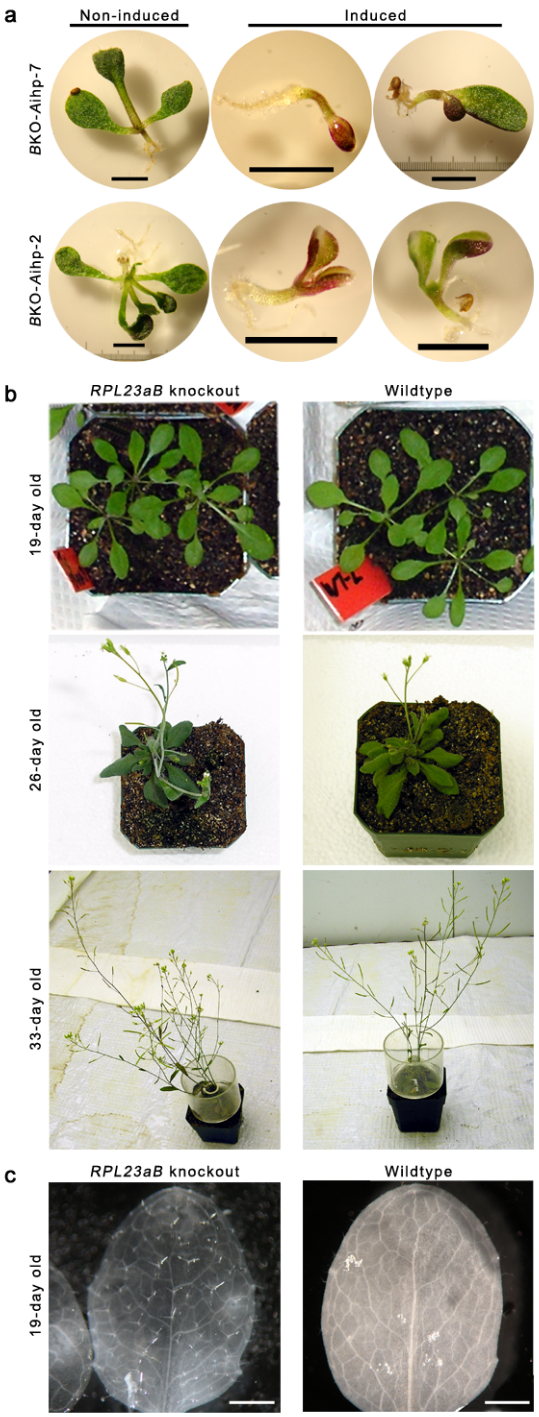

Figure 3.1 Phenotype of *RPL23aB* knockouts (**b–c**) or *B*KOs with silenced *RPL23aA* (**a**). **a** Twelve day-old *B*KO–*A*ihp–2 and –7 T_2 seedlings grown on basal media augmented with 25 µg ml^{-1} hygromycin, and 0 (non-induced) or 10 µM estradiol (induced). Bars are 2 mm. **b** Nineteen, 26, and 33 day-old *B*KO and WT plants grown in soil. **c** Darkfield micrographs showing first leaf venation of 19 day-old *B*KO and WT plants. Bars are 1 mm.

accumulated divergently in response to very specific treatments. For example, both paralogs were upregulated in response to the auxin, IAA, and the cytokinin, 6-benzylaminopurine, while in response to heavy metal stress by copper sulfate *RPL23aA* transcript abundance decreased whereas abundance of *RPL23aB* remained static (McIntosh and Bonham-Smith, 2005). To buildon these previous findings, I have used a quantitative RT-PCR approach to transcriptionally profile paralog levels in WT and *B*KO plants during development and in response to temperature and light stresses. To that end, plants of each genotype were treated (see Materials and Methods), total RNA was extracted, and two-step qRT-PCR was conducted using *ACT7* as an internal control to standardize *RPL23aA* and *RPL23aB* transcript levels. Based on threshold cycle values, the level of *ACT7* did not vary appreciably within each treatment (data not shown).

3.3.3 Paralog expression in seedlings and mature tissues

In WT plants the transcript level of *RPL23aA* was greater than that of *RPL23aB* in seedlings and all mature plant tissues (Figure 3.2), consistently comprising about 75% of the total *RPL23a* transcript pool (range 69% in stem to 76% in seedling). Both transcripts were most abundant in seedlings, buds, open flowers and large siliques, while significantly lower accumulation was detected in mature leaves and stems. In green elongating siliques, *RPL23aA* transcripts were significantly less abundant than in seedlings (~73% reduction) and *RPL23aB* transcripts also showed a trend of reduced accumulation (~68 % reduction, $P = 0.096$). The accumulation of *RPL23aA* transcripts in *B*KOs mirrored that in WT plants, with the exception of elongated siliques where accumulation was reduced relative to WT and *B*KO seedlings (Figure 3.2).

3.3.4 Paralog expression during photoinhibition

Photoinhibition is a reduction in photosynthetic capacity due to light exposure beyond what can be utilized photochemically (Gray et al., 2003; Oquist et al., 1992). It results from oxidative damage to the D1 reaction centre protein of photosystem II (PSII) and/or the increased dissipation of light energy through non-photochemical means via inactivation of PSII reaction centres (Aro et al., 1993; Gray et al., 2003; Oquist et al., 1992). It induces a stress response in plants that causes global transcriptional changes and reprogramming of metabolic pathways (Pnueli et al., 2003; Scarpeci and Valle, 2008; Vandenabeele et al., 2003). To determine the effect of this stress response on expression of *RPL23a* paralogs, I exposed non-acclimated WT

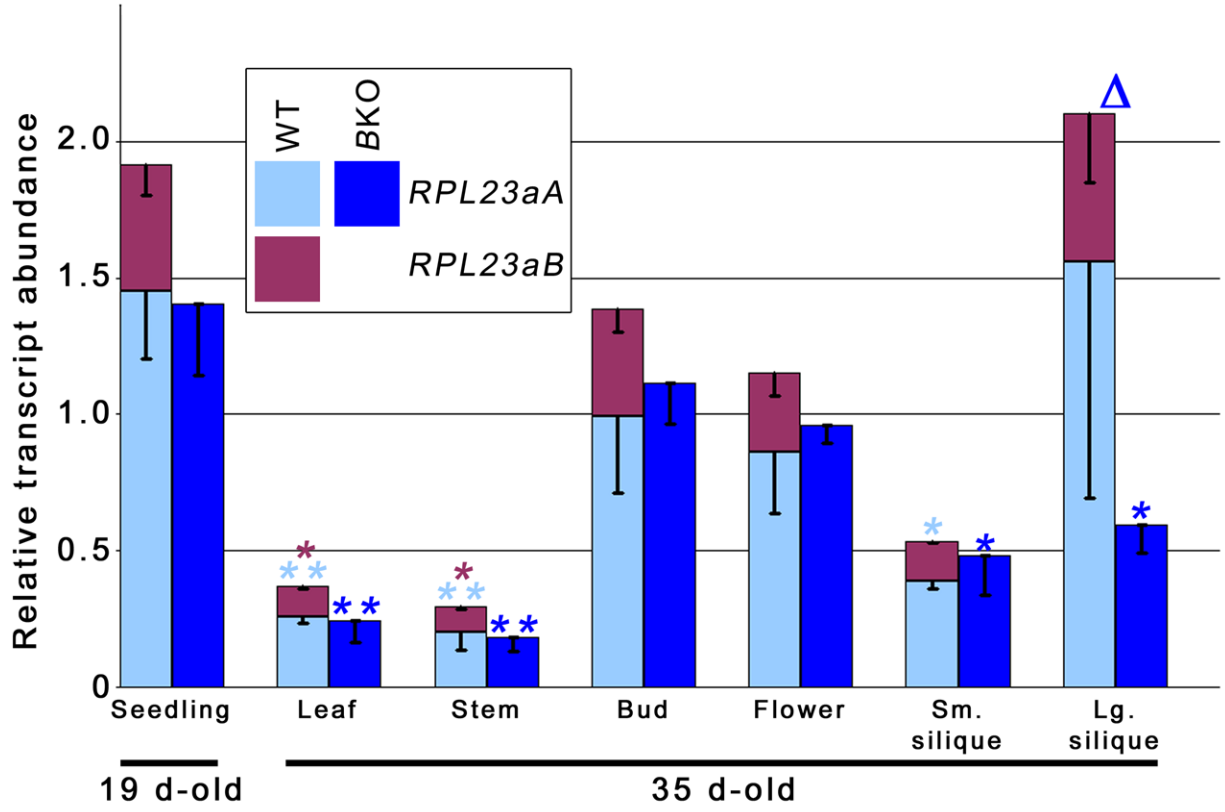

Figure 3.2 Quantification of *RPL23aA* and *RPL23aB* transcript abundance in wildtype and *RPL23aB* knockout whole seedlings (15–19 day-old) and mature plant tissues (35 day-old). Light blue and dark blue columns represent the *ACT7* standardized level of *RPL23aA* in WT and *B*KO plants, respectively. Purple columns represent the standardized level of *RPL23aB* in WT plants. Black bars show SE. For each genotype, transcript levels in mature tissues that differ significantly at $P \leq 0.05$ and $P < 0.01$ from levels in seedlings are indicated by asterisks (* and **, respectively) above columns. The Δ symbol between columns indicates a significant difference in *RPL23aA* levels between WT and *B*KO tissues.

and *B*KO plants to high irradiance and low temperature, conditions which have previously been shown to predispose plants to rapid photoinhibition (Gray et al., 2003; Huner et al., 1993). Following 1–3 h photoinhibition *COR15A* (positive control), a cold and high light-responsive gene (Kimura et al., 2003; Lin and Thomashow, 1992), showed a clear induction in WT and *B*KO plants relative to pre-treatment, indicating that the light regime used caused a stress response (Figure 3.3a). I observed a basal level of *COR15a* expression under non-stressed conditions, and this is in agreement with previous findings (Sakuma et al., 2006; Xiong et al., 2001). In WT and *B*KO plants, *RPL23a* paralogs showed a trend of increased transcript abundance during the photoinhibition, but due to variability within replicates these differences were not significant (Figure 3.3b). During recovery, transcript levels of *RPL23aB* in WT plants dropped significantly, while those of *RPL23aA* showed a downward trend in both WT and *B*KO plants. When replicates were analyzed independently, each replicate showed a transient increase in transcript levels after 1–5 h of photoinhibition, followed by a decrease in levels (data not shown). On the assumption that a certain threshold of irradiance might trigger the spike, and based on the observed variation in irradiance between replicates (e.g. replicate 1 irradiance = 1150–1200 µmol photons m^{-2} s^{-1}, replicate 2 irradiance = 1800–2400), the data were reanalyzed with values for the spike pooled into a single time category (1–5, Figure 3.3c). This analysis showed that *RPL23aB* transcript levels in WT plants increased by ~43% during photoinhibition relative to pre-treatment levels, and subsequently decreased during recovery ($P < 0.06$). Similarly, photoinhibition led to a ~48% increase in transcript levels of *RPL23aA* in *B*KO plants, followed by a decrease to ~40% of pre-treatment levels during recovery. Consistent with mature tissue experiments, *RPL23aA* levels between WT and *B*KO plants were similar during photoinhibition and recovery.

3.3.5 Paralog expression during low temperature stress

Exposure to low, non-freezing temperatures induces a well characterized signaling cascade that alters gene expression to provide increased tolerance to freezing and drought (Fowler and Thomashow, 2002; Kim, 2007; Yamaguchi-Shinozaki and Shinozaki, 2006). I grew WT and *B*KO plants for 19 d at 23/18 ºC, then transferred them to 4 ºC for 28 d to monitor expression of *RPL23a* paralogs during cold acclimation. *COR15A* was upregulated in WT and *B*KO plants relative to pre-treatment levels following 1 h cold treatment, and was strongly induced by 4 h

Figure 3.3 Quantification of *RPL23aA* and *RPL23aB* transcript abundance in 15–19 day-old wildtype and *RPL23aB* knockout seedlings photoinhibited at 4 °C and 1150–2400 µmol photons m^{-2} s^{-1} for 5 h and then allowed to recover for 48 h at 20 °C and <3 µmol photons m^{-2} s^{-1}. **a** Induction of *COR15A* (positive control) during photoinhibition. Gene specific primers were used to amplify *COR15A* (C) and *ACT7* (A; amplification control) from total RNA extracts of WT and *B*KO plants prior to stress-treatment (0 h) and following 1 h and 3 h of photoinhibition. Amplicons were 211 and 580 bp for *ACT7* and *COR15A*, respectively. Agarose gels were stained with EtBr. **b, c** Quantification of *RPL23a* paralogs. Columns and symbols as in Figure 3.2 legend. Asterisks indicate significant differences in transcript levels relative to time 0 h (pre-treatment). **c** Reanalysis of photoinhibition data from (**b**) to emphasize the transient increase in *RPL23aA* and *RPL23aB* levels. Time 1–5 shows the average maximum level of transcript accumulation for four biological replicates.

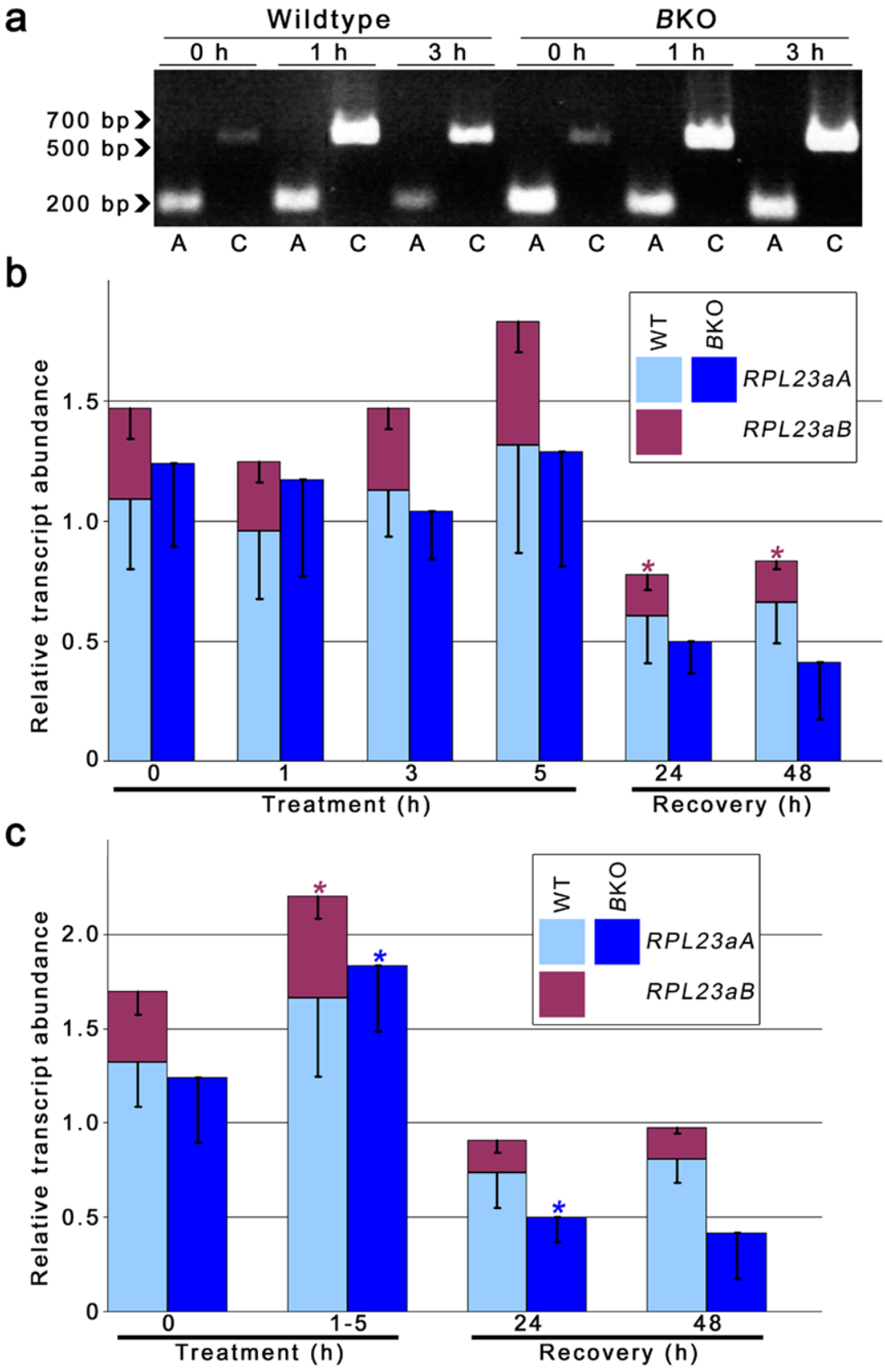
a
Wildtype
BKO
0 h
1 h
3 h
0 h
1 h
3 h
700 bp
500 bp
200 bp
A C A C A C A C A C A C
b
Relative transcript abundance
1.5
1.0
0.5
0
WT
BKO
RPL23aA
RPL23aB
0
1
3
5
24
48
Treatment (h)
Recovery (h)
c
Relative transcript abundance
2.0
1.5
1.0
0.5
0
WT
BKO
RPL23aA
RPL23aB
0
1-5
24
48
Treatment (h)
Recovery (h)

(Figure 3.4a). In contrast, transcript levels for *RPL23a* paralogs in both WT and *B*KO plants were relatively stable until 24 h after transfer to 4 ºC, at which time the abundance of *RPL23aB* in WT plants increased ~61% relative to pre-treatment levels (Figure 3.4b). Upregulation of *RPL23aB* continued through the 48 and 168 h samplings, and reached a maxima of 154% of pre-treatment levels at 336 h in leaves that had emerged post-cold transfer. In contrast, leaves that had emerged prior to cold transfer had similar *RPL23aB* levels at 336 h to whole seedlings at 0 h. Levels of *RPL23aA* were relatively static during cold treatment in both WT and *B*KO plants, but were highly upregulated in new leaves emerging during cold treatment, increasing to ~248 and ~208% of pre-treatment levels in WT and *B*KO plants, respectively (Figure 3.4b). During the 24 recovery period, both paralogs were rapidly and progressively downregulated in WT plants, dropping to ~16 and ~13% of pre-treatment levels for *RPL23aA* and *RPL23aB*, respectively, by 24 h recovery. The downregulation was slightly less rapid for *RPL23aA* in *B*KOs, as no significant decrease from pre-treatment levels was detected until 1 hr recovery. However, by 24 h recovery *RPl23aA* transcripts had decreased to ~10% of pre-treatment levels. Transcript abundance of *RPL23aA* was roughly equivalent in both genetic backgrounds during cold treatment, except after 336 h, at which time the level of *RPL23aA* was greater in older leaves of *B*KOs, which had emerged prior to cold treatment, than in older leaves of WT plants.

3.3.6 Paralog expression during high light stress

Photosystem II excitation pressure, a measure of the redox status of the plastoquinone Q_A electron acceptor, can be modulated by both temperature and irradiance (Gray et al., 1996; Huner et al., 1998). Plant growth under moderate to high irradiance at non-cold acclimating temperatures reportedly increases PSII excitation pressures and tolerance to photoinhibition (Gray et al., 2003; Gray et al., 1996). This process of photosynthetic acclimation results from altered stoichiometry of photosystem components, changes in pigment profiles, increased non-photochemical quenching, and redistribution of photosytem redox states (Bailey et al., 2004; Bailey et al., 2001). To determine the affect of moderate to high irradiance on transcript abundance of *RPL23a* paralogs, I grew WT and *B*KO plants for 19 d at ~120 µmol photons m^{-2} s^{-1} and then transferred them to 300–330 µmol photons m^{-2} s^{-1} for 14 d. Only a mild induction of *COR15A* was observed in WT and *B*KO plants following 1–4 h high-light stress treatment (Figure 3.5a), suggesting that this irradiance regime was less of a shock than the photoinhibition stress. In WT plants, transcript abundance of both paralogs was relatively stable until 48 h

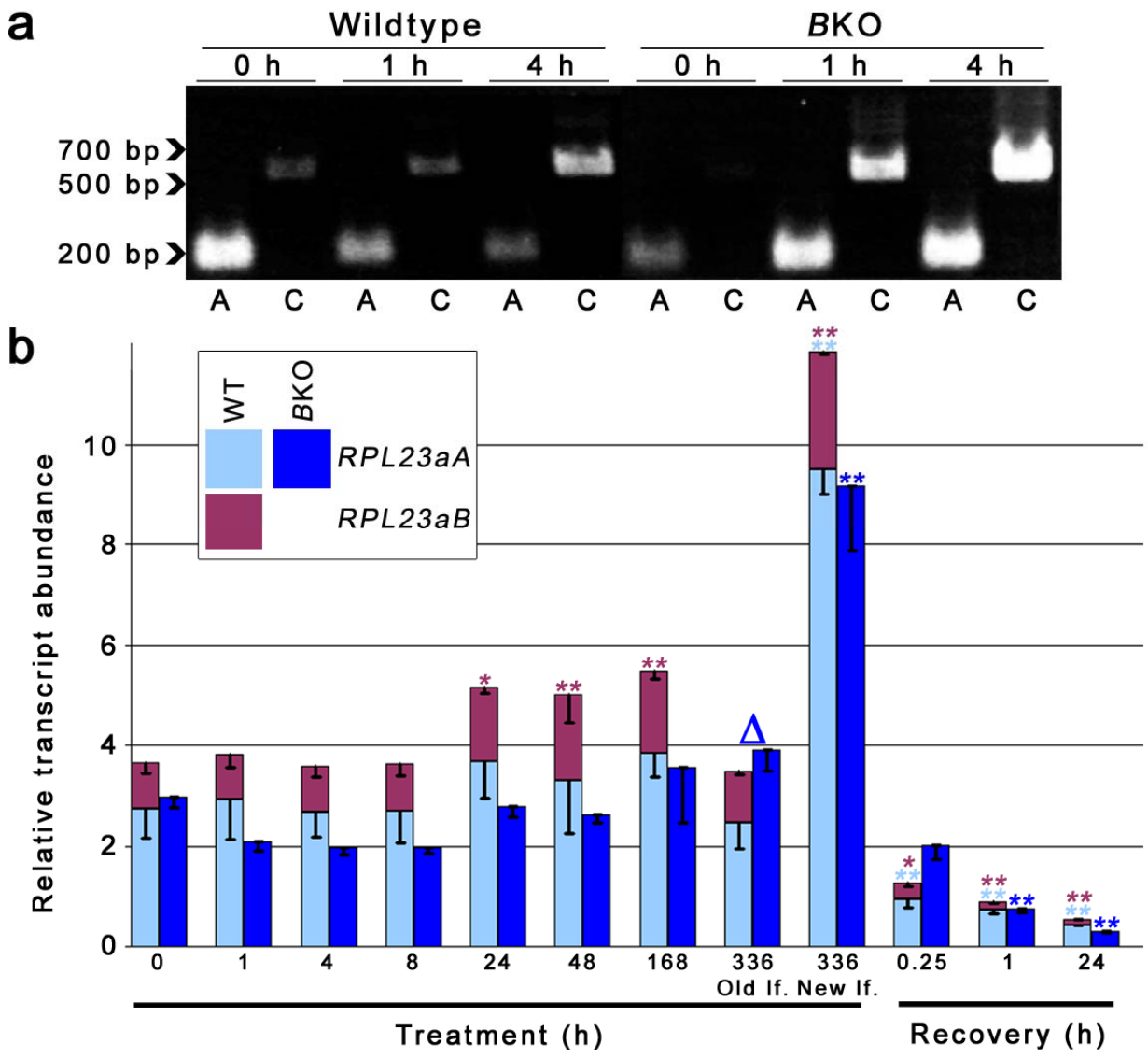

Figure 3.4 Quantification of *RPL23aA* and *RPL23aB* transcript abundance in 19 day-old wildtype and *RPL23aB* knockout seedlings incubated at 4 °C and 90–100 µmol photons m^{-2} s^{-1} for 28 d, and then allowed to recover for 24 h under pre-treatment conditions. **a** Induction of *COR15A* (positive control) during low temperature stress. See Figure 3.3 legend for details. **b** Quantification of *RPL23a* paralogs. Columns and symbols as in Figure 3.2 and 3.3 legends. After 336 h cold stress, leaves that had emerged prior to cold treatment (old lf.) were harvested separately from leaves that had emerged after treatment (new lf.)

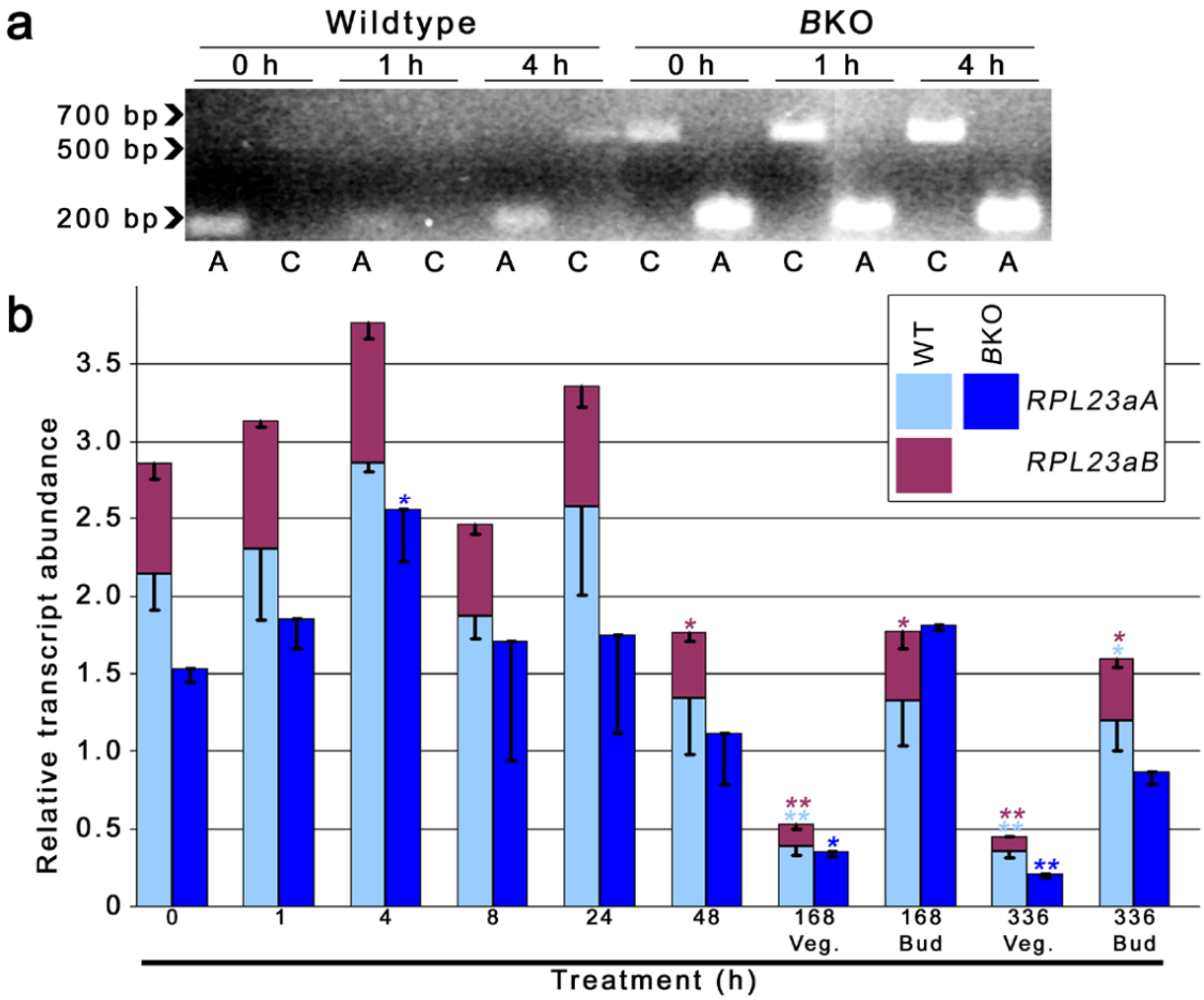

Figure 3.5 Quantification of *RPL23aA* and *RPL23aB* transcript abundance in 19 day-old wildtype and *RPL23aB* knockout seedlings incubated at 17/23 °C and 0/300–330 µmol photons m^{-2} s^{-1} for 18 d. **a** Induction of *COR15A* (positive control) during high light stress. See Figure 3.3 legend for details. Intervening lanes have been removed. **b** Quantification of *RPL23a* paralogs. Columns and symbols as in Figure 3.2 and 3.3 legends. After 168 and 336 h light stress, vegetative (veg.) and reproductive (bud) tissues were harvested separately.

treatment, at which time the levels decreased relative to pre-treatment ($P = 0.09$ and $P < 0.05$ for *RPL23aA* and *RPL23aB*, respectively; Figure 3.5b). By 168–336 h treatment, transcript abundance in vegetative tissues was ~16–18 and ~14–20% of pre-treatment levels for *RPL23aA* and *RPL23aB*, respectively. Paralog expression was higher in buds than in vegetative tissues at 168 and 336 h, but after 336 h treatment remained significantly lower than pre-treatment levels (Figure 3.5b). Abundance of *RPL23aA* transcripts in *B*KOs was transiently increased 4 h after treatment, and then steadily decreased to a low of ~14% pre-treatment levels in vegetative tissues following 336 h treatment. Consistent with WT plants, *RPL23aA* transcript levels were higher in bud tissues of *B*KOs than in vegetative tissues (Figure 3.5b). No significant differences were observed between levels of *RPL23aA* in WT and *B*KO plants during high light stress, although the level of *RPL23aA* in buds of *B*KOs dropped significantly between 168 and 336 h treatment and the corresponding time points in WT plants has similar levels of *RPL23aA*.

3.3.7 *RPL23a* transcript levels are reduced in *RPL23aB* knockouts

My results indicated that *RPL23aA* transcript abundance in *B*KOs paralleled the level in WT plants, suggesting that *B*KOs are deficient in total *RPL23a* transcripts. To confirm this deficiency, data from all experiments was reanalyzed such that the level of *RPL23aA* in *B*KOs was compared to the total *RPL23a* transcript level (*RPL23aA* + *RPL23aB*) in WT plants. The level of *RPL23a* transcript was found to be significantly less in *B*KOs than WT plants for at least one sampling period or tissue type from each experiment (Table 3.1). This was especially true for the low temperature and high light experiments, where *RPL23a* transcript abundance after 0–48 h of respective treatments was 32–48% less in *B*KOs than in WT plants (Table 3.1). However, no abnormal phenotype developed during or following any of the temperature or light-stress treatments (i.e. photoinhibition, low temperature and high light).

3.4 Discussion

Feedback regulation of a small number of r-proteins has been demonstrated in yeast and animals, mediated by the binding of r-proteins to their own pre-mRNA, which impairs splicing and often leads to rapid degradation of the non-spliced transcripts (reviewed in Ivanov et al., 2006). This form of regulation has been suggested to occur for the two member RPS28 family of peach (*Prunus persica*) based on the finding that non-spliced transcripts accumulate in non-

Table 3.1 Comparison of *RPL23a* transcript levels in wildtype and *RPL23aB* knockout plants. The difference between average total *RPL23a* transcript abundance in wildtype and *B*KO plants (mean difference) is listed along with results of the corresponding t statistic (t-stat.) and P-value ($P[H_0]$) for the statistical test of the null hypothesis that the total level of *RPL23a* transcripts is equivalent in WT and *B*KO plants. Positive and negative mean values indicate greater transcript abundance in wildtype and *B*KO plants, respectively. NS, no significant difference (H_0 not rejected). *, ** and *** indicate that transcript levels are significantly different at $P < 0.1$, 0.05 and 0.01, respectively, as determined by pairwise comparisons of least-squares means (H_0 rejected). Experiments were analyzed in separate mixed model ANOVAs.

Experiment				Experiment			
Seedling & Mature Tissues	Mean diff.	t-stat.	$P(H_0)$	Photoinhibition	Mean diff.	t-stat.	$P(H_0)$
Seedling	0.51	0.99	NS	0 h	0.23	0.95	NS
Leaf	0.13	0.24	NS	1 h	0.07	0.53	NS
Stem	0.07	0.13	NS	3 h	0.43	1.50	NS
Bud	0.27	0.49	NS	5 h	0.54	1.81	*
Flower	0.19	0.35	NS	24 h recovery	0.28	1.01	NS
Small silique	0.05	0.09	NS	48 h recovery	0.42	0.84	NS
Large silique	1.51	2.94	***				

Experiment				Experiment			
Low temperature	Mean diff.	t-stat.	$P(H_0)$	High light	Mean diff.	t-stat.	$P(H_0)$
0 h	0.67	0.83	NS	0 h	1.33	2.64	**
1 h	1.73	2.12	**	1 h	1.29	2.56	**
4 h	1.62	1.99	*	4 h	1.21	2.41	**
8 h	1.65	2.03	**	8 h	0.75	1.49	NS
24 h	2.37	2.91	***	24 h	1.61	3.22	***
48 h	2.40	2.96	***	48 h	0.65	1.30	NS
168 h	1.91	2.36	**	168 h veg.	0.18	0.36	NS
336 h old leaf	-0.40	-0.50	NS	168 h bud	-0.04	-0.08	NS
336 h new leaf	2.67	4.20	***	336 h veg.	0.24	0.49	NS
15 min recovery	-0.84	-1.29	NS	336 h bud	0.73	1.45	NS
1 h recovery	0.13	-0.02	NS				
24 h recovery	0.11	-0.06	NS				

mitotically active tissues (e.g. expanded leaves, mature stems), while only spliced transcripts are found in young, developing tissues (Giannino et al., 2000). My results would suggest against the existence of an analogous feedback mechanism regulating the RPL23a family in Arabidopsis. Loss of *RPL23aB* caused no appreciable increase in the level of *RPL23aA* transcript during development or in response to temperature and light stresses. Moreover, my results are consistent with experiments in yeast demonstrating that no intergenic transcriptional compensation occurred following individual disruption of *RPS17A* or *RPS17B* (Abovich et al., 1985). These single deletion haploid strains also had decreased growth rates and imbalanced ratios of 40 S : 60 S subunits, indicating an additional lack of post-transcriptional dose compensation. Conversely, the *B*KOs in my experiments developed no abnormal phenotype and showed comparable growth rates to WT plants. This suggests that either *RPL23aA* is produced in sufficient quantities to fulfill biological requirements for ribosome biogenesis, or that the level of RPL23aA is upregulated post-transcriptionally, perhaps via increased ribosome loading. The latter hypothesis is supported by work on fission yeast (*Schizosaccharomyces pombe*) demonstrating that deficiency in SSU production due to loss of an arginine methyltransferase (*rmt3*) results in the shift of several r-protein transcripts to larger polysomes (Bachand et al., 2006).

I have shown that both *RPL23a* paralogs respond similarly to stress and developmental stimuli in WT plants. This is exemplified by my finding that despite large differences in total transcript abundance, the ratio of *RPL23aA* to *RPL23aB* was stably at ~3 : 1 (low of 2.6 : 1.4 during cold stress, high of 3.3 : 0.7 during recovery from photoinhibition and cold stress). This suggests that both genes possess similar regulatory elements for enhancing and repressing transcription. Recent studies have identified two essential *cis*-acting elements governing the upregulation of genes in mitotically active tissues: the *PCNA* site II motif (also named Up1, $^{5'}$TGGGCY$^{3'}$) and the interstitial telomeric repeat (*telo* box or Up2, $^{5'}$AAACCCTA$^{3'}$) (reviewed in McIntosh and Bonham-Smith, 2005). Site II motifs have been shown to be sufficient to direct reporter gene expression to zones of active cell division, and this expression is strongly increased by the presence of a *telo*-box, which does not function independently (Manevski et al., 2000; Tatematsu et al., 2008; Tremousaygue et al., 2003). Site II motifs have been shown to interact with TCP-domain transcription factors (Kosugi and Ohashi, 1997, 2002; Li et al., 2005a; Tremousaygue et al., 2003), which in turn associate with the Arabidopsis *telo*-box binding protein, AtPurα

(Tremousaygue et al., 2003; Tremousaygue et al., 1999). The finding that DNase I hypersensitivity maps next to the *telo*-box of Arabidopsis *PCNA1* (Kodama et al., 2007), and that the human homolog of AtPurα has DNA helix destabilizing properties (Darbinian et al., 2001), suggest that these elements might function in chromatin remodeling and mediate binding of additional transcription factors and/or the TATA box-binding protein–RNA pol II complex. The *telo*-box and site II motifs are present together in the RRs of at least 153 r-protein genes (Tremousaygue et al., 2003), and analysis of the RRs of *RPL23a* paralogs using the PLACE database (Higo et al., 1999) determined that each paralog possesses three of each motif within 300 bp of transcription start sites, as well as sharing auxin response and root-specific elements (present study, McIntosh and Bonham-Smith, 2005). It is interesting that site II motifs, in addition to their role in upregulating genes in cycling cells, also function as negative regulators of the Arabidopsis alternative oxidase gene, *AtOX1c* (Ho et al., 2007) and along with *telo*-boxes are found in RRs of genes repressed by *A. tumefaciens* infection (Ditt et al., 2006). These findings suggest that *cis*-acting regulatory elements conserved in both *RPL23aA* and *RPL23aB*, specifically the site II and *telo*-box motifs, coordinate their expression in response to developmental and stress stimuli.

Low temperature stress led to the upregulation of *RPL23aA* and *RPL23aB*, especially in leaves that emerged following transfer to the cold. Unlike the cold responsive CRT/DRE binding factor (CBF) genes that are rapidly and markedly induced within 30 min of cold treatment (Gilmour et al., 1998), the *RPL23a* paralogs were induced slowly (≥24 h) and accumulated to a maximum of 150–250% of their pre-treatment levels. This result is in agreement with findings from soybean (*Glycine max*) where three r-proteins, RPS6, RPS13 and RPL37, are upregulated within 3–9 d of cold-treatment (Kim et al., 2004). Additional support is provided by experiments showing upregulation of one or more r-protein transcripts in response to cold-treatment of many plant species, including Arabidopsis (Jung et al., 2003; Oono et al., 2006), canola (Brassica napus, Saez-Vasquez et al., 1993), sunflower (Helianthus annuus, Fernandez et al., 2008) and trifoliate orange (Poncirus trifoliata, Zhang et al., 2005a). The cold response in Arabidopsis involves induction of the CBF regulon, a large group of genes containing CRT/DRE elements in their promoters (Fowler and Thomashow, 2002; Gilmour et al., 1998). This regulon includes a large number of hydrophilic proteins that protect against the formation of lipid structures with deleterious affects on cell membranes (Steponkus et al., 1998; Thomashow, 1999). These

hydrophilic proteins are encoded by the COR/LEA gene family and are the largest group of genes that exhibit long-term upregulation following cold treatment (Fowler and Thomashow, 2002). It is possible that the cold induction of r-proteins, and consequently ribosomes, functions to maintain active translation of cryoprotective gene transcripts (i.e. COR/LEA) despite a temperature-dependent reduction in peptidyl-transferase activity.

Transfer of nonacclimated plants to cold temperature under constant irradiance leads to the production of reactive oxygen species (Huner et al., 1998), which are also produced under high irradiance and constant temperature, and thus some overlap exists between responses to cold and high light. For example, Fowler and Thomashow (2002) report that reactive oxygen detoxification machinery is rapidly and transiently induced following transfer of Arabidopsis to 4 °C. A rapid response to oxidative stress has also been reported following high light treatment (Kimura et al., 2003; Rossel et al., 2002; Vanderauwera et al., 2005), and following treatment of Arabidopsis with hydrogen peroxide (Desikan et al., 2000) or the superoxide anion-generating chemical, methyl viologen (Scarpeci et al., 2008). If this induction requires increased translational capacity, it could explain my finding that high light (300–330 and 1150–2400 μmol photons m^{-2} s^{-1}) led to a transient increase in *RPL23aA* and *RPL23aB* levels. Upregulation of a subset of r-proteins has also been demonstrated following 2 h treatment with methyl viologen (Scarpeci et al., 2008) and following high-light treatment of non-catalase-deficient and catalase deficient Arabidopsis plants, the latter of which accumulate hydrogen peroxide due to impaired scavenging (Vanderauwera et al., 2005). One class of oxidative-stress induced genes are heat shock proteins (HSPs, Rossel et al., 2002; Scarpeci et al., 2008), and it is interesting that site II motifs are found in the upstream RR of several HSPs (Scarpeci et al., 2008), suggesting that this element could be involved in the stress-induced response of both HSPs and r-proteins. The observed decrease in transcript levels of *RPL23a* paralogs in vegetative tissues following 168–336 h high light treatment probably reflects the reduced expression of paralogs in mature tissues (cf. Figure 3.1 and 3.5), and the short-lived nature of the induction. Similarly, the reduced levels in bud tissue after 336 h of high light treatment are consistent with the levels observed in buds from plants of comparable age grown under 100 μmol photons m^{-2} s^{-1}.

During recovery from both photoinhibition and low temperature stress the *RPL23a* paralogs were significantly downregulated. This is in agreement with the observed downregulation of *RPL23aB* during recovery from 24 h cold-treatment at 15 °C, and during recovery from

wounding (McIntosh and Bonham-Smith, 2005). However, this earlier study reported conflicting results for *RPL23aA*, which was either upregulated during recovery (cold-treatment) or remained at pre-treatment levels (wounding). While I cannot speculate on the observed differences due to wounding, it is possible that the differences in response to cold-treatment are due to methodology. The present study used a 28 d cold-treatment at 4 °C, which is sufficient to allow for cold acclimation (Cook et al., 2004; Gray et al., 2003), whereas the earlier study used a 24 h cold stress at 15 °C prior to allowing recovery (McIntosh and Bonham-Smith, 2005). There have been few studies characterizing gene expression during stress recovery, but microarray analyses of Arabidopsis during cold deacclimation and during rehydration following cold acclimation and drought stress, respectively, demonstrated a small number of r-proteins are repressed during recovery (Oono et al., 2003; Oono et al., 2006); these studies did not specifically identify either *RPL23a* paralog. It is possible that upregulation of ribosomal protein synthesis during cold and light stress creates a surplus of ribosomes that is compensated for by reduced expression of r-proteins during recovery. However, it is also likely that both the increased age of harvested material during recovery and the potential reduction in plant health following stress treatment contributed to reduced levels of *RPL23a* transcripts.

In this study I have used a *B*KO line to investigate the ability of Arabidopsis to compensate for loss of a single paralog under conditions that require reprogramming of gene expression and modulation of protein synthesis. No compensatory induction of *RPL23aA* transcription was detected in *B*KOs, and this is consistent with the observations that an abnormal phenotype is produced following loss of single r-protein paralogs (Chen et al., 2006; Ito et al., 2000; Nishimura et al., 2004; Pinon et al., 2008; Revenkova et al., 1999; Van Lijsebettens et al., 1994; Vanderhaeghen et al., 2006; Weijers et al., 2001; Yao et al., 2008). To date, *rps27b* is the only other characterized r-protein mutant lacking an abnormal phenotype under normal growing conditions and in response to most abiotic stresses (oxidative stress, dehydration-stress and heat-stress). This mutant exhibits hypersensitivity to genotoxic stress induced by UV-C irradiance or methyl methane sulfate-treatment (Revenkova et al., 1999), possibly reflecting an extra-ribosomal role for this paralog. An extra-ribosomal role for RPL23aB is not likely given that it has very high sequence conservation with RPL23aA, shows overlapping transcript expression (present work, McIntosh and Bonham-Smith, 2005) and intracellular localization (Degenhardt and Bonham-Smith, 2008a) relative to its paralog, and is detected in ribosomal fractions (Carroll

et al., 2008). Another possibility is that expression of *RPL23aA*, and potentially *RPL23aB*, is controlled at the translational level by a mechanism unique from other r-proteins. In fission yeast, it has been reported that loss of *Cpc2/RACK1* causes a specific decrease in the ribosome loading of *Rpl25-1* (the yeast *RPL23a* ortholog) transcripts, suggesting that Cpc2/RACK1 may recruit *Rpl25-1* to the ribosome for translation (Shor et al., 2003). An analogous mechanism in Arabidopsis may allow a specific increase in ribosome loading of *RPL23aA* transcripts in *B*KO plants. Future experiments will be required to address the specific spatiotemporal requirements for RPL23aB, and to identify whether cellular machinery operates to prevent the deleterious effects resulting from loss of certain r-proteins.

4 CHAPTER 4. ARABIDOPSIS RIBOSOMAL PROTEINS RPL23aA AND RPL23aB ARE DIFFERENTIALLY TARGETED TO THE NUCLEOLUS AND ARE DISPARATELY REQUIRED FOR NORMAL DEVELOPMENT.

A version of this chapter has been published in Plant Physiology. Under the supervision of PC Bonham-Smith, I designed and conducted all experiments and wrote the manuscript. Permission to use was obtained from the publisher and is contingent on the following citation.

Degenhardt, R.F. and Bonham-Smith, P.C. (2008) Arabidopsis ribosomal proteins RPL23aA and RPL23aB are differentially targeted to the nucleolus and are disparately required for normal development. *Plant Physiology*, 147, 128-142.

Plant Physiology URL: www.plantphysiol.org

That plant r-protein genes show overlapping transcript accumulation suggests that many r-protein genes may be functionally redundant or development/tissue/stress specific. Here I characterized the localization and gene silencing phenotypes of a LSU r-protein family, RPL23a, containing two expressed genes (*RPL23aA* and *RPL23aB*). Live cell imaging of RPL23aA and RPL23aB in tobacco with a C-terminal fluorescent-protein tag demonstrated that both isoforms accumulated in the nucleolus, however only RPL23aA was targeted to the nucleolus with an N-terminal fluorescent protein tag, suggesting divergence in targeting efficiency of localization signals. Independent knockdowns of endogenous *RPL23aA* and *RPL23aB* transcript levels using RNAi determined that a *RPL23aB* knockdown did not alter plant growth or development. Conversely, a knockdown of *RPL23aA* produced a pleiotropic phenotype characterized by growth retardation, irregular leaf and root morphology, abnormal phyllotaxy and vasculature, and loss of apical dominance. Comparison to other mutants suggests that the phenotype results from reduced ribosome biogenesis, and I postulate a link between biogenesis, microRNA-target degradation and maintenance of auxin homeostasis. An additional RNAi construct that coordinately silenced both *RPL23aA* and *RPL23aB* demonstrated that this family is essential for viability.

4.1 Introduction

The ribosome is a massive enzyme (2.5–4.5 MD) responsible for catalyzing protein synthesis. It consists of two subunits of unequal size that exist freely in the cell, but assemble together on mRNA to become translationally competent. Plant cytoplasmic ribosomes synthesize the majority of cellular proteins (Bailey-Serres, 1998; Bogorad, 1975), and in Arabidopsis are comprised of four rRNAs (SSU 18 S and LSU 26 S, 5.8 S and 5 S) and 81 r-proteins (33 SSU, 48 LSU) (Barakat et al., 2001; Chang et al., 2005). Ribosomes contain only a single copy of nearly all r-proteins (Ban et al., 2000; Guarinos et al., 2003; Hanson et al., 2004; Schuwirth et al., 2005; Wimberly et al., 2000), yet in plants, r-proteins are encoded by large multi-gene families containing more than one transcriptionally active member (Barakat et al., 2001; Hulm et al., 2005; McIntosh and Bonham-Smith, 2005; Ouyang et al., 2007; Popescu and Tumer, 2004). For example, the Arabidopsis genome contains 254 genes for the 81 r-proteins, with families of between two and five expressed members (Barakat et al., 2001; Chang et al., 2005). This high degree of paralogy suggests that many r-protein genes may be functionally redundant or development/tissue/stress specific.

Arabidopsis RPL23a is part of a universally conserved r-protein family (Lecompte et al., 2002), which bind directly to LSU rRNA and are essential for ribosome biogenesis (El-Baradi et al., 1987; El-Baradi et al., 1984; El-Baradi et al., 1985; Rutgers et al., 1991). Structural studies have mapped its yeast and bacterial counterparts (L25 and L23, respectively) to the LSU, adjacent to the polypeptide exit tunnel (Nissen et al., 2000; Spahn et al., 2001). This position suggests a role for RPL23a in protein translocation and secretion, and this role has been validated in both prokaryotes and eukaryotes (Beckmann et al., 1997; Halic et al., 2004; Maier et al., 2005; Menetret et al., 2005; Morgan et al., 2002; Pool et al., 2002). There are two members of the RPL23a family in Arabidopsis, *RPL23aA* and *RPL23aB*. Transcript expression profiles have shown that *RPL23aA* is more abundant than *RPL23aB* in all tissues, and that accumulation of each differs in response to cold-, wounding- and copper-stress (McIntosh and Bonham-Smith, 2005). Both isoforms are incorporated into the ribosome (Carroll et al., 2008; Chang et al., 2005; Giavalisco et al., 2005), and RPL23aA functionality was confirmed by its ability to complement a yeast *l25* mutant (McIntosh and Bonham-Smith, 2001).

The consequences of overlapping r-protein expression in plants have yet to be fully elucidated. In yeast, 59 of 79 r-proteins are encoded by two expressed paralogs, producing identical or near-

identical r-protein isoforms. Although these paralogs can be transcribed at divergent levels (Planta, 1997; Tornow and Santangelo, 1994), a high transcription rate from one paralog is compensated for by a low rate from the other, resulting in a consistent transcript level for each r-protein (Planta, 1997; Warner et al., 1985). As with yeast, most of Arabidopsis r-protein paralogs encode very similar proteins. However, unlike yeast, there is no evidence suggesting that transcript levels among paralogs are linked in a regulated manner. For example, hormone and stress treatment of Arabidopsis seedlings leads to changes in transcript levels of single paralogs from the *RPS15a* and *RPL23a* families, but has no affect on the levels of the other expressed paralogs (Hulm et al., 2005; McIntosh and Bonham-Smith, 2005). Further, despite overlapping transcript expression, phenotypic characterization of single paralog silencing or knockout lines suggest that paralogs are not functionally equivalent. In tobacco for example, silencing *RPL3A* led to an increase in *RPL3B* transcript levels, but this increase was unable to compensate for the reduced *RPL3A* levels, resulting in abnormal growth and development (Popescu and Tumer, 2004). In Arabidopsis, *rps13b* and *rps18a* T-DNA insertional mutants develop narrow, pointed first leaves, and have stunted root growth and delayed flowering; in both cases Northern analyses confirmed that transcript levels from paralogs, were unaffected (Ito et al., 2000; Van Lijsebettens et al., 1994). It remains to be determined whether these findings result from a biological shortage of r-proteins for ribosome biogenesis caused by the loss of one copy from a redundant family, or if they are indicative of specialized functions for specific paralogs.

In the present work, I investigated whether the two Arabidopsis *RPL23a* paralogs are equivalent with respect to cellular localization and phenotypic response to gene knockdowns. Accordingly, C- and N-terminal RPL23a-fluorescent protein fusions were made and their localization followed *in vivo* in a heterologous tobacco system. I found that the two isoforms have different affinities for nucleolar accumulation, with RPL23aA predominating. I then designed estrogen-inducible, RNAi-mediated silencing constructs targeting *RPL23aA* and *RPL23aB*, independently and coordinately. *RPL23aA s*ilencing resulted in growth retardation and morphological abnormalities, while *RPL23aB* silencing had no affect. I also showed, for the first time in plants, that coordinate silencing of both *RPL23aA* and *RPL23aB* is lethal. My results indicate that the two RPL23a isoforms are not of equivalent importance for normal plant development.

4.2 Materials and Methods

4.2.1 Plant material

Arabidopsis cultivar Columbia-0 and tobacco cultivar Petit Havana were used for all experiments. Unless otherwise stated, Arabidopsis was plated on basal media. Growth conditions are provided in Appendix C.

4.2.2 Fluorescent protein and RNAi constructs

Standard techniques were followed for all molecular cloning (Sambrook et al., 1989). All cloning products were verified by automated sequencing (NRC/PBI). The fluorescent proteins used were monomeric GFP modified for plants (mGFP5, Haseloff et al., 1997), monomeric RFP (mRFP) (Campbell et al., 2002), and EGFP (ClonTech, Palo Alta, CA). Details of cloning methodology are available in Appendix C.

For RNAi-mediated gene silencing, targeted regions of *RPL23aA* and *RPL23aB* were cloned in sense and antisense orientation, separated by an intron, into the binary vector pER8 (Zuo et al., 2000), creating the estrogen inducible, hairpin RNA forming casettes, RPL23aA–ihp, RPL23aB–ihp and RPL23a–ihp. The pER8 vector system is strictly regulated by estrogen, and shows no non-specific effects on plant growth or development (Zuo et al., 2000). Details of cloning methodology are available in Appendix C.

4.2.3 Transient expression in tobacco

Fluorescent protein constructs within binary vectors were used to transform *A. tumefaciens* strain LBA4404 (Hoekema et al., 1983) via electroporation. All constructs in pGREEN were coelectroporated with pSOUP, which must be coresident in *A. tumefaciens* to provide the replication functions, in *trans*, for pGREEN (Hellens et al., 2000). Tobacco infiltrations were carried out following previously described protocols (Batoko et al., 2000; Brandizzi et al., 2002a; Sparkes et al., 2006). Following infiltration, tobacco plants were returned to the growth chamber for 48–72 h prior to visualization with the CLSM.

4.2.4 Confocal microscopy

Live cell imaging was conducted with an inverted Zeiss LSM 510 META CLSM using previously described settings (Brandizzi et al., 2002a; Runions et al., 2006), with the exception that a 585–615 nm bandpass filter was used to detect mRFP. These settings prevented spectral

bleed-through of fluorescence emission from EGFP/GFP5 + mRFP during coexpression experiments. Acquired Images were processed with Zeiss LSM Image Browser software and exported to Adobe Photoshop 7.0 software (San Jose, CA) for figure preparations.

4.2.5 Generation and induction of stable RNAi transgenics

Stable transgenics carrying the inducible silencing cassettes were generated via the floral dip protocol (Clough and Bent, 1998). As a negative control, Arabidopsis was transformed with the pER8 empty vector using the same technique. T_3 transgenic lines, created by selecting each successive generation on basal media supplemented with 25 μg ml^{-1} hygromycin (Invivogen) and 200 μg ml^{-1} cefotaxime (Sanofi-Aventis), were used for RNAi studies. Seed from independently transformed lines was plated on basal media supplemented with 0–100 μM estradiol. Transgenics grown on non-inductive media (0 μM estradiol) were occasionally transferred to inductive media (2–100 μM estradiol) to observe responses.

4.2.6 Dark-field microscopy

Digital images of transgenics were taken with a Zeiss Stemi 2000-C stereomicroscope. Root sections were observed following staining with Toluidine blue. Vasculature was examined by fixing 14–18-day-old seedlings overnight in 3:1 ethanol:acetic acid. Fixed seedlings were processed through an ethanol series (80, 90, 95 and 100% ethanol) and cleared by incubation overnight in saturated chloral hydrate. Images were taken at 100–200× zoom with a Zeiss Axioskop microscope equipped with a darkfield diaphragm. Approximately 8–10 cleared seedlings were analyzed for each genotype (pER8–ihp–4 and RPL23aA–ihp–4).

4.2.7 Quantitative PCR

Quantitative PCR was performed using RNA extracted from 10–18 day-old whole seedlings with an iQ5 Real-Time PCR Detection System (Bio-Rad). For each sample, amplifications of *RPL23aA*, *RPL23aB* and *ACT7* were performed in triplicate, within the same qPCR run, and only one amplicon was produced per reaction. The *ACT7* gene was used as an internal control to standardize *RPL23aA/B* levels in induced and non-induced transgenics, and threshold cycle (Ct) changes were compared to standardized levels in non-induced wild-type seedlings of equivalent age using the comparative Ct method (Livak and Schmittgen, 2001). The entire procedure (RNA extraction, first-strand synthesis, qPCR) was repeated for a minimum of three biological replicates. Data was obtained using the iQ5 Optical System software (Bio-Rad) and

subsequently exported to Microsoft Excel (Redmond, WA) for summarizing. Detailed methodology for RNA extractions, first-strand synthesis, primer selection and validation, and qPCR optimization are available in Appendix C.

4.3 Results

4.3.1 RPL23a isoform comparison

RPL23aA and *RPL23aB* share 68.8% identity at the transcript level [83.7 % between open reading frames (ORFs)], but encode proteins exhibiting 94.8% amino acid identity. They also share a high degree of primary sequence conservation with other eukaryotic orthologs (Figure 4.1a), especially within the C-terminal domain that binds LSU rRNA (Rutgers et al., 1991). The eukaryotic L23a/L25 r-proteins possess an N-terminal extension region that is absent from prokaryotic counterparts, and contains the NLS (Jakel and Gorlich, 1998; Rutgers et al., 1990; Schaap et al., 1991). Although the NLS of plant RPL23a's has yet to be experimentally determined, all residue differences between Arabidopsis RPL23a isoforms reside within the N-terminal region (Figure 4.1a). Further, two of these differences occur within a classical monopartite NLS [Figure 4.1a, consensus $(K/R)_2XK/R$, where X denotes any residue] that purportedly also functions as a nucleolar localization signal (NoLS, Dingwall and Laskey, 1991; Horke et al., 2004; Kalderon et al., 1984; Weber et al., 2000).

4.3.2 C-terminally-tagged RPL23a isoforms localize to the nucleolus

To investigate whether differences in putative RPL23a NLS/NoLS domains have any impact on localization patterns, I designed RPL23aA/B C-terminal fusions with monomeric red fluorescent protein (mRFP) separated by a glutathione-*s*-transferase (GST) linker. The GST linker was added to increase translational fusion mass beyond the size exclusion limit of nuclear pore complexes (>60 kD), and to enable affinity purification of bound proteins (Grebenok et al., 1997; Merkle, 2003); it did not interfere with localization in any noticeable way (see also Kishi et al., 1996; Ookata et al., 1995). C-terminal fusions were investigated because it has previously been shown that attachment of a small (~2 kD) FLAG-HIS tag to the C-terminus of RPL23aA did not disrupt the ability of the fusion protein to incorporate into ribosomes and form polysomes (Zanetti et al., 2005). RPL23a orthologs are known to be involved in LSU biogenesis within the nucleolus (Jeeninga et al., 1996; van Beekvelt et al., 2001), and hence I hypothesized that Arabidopsis RPL23a would accumulate to the greatest extent in the nucleolus. To enable

Figure 4.1 Alignment and localization of the Arabidopsis RPL23a isoforms. **a** Clustal alignment of the two Arabidopsis RPL23a isoforms (*At*RPL23aA and RPL23aB) with tobacco RPL23a (*Nt*RPL23a), two rice RPL23a isoforms (*Oryza sativa*; *Os*RPL23a-1, LOC_Os01g24690; *Os*RPL23a-2, LOC_Os04g42270), human RPL23a (*Homo sapiens*; *Hs*RPL23a) and yeast RPL25 (*Saccharomyces cerevisiae*; *Sc*RPL25). Identical and similar residues shared by four or more orthologs are shaded black and gray, respectively, while those shared by three or less orthologs are shaded white. Experimentally determined domains responsible for nuclear localization in human (Jakel and Gorlich, 1998) and yeast (Schaap et al., 1991) are highlighted in yellow. The C-terminal domain, which contains rRNA binding capacity, is highlighted red (Kooi et al., 1994; Rutgers et al., 1991). Putative monopartite NLSs [(K/R)XK/R] in Arabidopsis are delineated by green brackets. Numbering is for reference only. **b**–**i** CLSM images of tobacco epidermal cells transiently coexpressing FIB2–EGFP and RPL23aA–mRFP (**b**–**c**), or FIB2–EGFP and RPL23aB–mRFP (**d**–**e** and **i**), or expressing RPL23aB–mRFP alone (**f**–**h**). Nucleolar and nucleoplasmic signals are indicated by transparent white arrowheads and small white arrows, respectively (**b**–**i**). White arrowheads point to cajal bodies (Beven et al., 1995) (left panels in **b**–**e**). Images of the same optical slice were merged to show signal overlap (right panels in **b**–**e** and **i**). Bars = 10 μm.

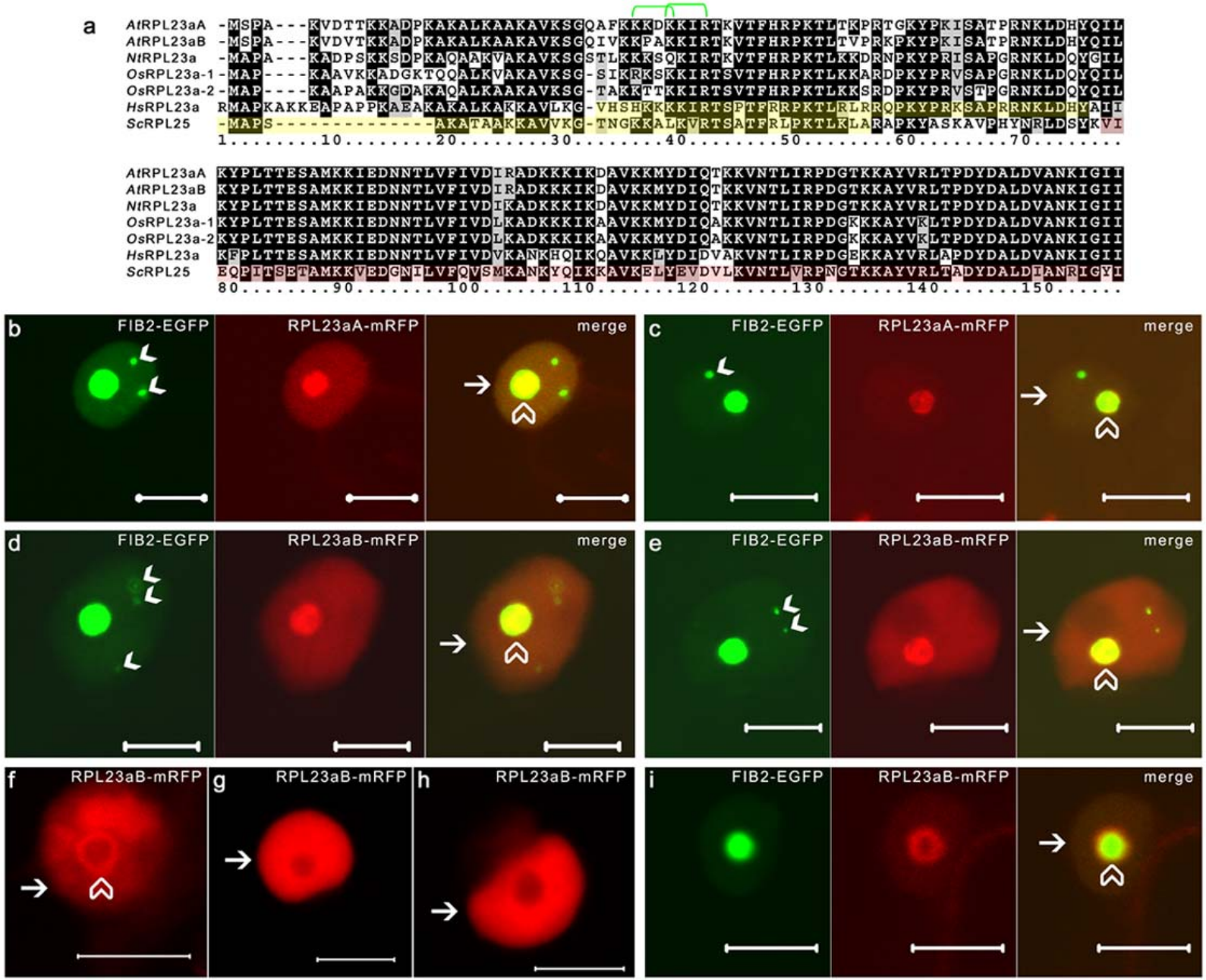
a
AtRPL23aA -MSPA---KVDTTKKADPKAKALKAAKAVKSGQAFKKKDKKIRTKVTFHRPKTLTKPRTGKYPKISATPRNKLDHYQIL
AtRPL23aB -MSPA---KVDVTKKADPKAKALKAAKAVKSGQIVKKPAKKIRTKVTFHRPKTLTVPRKPKYPKISATPRNKLDHYQIL
NtRPL23a -MAPA---KADPSKKSDPKAQAAKVAKAVKSGSTLKKKSQKIRTKVTFHRPKTLKKDRNPKYPRISAPGRNKLDQYGIL
OsRPL23a-1 -MAP----KAAVKKADGKTQQALKVAKAVKSG-SIKRKSKKIRTSVTFHRPKTLKKARDPKYPRVSAPGRNKLDQYQIL
OsRPL23a-2 -MAP----KAAPAKKGDAKAQALKAAKAVKSG-TAKKTTKKIRTSVTFHRPKTLKKSRDPKYPRVSTPGRNKLDQYQIL
HsRPL23a RMAPKAKKEAPAPPKAEAKAKALKAKKAVLKG-VHSHKKKKIRTSPTFRRPKTLRLRRQPKYPRKSAPRRNKLDHYAII
ScRPL25 -MAPS--------------AKATAAKKAVVKG-TNGKKALKVRTSATFRLPKTLKLARAPKYASKAVPHYNRLDSYKVI
1.....10.....20.....30.....40.....50.....60.....70.....
AtRPL23aA KYPLTTESAMKKIEDNNTLVFIVDIRADKKKIKDAVKKMYDIQTKKVNTLIRPDGTKKAYVRLTPDYDALDVANKIGII
AtRPL23aB KYPLTTESAMKKIEDNNTLVFIVDIRADKKKIKDAVKKMYDIQTKKVNTLIRPDGTKKAYVRLTPDYDALDVANKIGII
NtRPL23a KYPLTTESAMKKIEDNNTLVFIVDIKADKKKIKDAVKKMYDIQTKKVNTLIRPDGTKKAYVRLTPDYDALDVANKIGII
OsRPL23a-1 KYPLTTESAMKKIEDNNTLVFIVDLKADKKKIKAAVKKMYDIQAKKVNTLIRPDGKKKAYVKLTPDYDALDVANKIGII
OsRPL23a-2 KYPLTTESAMKKIEDNNTLVFIVDLKADKKKIKAAVKKMYDIQAKKVNTLIRPDGKKKAYVKLTPDYDALDVANKIGII
HsRPL23a KFPLTTESAMKKIEDNNTLVFIVDVKANKHQIKQAVKKLYDIDVAKVNTLIRPDGEKKAYVRLAPDYDALDVANKIGII
ScRPL25 EQPITSETAMKKVEDGNILVFQVSMKANKYQIKKAVKELYEVDVLKVNTLVRPNGTKKAYVRLTADYDALDIANRIGYI
80.....90.....100.....110.....120.....130.....140.....150.....
b
FIB2-EGFP
RPL23aA-mRFP
merge
c
FIB2-EGFP
RPL23aA-mRFP
merge
d
FIB2-EGFP
RPL23aB-mRFP
merge
e
FIB2-EGFP
RPL23aB-mRFP
merge
f
RPL23aB-mRFP
g
RPL23aB-mRFP
h
RPL23aB-mRFP
i
FIB2-EGFP
RPL23aB-mRFP
merge

definitive identification of nucleolar accumulation I used a nucleolar marker, *At*FIBRILLARIN2 (FIB2), with a C-terminal enhanced GFP (EGFP) tag (Barneche et al., 2000). FIB2 specifically localizes to the nucleolus, where it directs a requisite step in rRNA processing and ribosome assembly (Barneche et al., 2000; Tollervey et al., 1993). RPL23aA/B–mRFP chimerics were transiently coexpressed with the FIB2–EGFP marker in tobacco epidermal cells via infiltration with transformed *A. tumefaciens* (Sparkes et al., 2006). Cells imaged with a confocal laser scanning microscope (CLSM) 72-h post-infiltration showed strong nucleolar accumulation of FIB2–EGFP (Figure 4.1b–e, i, left panels) and weaker but clearly discernible nucleolar signals for RPL23aA–mRFP (Figure 4.1b–c, middle panels) and RPL23aB–mRFP (Figure 4.1d–e, middle panels). FIB2–EGFP also localized to mobile cajal bodies (Figure 4.1b–e, see Appendix C for details on cajal bodies and nucleoli properties), which are non-membrane bound inclusions associated with nucleoli (Beven et al., 1995; Kim et al., 2007).

While both RPL23a isoforms were capable of localizing to the nucleolus, RPL23aB–mRFP was occasionally unable to target the core of the nucleolus (Figure 4.1f–i), instead accumulating only at the nucleolus' periphery (13.6% of cells, n = 66; Figure 4.1f and i) or being excluded altogether (19.7% of cells, n = 66; Figure 4.1g–h). Further, although non-nucleolar targeting of RPL23aA-mRFP was observed (10.4% of cells, n = 67), it was a significantly more common occurrence with RPL23aB-mRFP (33.3% of cells, P = 0.001). Alignment of Arabidopsis RPL23a isoforms with tobacco RPL23a (Gao et al., 1994) showed that RPL23aB had two non-conservative K substitutions within putative NLS/NoLS domains (Figure 4.1a, reference numbering positions 38 and 56) relative to RPL23aA and *Nt*RPL23a. To examine whether these substitutions might confer a competitive advantage for nucleolar accumulation to RPL23aA, I coexpressed both RPL23aA and RPL23aB in the same tobacco epidermal cells. Accordingly, two additional fusion-protein constructs were made where the C-terminal mRFP tag of RPL23aA and RPL23aB was replaced with a GFP variant modified for plant expression, GFP5 (Haseloff et al., 1997). Coexpression of RPL23aA–GFP5 with RPL23aB–mRFP resulted in a high rate of co-exclusion from the nucleolus (40% of cells, n = 25; data not shown). Yet in all instances where nucleolar localization was observed, RPL23aA–GFP5 successfully targeted the nucleolus (100% of cells, n = 13), whereas accumulation of RPL23aB–mRFP was inconsistent, as it was frequently excluded or peripherally localized (40 and 20% of cells, respectively, n = 13; Figure 4.2a–b). However, when the two isoforms were coexpressed with the converse set of fluorescent

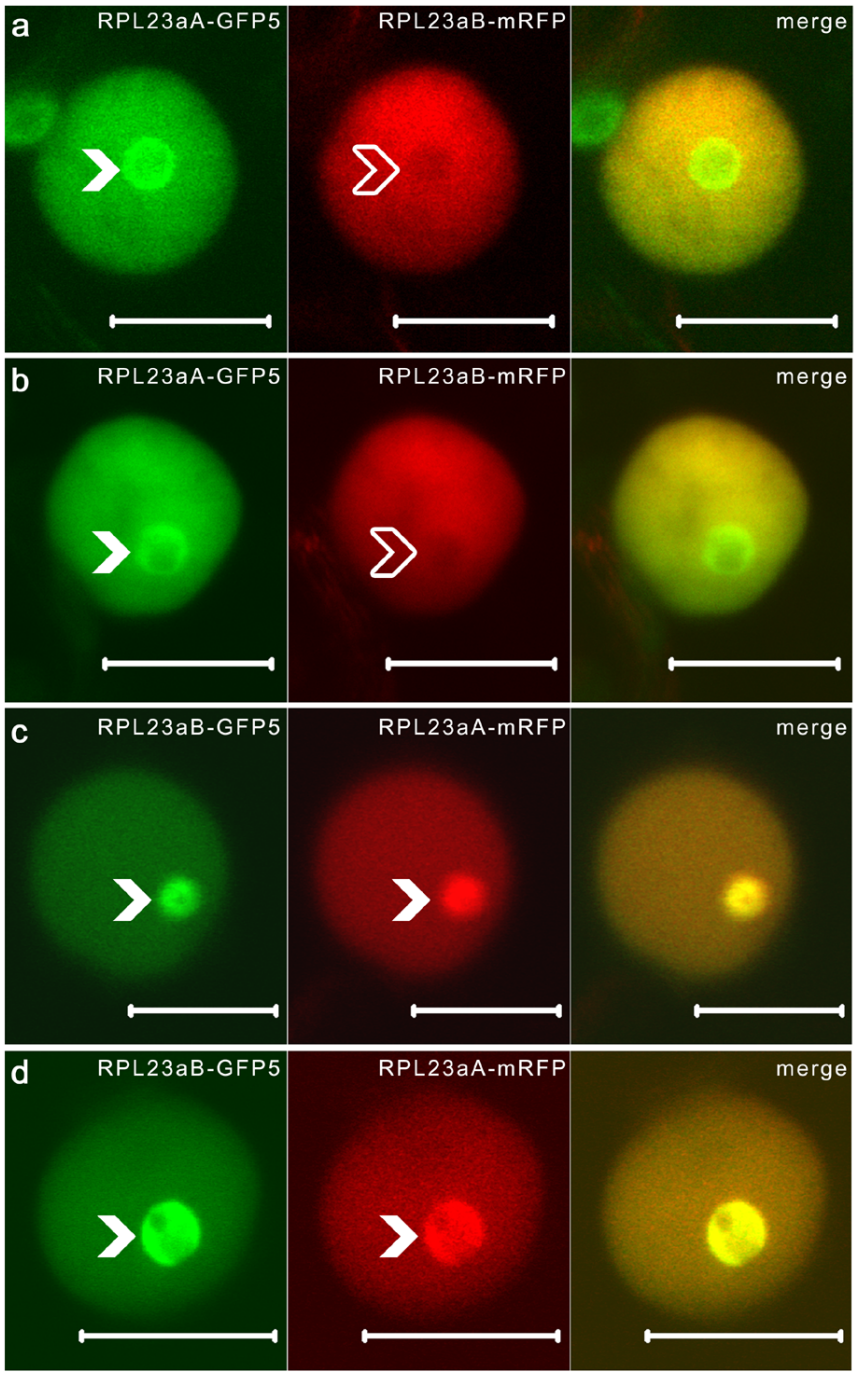

Figure 4.2 Nucleolar colocalization of C-terminally tagged RPL23aA and RPL23aB in tobacco epidermal cells is fluorophore-dependent. **a**–**d** CLSM images of tobacco epidermal cells transiently coexpressing RPL23aA–GFP5 and RPL23aB–mRFP (**a**–**b**), or RPL23aA–mRFP and RPL23aB–GFP5 (**c**–**d**). Solid white arrowheads point to nucleoli; transparent white arrowheads point to nucleolus exclusion zones. Images of the same optical slice were merged to show signal overlap (right panels in **a**–**d**). Bars = 10 μm.

protein tags, RPL23aA–mRFP and RPL23aB–GFP5 showed co-nucleolar accumulation (100% of cells, n = 13; Figure 4.2c–d). These contradictory findings suggest that the fluorescent protein tags may be affecting RPL23aA/B localization (discussed below), but nevertheless indicates that both isoforms accumulate in the nucleolus.

4.3.3 N-terminally-tagged RPL23aB is excluded from the nucleolus

The N-terminal domain of the yeast RPL23a ortholog is necessary for both nuclear localization and LSU biogenesis (van Beekvelt et al., 2001). To determine if I could interfere with the ability of the N-terminal domain of Arabidopsis RPL23a to direct nuclear/nucleolar accumulation, the RPL23a fusion protein constructs were redesigned such that the GFP5 tag was N-terminal, separated from RPL23aA and RPL23aB by the GST linker. As a control, I coexpressed GFP5–RPL23aA/B with free mRFP, which labels the cytoplasm and nucleoplasm, but is actively excluded from the nucleolus (Campbell et al., 2002). Shifting the 466 residue fluorescent protein tag to the N-terminus completely disrupted GFP5–RPL23aB nucleolar localization (0% of cells showed nucleolar-localization, n = 50), resulting in a solely cytoplasmic and nucleoplasmic distribution (Figure 4.3c–d and f). However, the N-terminal tag did not interfere with nucleolar targeting of RPL23aA (100% of cells showed nucleolar-localization, n = 50), which accumulated within the nucleolus at levels indistinguishable from RPL23aA–GFP5 (Figure 4.3a–b and e; cf. Figure 4.2a–b).

4.3.4 Silencing of RPL23aA produces a strong *pfl* phenotype

As my previous results suggested that the two RPL23a isoforms are differentially accumulated in the nucleolus, I wanted to investigate the resulting phenotypical consequences of paralog knockdowns in Arabidopsis. Correspondingly, I individually silenced *RPL23aA* and *RPL23aB* by engineering paralog-specific self-complementary segments of 3' UTRs within an estradiol-regulated vector, pER8 (Guo et al., 2003; Zuo et al., 2000). Consistent with my results from the characterization of an *rpl23ab* T-DNA knockout line (Chapter 3), none of the three T_3 transgenic *RPL23aB*-silencing lines (RPL23aB–ihp–1 to RPL23aB–ihp–3) showed any abnormal phenotype when grown on inductive media (Figure 4.4a). However, T_3 transgenic *RPL23aA*-silencing lines (RPL23aA–ihp–1 to RPL23aA–ihp–5) showed retarded growth and developmental abnormalities when plated on inductive media, which were most severe in line RPL23aA–ihp–4. Initially, this line developed narrow, pointed first leaves on short, stubby

Figure 4.3 RPL23aB with an N-terminal GFP5 tag is unable to accumulate in the nucleolus in tobacco epidermal cells. **a**–**d** CLSM images of tobacco epidermal cells transiently coexpressing GFP5–RPL23aA and free mRFP (**a**–**b**), or GFP5–RPL23aB and free mRFP (**c**–**d**). **e**–**f** Close-up images of cells expressing GFP5–RPL23aA (**e**) or GFP5–RPL23aB (**f**). Solid white arrowheads point to nucleoli (**a**–**b** and **e**) and transparent white arrowheads point to nucleolar exclusion zones (**c** and **f**). Free mRFP delineates the cytoplasm and nucleoplasm (middle panels in **a**–**d**). Images of the same optical slice were merged to show signal overlap (right panels in **a**–**d**). Bars = 10 μm.

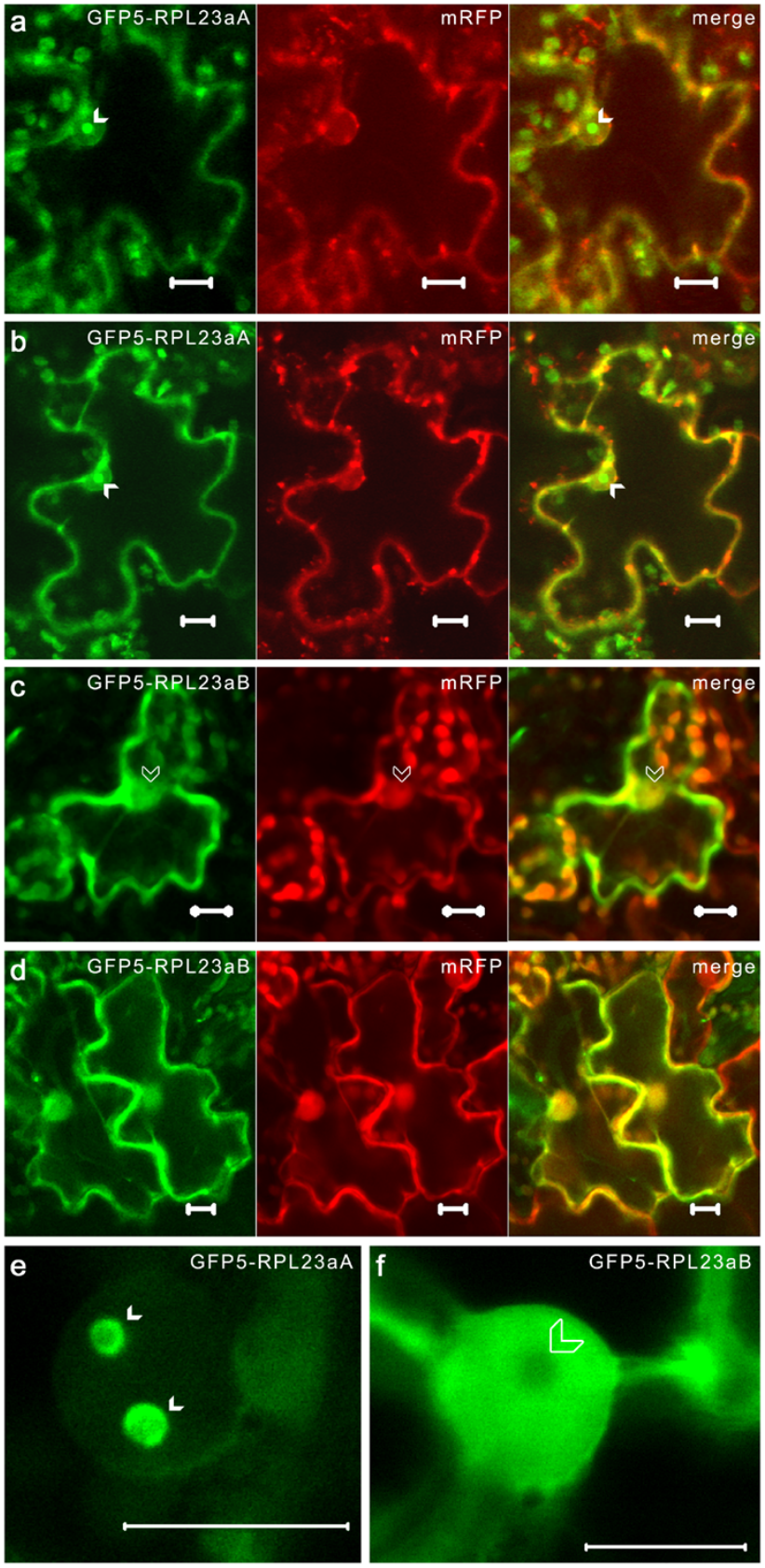
a
GFP5-RPL23aA
mRFP
merge
b
GFP5-RPL23aA
mRFP
merge
c
GFP5-RPL23aB
mRFP
merge
d
GFP5-RPL23aB
mRFP
merge
e
GFP5-RPL23aA
f
GFP5-RPL23aB

Figure 4.4 Characterization of Arabidopsis *RPL23aA* and *RPL23aB* silencing mutants. **a** 10-day-old seedlings grown on basal media without or with 10–50 μM estradiol (non-induced and induced, respectively). Images shown are representative of T_3 transgenics expressing the *RPL23aA* and *RPL23aB*-silencing cassette (RPL23aA–ihp and RPL23aB–ihp, respectively), or the empty vector control (pER8–ihp). Misshapen leaves with a 'pointed' morphology are indicated by arrowheads. **b** 13-, 18-, and 21-day-old pER8–ihp–2 and RPL23aA–ihp–4 grown on inductive media as above. Bar is 2 mm. **c** Comparison of the first four leaves from 13-day-old pER8–ihp–2 and RPL23aA–ihp–4 T_3 transgenic seedlings grown on inductive media. Leaves are ordered chronologically (oldest to youngest) left to right. Bars are 2 mm. **d** Abnormal leaf and root morphology of 18-day-old RPL23aA–ihp–4 transgenics grown on inductive media. A segment of root from an 18-day-old pER8–ihp–2 transgenic seedling is shown for comparison. Roots are stained with toluidine blue. Arrowheads point to lateral roots. **e** Darkfield micrographs showing leaf venation of 14–18-day-old pER8–ihp–2 and RPL23aA–ihp–4 T_3 transgenic seedlings grown on inductive media and cleared with chloral hydrate. Shown are the first, second and third leaves, and the hypocotyl/petiole junction. Arrow shows bifurcation of midveins in the petiole of RPL23aA–ihp–4 transgenics. **f** 38- and 74-day-old (top and bottom panels, respectively) pER8–ihp–2 and RPL23aA–ihp–4 T_3 transgenic seedlings grown on inductive media. Arrows in top panels point to rosette flowering branches in RPL23aA–ihp–4 transgenics. Bars are 2 cm. **g** qRT-PCR quantification of *RPL23aA* and *RPL23aB* transcript abundance in RPL23aA–ihp–1 to –5, RPL23aB–ihp–1 to –3, and pER8–ihp–2 to –4 T_3 Arabidopsis transgenic seedlings plated on inductive media. Vertical and horizontal hatched lines represent the *ACT7* standardized level of *RPL23aA* and *RPL23aB* transcripts, respectively, in transgenic lines on inductive media normalized to the transcript level in non-induced wild-type seedlings (set to 1). Black bars represent SEM. Gray bar represents 100% of wild-type transcript abundance. Asterisks highlight the lines depicted in (**a**) through (**f**).

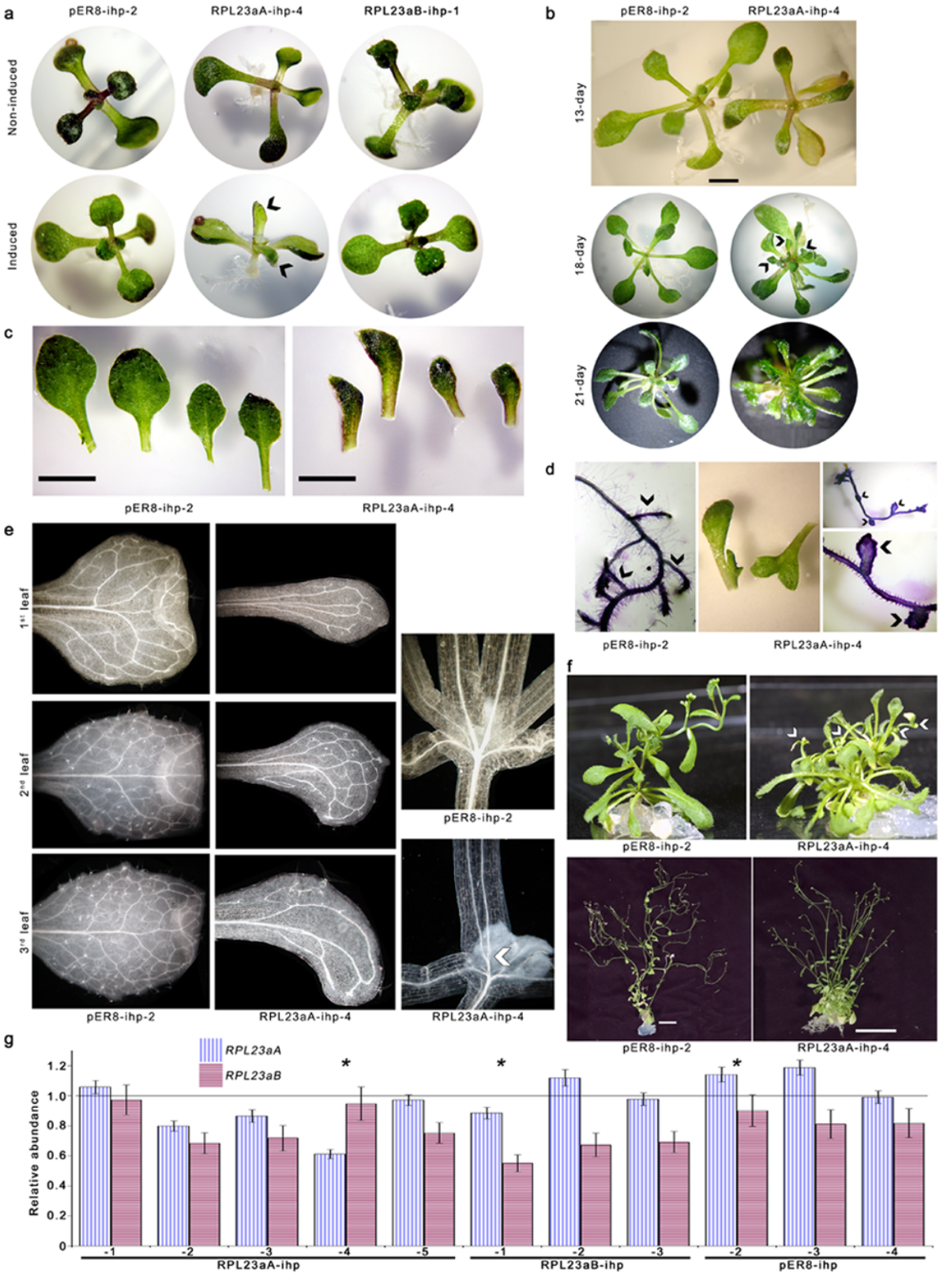
a
pER8-ihp-2
RPL23aA-ihp-4
RPL23aB-ihp-1
Non-induced
Induced
b
pER8-ihp-2
RPL23aA-ihp-4
13-day
18-day
21-day
c
pER8-ihp-2
RPL23aA-ihp-4
d
pER8-ihp-2
RPL23aA-ihp-4
e
1st leaf
2nd leaf
3rd leaf
pER8-ihp-2
RPL23aA-ihp-4
RPL23aA-ihp-4
pER8-ihp-2
f
pER8-ihp-2
RPL23aA-ihp-4
pER8-ihp-2
RPL23aA-ihp-4
g
RPL23aA
RPL23aB
Relative abundance
0
0.2
0.4
0.6
0.8
1.0
1.2
*
*
*
-1
-2
-3
-4
-5
RPL23aA-ihp
-1
-2
-3
RPL23aB-ihp
-2
-3
-4
pER8-ihp

petioles (Figure 4.4a and c). With further development, it produced leaf or leaf-life organs prolifically (Figure 4.4b), with an average of 26 leaf organs at bolting (SEM = 0.88, n = 7) compared to an average of 11 (SEM = 0.24, n = 30) on the induced empty vector control pER8–ihp transgenics. RPL23aA–ihp–4 transgenics also produced irregularly shaped or fused older leaves (Figure 4.4b and d), showed delayed transition to reproductive growth when plated on inductive media (some induced seedlings had not flowered at 7 weeks of age, data not shown), and was shorter than pER8–ihp controls at maturity (15.3 cm, SEM = 1.8 cm, versus 20.4 cm, SEM = 0.9; Figure 4.4f). Apical dominance was lost, with older RPL23aA–ihp–4 plants showing substantially increased rosette branching (RPL23aA–ihp–4 = 8.8 rosette reproductive shoots, SEM = 1.4; pER8–ihp–4 = 3.3, SEM = 0.6; Figure 4.4f). The RPL23aA–ihp–4 line also had substantially reduced root growth and an abnormal root phenotype characterized by short root hairs and malformed lateral roots (Figure 4.4d). The atypical leaf phenotype of RPL23aA–ihp–4 resembled that of *pfl* mutants characterized for *RPS13B* and *RPS18A* knockouts (Ito et al., 2000; Van Lijsebettens et al., 1994), but was unique with respect to a greater delay in the transition to reproductive growth, reduced seed production (data now shown), increased leaf number, longer persistence of the 'pointed'-morphology (Figure 4.4b), and abnormal root growth (Figure 4.4d). Nishimura et al. (2005) have reported that a RPL24B knockout also develops a *pfl* phenotype, as well as additional defects in patterning of cotyledon vasculature and the gynoecium, which were attributed to a specific role for RPL24 in regulating expression of auxin polar transport and response factors. As RPL23aA–ihp–4 has aberrant phyllotaxis, apical dominance and root development, all of which are auxin-mediated processes (Chatfield et al., 2000; Reed et al., 1998; Reinhardt, 2005), I investigated whether vascular patterning was also disrupted. Chloral-hydrate cleared RPL23aA–ihp–4 seedlings were examined and found to have venation that deviated dramatically from the closed, reticulate venation of pER8–ihp controls (Figure 4.4e). Mutant leaves had substantially reduced venation, little to no tertiary or quaternary veins, open vein loops with distal segments ending freely in the lamina, and aberrant anastamosis that was most apparent in the first leaves where the midvein bifurcated close to the hypocotyl-petiole junction (Figure 4.4e). Veins also exhibited reduced lateral orientation, with a predominance for base to tip alignment. I did not observe any defects in gynoecium patterning of RPL23aA–ihp–4 plants that had been transferred at bolting to fresh media augmented with estradiol. However, the inducible system I utilized was not readily amenable to analysis of

reproductive organs or fertility due to the half-life of the inducer and the requirement of growing transgenics on sealed plates for both sterility and to prevent rapid oxidation of estradiol.

To ascertain whether the observed phenotypes corresponded to *RPL23aA* transcript levels, qRT-PCR was conducted on RNA from transgenic seedlings (10–13-days-old) grown on inductive and non-inductive media. The greatest downregulation in *RPL23aA* transcript was recorded for induced RPL23aA–ihp–4 seedlings (~40% reduction in transcript level; Figure 4.4g), while transcript levels in induced empty vector control pER8–ihp transgenics (Figure 4.4g), and in induced wild-type seedlings (data not shown), were unaltered. Silencing of *RPL23aB* was observed in all RPL23aB–ihp transgenic lines (~30–45% reduction transcript level). A small degree of cross-silencing was also observed in some of the RPL23aA/B–ihp transgenic lines (A–ihp–2 and –3, B–ihp–1), but did not lead to development of an abnormal phenotype. My results suggest that the *pfl* phenotype is strongly correlated to *RPL23aA* transcript level.

4.3.5 The RPL23a family is essential for viability

The purported involvement of RPL23a orthologs in numerous critical ribosomal functions suggest that RPL23a should be essential for plant viability. To test this hypothesis, I designed an RNAi construct that targets a highly conserved region of the ORFs. T_3 seed from six transgenic lines (RPL23a–ihp–3 to RPL23a–ihp–7) were screened on inductive media and the majority of lines showed acute growth defects, characterized by severely retarded development, reduced root growth, atypical leaf and root morphology, accumulation of anthocyanins, prolific leaf organ development, delayed transition to reproductive growth, flower abortion and early senescence (Figure 4.5c–d, reproductive defects data not shown). Two lines (RPL23a–ihp–5 and –6) were non-viable on inductive media and died post-germination (Figure 4.5a–b). Line RPL23a–ihp–5 was grown for 14-days on non-inductive media and transferred to inductive media; thereafter it began to show symptoms consistent with protein synthesis inhibition (impeded growth, chlorosis, necrosis), which progressively worsened and proved lethal 14–21-days post-induction (data not shown). To confirm that observed phenotypes were a direct result of silencing *RPL23aA* and *RPL23aB*, I conducted qRT-PCR analyses on RNA from transgenic seedlings (10–13-days-old) grown on inductive and non-inductive media. Transcript levels of *RPL23aA* and *RPL23aB* were dramatically lower in induced seedlings of lines RPL23a–ihp–5 to –7 relative to wild-type

Figure 4.5 The Arabidopsis RPL23a family is essential for viability. **a–c** Representative images of 11-day-old (**a**) and 18-day-old (**b**–**c**) T_3 transgenics expressing the *RPL23a* family-silencing cassette (RPL23a–ihp) germinated on basal media without or with 10–50 μM estradiol (non-induced and induced, respectively). Bars are 2 mm. Abnormal leaf morphology of RPL23a–ihp–5 transgenics on non-inductive media, indicated by black arrow, suggests leaky expression. **d** Aberrant leaf morphology apparent on 29 day-old RPL23a–ihp–7 transgenics grown on inductive media. Black arrows indicate leaves with particular anomalous form. **e** qRT-PCR quantification of *RPL23aA* and *RPL23aB* transcript abundance in RPL23a–ihp–3 to –8 T_3 Arabidopsis transgenic seedlings plated on inductive media. Vertical and horizontal hatched lines represent the *ACT7* standardized level of *RPL23aA* and *RPL23aB* transcripts, respectively, in transgenic lines on inductive media normalized to the transcript level in non-induced wild-type seedlings (set to 1). Black bars represent SEM. Gray bar represents 100% of wild-type transcript abundance. Asterisks highlight the lines depicted in (**a**) through (**d**).

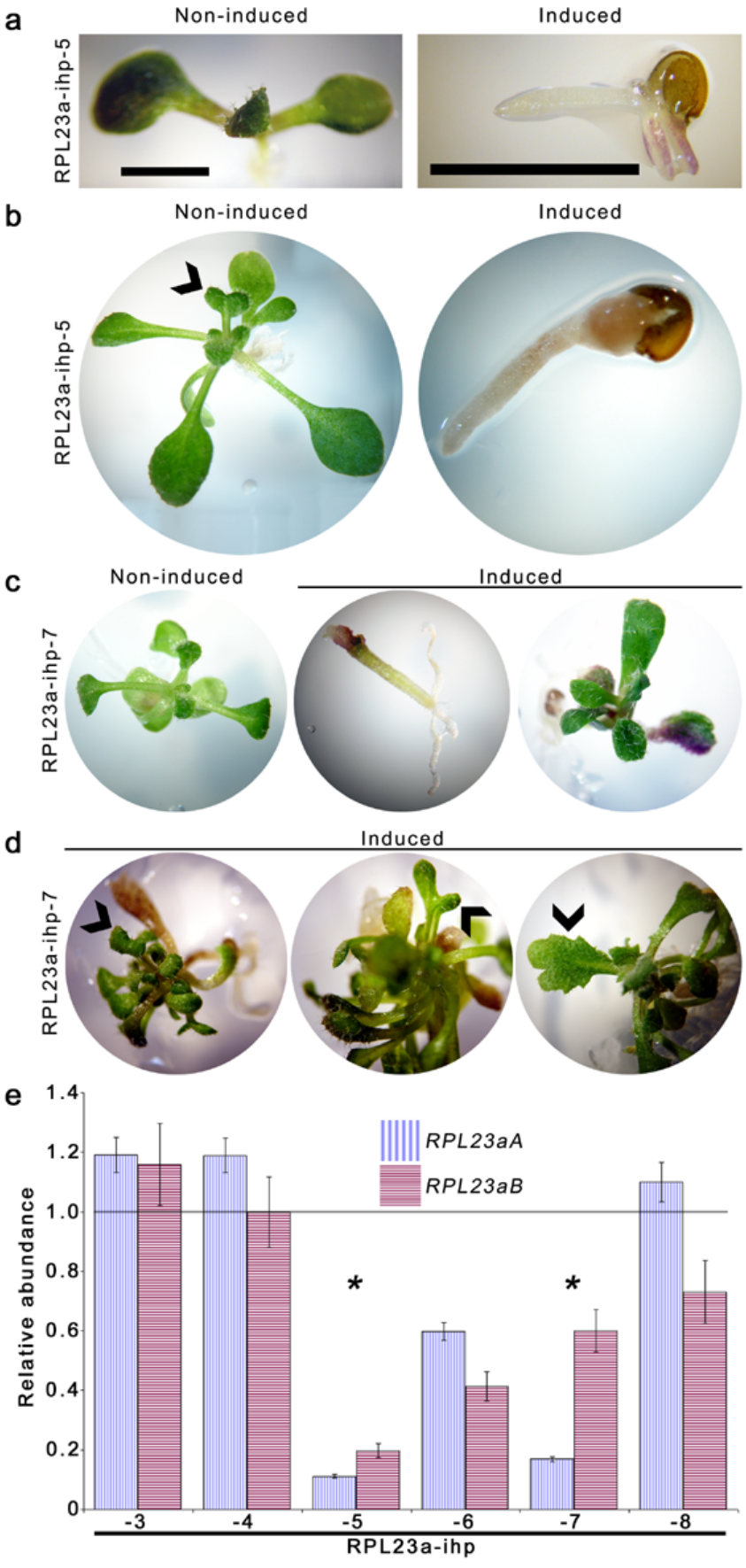
a
Non-induced
Induced
RPL23a-ihp-5
b
Non-induced
Induced
RPL23a-ihp-5
c
Non-induced
Induced
RPL23a-ihp-7
d
Induced
RPL23a-ihp-7
e
Relative abundance
1.4
1.2
1.0
0.8
0.6
0.4
0.2
0
RPL23aA
RPL23aB
*
*
-3
-4
-5
-6
-7
-8
RPL23a-ihp

(Figure 4.5e). Line –7, which had a survival rate of ~10–20% when plated on inductive media, had decreased levels of *RPL23aA* and increased levels of *RPL23aB* relative to line –6, which had a survival rate of <5% on inductive media. This suggests that *RPL23aB* may be capable of functionally compensating for *-A*. Overall, findings show that, consistent with its orthologs, the Arabidopsis RPL23a family is essential for viability.

4.4 Discussion

I have shown that both RPL23a isoforms accumulate in the nucleolus when transiently expressed in tobacco, providing further support for the hypothesis that this family contributes to ribosome heterogeneity (see Appendix C for further discussion) (Carroll et al., 2008; Chang et al., 2005; Giavalisco et al., 2005). I found that only RPL23aA is able to tolerate N-terminal GFP5 fusions and C-terminal fusion to mRFP without disrupting localization. Nucleolar-targeting of RPL23aB was completely disrupted by N-terminal fusions with GFP5, yet these fusions did not impede nuclear localization, as this construct readily accumulated in the nucleoplasm (Figure 4.3c–d and f) despite being larger than the size exclusion limit of the plant nuclear pore complex (Merkle, 2003). It could also be argued that nuclear localization of GFP5–RPL23aB results from overexpression of this construct and its slow diffusion into the nucleus (Bohnsack et al., 2002; Haasen et al., 1999), but this is not supported by my observations of nuclear localization in cells with only low expression levels (data not shown). Nucleolar targeting of RPL23aB was also impaired by C-terminal fusion with mRFP, but not by an equivalent fusion to GFP5. This may be explained, at least partially, by the biochemical properties of the GST–mRFP/GFP5 tags. Using the EMBOSS toolbox (Rice et al., 2000) I determined that the GST–GFP5 tag is more positively charged (pI = 6.31) and more basic than the GST–mRFP tag (pI = 6.16). RPL23a, like most r-proteins associating with negatively charged rRNA within the nucleolus (Brodersen et al., 2002; Klein et al., 2004), is positively charged (pI = 10.91–10.94) and basic. Thus the GST–GFP5 tag, attached to RPL23aA and RPL23aB, would be less likely to impede nucleolar localization via charge repulsion than the GST–mRFP tag. Nonetheless, I found that only RPL23aB localization was significantly disrupted by the mRFP tag, and thus I propose that RPL23aA has a stronger NoLS(s), or greater affinity for nucleolus-localized ligands.

I have shown that there are differences in nucleolar targeting of tagged isoforms, but not of nuclear accumulation, suggesting that the 9 residue differences between RPL23aA and RPL23aB

disrupt one or more NoLSs, or reduce efficiency of NoLS(s). One divergent region between the RPL23a isoforms occurs within a stretch of basic amino acids containing a putative NoLS/NLS (Dingwall and Laskey, 1991; Horke et al., 2004; Kalderon et al., 1984; Weber et al., 2000). In RPL23aA, this putative NoLS conforms to the core consensus sequence for nucleolin binding in mammals [$(K/R)_2XK$] (Intine et al., 2004; Lee et al., 1998; Wang et al., 2005a; Xue et al., 1993). Nucleolin is a major nucleolar protein, involved in RNA pol I transcription of rDNA, rRNA processing and nucleocytoplasmic trafficking of RNA and RNPs (Bouvet et al., 1998; Ginisty et al., 1998; Mongelard and Bouvet, 2007; Roger et al., 2003). It has recently been reported that nucleolin also functions in rDNA condensation and maintaining the nucleolus' structure in plants (Pontvianne et al., 2007). A nucleolin-binding motif in RPL23aA could explain why this isoform shows greater affinity for nucleolar accumulation than RPL23aB, which lacks a consensus nucleolin-binding motif. Nucleolin could function as a nucleolar 'anchor' for the r-protein prior to its assembly into pre-ribosomal particles, in the same manner as nucleolin-containing U3 snoRNPs bind to rDNA to prepare for processing of nascent rRNA transcripts (Caparros-Ruiz et al., 1997). A similar mechanism may function in the monocot rice, which also has two members to its RPL23a family. Only one rice isoform has a putative nucleolin-binding motif (OsRPL23a-1, Figure 4.1a), suggesting that one member of both the rice and Arabidopsis RPL23a families may have lost (or gained) its nucleolin-binding capacity following the respective duplication events that created the paralogs.

RPL23aA silencing results in development of a pleiotropic phenotype with symptoms similar to other characterized r-protein mutants, *RPS5B, RPS13B*, *RPS18A* and *RPL24B* (Ito et al., 2000; Nishimura et al., 2005; Van Lijsebettens et al., 1994; Weijers et al., 2001). In each case, loss/reduction of an r-protein leads to reduced cell division, retarded growth, morphological abnormalities and late-flowering. Further, vascular patterning is disrupted in all r-protein mutants (Ito et al., 2000; Nishimura et al., 2005; Weijers et al., 2001), except possibly for *RPS18A* where vasculature was not examined (Van Lijsebettens et al., 1994). This phenotype has been replicated in a recently characterized Arabidopsis nucleolin gene knockout mutant, *Atnuc-l1* (Kojima et al., 2007; Petricka and Nelson, 2007; Pontvianne et al., 2007). As described above, nucleolin has an established role in rDNA transcription and rRNA processing (Ginisty et al., 1999). For the latter, it assembles with the U3 snoRNP complex that cleaves nascent rRNA at the 5' external transcribed spacer primary processing site (Caparros-Ruiz et al., 1997; Saez-

Vasquez et al., 2004). In the *Atnuc-l1* mutant, pre-rRNA precursor accumulation is decreased, and primary cleavage and subsequent pre-rRNA processing are disrupted (Kojima et al., 2007; Petricka and Nelson, 2007; Pontvianne et al., 2007). In yeast, the RPL23a ortholog is required for efficient pre-rRNA processing (van Beekvelt et al., 2001), and both RPS13 and RPS18 are universally conserved, core structural components of the SSU that bind 18 S rRNA and are associated with the pre-rRNA processing complex (Brodersen et al., 2002; Pontvianne et al., 2007; Xiang and Lee, 1989; Yusupov et al., 2001). The striking similarity of phenotype between *rpl23aa, rps5b, rps13b, rps18a, rpl24b* and *Atnuc-l1* mutants may thus represent the *in vivo* response to decreased production of processed rRNAs, and the concomitant effects on ribosome biogenesis and protein production, with the observed severity gradient being a measure of the extent of the reduction in mature rRNAs. In this scenario, r-proteins likely act indirectly on pre-rRNA processing, with their binding required to induce conformational changes that facilitate pre-rRNA processing, or allow the association of other r-proteins and factors involved in processing (Ban et al., 2000; Mandiyan et al., 1991; van Beekvelt et al., 2001; Wimberly et al., 2000).

It is interesting that the phenotype obtained by silencing *RPL23aA* is not only similar to other r-protein and ribosome biogenesis mutants, but also to plants with disrupted auxin-responsiveness/polar auxin transport. For example, vascular patterning abnormalities similar to those resulting from impaired ribosome biogenesis have also been reported for *ettin/auxin response factor(arf)3* and *monopteros/arf5*, which are auxin-regulated transcription factor mutants (Nemhauser et al., 2000; Przemeck et al., 1996; Sessions et al., 1997); *pin-formed1*, an auxin efflux transporter mutant (Bennett et al., 1995; Goto et al., 1991; Petrasek et al., 2006), *auxin resistant1/axr1*, a mutant with reduced expression of a subunit of an enzyme complex that activates the auxin-regulated SCF^{TIR} ubiquitin-ligase (del Pozo et al., 2002; Deyholos et al., 2003), *hve1/cand1*, a mutant with reduced levels of a regulator of SCF^{TIR} assembly (Alonso-Peral et al., 2006), and *lop1/tornado1* and *tornado2*, which are mutant in establishing/maintaining auxin homeostasis (Carland and McHale, 1996; Cnops et al., 2006; Cnops et al., 2000). Moreover, treatment of wild-type plants with inhibitors of polar auxin transport has also been reported to disrupt vasculature, causing veins to be restricted to leaf margins and disrupting the midvein (Mattsson et al., 1999; Sieburth, 1999). Petricka and Nelson (2007) determined that auxin response maxima (detected with a synthetic reporter construct,

DR5–GUS, Sabatini et al., 1999; Ulmasov et al., 1997), which predict future sites of higher order venation (primary, secondary, tertiary, etc) (Mattsson et al., 2003), were mislocalized in developing leaves of their *Atnuc-l1* mutant, such that response maxima were not observed in leaf margins or at sites predicting tertiary or quaternary vein development. This reduction in marginal auxin response maxima was maintained when *Atnuc-l1* leaves were treated with an inhibitor of polar auxin transport, which in wild-type plants restricts response maxima to leaf margins (Mattsson et al., 2003; Petricka and Nelson, 2007). It is suggested that the observed pointed/narrow leaf and abnormal venation phenotypes result from a lack of marginal auxin sources/response factors, causing a reduction in auxin-mediated laterally-directed cell division and negating procambial differentiation at leaf margins, leading to a decrease in lateral expansion of the leaf and reduced vasculature with predominantly base to tip vein orientation (Petricka and Nelson, 2007). A more general reduction of auxin-response would also explain my observation of a loss of apical dominance, as auxin/auxin-responsiveness at the shoot apex is responsible for preventing the formation of lateral buds (Cline, 1991; Lincoln et al., 1990). Thus, perhaps the simplest explanation for the observed relationship between ribosome biogenesis and auxin transport/responsiveness is that synthesis of specific response/trafficking proteins is decreased below a certain required spatiotemporal threshold, disrupting auxin-regulated development and altering patterning. However, this explanation would seem to require a very specific reduction in the translation of auxin-response/trafficking genes.

Another possibility, is that auxin homeostasis is linked to cellular translational status through microRNAs (miRNAs). miRNAs are a class of small RNAs (~22 nts) that originate from long single-stranded RNAs (ssRNAs) transcribed from endogenous genes by RNA pol II (Xie et al., 2005). The ssRNAs possess internal complementarity allowing fold-back and formation of double-stranded RNA (dsRNA) that is processed by DICER-LIKE1 (DCL1) in conjunction with the dsRNA-binding protein, HYL1 (reviewed in Mallory and Vaucheret, 2006a). The dsmiRNAs are subsequently methylated by HEN1 and loaded onto ARGONAUTE1 (ARG1), which facilitates miRNA maturation and directs cleavage of transcripts with near-perfect complementarity to the miRNAs. Support for a link between miRNAs and auxin homeostasis is two-fold. First, mutants in miRNA biogenesis (*dcl1*, *hyl1*, *hen1*, *arg1*) have a range of severe pleiotropic symptoms consistent with disrupted auxin responses, including altered leaf morphology, reduced stature, aberrant gynoecium patterning, decreased apical dominance,

atypical phyllotaxis and irregular vasculature (Bohmert et al., 1998; Chen et al., 2002; Jacobsen et al., 1999; Lu and Fedoroff, 2000). Secondly, several experimentally and computationally determined targets of miRNAs are involved in the auxin response, including *TIR1*, a component of the SCF^{TIR} complex, *NAC1/NAM*, an auxin signal transducer, and *ARFs 6*, *8*, *10*, *16* and *17*, (Bonnet et al., 2004; Vazquez et al., 2004; Xie et al., 2007) (reviewed in Eckardt, 2005; Mallory and Vaucheret, 2006a). How then, are miRNA-mediated processes dependent on translational status? A possible answer comes from recent experiments in Drosophila, where Eulalio et al. (2007) fused the 3' UTR of different miRNA targets to the firefly luciferase ORF and quantified luciferase transcript levels in cell culture following incubation with or without cognate miRNAs. Transcript levels were shown to decrease significantly following incubation with miRNAs, however treatment of cells with translation inhibitors (cycloheximide, homoharringtonine, and hippuristanol) caused the stabilization of a subset of miRNA-targets. Eulalio et al. (2007) attributed the translational dependency of miRNA-target degradation on the possibility that silencing of some targets is initiated after translation commences. A similar mechanism operating in plants would provide an elegant model to explain my findings. Under normal conditions, translation in mitotically-active tissues is occurring at a very high rate, allowing the accurate degradation of miRNA targets (which include a large number of auxin response transcripts), and the maintenance of auxin homeostasis. However, when ribosome biogenesis, and consequently translation, are impaired, some miRNA targets are stabilized resulting in the disruption of auxin feedback cycles, leading to an array of developmental abnormalities. This model could, for example, explain my finding of reduced apical dominance; it has previously been shown that transgenic Arabidopsis expressing an engineered miRNA resistant version of *ARF17* have increased levels of *ARF17* transcript (Mallory et al., 2005). This line had a variety of auxin-related developmental defects, and showed an increase in transcript levels of 2 auxin-conjugating enzymes, *GH3.2/YDK1* and *GH3.3*, suggesting that *ARF17* functions as a repressor of the conjugating enzymes. Overexpression of *YDK1* has previously been shown to result in reduced apical dominance (Takase et al., 2004), presumably because of a reduction in free auxin acting on the meristem to inhibit the formation of lateral buds. It is clear from the phenotypes of auxin response-, miRNA synthesis-, and ribosome biogenesis-mutants that the regulation of auxin homeostasis is very complex, but it is an intriguing possibility that a common link relates all three processes.

I observed that no abnormal phenotype was detected as a result of silencing *RPL23aB*, or in a T-DNA insertion *rpl23ab* knockout line (Chapter 3). This adds to the mounting body of evidence indicating that, despite often overlapping transcript accumulation patterns, disparity exists in the requirement of r-protein paralogs for normal development (Barakat et al., 2001; McIntosh and Bonham-Smith, 2006). For example, expression profiles of Arabidopsis *RPS5A–B* (Weijers et al., 2001), *RPS18A–C* (Van Lijsebettens et al., 1994; Vanderhaeghen et al., 2006) and *RPL23aA–B* (McIntosh and Bonham-Smith, 2005) indicate that transcripts from all paralogs accumulate to the highest levels in mitogenic tissues (e.g. meristems, young leaves), and the lowest in non-dividing tissues. In all cases, the absolute transcript level varies, but the relative contribution from each paralog remains fairly constant. This is exemplified by transcript profiling of *RPS18A–C*, indicating that *RPS18A*, *RPS18B*, and *RPS18C* represent ~27, 16, and 57%, respectively, of the total *RPS18* transcript pool (Vanderhaeghen et al., 2006). Yet, for each of these families it has been demonstrated that knockout or knockdown mutants of a single paralog triggers development of the atypical phenotype (*RPS5B*, *RPS18A* and *RPL23aA*, present work, Van Lijsebettens et al., 1994; Weijers et al., 2001). These findings could easily be reconciled if the abnormal phenotype-triggering mutation disrupted the predominantly expressed gene, or if a corresponding mutation in another paralog induced the same phenotypic response, but this is not supported by experimental data. For example, *RPS18A* represents roughly only ¼ of the total *RPS18* transcript, and yet its loss produces the *pfl* phenotype (Van Lijsebettens et al., 1994). Similarly, this phenotype was reproduced in a knockout of *RPS13B*, which also makes only a small contribution to the *RPS13* transcript pool (Ito et al., 2000). It could also be the case that differential spatiotemporal expression of paralogs leads to observed knockout/knockdown phenotypes. It has been shown that *RPS5B* is predominately localized to cell division zones, while *RPS5A* is found in less mitotically-active regions (Weijers et al., 2001). Yet, this too would be an oversimplified explanation given our findings of overlapping GUS-staining directed by *RPL23aA* and *RPL23aB* 5' RRs (Chapter 2). Moreover, evidence to date suggests that plant r-protein paralogs are differentially required for "normal" development, with ancillary paralogs functioning only under exceptional conditions, perhaps mediated through spatiotemporal regulation, stimulus-induced expression, assumption of extra-ribosomal roles (reviewed in Wool, 1996), or via disparity in cognate binding partners (e.g. affinity for nucleolin).

I have demonstrated for the first time in a higher eukaryote that the *RPL23a* family is essential for viability. This is in agreement with previous findings in numerous prokaryotes, yeast and *Caenorhabditis elegans* (Kamath et al., 2003; Zhang et al., 2004). Induction of the *RPL23a*-family silencing construct results in a range of severe pleiotropic phenotypes characterized by developmental defects, reduced shoot and root growth, flower abortion, and in the most severe case, death upon germination. Given the established importance of RPL23a, my inducibly lethal *RPL23a*-silencing lines could be useful tools for the *in vivo* analysis of rRNA processing, LSU assembly and protein synthesis defects. This adds RPL23a to a growing list of r-proteins from higher eukaryotes that are essential for viability, including RPS5 from Arabidopsis (Weijers et al., 2001), and RPS2, RPS3, RPS4, RPS5, RPS6, RPS13, RPS14, RPL5, RPL9, RPL14, RPL19, RPL38 from fruit fly (reviewed in Marygold et al., 2005; Saboe-Larssen et al., 1998).

Herein I have demonstrated that the Arabidopsis RPL23a paralogs are differentially targeted to the nucleolus. Disparity within a putative NoLS appears to be responsible, but future work is necessary to determine whether this directly affects their respective abilities to bind to the nucleolus structural protein, nucleolin. I have shown by RNAi-mediated silencing that *RPL23aB* is phenotypically dispensable, while *RPL23aA* knockdown leads to a severe *pfl* phenotype that is possibly due to impaired pre-rRNA processing and consequential effects on miRNA-target stability and auxin homeostasis. How directly r-proteins, and particularly RPL23a, are involved in pre-rRNA processing has yet to be elucidated. I have determined that the RPL23a family is essential for survival by the non-viability of transgenic lines that silence both paralogs. These lines have a normal lifecycle on non-inductive media, and thus may be useful tools for studying ribosome biogenesis at different developmental stages.

5 CHAPTER 5. REGULATION OF RIBOSOMAL PROTEIN RPL23a LEVELS IN ARABIDOPSIS BY PROTEASOME-MEDIATED DEGRADATION

Previous work (Chapters 2 and 3) has provided evidence that regulation of *RPL23a* expression occurs at both the transcriptional and translational level. Here we investigated whether regulation also occurs at the post-translational level via protein turnover. Tagged RPL23a r-proteins and specific inhibitors of the 26 S proteasome were used to monitor the distribution and stability of r-proteins in Arabidopsis and tobacco. In Arabidopsis, fluorescent protein tagged isoforms of RPL23a were found to be unstable, but could be stabilized by treatment with a proteasome-inhibitor. In tobacco, tagged Arabidopsis r-proteins were more stable, but predominantly were found in a polyubiquitylated form. Results suggest that plants have an analogous system to mammals for the proteasome-mediated degradation of excess r-proteins that operates to ensure an equimolar quantity of r-proteins for subunit biogenesis.

5.1 Introduction

Translation in the model flowering plant Arabidopsis is conducted by three distinct populations of ribosomes: the bacterial-like 70 S ribosomes of the mitochondria and plastids, and the larger 80 S cytoplasmic and endoplasmic reticulum-associated ribosomes. The latter consists of two subunits (60 S and 40 S), four rRNAs (18 S, 26 S, 5.8 S and 5 S) and 81 r-proteins (Barakat et al., 2001; Chang et al., 2005). All r-proteins of the 80 S ribosome are present as single-copies except for the acidic phosphoproteins that assemble into a multimeric lateral stalk (Ban et al., 2000; Guarinos et al., 2003; Hanson et al., 2004; Schuwirth et al., 2005; Spahn et al., 2001; Wimberly et al., 2000). However, in plants r-proteins are encoded from multigene families (2–7 members) containing more than one expressed member (Barakat et al., 2001; Hulm et al., 2005; McIntosh and Bonham-Smith, 2005; Ouyang et al., 2007; Popescu and Tumer, 2004). In some cases family members are differentially expressed in a tissue-, stress-, or development-specific manner. For example, in the Arabidopsis RPL11 family, the RR of *RPL11C* directed reporter gene expression in meristematic regions of vegetative and reproductive tissues, while expression from -A was restricted to regions of the root and anthers (Williams and Sussex, 1995). Nevertheless, most studies suggest that expression of family members is largely overlapping, and is greater in meristems and rapidly growing tissues (Barakat et al., 2007; Hulm et al., 2005; McIntosh and Bonham-Smith, 2005; Van Lijsebettens et al., 1994;

Williams and Sussex, 1995). Proteomic analyses of the cytoplasmic ribosome have confirmed that overlapping expression of family members provides a source of ribosome heterogeneity (Carroll et al., 2008; Chang et al., 2005; Giavalisco et al., 2005). For example, isolated ribosomal fractions contained peptide signatures matching all members of the RPS3 family (RPS3A–C), and three of four members of the RPL7, RPL13a and RPL35 families (Carroll et al., 2008).

Eukaryotes employ a variety of strategies to govern equimolar accumulation of r-proteins (reviewed in McIntosh and Bonham-Smith, 2006). In budding yeast, 59 of 79 r-proteins are encoded from two-member gene families and regulation occurs predominantly at the transcriptional level (Planta and Mager, 1998; Sengupta et al., 2004). Transcripts have short half-lives (Kim and Warner, 1983; Li et al., 1999) and accumulate to roughly equivalent cellular levels for each r-protein due to transcriptional compensation within families (i.e. if one paralog is transcribed at a high rate, the other is transcribed at a low rate) (Planta, 1997; Tornow and Santangelo, 1994; Warner et al., 1985). Regulation also occurs at the post-transcriptional level via the turnover of r-proteins produced in excess of biological demands (El-Baradi et al., 1986; Tsay et al., 1988). Copy number of r-protein genes in animals is highly variable. In mammals, gene families are very large, but generally only one copy is expressed and the remainder are present as inactive, processed pseudogenes (Wool et al., 1995; Zhang et al., 2003). By contrast, invertebrates tend to have smaller gene families containing 1–3 expressed members (Barthelemy et al., 2007; Marygold et al., 2007; Semple and Wolfe, 1999). The r-protein transcripts of both animals and fission yeast have relatively long half-lives (Geyer et al., 1982; Lackner et al., 2007), and regulation occurs principally post-transcriptionally via the coordinated recruitment of r-protein transcripts to polysomes in response to growth stimuli (Bachand et al., 2006; Garcia-Martinez et al., 2007; reviewed in Meyuhas, 2000). Additionally, animal r-proteins not incorporated into ribosome subunits are rapidly degraded (Pierandrei-Amaldi et al., 1985). The mechanisms used for coordinate regulation of plant r-proteins are largely unknown, although there is evidence indicating a role for transcriptional, posttranscriptional, translational and posttranslational-regulation (reviewed in McIntosh and Bonham-Smith, 2006).

Recently, a combination of quantitative mass spectrometry and bioimaging has been used to investigate the synthesis, nucleocytoplasmic transport, mobility and degradation of nucleolar proteins in HeLa cells (Andersen et al., 2005; Lam et al., 2007). These studies found that newly

synthesized r-proteins are targeted to the nucleolus more rapidly than other nucleolar proteins, and far in excess of physiological demands (Lam et al., 2007). When no nascent rRNA transcripts are present for subunit assemble, the excess r-proteins begin to shuttle between the nucleolus and the nucleoplasm, where they are exposed to the 26 S proteasome and degraded (Lam et al., 2007; Matsumoto et al., 2005a). A similar mechanism is postulated to exist in yeast (Warner, 1989) given the short half-life of unused r-proteins (reviewed in Warner, 1989), and the finding that ectopically expressed r-proteins are highly unstable (Gritz et al., 1985; Warner et al., 1985), but can be stabilized by depletion of the corresponding endogenous r-protein (Abovich et al., 1985). Under this model, the rate-limiting step governing production of ribosome subunits is the synthesis of rRNA (Lam et al., 2007). In the present work I investigated the existence of a proteasome-mediated degradation pathway for excess r-proteins in plants. Fluorophore-tagged RPL23aA/B were expressed in Arabidopsis and tobacco and their accumulation patterns and relative stability were observed. Specific inhibitors of the 26 S-proteasome were used to determine r-protein dynamics in Arabidopsis. I show that fluorophore-tagged RPL23aA/B are unstable in Arabidopsis, but can be stabilized by treatment with a proteasome inhibitor. In tobacco, a portion of the tagged r-protein accumulated in the nucleolus (Degenhardt and Bonham-Smith, 2008a), but predominantly occurred as a ubiquitylated degradation intermediate. Similarly, chemical inhibition of the Arabidopsis 26 S-proteasome resulted in the accumulation of N-terminally tagged RPL23aA and RPL23aB fusion proteins as ubiquitylated intermediates. Results suggest that coordinate regulation of plant r-proteins involves the proteasome-mediated degradation of r-proteins produced in excess of biological requirements.

5.2 Materials and Methods

5.2.1 Plant material and growth conditions

Arabidopsis cultivar Columbia-0 was grown in a vermiculite/peat soil (Redi-Earth, WR Grace & Co.), or on basal media. Prior to plating, Arabidopsis seed was vapor phase sterilized for 16–20 h (Clough and Bent, 1998) or sterilized in a bleach solution (2.625% sodium hypochlorite, 0.5% Tween 20 [Calbiochem]) for 5 min followed by sequential washes with water. Plated or soil-sown Arabidopsis seed was stratified at 4ºC for three days and then placed in a growth chamber with a 23º/18ºC temperature regime and a 16 h/8 h photoperiod of ~120 µmol photons m^{-2} sec^{-1}. For protoplasts, Arabidopsis seed was bleach-sterilized, plated on 1X MS medium

(0.6% phytagar) and grown under a 23º/18ºC temperature regime and a 12 h/12 h photoperiod of ~100 µmol photons m^{-2} sec^{-1}. Tobacco cultivar Petit Havana seed was sown in peat/perlite soil (Sunshine Mix 1, Sun Gro, Vancouver, BC, Canada) and plants were grown in a growth chamber with a 23º/18ºC temperature regime and a 16 h/8 h photoperiod of ~170 µmol photons m^{-2} sec^{-1}.

5.2.2 Arabidopsis biolistics and stable transformations

Creation of N- and C-terminally-tagged RPL23aA/B fusion proteins, and the free mRFP control, were previously described (Degenhardt and Bonham-Smith, 2008a). For the transient expression of fluorescent protein constructs using biolistics, 14–18 day-old Arabidopsis seedlings were transferred to 6 cm Petri-plates containing fresh ½ MS media (0% sucrose) and subjected to biolistic infiltration with a PDS-1000/He Biolistic Particle Delivery System (Bio-Rad) modified as follows from manufacturer's instructions: uncut plasmid DNA (0.5–4 µg μl^{-1}) was precipitated onto 1 µm (Bio-Rad) or 1.6+ µm gold particles (Sigma-Aldrich), and whole seedlings (abaxial side up) were bombarded using 900 and 1100 PSI rupture discs (Bio-Rad). Following bombardment, seedlings were turned upright and returned to the growth chamber for 48–96 h prior to CLSM visualization.

The floral dip protocol (Clough and Bent, 1998) was used to stably transform Arabidopsis. Transformants were selected on ½ MS media supplemented with 25 µg ml^{-1} hygromycin (Invivogen) and 200 µg ml^{-1} cefotaxime (Sanofi-Aventis). Fluorescent protein imaging (CLSM) and Western blotting were performed on T_3 transgenic lines.

5.2.3 Confocal microscopy

CLSM was conducted using previously described settings (Brandizzi et al., 2002a; Degenhardt and Bonham-Smith, 2008a; Runions et al., 2006). For co-visualization of GFP fluorescence and chloroplast autofluorescence in protoplast experiments, a 650 nm longpass filter was used along with a 515-nm dichromatic beam splitter. Image processing was done with Zeiss LSM Image Browser software and figures were prepared using Adobe Photoshop 7.0 software.

5.2.4 Quantitative RT-PCR

Procedures for RNA extraction, first-strand synthesis and qPCR were previously described (Degenhardt and Bonham-Smith, 2008a). Total RNA for qRT-PCR was extracted from 10–18 day-old whole seedlings. Quantification of the *GFP5–RPL23aA/B* transgenes was carried out with GFP5_qRT_F ($^{5'}$GCGTCAAGGAGGACGGAAACATC$^{3'}$) and GFP5_qRT_R

($^{5'}$GCGAAAGGGCAGATTGTGTGGAC$^{3'}$) primers. The identity of the amplicon was confirmed by automated sequencing (NRC-PBI). A minimum of three biological replicates were analyzed. Processing of optical data was done with the iQ5 Optical System software (Bio-Rad) and data analysis was conducted using Microsoft Excel.

5.2.5 Proteasome inhibition in protoplasts, excised leaves and whole seedlings

Arabidopsis leaf protoplasts were prepared from 17–45 day-old wildtype and T_3 GFP5–L23aA/B stable transgenic plants, grown on 1X MS media supplemented with 0 (WT) or 25 μM hygromycin (T_3 lines). The T_3 lines A3 and B2 were selected because they had the greatest transgene expression. Protoplasts were isolated essentially following previously described methods (Yoo et al., 2007), with the exception that protoplasts were resuspended in culture media **(**0.4 M mannitol, 15 mM MgCl, 4 mM MES and 0.442% MS medium, pH 5.7**)** supplemented with 25–50 μM *clasto*-lactacystin-β-lactone (Sigma-Alrich). After 1.5–24 hours of incubation at room temperature in the dark with gentle shaking (60 RPM) protoplasts were either viewed with a CLSM or pelletted at 200 *g* for 2 minutes and frozen in $N_{2(l)}$ for protein extraction.

For proteasome inhibition in intact leaves, wildtype and T_3 stable transgenics expressing *GFP5–L23aA/B* were grown as above for 29 days, at which time leaves were removed and vacuum infiltrated with 50 μM β-lactone using previously described methods (Hori and Watanabe, 2005). After 5–23 hours incubation at room temperature in the dark with shaking (200 RPM) protoplasts were viewed by CLSM.

5.2.6 Ribsome/polysome isolations

The ribosomal fraction of non-transformed tobacco, and tobacco transiently expressing FIB2–EGFP, and RPL23aA and RPL23aB with N- and C-terminal GFP5-tags were isolated essentially as previously described (Williams et al., 2003; Zanetti et al., 2005), with the following modifications: 1.25 mL of polysome extraction buffer (PEB) was added to ~700 mg of manually pulverized tissue, PEB contained 114.4 mM β-mercaptoethanol instead of DTT, and an SW55 Ti rotor (Beckman, Fullerton, CA) was used in place of a 70 Ti rotor. The polysomal fraction from the same plant material was isolated using the above-mentioned PEB recipe and fractions were separated as previously described (Kawaguchi and Bailey-Serres, 2005; Kawaguchi et al., 2003).

A total of 10 fractions were collected: the top and bottom 5 (non-ribosomal and polysomal/ribosomal, respectively) were pooled separately. Protein was precipitated by incubation overnight in 10 volumes 1:9 TCA:acetone at -20°C, followed by resuspension in 2 mL water. Sucrose was removed by chloroform/methanol precipitation, and the protein pellet was resuspended in 1X Laemmli SDS buffer (Laemmli, 1970).

5.2.7 Immunodetection of GFP fusion proteins and r-proteins

Total soluble protein from tobacco and Arabidopsis plants stably transformed with, or transiently expressing, N-terminal GFP fusion proteins was isolated as previously described (Ni et al., 1996; Wang et al., 2005b). Protein from Arabidopsis protoplasts was isolated using the method of Crofts et al. (1999). Proteins from ribosomal/polysomal fractions were isolated as described above. Soluble proteins were separated through 10–12% SDS-PAGE gels, and detected using the enhanced chemiluminescence system (GE Healthcare, Piscataway, NJ) with a rabbit polyclonal GFP antibody (Santa Cruz Biotechnology, Santa Cruz, CA and abcam, Cambridge, MA). For the identification of polyubiquitylated fusion proteins, membranes probed with anti-GFP were stripped by incubating in stripping buffer (62.5 mM Tris-Cl, pH 6.7, 100 mM β-mercaptoethanol, 2% SDS) for 1 hour at 65ºC with occasional agitation. These membranes were then reprobed with a rabbit polyclonal antibody to ubiquitin (Rockland Immunochemicals, Gilbertsville, PA). Equal loading was evaluated by staining membranes with 0.2% Ponceau S (Sigma-Aldrich) or Coomassie-Blue.

5.3 Results

5.3.1 Fluorescent protein tagged RPL23a isoforms are not stable in Arabidopsis

I recently characterized the localization of Arabidopsis RPL23aA and RPL23aB tagged with a fluorescent protein in a heterologous tobacco system (Chapter 4, Degenhardt and Bonham-Smith, 2008a). RPL23a is the plant ortholog of a universally conserved r-protein family (Lecompte et al., 2002). It binds directly to 23–28S rRNA, is essential for ribosome biogenesis (El-Baradi et al., 1987; El-Baradi et al., 1984; El-Baradi et al., 1985; Rutgers et al., 1991), and with RPL35 forms a “promiscuous binding site” (Halic et al., 2004) responsible for cotranslational targeting and translocation of nascent polypeptides (Beckmann et al., 1997; Halic et al., 2004; Maier et al., 2005; Menetret et al., 2005; Morgan et al., 2002; Pool et al., 2002). Although it has been

demonstrated that fusing a small FLAG–His_6 tag (~2 kD) to the C-terminus of RPL23aA does not prevent the fusion protein from incorporating into Arabidopsis ribosomes or forming polysomes (Zanetti et al., 2005), my previous studies did not examine ribosomal incorporation of RPL23aA/B with a much larger glutathione *S*-transferase–GFP tag (GST–GFP5; 466 residue, 53.4 kD). To determine if GST–GFP5 tagged r-proteins were incorporated into ribosomes, I conducted Western blot analyses using a GFP antibody on ribosomal pellet-, sucrose-gradient separated polysomal-, and non-ribosomal-fractions from tobacco leaves transiently expressing C- and N-terminally-tagged RPL23aA/B. Despite weak expression of tagged RPL23a isoforms in tobacco leaves used for Westerns (Figure 5.1a), a faint band corresponding to the molecular weight of the fusion protein (~70.8 kD) was detected in ribosomal/polysomal fractions from leaves expressing C- and N-terminally tagged RPL23aA (Figure 5.1b, d; data not shown for polysomal fraction of RPL23aA–GFP5) and C-terminally tagged RPL23aB (Figure 5.1d; data not shown for ribosomal pellet fraction of RPL23aB–GFP). However, no product was detected in the corresponding fractions from leaves expressing an EGFP-tagged nucleolar marker (FIB2, Figure 5.1d, data not shown for ribosomal pellet fraction, Barneche et al., 2000; Degenhardt and Bonham-Smith, 2008a), or GFP5–RPL23aB (Figure 5.1d; data not shown for ribosomal pellet fraction), which I previously found to be excluded from the nucleolus (Figure 5.1a, Degenhardt and Bonham-Smith, 2008a), or from non-transformed tobacco (Figure 5.1b, d). A band corresponding to the fusion protein was also detected in non-ribosomal fractions of C-terminally tagged RPL23aA/B (Figure. 5.1b, d), indicating that a portion of these fusion proteins were not incorporated into ribosomes in tobacco.

Having established that RPL23aA/B fusion proteins assemble as endogenous r-proteins, I attempted to express these constructs in Arabidopsis to evaluate their relative expression when expressed ectopically under the control of the CaMV 35S promoter. To verify localization patterns, the GFP5 tag was swapped with a mRFP tag to allow for coexpression with FIB2–EGFP. Biolistics was used to infiltrate epidermal cells of Arabidopsis seedlings with C-terminally tagged RPL23a and FIB2. Forty-eight h post-bombardment, FIB2–EGFP was highly expressed and accumulated in nucleoli (Figure 5.2a–b), however no fluorescence from RPL23aA/B–mRFP was detected. No fluorescence was observed regardless of incubation period post-bombardment (24–96 h), plasmid concentration (0.5–4 $\mu g\ \mu l^{-1}$), age or size of bombarded leaves, and was consistent when plants were bombarded with RPL23aA/B–GFP5 constructs

Figure 5.1 RPL23aA and RPL23aB fusion proteins are incorporated into ribosomes. **a** CLSM images of tobacco epidermal cells transiently expressing N- and C-terminally tagged RPL23aA and RPL23aB. Nucleoli and nucleolar exclusion zones are indicated by solid and transparent white arrowheads, respectively. White bars = 5 μm. **b** Western blot using an anti-GFP antibody of the ribosomal pellet (even lanes) and ribosome-depleted crude fraction (odd lanes) from non-transformed tobacco (lanes 7–8) or tobacco leaves transiently expressing RPL23aA–GFP5 (lanes 1–2), GFP5–RPL23aA (lanes 3–4), and GFP5–RPL23aB (lanes 5–6). Large black arrowheads show positions of molecular mass markers; smaller black arrowheads show products detected in ribosomal or crude fractions not detected in the non-transformed control. **c** Ponceau S-staining of nitrocellulose membrane in (**a**) to show loading. **d** Western blot as in (**a**) of sucrose-gradient fractionated polysomal (even lanes) and non-polysomal (odd lanes) proteins from nontransformed tobacco (lane 7–8), or tobacco leaves transiently expressing RPL23aB–GFP5 (lane 1–2), GFP5–RPL23aA (lane 3–4), and FIB2–EGFP (5–6). Arrowheads as in (**a**). **e** Ponceau S-staining of nitrocellulose membrane in (**c**) to show loading.

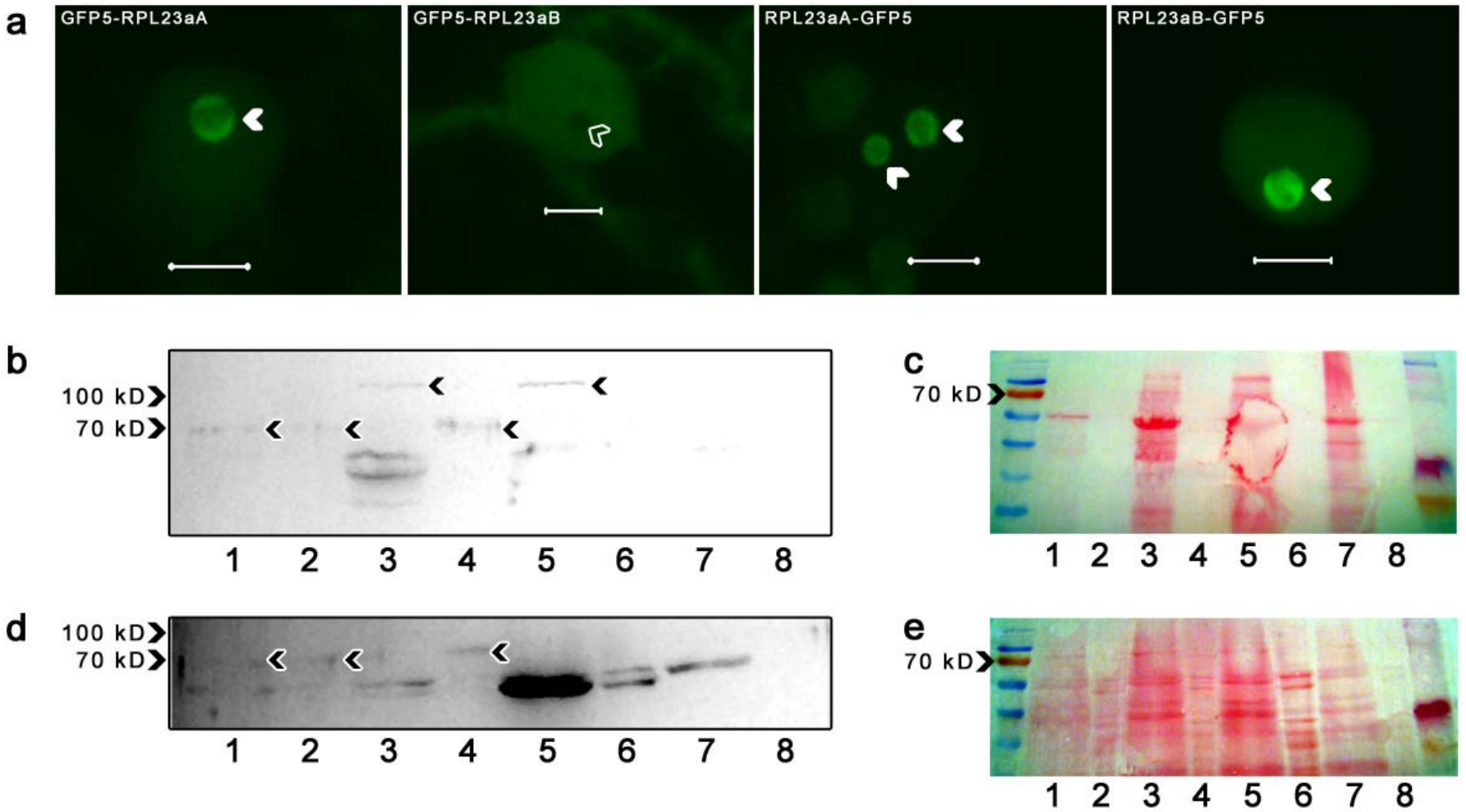
a
GFP5-RPL23aA
GFP5-RPL23aB
RPL23aA-GFP5
RPL23aB-GFP5
b
100 kD
70 kD
1 2 3 4 5 6 7 8
c
70 kD
1 2 3 4 5 6 7 8
d
100 kD
70 kD
1 2 3 4 5 6 7 8
e
70 kD
1 2 3 4 5 6 7 8

Figure 5.2 RPL23a–fluorescent protein fusions are not stable in Arabidopsis. **a–b** Representative CLSM images of Arabidopsis epidermal cells infiltrated via bombardment using gold particles coated with RPL23aA–mRFP + FIB2–EGFP constructs (**a**), or RPL23aB–mRFP + FIB2–EGFP constructs (**b**). Images of the same optical slice were merged to show signal overlap (right panel in **a**–**b**). Solid white arrowheads indicate nucleoli. Bars = 10 µm. **c** Agarose gel of EvaGreen-stained *RPL23aA/B–GFP5* PCR products amplified from Arabidopsis seedlings 48 h after particle bombardment with 1 µg (columns A1 and B1) or 2 µg (columns A2 and B2) of RPL23aA/B–GFP5 constructs. Amplicon is 236 bp. **d** qRT-PCR quantification of *RPL23aA–GFP5* and *RPL23aB–GFP5* transcript abundance from bombarded Arabidopsis seedlings (x-axis labels as in **c**). Vertical hatched lines represent the *ACT7* level (standardized to a value of 1); horizontal hatched lines represent the relative level of *RPL23aA–GFP5* (columns A1–A2) or *RPL23aB–GFP5* (columns B1–B2). Bars represent SEM. **e** Western blot with an anti-GFP antibody of Arabidopsis seedlings bombarded with RPL23aA–GFP5 and RPL23aB–GFP5 constructs (lane 1 and 2, respectively), non-transformed control seedlings (lane 3), or tobacco transiently expressing GFP5–RPL23aB (lane 4, positive control). Black arrowheads show positions of molecular mass markers. **f** Ponceau S-staining of nitrocellulose membrane (**e**) showing equal loading.

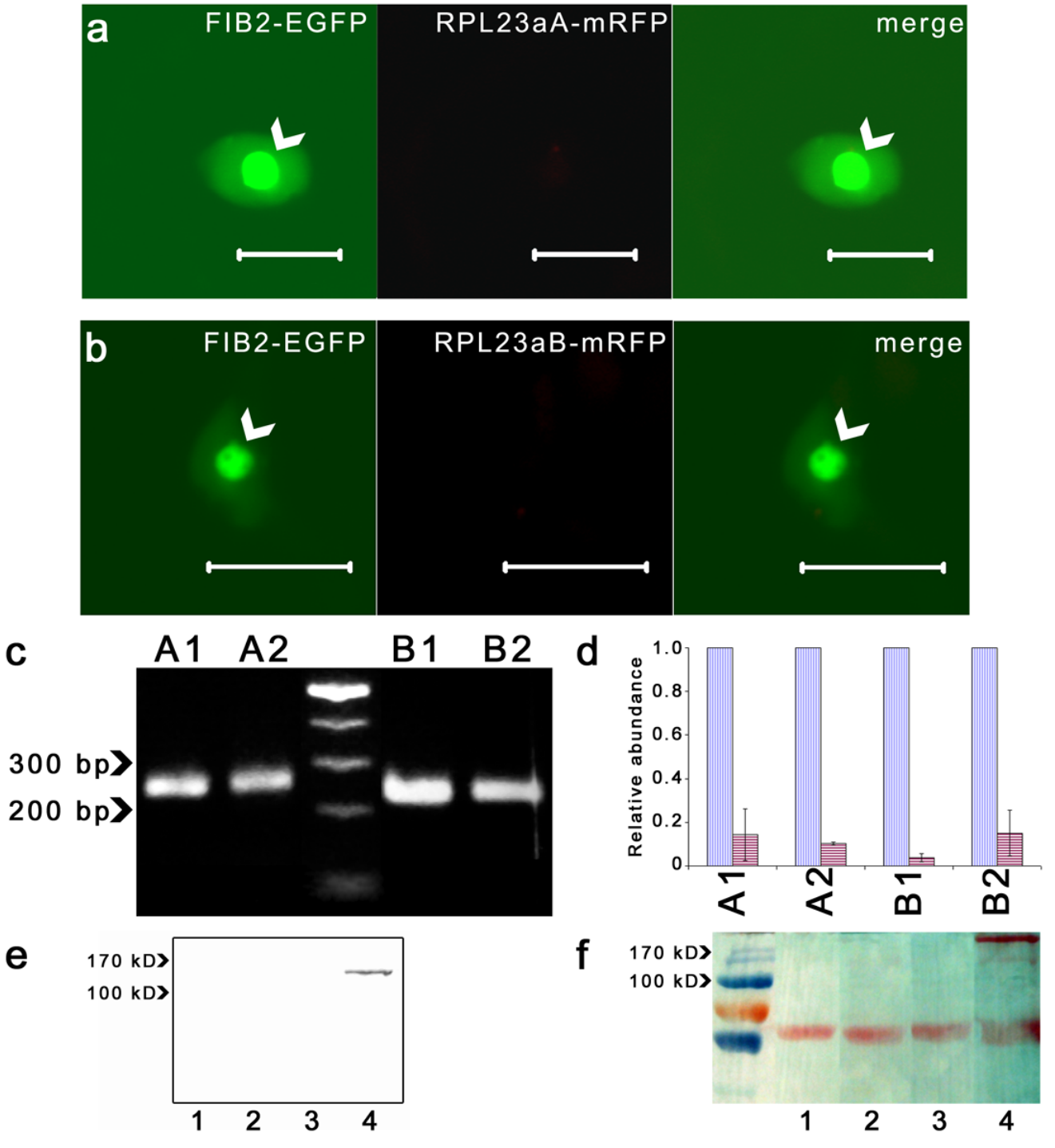
a
FIB2-EGFP
RPL23aA-mRFP
merge
b
FIB2-EGFP
RPL23aB-mRFP
merge
c
A1
A2
B1
B2
300 bp
200 bp
d
Relative abundance
1.0
0.8
0.6
0.4
0.2
0
A1
A2
B1
B2
e
170 kD
100 kD
1
2
3
4
f
170 kD
100 kD
1
2
3
4

alone (data not shown). To determine if the fusion protein constructs were being transcribed, I performed quantitative RT-PCR (qRT-PCR) on RNA from seedlings bombarded with RPL23aA–GFP5 and RPL23aB–GFP5. Results indicated that, although *RPL23aA–GFP5* and *RPL23aB–GFP5* transcripts were present (Figure 5.2c), abundance was 7–10-fold and 7–28-fold less than the actin internal control gene, *ACT7*, respectively (Figure 5.2d). This finding suggested that my inability to express RPL23aA/B–GFP5/mRFP fusions in Arabidopsis was not due to an inability to accumulate transcript, especially given the relatively poor transformation efficiency using the particle bombardment technique (i.e. less than 5% of cells bombarded with FIB2–EGFP showed expression), and the concomitant dilution of transgene signal. To determine if the fusion protein transcripts were being translated at levels undetectable by confocal laser scanning microscopy (CLSM), Western blots of RPL23aA/B–GFP5-bombarded seedlings, wildtype Arabidopsis seedlings (negative control) and tobacco leaves 72 h post-infiltration with the GFP5–RPL23aB constructs (positive control), were carried out using a GFP5 antibody. While no product was detected in the negative control or the bombarded Arabidopsis seedlings, a protein with >100 kD mass was identified from tobacco expressing GFP5–RPL23aB (Figure 5.2e). Although heavier than the predicted mass of the fusion protein (~70.8 kD), a similar size product was recognized by anti-GFP in the ribosome-depleted crude fraction of tobacco leaves expressing GFP5–RPL23aB (Figure 5.1b), and in a crude protein extract from tobacco expressing GFP5–RPL23aA (Figure 5.3a). No product was detected in non-transformed tobacco (Figure 5.3a and c**)**. This product did not appear to be a dimer, as it was stable even when boiled for 20 min with 0.7 M β-mercaptoethanol, or for 5 min with 20% SDS and 400 mM DTT (data not shown). Moreover, by loading more protein a product of the appropriate mass (~71 kD) was detected (Figure 5.5e), although it appeared much fainter than the heavier products.

These findings in Arabidopsis seedlings suggested that RPL23aA/B–GFP5 was being degraded post-translationally, but the possibility remained that the fusion proteins were expressed at levels undetectable by my technique. To increase expression, I generated stable transgenic Arabidopsis lines via floral dip using the N-terminal GFP5 tagged RPL23aA/B constructs under control of the enhanced CaMV 35S promoter (Saint-Jore et al., 2002), which I had previously found produced higher expression levels in tobacco than C-terminally tagged constructs (data not shown). qRT-PCR conducted on four and three T_3 lines independently transformed with GFP5–RPL23aA and GFP5–RPL23aB, respectively, determined that one transgenic line for each construct had

Figure 5.3 Stably transformed Arabidopsis are unable to express GFP5–RPL23aA/B despite high levels of transcript. **a** and **c** Western blot using an anti-GFP antibody of T_3 Arabidopsis seedlings transformed with GFP5–RPL23aA lines A1–A4 (**a**, lanes 2–5), or with GFP5–RPL23aB lines B1–B3 (**c**, lanes 2–4), non-transformed Arabidopsis seedlings (**a** and **c**, lane 1), non-transformed tobacco (**a**, lane 7; **c**, lane 6), and tobacco transiently expressing GFP5–RPL23aA (**a**, lane 6), or GFP5–RPL23aB (**c**, lane 5). Large black arrowheads show positions of molecular mass markers; smaller black arrowheads show products detected by GFP antibody. **b** and **d** Coomassie-Blue staining of nitrocellulose membranes (**a** and **c**, respectively) showing equal loading. **e** qRT-PCR of *GFP5–RPL23aA* and *RPL23aB* transcript abundance in T_3 Arabidopsis transgenic seedlings. Vertical hatched lines represent the *ACT7* level (standardized to a value of 1); horizontal hatched lines represent the relative level of *GFP5–RPL23aA* in transgenics lines A1–A4, and of *GFP5–RPL23aB* in transgenic lines B–1 to B–3. Bars represent SEM. **f** CLSM images of T_2 Arabidopsis transgenic seedlings (line mRFP–6) expressing free mRFP. The transparent white arrowhead indicates a nucleolar exclusion zone.

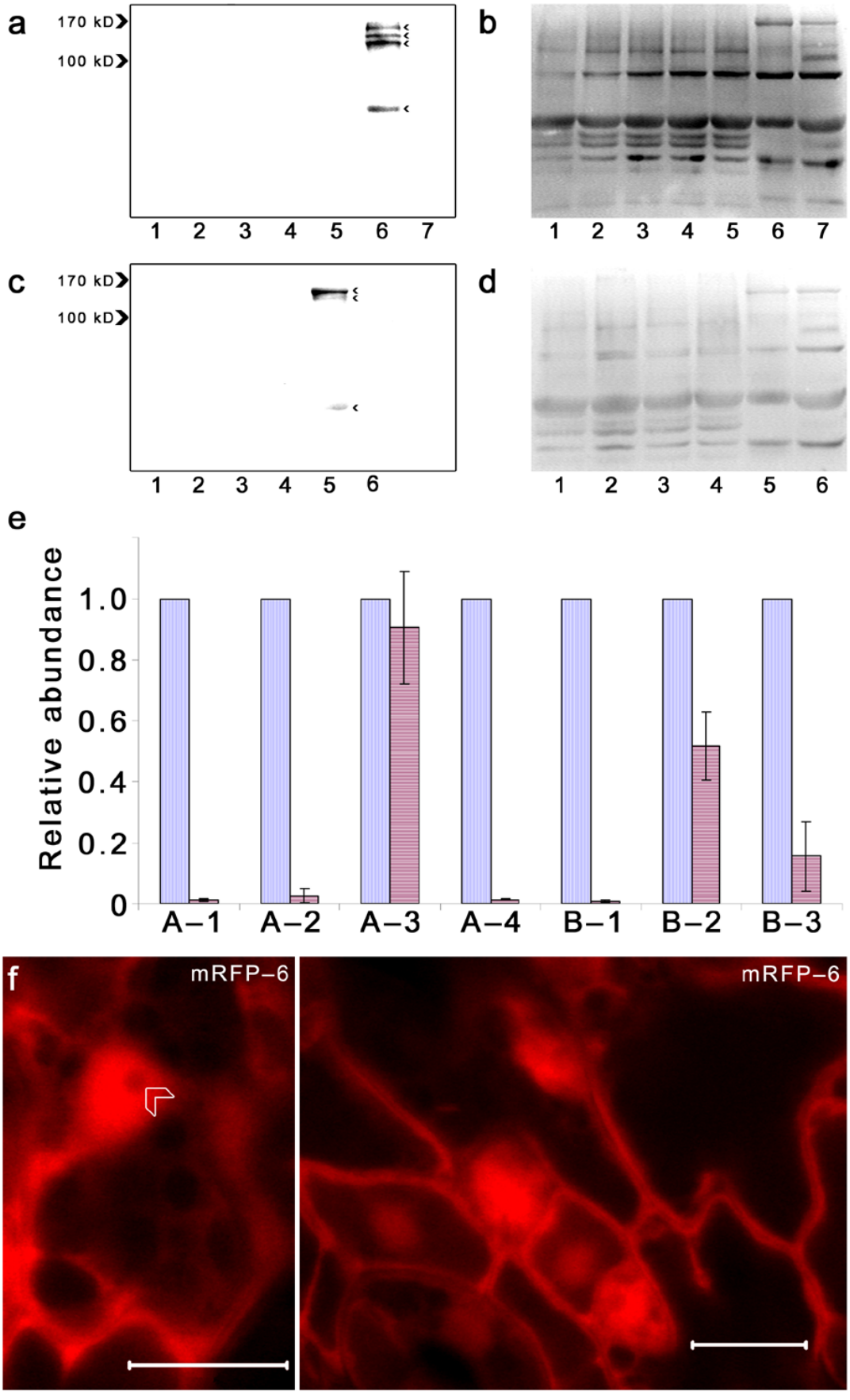
a
170 kD
100 kD
1 2 3 4 5 6 7
b
1 2 3 4 5 6 7
c
170 kD
100 kD
1 2 3 4 5 6
d
1 2 3 4 5 6
e
Relative abundance
1.0
0.8
0.6
0.4
0.2
0
A–1
A–2
A–3
A–4
B–1
B–2
B–3
f
mRFP–6
mRFP–6

increased *GFP5–RPL23aA*/*B* transcript abundance relative to biolistic experiments (Figure 5.3e, lines A3 and B2). However, no translated fusion protein product was detected in any transgenics via CLSM imaging, or Western blot analysis using an anti-GFP antibody (Figure 5.3a–d). This was not a consequence of transformation procedure or a promoter problem, as Arabidopsis plants stably transformed with free mRFP, under control of the same CaMV 35S promoter, showed high expression levels (Figure 5.3f).

5.3.2 Degradation of tagged RPL23a isoforms is proteasome mediated

The mechanism postulated for degradation of r-proteins produced in excess of biological requirements in yeast and mammals (Abovich et al., 1985; Lam et al., 2007; Pierandrei-Amaldi et al., 1985; Warner et al., 1985) is believed to involve the polyubiquitylation of target r-proteins within the nucleus, which constitutes the primary signal for their subsequent degradation by the 26 S-proteasome (Pickart, 2000). To determine if an analogous mechanism operates in Arabidopsis, I generated protoplasts from the two stable T_3 transgenic lines with the highest expression of *GFP5–RPL23aA*/*B* transcripts (lines A3 and B2) and treated them with *clasto*-lactacystin-β-lactone (hereafter β-lactone), a specific inhibitor of the 26 S-proteasome (Brandizzi et al., 2003; Di Cola et al., 2005; Lam et al., 2007). Seventeen hours after treatment with 25 μM β-lactone, GFP fluorescence was detected from both A3 and B2 protoplasts (Figure 5.4a). In A3, the GFP signal derived from faint spherical structures that may represent nucleoli, while in B2 the signal had a punctuate distribution with no apparent nucleolar signal. Not withstanding chloroplast autofluorescence, no GFP signal was detected from A3 or B2 protoplasts prior to treatment, or from wildtype (WT) protoplasts after 15 hours treatment with 25 μM β-lactone (Figure 5.4a). Similar results were obtained when excised leaves from T_3 transgenic lines A3 and B2 were vacuum infiltrated with β-lactone. While no GFP signal was detected pre-treatment (data not shown), or from WT leaves treated for 12 hours with 50μM β-lactone, a putative nucleolar signal was detected in treated A3 leaves (Figure 5.4b). In contrast to results obtained from protoplasts, no signal was detected from treated B2 leaves (data not shown). To confirm GFP5–RPL23aA/B protein expression in transgenic plants treated with β-lactone, western blots were conducted on crude protein extracted from treated and untreated A3, B2 and WT protoplasts, using an anti-GFP antibody. After 15 hours of treatment, products of the anticipated size of the GFP–L23aA/B fusion proteins (~70.8 kD) could be detected in A3 and B2 protoplasts,

Figure 5.4 N-terminally tagged RPL23aA and RPL23aB fusion proteins are expressed in Arabidopsis following proteasome inhibition. **a** Protoplasts isolated from 25-day old wildtype Arabidopsis seedlings (WT) or T_3 seedlings transformed with *GFP5–RPL23aA* or *GFP5–RPL23aB* (line A3 and B2, respectively) were treated with 25 μM β-lactone for 17 hours and viewed with a CSLM. Representative images taken from untreated transgenic protoplasts (0 hours, top panels), and from WT (bottom-left panel) and transgenic protoplasts 17 hours post-treatment with 25 μM β-lactone (bottom-right panels). Chloroplast (Cp) autofluorescence was visualized with a 650 nm longpass filter, and was also visible using GFP5-specific settings (note overlap in merge images). A bright field microscopy image is also shown for post-treatment WT protoplasts. Transparent white arrowheads point to faint spheres observed only in post-treatment A3 protoplasts, while solid arrowheads show some of the smaller spots observed in post-treatment B2 protoplasts. Bars = 10 μm. **b** Excised leaves from 29 day old Arabidopsis seedlings as in (**a**) were treated with 50 μM β-lactone for 12 hours and viewed with a CLSM. Representative post-treatment images labeled as in (**a**) are shown. A bright field microscopy image is shown for post-treatment WT leaves. Transparent white arrowheads point to putative nucleoli observed only in post-treatment A3 leaves. Bars = 10 μm.

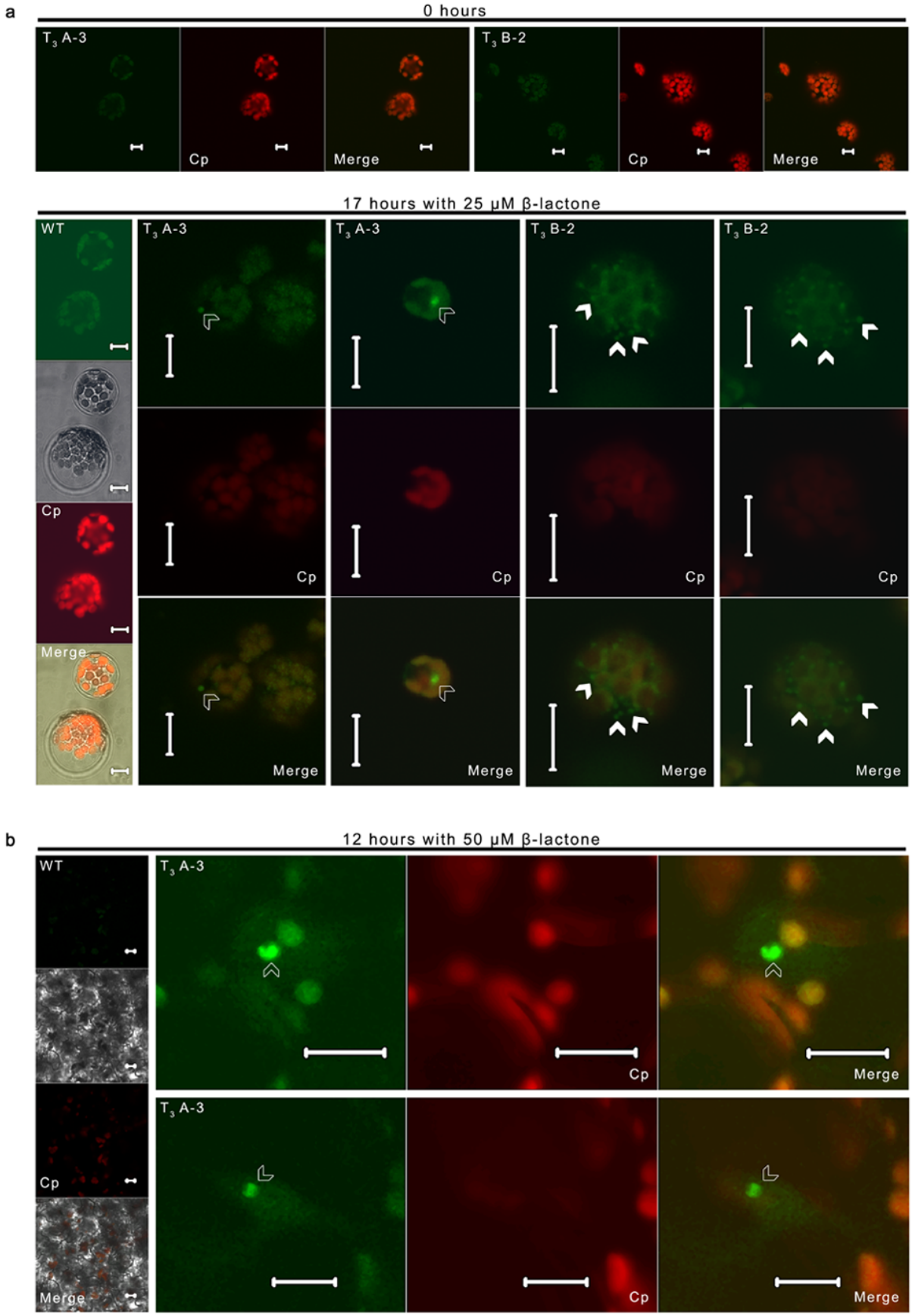
a
0 hours
T3 A-3
Cp
Merge
T3 B-2
Cp
Merge
17 hours with 25 μM β-lactone
WT
T3 A-3
T3 A-3
T3 B-2
T3 B-2
Cp
Merge
b
12 hours with 50 μM β-lactone
WT
T3 A-3
Cp
Merge
T3 A-3
Cp
Merge

but not in WT (Figure 5.5a–b). Additional products of higher and lower molecular weight (1 of >100 kD, 3 of >55 kD and <70 kD, and 1 of ~35 kD) were also detected exclusively in treated A3 and B2 protoplasts, as well as a product of ~50 kD (Figure 5.5a–b). Following 24 hours of treatment with β-lactone, the ~50 kD product became more predominant (Figure 5.5c–d).

Addition of a polyubiquitin chain to a target protein is reported to result in substantial reduction in electrophoretic mobility, and dependent on the size of the chain, can result in identification of multiple products (Causevic et al., 2001; Kopito and Sitia, 2000; Moon et al., 2004). To investigate whether the high molecular weight products detected in the Westerns of tobacco leaves 72 h after infiltration with GFP5–RPL23aA/B constructs were polyubiquitylated, anti-GFP probed membranes were stripped and reprobed with a ubiquitin (UBI) antibody. High molecular weight peptides identical to those identified with anti-GFP were detected, as well as a ~50 kD peptide also identified by anti-GFP (Figure 5.5e–g). These products were not detected in WT tobacco using either the anti-GFP or anti-UBI antibodies.

5.4 Discussion

I have provided evidence for a proteasome-mediated degradation pathway operating dynamically to regulate r-protein levels in plants. This is consistent with results from yeast, HeLa cells, Drosophila and *X. laevis* embryos indicating that r-proteins produced in excess of biological requirements are degraded (Andersen et al., 2005; Cherry et al., 2005; Lam et al., 2007; Pierandrei-Amaldi et al., 1985; Warner et al., 1985). My tagged r-proteins, which would be in biological excess given their ectopic expression from the CaMV 35S promoter, were degraded, or targeted for degradation, in both Arabidopsis and tobacco. It is likely that the GST–fluorescent protein tags, with a mass of ~50 kD, would reduce the efficiency of fusion protein incorporation into pre-ribosomal particles within the nucleolus relative to endogenous wildtype RPL23aA and RPL23aB, and this alteration in kinetics would increase the likelihood of their degradation. The model proposed by Lam et al. (2007) suggests that proteasome-mediated r-protein degradation occurs in the nucleoplasm, and not the nucleolus, because of previous findings that the mammalian nucleolus is devoid of proteasome activity (Rockel et al., 2005). However, it is intriguing that proteomic analysis of the Arabidopsis nucleolus identified 26 S-proteasome components that were not found in the corresponding analysis of human nucleoli (Andersen et al., 2002; Brown et al., 2005; Pendle et al., 2005).

Figure 5.5 N-terminally tagged RPL23aA and –B fusion proteins are degraded via a proteasome mediated pathway. **a** and **c** Western blot using an anti-GFP antibody of Arabidopsis protoplasts 15 (**a**) and 24 (**c**) hours post-treatment with 25 μM β-lactone. Shown are wildtype protoplasts preceding and following treatment (**a**, lane 1 and 4, respectively), A3 protoplasts preceding treatment (**a**, lane 2; **c**, lane 1) and following 15 (**a**, lane 5) or 24 hour treatments (**c**, lane 3), and B2 protoplasts preceding treatment (**a**, lane 3; **c**, lane 2) and following 15 (**a**, lane 6) or 24 hour treatments (**c**, lane 4). Large black arrowheads show positions of molecular mass markers; smaller black arrowheads show products detected in treated A3 or B2 that were not detected in WT. **b** and **d** Ponceau S-staining of nitrocellulose membranes (**a** and **c**, respectively) to show equal loading. **e**–**f** Western blots of nontransformed tobacco (**e**–**f**, lane 3), or of tobacco transiently expressing GFP5–RPL23aA (**e**–**f**, lane 1) or GFP5–RPL23aB (**e**–**f**, lane 2). Blots were probed with an anti-GFP antibody (**e**) and subsequently stripped and reprobed with an anti-ubiquitin antibody (**f**). Large black arrowheads show positions of molecular mass markers; smaller black arrowheads show products detected in GFP5–RPL23aA/B-expressing tobacco, by respective antibodies, that were not detected in nontransformed tobacco. The region of (**e**) delineated by the rectangular box was enlarged and its contrast digitally increased to show the presence of a faint product of approximately 71 kD size. **g** Ponceau S-staining of nitrocellulose membrane (**e**–**f**) showing equal loading.

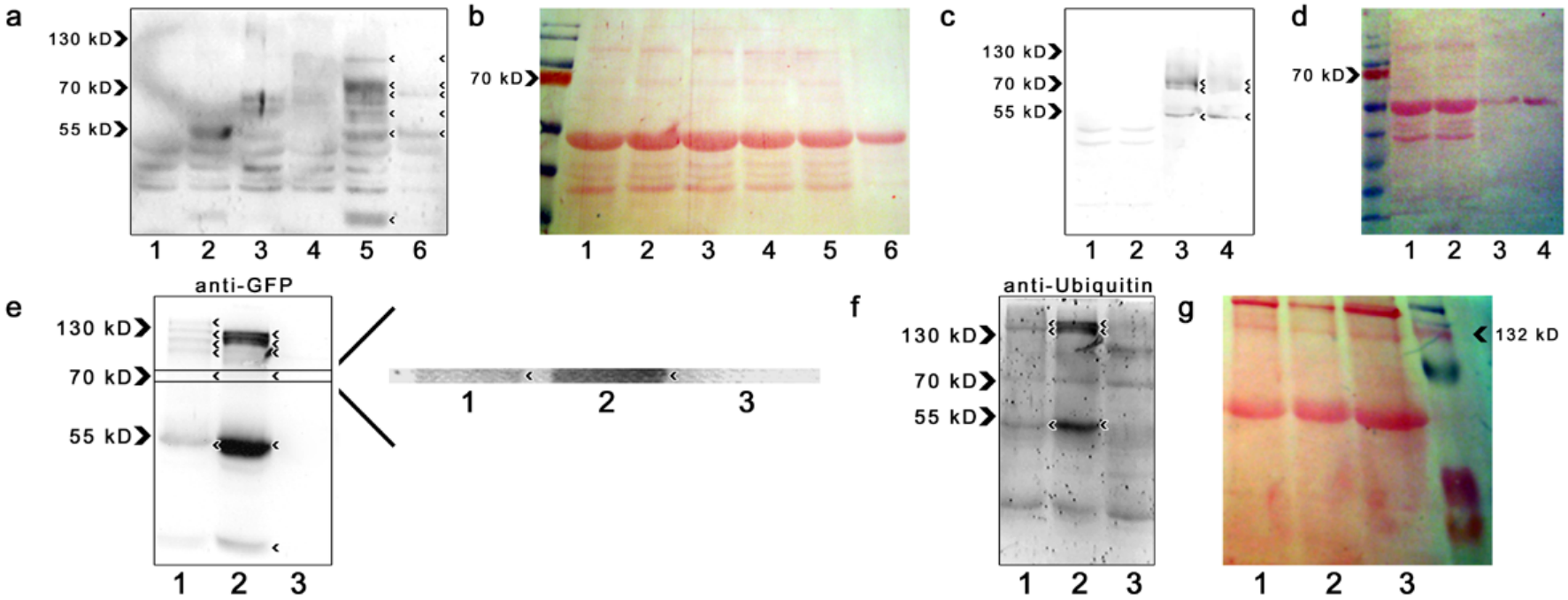
a
130 kD
70 kD
55 kD
1 2 3 4 5 6
b
70 kD
1 2 3 4 5 6
c
130 kD
70 kD
55 kD
1 2 3 4
d
70 kD
1 2 3 4
e
anti-GFP
130 kD
70 kD
55 kD
1 2 3
1 2 3
f
anti-Ubiquitin
130 kD
70 kD
55 kD
1 2 3
g
132 kD
1 2 3

Although I was capable of expressing tagged RPL23aA/B transiently in tobacco, I noted that Western analysis detected multiple products with reduced electrophoretic mobility relative to the fainter product of expected mass. I found that these large products were also detected by an anti-UBI antibody, indicating that they had been targeted for degradation via addition of a polyubiquitin chain. This is consistent with the empirically determined ubiquitylation and proteasome-inhibitor sensitive degradation of other plant proteins, such as PEPC kinase (Agetsuma et al., 2005), sucrose synthase (Hardin and Huber, 2004), and phytochrome A (Clough and Vierstra, 1997). It is possible that steric hindrance or misfolding of my fusion proteins directed them into a proteasome-mediated degradation pathway, but it should be noted that the fusion proteins were properly localized to the nucleolus (Degenhardt and Bonham-Smith, 2008a), were incorporated into ribosomes and polysomes, and that few plant studies have reported β-lactone sensitivity in the degradation of misfolded proteins (Brandizzi et al., 2003; reviewed in Urade, 2007). Thus my results suggest that Arabidopsis and tobacco r-proteins are ubiquitylated en route to degradation by the 26 S proteaseome, which is in agreement with proteomic analyses of ubiquitylated Arabidopsis proteins isolated by affinity purification of GST-tagged ubiquitin binding domains (Maor et al., 2007). Almost 10% of the total ubiquitylated proteins identified (26 of 294) were r-proteins. My ability to detect expression in tobacco may therefore be a consequence of the high expression level I observed, and/or a measure of the efficiency and speed of the degradation pathway for Arabidopsis r-proteins in a heterologous versus native system. In Arabidopsis, previous reports of localization of r-proteins tagged with fluorescent proteins (N-terminal GFP–r-protein fusions) have used cultured protoplasts transiently transformed with hypervirulent *A. tumefaciens*, purportedly directing very high expression levels (Koroleva et al., 2005; Pendle et al., 2005). By contrast, I obtained relatively low expression of my fusion proteins in Arabidopsis (transcripts from transgenes never accumulated to higher levels than the *ACT7* internal control). Moreover, although I never observed fluorescence from my fusion protein constructs expressed in stably transformed Arabidopsis, I was able to detect a product of ~71 kD by isolating protoplasts from younger seedlings (17-days old) transformed with GFP5–RPL23aA (but not GFP5–RPL23aB) (data not shown). Thus it would seem that my inability to observe fluorescence from the tagged RPL23a isoforms resulted from both low expression and rapid degradation of the fusion protein.

The model of Lam et al. (2007) dictates that synthesis of rRNA is the limiting factor in ribosome biogenesis at the expense of surplus production of r-proteins. My data is in agreement with this model given that ectopically expressed tagged RPL23a isoforms were found to accumulate as ubiquitylated intermediates in tobacco, and in Arabidopsis following proteasome inhibition. However, an alternate but not mutually exclusive model suggests that ribosome biogenesis is limited by the component in shortest supply (Marygold et al., 2007). This model is based on the *Minute* phenotype of *D. melanogaster* that develops as a result of r-protein haploinsufficiency (reviewed in Marygold et al., 2007), and the finding that RNAi-mediated depletion of single *D. melanogaster* r-proteins leads to a reduction in levels of other r-proteins (Cherry et al., 2005). In this case, ribosome biogenesis is downregulated to the level dictated by the haploinsufficient r-protein, presumably because the rates of transcription and mRNA turnover are fixed. In fission yeast, Bachand et al. (2006) reported that a decrease in the production of ribosomal SSUs due to depletion of an rpS2 arginine methyltransferase was compensated for by increased polysome loading of SSU r-protein transcripts. This autoregulation provides tentative support for both models and adds to the body of evidence indicating that eukaryotes have evolved diverse regulatory mechanisms to optimize protein translation and prevent the energetically costly, and potentially lethal, overaccumulation of ribosome components.

6 SUMMARY AND CONCLUSIONS

The work described in this thesis investigated r-protein paralogy in Arabidopsis via specific examination of the two-member *RPL23a* gene family. Here the topic of r-protein paralogy is discussed and the major findings of my research are summarized.

Whole and partial genome duplication events have led to the duplication of genes for all 81 r-proteins that form the cytosolic ribosome (Barakat et al., 2001; Cannon et al., 2004; Maere et al., 2005; Simillion et al., 2002). Although some copies have may lost functionality within the ribosome (for example L7A and S15aC, Barakat et al., 2007; Chang et al., 2005; Hulm et al., 2005), and others have presumably been lost altogether from the genome, all families contain at least two members that are transcribed and appear to have undergone purifying selection (Barakat et al., 2001), suggesting a requirement for multiple copies. It has been postulated that r-protein copies are necessary to meet the translational needs of growing tissues while maintaining the capacity to rapidly respond to development/stress-specific stimuli (McIntosh and Bonham-Smith, 2006; Van Lijsebettens et al., 1994). This is supported by findings that single paralogs from the Arabidopsis *RPS15a* and *RPL23a* families are up/down regulated in response to hormone and stress treatments, with no corresponding affects on levels of the other expressed paralogs (Hulm et al., 2005; McIntosh and Bonham-Smith, 2005). Analyses of Arabidopsis r-protein gene knockouts suggest that each paralog is required for normal development, regardless of the relative contribution of that paralog to the total expression of the family (Ito et al., 2000; Nishimura et al., 2004; Pinon et al., 2008; Revenkova et al., 1999; Van Lijsebettens et al., 1994; Weijers et al., 2001; Yao et al., 2008). This further suggests that regulation of individual r-protein genes is wholly independent, with plants unable to compensate for loss of single paralogs by upregulating remaining copies.

Previous research on the Arabidopsis RPL23a gene family has shown the functionality of the RPL23aA isoform via its ability to complement a yeast *l25* mutant (McIntosh and Bonham-Smith, 2001). Semi-quantitative RT-PCR was used to measure transcript levels of each paralog, determining that transcripts of *RPL23aA* and *RPL23aB* are most abundant in mitotically active tissues, but accumulate divergently in response to very specific treatments (McIntosh and Bonham-Smith, 2005). Fusion of a small (~2 kD) FLAG-HIS tag to the C-terminus of RPL23aA was demonstrated to not disrupt the ability of the fusion protein to incorporate into ribosomes

and form polysomes (Zanetti et al., 2005). My research has expanded on earlier findings to gain insight into r-protein paralogy. Specifically, I have improved our understanding of how the RPL23a paralogs are regulated, and determined the predominance of RPL23aA during development. My specific objectives were to 1) identify *cis*-acting elements necessary for regulating expression of each RPL23a paralog; 2) establish the requirement for RPL23a paralogs during development; 3) investigate whether Arabidopsis compensates for loss of *RPL23aB* by upregulating transcription of *RPL23aA*; 4) characterize the subcellular localization of RPL23aA and RPL23aB; and 5) determine the involvement of protein turnover in regulating RPL23a accumulation.

To define the *cis*-acting elements necessary for regulating expression of each RPL23a paralog (objective 1), the RR deletion series of McIntosh (2005) was expanded to include a 3' RR deletion series and constructs lacking the 5' UTR intron (Chapter 2). These studies confirmed the importance of the site II motif and *telo*-box for conferring expression in mitotically active tissues (cf. Li et al., 2006; Tatematsu et al., 2005; Tremousaygue et al., 2003). I provided evidence that the *telo*-box is able to direct expression in a context-specific manner without a site II motif. This is in contrast to previous reports that only the site II motif functions independently in conferring expression to zones of cell division (Tremousaygue et al., 2003). It is possible that *telo*-box driven expression requires synergistic interaction with other features, such as the CAAT-boxes that bind trimeric nuclear factor Y (NF-Y) complexes (Gusmaroli et al., 2001, 2002). I determined that reporter gene expression driven by RRs did not strictly require leader intron splicing, although intron mediated enhancement may have occurred due to unidentified *cis*-elements present within leader introns (cf. Fu et al., 1995; Jeong et al., 2007; Rose and Beliakoff, 2000; Vitale et al., 2003). Using a transient expression strategy in Arabidopsis protoplasts, I determined that O_2 deprivation- and sucrose-starvation-mediated repression of *RPL23a* paralog transcription depends on the *telo*-box alone, or in conjunction with the TATA-box, the site II motif and/or possibly the *RPL23aB*-specific fermentation motif $^{5'}$AAACAAA$^{3'}$ (Mohanty et al., 2005). This contrasts with previous studies where the site II motif is ascribed the predominant role in transcriptional repression (Ditt et al., 2006; Ho et al., 2007). Lastly, I conducted a bioinformatic-based full-length cDNA comparison between Arabidopsis RPL23a paralogs, 215–220 r-proteins genes, and RPL23a orthologs from 55 different eukaryotic species. This study revealed that RPL23a cDNAs have many characteristics of translationally regulated

transcripts that are associated with heavy polysomes (Kawaguchi and Bailey-Serres, 2005), and determined that the *telo*-box is a conserved 5' UTR element of most angiosperms.

I used two methods to investigate the requirement for RPL23a paralogs during development (objective 2). A hemizygous *RPL23aB* knockout was obtained, made homozygous, and the loss of *RPL23aB* transcripts confirmed by RT-PCR and qRT-PCR (Chapter 3). This mutant was grown along-side wildtype plants under non-stressed conditions and under cold-temperature, high-light and photoinhibition-stresses, which result in global reprogramming of the cellular proteome (Kultz, 2005) and presumably require modulation of ribosome biogenesis. No abnormal phenotype developed in the *rpl23ab* knockout under any condition tested. I then used RNA-interference to individually and coordinately silence each *RPL23a* paralog (Chapter 4). Consistent with the knockout results, knockdown of *RPL23aB* produced no abnormal phenotype. In contrast, knockdown of *RPL23aA* led to a pleiotropic phenotype characterized by growth retardation, irregular leaf and root morphology, abnormal phyllotaxy and vasculature, and loss of apical dominance. This phenotype was generally more severe than that of other r-protein knockouts (Ito et al., 2000; Nishimura et al., 2004; Pinon et al., 2008; Revenkova et al., 1999; Van Lijsebettens et al., 1994; Yao et al., 2008), and resembled many known auxin response mutants (for example the *tornado1* and *tornado2* mutants that have disrupted auxin distribution, Carland and McHale, 1996; Cnops et al., 2006; Cnops et al., 2000). This latter finding led me to develop a model wherein a full r-protein complement is necessary to maintain active translation, which in turn facilitates the degradation of a subset of miRNA-regulated auxin response/homoeostasis factors (Appendix D). This model is based on the findings that a subset of miRNA targets in Drosophila are stabilized via chemical-inhibition of translation (Eulalio et al., 2007). Given recent reports that several r-protein knockouts enhance the abaxialized phenotype of *asymmetric leaves1* (*as1*) and *as2* (Pinon et al., 2008; Yao et al., 2008), which normally function to repress miRNAs that target three class III HD-ZIPs involved in specifying adaxial fate (Fu et al., 2007; Li et al., 2005b; Ueno et al., 2007 , and references therein), it seems plausible that r-proteins and active translation are also required to protect a subset of miRNA-regulated transcripts from degradation, possibly via sequestration in polysomes (Pillai et al., 2007). Under this hypothesis, a full r-protein complement and active translation would be required to prevent the miRNA degradation of class III HD-ZIPs, hence promoting adaxial identity.

I also demonstrated that the *RPL23a* family is required for viability via the lethal phenotype resulting from coordinately silencing both paralogs (Chapter 4). This is in agreement with previous findings in numerous prokaryotes, yeast and *C. elegans* (Kamath et al., 2003; Zhang et al., 2004). This adds RPL23a to a growing list of r-proteins from higher eukaryotes that are essential for viability, including RPS5 (Weijers et al., 2001) and RPL5 (Yao et al., 2008) from Arabidopsis, RPS13, RPS7, RPL21, RPL23, RPL25.2, RPL35, and RPL43 from *C. elegans* (Kamath et al., 2003), and RPS2, RPS3, RPS4, RPS5, RPS6, RPS13, RPS14, RPL5, RPL9, RPL14, RPL19, RPL38 from Drosophila (reviewed in Marygold et al., 2005; Saboe-Larssen et al., 1998). It is interesting to note that loss of only one of the two expressed *C. elegans* isoforms of RPL25, the ortholog to RPL23a, is 100% embryo-lethal (RPL25.2), the other isoform conferring only 50–80% embryo-lethality (Kamath et al., 2003).

Transcript profiles of *RPL23a* paralog levels in wildtype and *rpl23ab* knockout plants under non-stressed conditions were obtained by qRT-PCR (Chapter 3) to investigate whether r-protein paralogs are feedback regulated at the transcript level (objective 3). Results demonstrated a lack of feedback regulation and suggest that paralogs are regulated independently. This is consistent with the absence of transcriptional compensation by remaining paralogs (*RPS18B* and *RPS18C*) following loss of *RPS18A* in Arabidopsis (Vanderhaeghen et al., 2006). Although it is possible that remaining transcripts are shifted to larger polysomes to maintain an adequate supply of r-proteins, the finding that all other characterized r-protein knockouts result in abnormal phenotype development (Chen et al., 2006; Ito et al., 2000; Nishimura et al., 2004; Pinon et al., 2008; Revenkova et al., 1999; Van Lijsebettens et al., 1994; Weijers et al., 2001; Yao et al., 2008) suggest that this is not the case. Moreover, evidence accumulated to date suggests that *RPL23aB* probably fulfills auxiliary requirements only under certain conditions, one of which may be wounding given the finding that the *RPL23aB* RR confers greater wound-inducibility of a reporter gene than that of *RPL23aA* (McIntosh, 2005). Yet another possibility is that expression of *RPL23aA* and/or *RPL23aB* is controlled by a unique mechanism from other r-proteins at the translational level. In fission yeast it has been reported that loss of *Cpc2/RACK1* causes a specific decrease in the ribosome loading of *Rpl25-1* transcripts, suggesting that Cpc2/RACK1 may recruit *Rpl25-1* to the ribosome for translation (Shor et al., 2003). An analogous mechanism in Arabidopsis may allow a specific increase in ribosome loading of *RPL23aA* transcripts in the *rpl23ab* mutant.

Subcellular localization of RPL23a isoforms (Objective 4) was examined by confocal microscopy analyses of isoforms tagged at N- and C-termini with fluorescent proteins (Chapter 4). Live cell imaging in a heterologous tobacco system demonstrated that both isoforms accumulated in the nucleolus with a C-terminal fluorescent-protein tag, whereas only RPL23aA was targeted to the nucleolus with an N-terminal fluorescent protein tag, suggesting divergence in targeting efficiency of localization signals. Specifically, RPL23aB has non-conservative K34 to P34 substitution within a putative monopartite, SV40 large T-antigen-like, NLS (^{33}KKDK^{36}) that is found in RPL23aA and reportedly confers nucleolar-targeting and nucleolin binding in mammals (Wang et al., 2005a; Xue et al., 1993). Nucleolin is one of the most abundant nucleolar proteins, and functions in rDNA transcription, rRNA processing, nucleocytoplasmic trafficking and maintenance of the nucleolar integrity (Ginisty et al., 1999; Pontvianne et al., 2007). If the putative nucleolin-binding motif of RPL23aA is functional, it would confer a competitive advantage by enabling this paralog to associate with nascent rRNA and assemble rapidly into the LSU (Appendix D). Support for nucleolin binding of an r-protein NoLS comes from the findings that several mammalian r-proteins bind to nucleolin *in vitro* (Bouvet et al., 1998) and that the putative nucleolin binding motif (consensus $[K/R]_2XK$) is found within the delineated NoLSs of a number of animal and yeast RPs including RPS6, RPS25, RPL5, RPL7a, RPL22 and RPL23a (Jakel and Gorlich, 1998; Kundu-Michalik et al., 2008). I postulate that this motif functions in a context-specific manner to facilitate both nuclear import and high affinity nucleolus-binding via interaction with nucleolin, resulting in efficient ribosome biogenesis.

To ascertain the role of the 26 S proteasome in regulating the equimolar accumulation of r-proteins (objective 5), tagged RPL23a isoforms were expressed in Arabidopsis under control the 35S CaMV promoter and the accumulation of fusion proteins was measured by Western blot analyses before and after chemical disruption of proteasome function (Chapter 5). Fluorophore-tagged RPL23a isoforms were shown to be unstable in Arabidopsis, but could be stabilized by treatment with the proteasome inhibitor. In tobacco, tagged isoforms predominantly accumulated as higher molecular weight products that were detected by a ubiquitin antibody, suggesting that they were degradation intermediates. This is consistent with findings in mammalian HeLa cells determining that newly synthesized r-proteins are targeted to the nucleolus more rapidly than other nucleolar proteins, in excess of physiological demands, and are in constant equilibrium between the nucleolus, where they can be retained if nascent rRNAs

are available for subunit assembly, and the surrounding nucleoplasm, where they are exposed to the 26 S proteasome and degraded (Lam et al., 2007; Matsumoto et al., 2005a). A similar mechanism is postulated to exist in yeast (Warner, 1989) given the short half-life of unused r-proteins (El-Baradi et al., 1986; Tsay et al., 1988; Warner, 1989), and the finding that ectopically expressed r-proteins are highly unstable (Gritz et al., 1985; Warner et al., 1985), but can be stabilized by depletion of the corresponding endogenous r-protein (Abovich et al., 1985). The findings presented here indicate that the 26 S proteasome may have been retained as a mechanism to prevent the excess accumulation of r-proteins over the ~1.5 billion years of evolution since the last common ancestor to animals, plants and fungi (Hedges and Kumar, 2003).

Paralogy of r-proteins appears to be a common characteristic of plants and anamniote eukaryotes (Barthelemy et al., 2007; Marygold et al., 2007; Merchant et al., 2007; Planta and Mager, 1998; Semple and Wolfe, 1999). Results presented indicate that the Arabidopsis *RPL23a* paralogs have diverged significantly from each other. Although both paralogs have retained core regulatory elements necessary for coordinating their response to development/stress signals, *RPL23aA* has become predominant. *RPL23aB* is not required during normal development and is expressed at a lower level than *RPL23aA* in all developing tissues. Further, the RPL23aA isoform may possess a stronger signal for retention in the nucleolus. Whether these differences are indicative of reductive evolution taking place on this family, or reflect neofunctionalization or a highly specialized requirement of *RPL23aB* remain to be determined.

7 APPENDIX A. SUPPLEMENTARY MATERIAL FOR CHAPTER 2

7.1 Supplementary Materials and Methods for Chapter 2

7.1.1 Molecular cloning

7.1.1.1 Deletion constructs in pCAMBIA1381z

Full-length and 5' truncated RRs of *RPL23aA* and *RPL23aB* were amplified by PCR from respective BACs (F12L6 and T26I12) using specific primers containing restriction sites (Table A.1; reverse primer L23aA–5'–R or L23aB–5'–R; forward primers L23aA–5'FR–F, L23aA–5'Δ1–F to L23aA–5'Δ6–F or L23aB–5'FR–F, L23aB–5'Δ1–F to L23aB–5'Δ6–F). 3' end deletions were obtained in an identical fashion using forward primers selected based on results from the 5' deletion GUS assays (Table A.1; L23aA–5'Δ4–F and L23aB–5'Δ2–F, for *RPL23aA* and *RPL23aB*, respectively) and RR specific reverse primers (Table A.1; L23aA–3'Δ2–R to L23aA–3'Δ5–R or L23aB–3'Δ2–R to L23aB–3'Δ5–R). All deletion fragments were digested and cloned into *Eco*RI/*Bam*HI sites of pCAMBIA1381z (CAMBIA, Canberra, Australia), generating CambiaRPL23aA/B 5'Δ1–GUS to 5'Δ6–GUS, and CambiaRPL23aA/B 3'Δ2–GUS to 3'Δ5–GUS constructs. To avoid internal enzyme sites, full 5' RRs were first cloned into the *Eco*RV site of pBluescript II KS+ (pBSKS+) and then subcloned into pCAMBIA1381z at unique *Eco*RI/*Sal*I (*RPL23aA*) or *Sal*I/*Pst*I (*RPL23aB*) restriction sites, generating CambiaRPL23aA/B 5'FR–GUS constructs.

7.1.1.2 *RPL23aA* and *RPL23aB* intron-less fragments in pCAMBIA1381z

Complementary oligonucleotides (Table A.1; L23aA–INL–F and L23aA–INL–R for *RPL23aA*; L23aB–INL–F and L23aB–INL–R for *RPL23aB*) contained terminal 5' *Eco*RI and 3' *Bam*HI restriction sites and were annealed by incubating 10 μM of each oligonucleotide at 95°C for 5 min in 1X Pfu reaction buffer (Fermentas). The resulting double-stranded fragments were digested and cloned into the *Eco*RI/*Bam*HI restriction sites of pCAMBIA381z, generating CambiaRPL23aA/B–INL–GUS constructs.

7.1.1.3 *RPL23aA* and *RPL23aB* second introns in pCAMBIA1381z

Second introns were amplified from BACs containing *RPL23aA* and *RPL23aB* gene sequences (F12L6 and T26I12, respectively) using specific primers (Table A.1; L23aA–int–F and L23aA–

int–R for *RPL23aA*; L23aB–int–F and L23aB–int–R) and cloned into the unique *Pst*I/*Bam*HI sites of a pMECA derivative containing the *Bam*HI/*Kpn*I -60 *Cauliflower Mosaic Virus* (*CaMV*) minimal promoter–GUS–nos cassette of pMD992 (Deyholos and Sieburth, 2000; Pylatuik et al., 2003), generating pMECA–*RPL23aA*/*B*–int. The *RPL23aA*/*B* 2nd intron–-60 *CaMV* minimal promoter fragments were subsequently cloned into *Pst*I/*Nco*I sites of pCAMBIA1381z, generating CambiaRPL23aA/B–INT–GUS constructs.

7.1.1.4 Deletion constructs in pGREENII0000

To generate the protoplast expression vector, two plasmids were created, a gateway plasmid and a destination plasmid. For the gateway plasmid, *erGFP7int* (Mankin and Thompson, 2001), was obtained from ABRC (plasmid pLM NC95), amplified using gene specific primers (Table A.1; erGFP7int–F and erGFP7int–R) and cloned into *Hind*III/*Spe*I sites of pCAMBIA0380 (CAMBIA), generating 0380–erGFP7int. For the destination plasmid, the *nopaline synthase* (*nos*) poly-A signal (terminator) was amplified from pCAMBIA1381z using specific primers (Table A.1; nos–F and nos–R) and cloned into *Spe*I/*Not*I sites of the pGREEN II0000 vector (Hellens et al., 2000), generating pGREEN–nos.

The 5' RR deletion fragments of *RPL23aA* and *RPL23aB* were digested from their respective CAMBIA1381z plasmids, and subcloned into *Eco*RI/*Bam*HI sites of 0380–erGFP7int, generating 0380RPL23aA/B 5'Δ1–erGFP7int to 5'Δ6–erGFP7int. The RPL23aA 5'Δ3–erGFP7int to 5'Δ6–erGFP7int and RPL23aB 5'Δ1–erGFP7int to 5'Δ6–erGFP7int fragments were subsequently subcloned into pGREEN–nos at *Eco*RI/*Spe*I sites, generating pGREEN–RPL23aA 5'Δ3–erGFP7int– to 5'Δ6–erGFP7int–nos and pGREEN–RPL23aB 5'Δ1–erGFP7int– to 5'Δ6–erGFP7int–nos. The RPL23aA 5'Δ1/Δ2–erGFP7int cassettes were digested with *Eco*RI and *Ksp*AI and subcloned into *Eco*RI/*Sma*I sites of pGREEN–nos, generating pGREEN–RPL23aA 5'Δ1/Δ2–erGFP7int–nos. The full-length 5' RR of *RPL23aA* was isolated from CambiaRPL23aA 5'FR–GUS, subcloned into *Eco*RI/*Sal*I sites of 0380–erGFP7int, then digested with *Eco*RI and *Ksp*AI, and subsequently cloned into *Eco*RI/*Sma*I sites of pGREEN–nos, generating pGREEN–RPL23aA 5'FR–erGFP7int–nos. The full-length 5' RR of *RPL23aB* was isolated from CambiaRPL23aB 5'FR–GUS, subcloned into *Sal*I/*Pst*I sites of 0380–erGFP7int, with subsequent cassette isolated and subsequently cloned into *Eco*RI/*Spe*I sites of pGREEN–nos, generating pGREEN–RPL23aB 5'FR–erGFP7int–nos.

The negative control was the erGFP7int fragment from 0380–erGFP7int cloned into *Eco*RI/*Spe*I sites of pGREEN–nos, generating pGREEN–erGFP7int–nos. For the positive control, a tandem repeat of the (*CaMV*) *35S* promoter was amplified from pCAMBIA1381z using specific primers (Table A.1; 35S–F and 35S–R) and cloned upstream of erGFP7int at *Apa*I/*Eco*RI sites in 0380–erGFP7int, generating 0380–35S–erGFP7int. The 35S–erGFP7int cassette was isolated and cloned into pGREEN–nos at *Eco*RI/*Spe*I sites, generating pGREEN–35S–erGFP7int–nos.

7.1.2 Stable Transgenics

Agrobacterium tumefaciens carrying binary vectors were cultured overnight in LB, and resuspended to a final OD_{600} of 0.8–1.0 in 5% sucrose and 0.01% (infiltration medium 1) or 0.05% (infiltration medium 2) Silwet-L77 (Lehle Seeds, Round Rock, TX). Bolting Arabidopsis plants (~5 week-old) were either dipped twice at one week intervals in infiltration medium 1 or immersed in infiltration medium 2 and subjected to 70–100 kPa vacuum for two min. Infiltrated plants (T_0) were returned to the growth chamber and allowed to grow to maturity. T_1 seed was plated on solid media augmented with 25 μg mL^{-1} hygromycin (Sigma; or Invivogen, San Diego, CA) and 200–300 μg mL^{-1} β-lactam antibiotic (ticarcillin disodium/potassium clavulanate, GlaxoSmithKline, Middlesex, UK; or cefotaxime, Sanofi-Aventis, Laval, PQ). Surviving T^1 plants were transferred to soil and grown until maturity. Hemizygous T_2 seed was plated on selective media as described above (minus β-lactam antibiotics).

7.1.3 RT-PCR

First strand synthesis was conducted using SuperScript II reverse transcriptase (RT, Invitrogen) as per manufacturer's instructions, with the modification that 200–400 ng total RNA was used as template, a gene-specific reverse primer was used (Table A.1; pC–GUS–R2), and reverse transcription was conducted for 30 min at 50 °C. The first strand product was used as template for PCR with Pfu polymerase (Stratagene, La Jolla, CA, or Fermentas) following the SuperScript II instructions. All PCR amplifications used the pC–GUS–R2 reverse primer and a forward primer specific for the construct being investigated (Table A.1; L23aA–RTintF for *RPL23aA* 5'FR–GUS and 5'Δ4–GUS; L23aA–5'Δ5–F for *RPL23aA* 5'Δ5–GUS; L23aA–5'Δ6–F for *RPL23aA* 5'Δ6–GUS; L23aB–RTintF2 for *RPL23aB* 5'FR–GUS and 5'Δ4–GUS; L23aB–5'Δ5–F for *RPL23aB* 5'Δ5–GUS; L23aB–5'Δ6–F for *RPL23aB* 5'Δ6–GUS; L23aA–5'Δ4–F for *RPL23aA* 3'Δ2–GUS and 3'Δ5–GUS; L23aB–5'Δ2–F for *RPL23aB* 3'Δ2–GUS and 3'Δ5–GUS).

Identification of a transcript resulting from a reverse-oriented 35S *CaMV* promoter in T_2 seedlings carrying the pCAMBIA1381z empty vector control used a vector specific forward primer and the *GUS* specific reverse primer (Table A.1; Cam1381z–Tcheck–F and pC–GUS–R2, respectively). All products were cloned into the *Eco*RV restriction site of the pBSKS+ vector prior to sequence analysis.

7.1.4 5' RACE

Transcription start sites of *RPL23aA* and *RPL23aB* were determined using three gene specific reverse primers per paralog (Table A.1; L23aA–RACE–GSP1 to –GSP3, and L23aB–RACE–GSP1 to –GSP3) and a 5' RACE kit (Invitrogen), as per manufacturer's instructions with the modification that final nested PCR was performed using Pfu polymerase (Stratagene). The final nested amplification was performed as follows: 30 cycles of PCR (2 cycles of 2 min at 94 °C, 30 s at 52 °C and 45 s at 72 °C, followed by 28 cycles of 30 s at 94 °C, 30 s at 52 °C and 45 s at 72 °C) with a final 10 min extension at 72 °C. Amplification products were cloned into the *Eco*RV site of pBSKS+, and the insert's identity determined by automated sequencing (NRC–PBI). OneStep RT-PCR (Qiagen) amplifications used 5' RACE reverse primers and forward primers designed immediately 3' to mapped TSSs (Table A.1; L23aA–RACE–GSP3 and L23aA–RTintF for *RPL23aA*, and L23aB–RACE–GSP3, L23aB–RTintF1 (3' to minor TSS) and L23aB–RTintF2 (3' to major TSS) for *RPL23aB*).

7.1.5 Protoplast isolation

Protoplasts were isolated essentially following previously described methods (Yoo et al., 2007), with the exception that whole seedlings were sliced with a razor into small pieces (≤ 10 mm^2), vacuum infiltrated for 10 min with cell wall digestion solution (1.5% cellulysin [Calbiochem, San Diego, CA], 0.4% macerase [Calbiochem], 0.4 M mannitol [BDH Chemicals, Poole, UK], 20 mM KCl, 20 mM MES, 10 mM $CaCl_2$, 0.1% BSA [Calbiochem], 5 mM β-mercaptoethanol [Sigma-Aldrich], pH 5.7), and incubated for 4 h in digestion solution at 60 RPM and 20 ºC. Prior to transformation, protoplasts were pelleted at 100 *g* for 2 min, resuspended in electroporation buffer (0.3 M mannitol, 150 mM KCl, 4 mM MES, pH 5.7) at a concentration of $1.7–2.00 \times 10^5$ cells ml^{-1}, and dispensed in 300 µL aliquots into 0.4 cm cuvettes (Bio-Rad, Mississauga, ON, Canada).

7.1.6 Quantitative RT-PCR

Primers for real-time PCR amplification of *neomycin phosphotransferase II* (*nptII*), and *erGFP7int* were designed to produce amplicons of <200 bp and have a uniform Tm of ~60 °C (Table A.1; erGFP7int–qRT–F and erGFP7int–qRT–R for *erGFP7int*; nptII–qRT–F and nptII–qRT–R for *nptII*). DNase I (Fermentas) was used to treat 1 µg total RNA as per manufacturer's instructions prior to first strand synthesis, which was conducted with 400 ng RNA and 5 pmol of each reverse primer (erGFP7int–qRT–R and nptII–qRT–R) using RevertAid H- RT (Fermentas), as per manufacturer's instructions.

7.2 Supplementary Results and Discussion for Chapter 2

7.2.1 Comparison of *RPL23a* transcript properties with eukaryotic orthologs and other Arabidopsis r-proteins identifies conserved and non-conserved features

Conserved transcript architecture is an important component of animal r-protein post-transcriptional regulation (Meyuhas, 2000). To identify important transcript sequence features in Arabidopsis *RPL23a* paralogs, *RPL23aA*/*B* cDNAs were compared to all Arabidopsis r-protein fl-cDNAs with >8 bp of 3' or 5' UTR sequence (215–220 r-protein genes) and to 101–103 *RPL23a* orthologous transcript assemblies from 55 eukaryotic species, including 4 Brassicales, 21 Magnoliopsida plants (eudicots), 4 Liliopsida plants (monocots), 3 gymnosperms, 6 nonvascular plants, 5 vertebrates, 6 invertebrates, 4 fungi, and 2 protists. Transcript properties of the Arabidopsis *RPL23a* paralogs tended to be consistent with those of other Arabidopsis r-proteins (Table A.2). *RPL23aA/B* have short, U-rich 5' UTRs with limited secondary structure and low free energies. The 3' UTRs are slighter shorter than average (190 versus 248 nt), have low G/C and high U-content and lower than average free energies. Upstream AUG start codons (uAUGs), which generally initiate a short (<20 codons) open reading frame (uORF) (Jin et al., 2005; Kawaguchi and Bailey-Serres, 2005), were not present in either *RPL23a* paralog 5' UTRs and this is in agreement with the very low proportion of Arabidopsis r-proteins possessing uAUGs (Table A.2). Traits of *RPL23aA/B* 5' and 3' UTRs tended to be conserved with closely related orthologs (i.e. Brassicales), but not with more distant relatives.

Optimal sequence context of the AUG start codon is important for initiation of translation. Analysis of ribosome loading in Arabidopsis under non-stressed and dehydration stressed conditions has shown that the most efficiently translated transcripts under both conditions have

an A-rich AUG context with consensus $^{-10}$AAAAAAAAAA<u>AUG</u>GC^{+5} (Kawaguchi and Bailey-Serres, 2005). The general AUG context for all Arabidopsis transcripts is $^{-10}$aaaaaaaA/Gaa<u>AUG</u>Gc^{+5}, where lowercase letters represent bases with a relative frequency of <50% that were most commonly found at respective positions. To determine if this context was preserved in r-proteins, the -10 to +6 region surrounding the AUG start codon from the Arabidopsis *RPL23a* paralogs, eukaryotic *RPL23a* orthologs and Arabidopsis r-protein transcripts was analyzed. The consensus AUG context of *RPL23aA/B* ($^{-10}$AUYUYRAGCY<u>AUG</u>UCU^{+6}) was found to be much less A-rich than the general AUG context, and was highly conserved with other Brassicales, but not with more distant relatives or with other Arabidopsis r-proteins (Figure A.1). Among dicots, the core region from -4 to +6 is well-conserved, especially C at positions -2 and +5, and A at position -1. The Arabidopsis r-proteins as a whole show a preference for purines at position -4 to -1, +4 and +6. The predominance of a purine at position -3 was detected in all groups except monocots (Figure A.1).

7.3 Supplementary Tables for Chapter 2

Gene	Accession No.	Oligonucleotide Primer		
		Primer ID	Primer Sequence (5' to 3')	Amplicon Length (bp)
RPL23aA	At2g39460	L23aA–5'–R	GCGGGATCCGGCTTGAAATGATTCTTCAC	N/A
		L23aA–5'FR–F	GGAGAGGAGGAGCAAATTGTTTACC	1503
		L23aA–5'Δ1–F	GCGGAATTCGGTAGAAGCCAGTTCAGC	883
		L23aA–5'Δ2–F	GCGGAATTCGACACGTTTGTATGTTTC	555
		L23aA–5'Δ3–F	GCGGAATTCGCAACCAAAAGAATCAGTG	396
		L23aA–5'Δ4–F	GCGGAATTCGGCCCATTTATTCAATCC	295
		L23aA–5'Δ5–F	GCGGAATTCCCTCTCCAGGTTCGTGTC	145
		L23aA–5'Δ6–F	GCGGAATTCGCTTCGCTTTCTGGGTTTC	66
		L23aA–3'Δ2–R	GCGGGATCCGAAACCCAGAAAGCGAAGC	248
		L23aA–3'Δ3–R	GCGGGATCCGGAGAGGTGAAGCCGCTG	157
		L23aA–3'Δ4–R	GCGGGATCCCCCTAACTTACGCCGCAAC	129
		L23aA–3'Δ5–R	GCGGGATCCCTTAGTTGGGTCTATAATG	77
		RPL23aA–INL–F	GAATTCTTAGGGTTTTGAGAATCAGCGGCTTCACCTCTCCAGATTTCGTGTGTGAAGAATCATTTCAAGCCGGATCC	77
		RPL23aA–INL–R	GGATCCGGCTTGAAATGATTCTTCACACACGAAATCTGGAGAGGTGAAGCCGCTGATTCTCAAAACCCTAAGAATTC	N/A
		L23aA–int–F	GCGCTGCAGGTACGATCTTTTCATTG	321
		L23aA–int–R	GCGGGATCCCTGCAAATTACATACAAC	N/A
		L23aA–RTintF	CAGCGGCTTCACCTCTCC	N/A

		L23aA–RACE–GSP1	CTGATGAGTGTGTTCACTTTC	N/A
		L23aA–RACE–GSP2	CTTAATCTTCTTCTTGTCAGCACG	N/A
		L23aA–RACE–GSP3	GGCTTGACCAGACTTCACAG	N/A
RPL23aB	At3g55280	L23aB–5'–R	GCGGGATCCTGCTCAAGATAGATTCTTTTC	N/A
		L23aB–5'FR–F	CATGAATTTGAGTTAGAGGATGG	1061
		L23aB–5'Δ1–F	GCGGAATTCCACTTGATTCACTTGTCATC	650
		L23aB–5'Δ2–F	GCGGAATTCGTCATTTTCCAATCCTTAAG	563
		L23aB–5'Δ3–F	GCGGAATTCCGATTTGGACTTTGGTTTG	447
		L23aB–5'Δ4–F	GCGGAATTCCGATCTAGGGTTTACGG	345
		L23aB–5'Δ5–F	GCGGAATTCGTGTCATTTTTCTCGTGC	148
		L23aB–5'Δ6–F	GCGGAATTCGCTAATTGCTATTGCTC	77
		L23aB–3'Δ2–R	GCGGGATCCCCCCAGAAAAGAAAATCAG	528
		L23aB–3'Δ3–R	GCGGGATCCGCGGCGAAACAGAAACCC	317
		L23aB–3'Δ4–R	GCGGGATCCGAGTAGATCCAAGTTGCTTG	297
		L23aB–3'Δ5–R	GCGGGATCCCTAAGGGAAGTGAAAATG	261
		RPL23aB–INL–F	GGATTCCCAAGCAACTTGGATCTACTCTAGGGTTTCTGTTTCGC CGCTCAGGTTTCGTGAAAAGAATCTATCTTGAGCAGGATCC	85
		RPL23aB–INL–R	GGATCCTGCTCAAGATAGATTCTTTTCACGAAACCTGAGCGGC GAAACAGAAACCCTAGAGTAGATCCAAGTTGCTTGGGAATTC	N/A
		L23aB–int–F	GCGCTGCAGGTACGCCTTTTTTTCTTTC	335
		L23aB–int–R	GCGGGATCCCTGCAAAAATAATGGAAC	N/A

		L23aB–RTintF1	CCAAGCAACTTGGATC	N/A
		L23aB–RTintF2	GGGTTTCTGTTTCGCCGC	N/A
		L23aB–RACE–GSP1	CTAATGAGGGTGTTGACTTTCTTGG	N/A
		L23aB–RACE–GSP2	GATCTTTTTCTTGTCAGCACGG	N/A
		L23aB–RACE–GSP3	CGCAGGCTTTTTAACGATTTGGCC	N/A
erGFP7int	ABRC CD3-420	erGFP7int–F	GCGAAGCTTATGAAGACTAATCTTTTTCTC	1011
		erGFP7int–R	GCGACTAGTTTAAAGCTCATCATGTTTG	N/A
		erGFP7int–qRT–F	TATCCTCGGCCGAATTGTACGTACAATTCAGTAAA	196
		erGFP7int–qRT–R	CGCATGGAACAGGTAGTTTTCCAGTA	N/A
CaMV 35S	AF234306	35S–F	GCGGGGCCCCCCAACATGGTGGAGCACG	805
		35S–R	GCGGAATTCAGAGATAGATTTGTAGAGAG	N/A
Nos terminator	AF234306	nos–F	GCGACTAGTCGTTCAAACATTTGGC	270
		nos–R	GCGGCGGCCGCCCCGATCTAGTAAC	N/A
GUS	AF234306	pC–GUS–R2	CCTGGCACAGCAATTGCCCGGC	N/A
pCAMBIA 1381z	AF234306	Cam1381z–Tcheck–F	GGAAACAGCTATGACCATGATTAC	N/A
nptII	EU048864	nptII–qRT–F	CTTTTCTGGATTCATCGACTGTG	133
		nptII–qRT–F	GATACCGTAAAGCACGAGGAAG	N/A

Table A.1 Oligonucleotide primer sequences used in cloning, 5’ RACE, and qRT-PCR.

		uAUGs (%)			uORFs		Length (nt)		Base content (%)								Free energy (ΔG; kcal/mol)	
						Length	5’	3’	5’ UTR				3’ UTR					
Group	Sample size	0	1	>1	%	(aa)	UTR	UTR	A	C	G	U	A	C	G	U	5’ UTR	3’ UTR
All Arabidopsis genes[1]	4151–15133	73	15	12	n/a	n/a	125	248	30.5*	19.5*	19.5*	30.5*	34*	16*	16*	34*	-35	-69
All Arabidopsis r-proteins	215–220	96.3	2.8	0.9	3.7	11	72	207	27.2	25.1	19.7	28.0	24.3	15.2	16.7	43.8	-18.5	-55.7
All *RPL23a* orthologs	101–103	77.0	13.0	10.0	20.8	23	90	180	23.1	24.6	24.7	28.0	24.7	15.9	19.8	39.6	-29.4	-52.8
All plants	84–85	82.0	9.6	8.4	16.7	21	91	189	22.9	23.8	24.8	28.5	24.1	15.4	19.4	41.1	-28.9	-54.6
Eudicots	62–63	83.4	9.5	7.1	16.7	21	92	186	23.8	22.5	23	30.7	24.4	14.3	18.3	43.1	-28.4	-52.9
Brassicales	20	90.0	0	10.0	10.0	9	82	148	22.6	21.5	23.7	32.2	22.2	16.8	15.6	45.4	-25.5	-36.1
Arabidopsis	**2**	**100**	**0**	**0**	**0**	**n/a**	**55**	**190**	**23.7**	**23.7**	**21.9**	**30.7**	**23.5**	**14.6**	**15.4**	**46.5**	**-15.2**	**-50.2**
Monocots	8–9	62.5	25.0	12.5	22.2	36	123	214	21.9	29.0	28.1	21.0	19.8	19.0	24.8	36.4	-44.6	-71.8
Gymnosperms	4–5	75.0	0	25.0	25.0	28	113	352	22.7	15.7	40.0	21.6	26.1	14.6	18.7	40.6	-38.2	-106.8
Nonvascular plants	9	77.8	22.2	0	22.2	17	63	180	16.9	32.2	24.4	26.5	25.1	20.0	22.2	32.7	-21.0	-59.3
All animals	12	50.0	25.0	25.0	41.7	25	92	124	23.3	26.6	25.1	25.0	29.4	18.6	21.7	30.3	-35.7	-39.6
Vertebrates	5	80.0	20.0	0	20.0	14	38	63	30.7	27.0	23.8	18.5	33.5	20.9	17.4	28.2	-13.4	-15.9
Invertebrates	7	28.5	28.6	42.9	57.1	27	131	167	21.7	26.5	25.4	26.4	28.3	17.9	22.9	30.9	-51.7	-56.5
All fungi	3–4	100	0	0	0	n/a	28	127	37.1	32.6	19.1	11.2	28.1	17.3	23.8	30.8	-3.3	-37.4
All protists	2	0	100	0	100	29	145	221	24.2	25.6	19.8	30.4	23.3	24.2	24.7	27.8	-48.2	-84.5

Table A.2 Comparison of Arabidopsis *RPL23a* paralog transcript properties with eukaryotic *RPL23a* orthologs from 55 species, and with 215–220 Arabidopsis r-protein transcripts. Percentage values for upstream AUG start codons (uAUGs) and upstream open reading frames (uORFs) indicate the proportion of transcripts within each group possessing described features. The uORF average length is calculated only from transcripts with uORFs. [1]Data for all Arabidopsis genes was from Kawaguchi and Bailey-Serres (2005). *Estimated values; only percent GC was reported. n/a, not available.

7.4 Supplementary Figures for Chapter 2

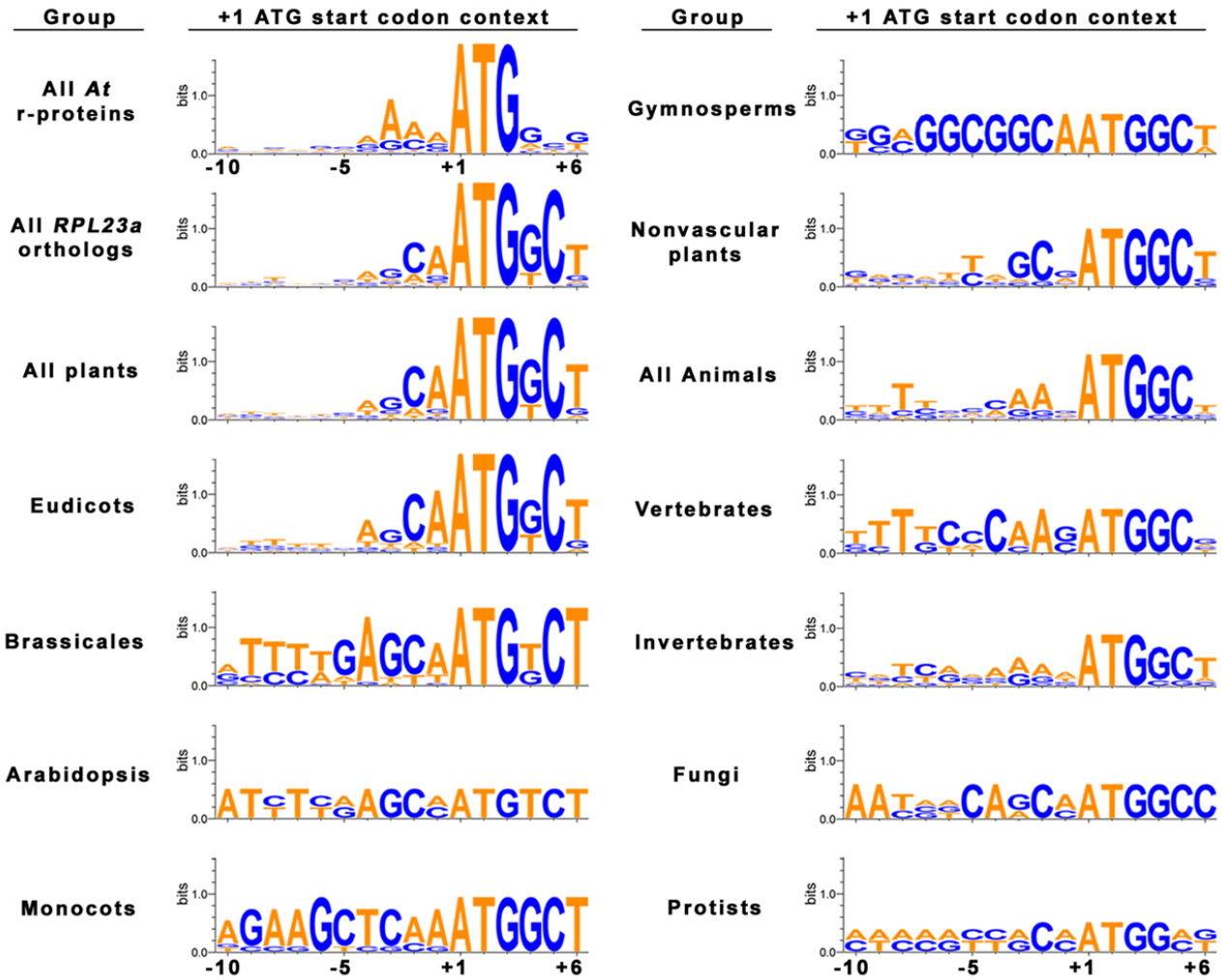

Figure A.1 Comparison of the sequence context of AUG (ATG) start codons of *RPL23a* paralog transcripts with eukaryotic *RPL23a* orthologs from 55 species, and with 215 Arabidopsis r-protein transcripts. The 16 nt sequence from -10 to +6 relative to +1 AUG start codon for all transcripts from each group was used to create a consensus sequence using Weblogo software (Crooks et al., 2004). Groups are as in Table A.2.

8 APPENDIX B. SUPPLEMENTARY MATERIAL FOR CHAPTER 3

8.1 Supplementary Tables for Chapter 3

Oligonucleotide Primer	
Primer ID	Primer Sequence
SAIL_LB	5'GCGTTCATAACCAATCTCGATACAC3'
SAIL-258-C12_RP	5'GCGTGACATCCAGACCAAGAAAGTG3'
SAIL-258-C12_LP	5'CGCAAAGTTGCTGGAATTGAAG3'
SALK_LB	5'GCGTTCATAACCAATCTCGATACAC3'
SALK-091329.46.50_RP	5'GCGTCGTCTTCTATTTCTCTTTTGCG3'
SALK-091329.46.50_LP	5'GCGACCACTTGAATTTTGGGTTG3'
SAIL-597-B08_RP	5'GCGTCGTCTTCTATTTCTCTTTTGCG3'
SAIL-597-B08_LP	5'GCGACCACTTGAATTTTGGGTTG3'
SAIL-444-A06_RP	5'GCGACCAGGTTAAACCGGGATTAG3'
SAIL-444-A06_LP	5'GCGTCTCCAGCTAAAGGTACGCC3'
L23aA_qRT_F	5'CAGATTTCGTGTGTGAAGAATCAT3'
L23aA_qRT_R	5'ACCAGTTCTAGGCTTGGTAAGAG3'
L23aB_qRT_F	5'CGTGAAAAGAATCTATCTTGAGCA3'
L23aB_qRT_R	5'AGGCTTTCTAGGAACGGTCAATG3'
ACT7_qRT_F	5'GATATTCAGCCACTTGTCTGTGAC3'
ACT7_qRT_R	5'CATGTTCGATTGGATACTTCAGAG3'

Table B.1 Oligonucleotide primer sequences used in zygosity confirmation, RT-PCR and qRT-PCR.

8.2 Supplementary Figures for Chapter 3

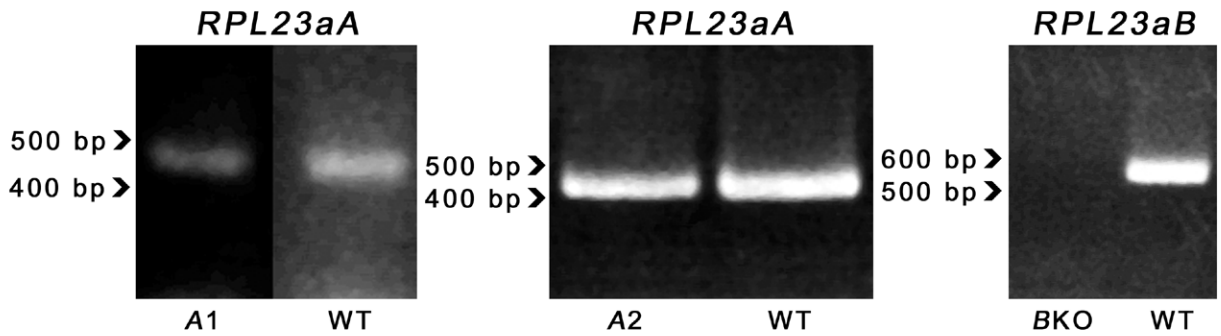

Figure B.1 RT-PCR analysis of homozygous T-DNA insertion lines. Gene specific primers were used to amplify *RPL23aA* or *RPL23aB* (Table B.1; RPL23A1F and RPL23A1R for *RPL23aA*, RPL23A2F and RPL23A2R for *RPL23aB*) from total RNA extracts of wildtype plants (WT), putative *RPL23aA* T-DNA knockout lines SAIL-258-C12 (*A*1) and SALK-091329.46.50 (*A*2), and putative *RPL23aB* T-DNA knockout line SAIL-597-B08 (*B*KO). For the SAIL-258-C12 image, intervening lanes have been removed. Thirty cycles were used for PCR and amplicons were 437 and 535 bp for *RPL23aA* and *RPL23aB*, respectively. Agarose gels were stained with EtBr.

9 APPENDIX C. SUPPLEMENTARY MATERIAL FOR CHAPTER 4

9.1 Supplementary Materials and Methods for Chapter 4

9.1.1 Plant growth conditions

Arabidopsis wildtype and transgenic seed were vapor-phase sterilized for 16–20 h (Clough and Bent, 1998) and plated on basal media. Seeds were stratified at 4ºC for three days and then placed in a growth chamber with a 23º/18ºC temperature regime and a 16 h/8 h photoperiod of ~120 µmol photons m^{-2} sec^{-1}. For tobacco experiments, seed was grown in soil in a growth chamber with a 23º/18ºC temperature regime and a 16 h/8 h photoperiod of ~170 µmol photons m^{-2} sec^{-1}.

9.1.2 Fluorescent protein constructs

C-terminal fluorescent protein tags were created by using RT-PCR to amplify *RPL23aA* and *RPL23aB* ORFs from total RNA. Briefly, approximately 100 mg of fresh Arabidopsis seedling tissue was flash frozen in $N_{2(l)}$ and ground to a fine powder. Total RNA was extracted using the RNeasy Plant Mini kit (Qiagen) following the manufacturer's instructions. ORFs were amplified using Superscript II RT (Invitrogen), modified from manufacturer's instructions as follows: isolated total RNA was treated with ~1 U DNase I (GE Healthcare) following manufacturer's instructions, reverse transcription was conducted using 200 ng of RNA as template incubated with an ORF-specific reverse primer (Table C.1, L23aA_R_EcoRI and L23aB_R_EcoRI) for 40 min at 48ºC. PCR amplification was conducted using 10% (2 µL) of the first-strand product as template, with ORF-specific reverse (L23aA_R_EcoRI; L23aB_R_EcoRI) and forward primers (Table C.1, L23aA_F_PstI and L23aB_F_PstI) and Pfu polymerase (Fermentas). RPL23aA and RPL23aB ORF PCR products were cloned into unique *Pst*I/*Eco*RI restriction sites in the pGEM4 vector (Promega) to create pGEM4–RPL23aA/B. These ORFs were subcloned into unique *Eco*RI/*Bam*HI sites within the pGREENI0029 binary vector (Hellens et al., 2000) using primers that substituted the 5' and 3' restriction sites for *Eco*RI and *Bam*HI, respectively, and removed the 3' stop codon, generating pGREENI0029–RPL23aA/B. The glutathione *S*-transferase (GST) linker was amplified by PCR from pGEX-4T-3 (GE Healthcare) using gene specific primers (Table C.1, GST_F_BamHI and GST_R_HindIII) and cloned into the unique *Bam*HI/*Hind*III sites of pGREENI0029–RPL23aA/B in-frame with RPL23aA/B, generating pGREENI0029–

RPL23aA/B–GST. GFP5 and mRFP were amplified by PCR from pVKH18En6–GFP5–mTALIN (Brandizzi et al., 2002c) and pVKH18En6–ST–mRFP (Runions et al., 2006; Saint-Jore et al., 2002), respectively, using gene specific primers (Table C.1, GFP_F_HindIII, GFP_R_SpeI, RFP_F_HindIII and RFP_R_SpeI) containing 3' stop codons and cloned into the unique *Hind*III/*Spe*I sites of pGREENI0029–RPL23aA/B–GST in-frame with RPL23aA/B–GST, generating pGREENI0029–RPL23aA/B–GST–GFP/RFP. Finally, a tandem repeat of the CaMV 35S promoter (35S) and a nopaline synthase (nos) poly(A) signal (terminator) were amplified by PCR from pCAMBIA1381z (CAMBIA) using gene specific primers (Table C.1, 35S_F_ApaI, 35S_R_EcoRI, nos_F_SpeI and nos_R_NotI) and cloned into the unique *Apa*I/*Eco*RI (35S) and *Spe*I/*Not*I (nos) sites of pGREENI0029-RPL23aA/B-GST-GFP5/mRFP, creating a fusion protein of RPL23aA/B–GST–GFP5/mRFP under the control of a tandem 35S promoter.

N-terminal tags were made in a similar manner. The GST linker was cloned into pBluescript II KS+ (pBSKS+) at the unique *Bam*HI/*Hind*III sites, creating pBSKS+–GST. Subsequently, RPL23aA/B ORFs were subcloned from pGEM4–RPL23aA/B into unique *Hind*III/*Sal*I sites in pBSKS+–GST using primers that replace the 5' and 3' sites with *Hind*III and *Sal*I, respectively, and that contain a 3' nested *Sac*I site, generating pBSKS+–GST–RPL23aA/B. The GST–L23aA/B cassette was subcloned into the binary vector pVKH18En6–GFP5–mTALIN at unique *Bam*HI/*Sac*I restriction sites, replacing mTALIN and creating a fusion protein of GFP5–GST–L23aA/B under the control of an enhanced 35S promoter.

The free mRFP control was created by digesting pVKH18En6–ST–mRFP with *Sal*I to linearize the vector immediately 5' to mRFP; the single-stranded overhanging DNA was filled in with Klenow fragment (Invitrogen) according to manufacturer's instructions, and cut with *Sac*I to release the mRFP fragment containing a 5' blunt end and 3' *Sac*I site. This fragment was cloned into pBSKS+ previously cut with *Not*I, blunt-ended with Klenow fragment and cut with *Sac*I, creating pBSKS+–mRFP. The mRFP fragment from pBSKS+–mRFP was subcloned into the binary vector pVKH18En6–GFP5–mTALIN at unique *Xba*I/*Sac*I sites, replacing GFP5–mTALIN. To make the 35S–FIB2–EGFP control, the FIB2–EGFP fragment from ppk100–FIB2–EGFP (Barneche et al., 2000) was subcloned into the binary vector pCAMBIA1380 (CAMBIA) at unique *Eco*RI/*Spe*I sites, creating pCAMBIA1380–FIB2–EGFP. Subsequently, a tandem repeat of the 35S promoter was amplified by PCR from pCAMBIA1381z (CAMBIA)

and cloned into the unique *Apa*I/*Eco*RI sites of pCAMBIA1380–FIB2–EGFP, creating a fusion protein of FIB2–EGFP under the control of a tandem 35S promoter.

9.1.3 RNAi constructs

For silencing of *RPL23aA*, a 148 bp region of the 3' UTR was chosen as the target sequence and amplified by PCR from the F12L6 BAC, obtained from ABRC, using specific primers (Table C.1, L23aA_Sense_F_XhoI, L23aA_Sense_R_HindIII, L23aA_Antisense_F_SpeI and L23aA_Antisense_R_PstI). To silence *RPL23aB*, a 205 bp region corresponding to the final 25 bp of the ORF and 180 bp of the 3' UTR were chosen as the target and amplified by PCR using specific primers (Table C.1, L23aB_Sense_F_XhoI, L23aB_Sense_R_HindIII, L23aB_Antisense_F_SpeI and L23aB_Antisense_R_PstI) from genomic DNA extracted from Arabidopsis seedling tissue using the DNeasy Plant Mini Kit (Qiagen), as per manufacturer's instructions. The targeted regions for silencing *RPL23aA* and *RPL23aB* independently showed 59.3% and 60.5% identity, respectively, to the corresponding regions on paralogs, with no stretch of perfect identity greater than 16 bp. For silencing of the *RPL23a* family, a 343 bp region of the *RPL23aA* ORF was chosen as the target and amplified by PCR from pGEM4–RPL23aA using specific primers (Table C.1, L23a_Sense_F_XhoI, L23a_Sense_R_HindIII, L23a_Antisense_F_SpeI and L23a_Antisense_R_PstI). The targeted region of the *RPL23aA* ORF shared 86.3% identity between paralogs and had several 17–20 bp stretches of perfect identity. Sense and antisense PCR products for each target were cloned into the intron-containing intermediate vector pSK–int (Guo et al., 2003) at unique *Xho*I/*Hind*III (sense) and *Pst*I/*Spe*I (antisense) sites. The resultant sense–intron–antisense cassette was subcloned into the unique *Xho*I/*Spe*I sites of the binary vector pER8 (Zuo et al., 2000), creating the estrogen inducible, hairpin RNA forming cassettes, RPL23aA–ihp, RPL23aB–ihp and RPL23a–ihp.

9.1.4 Quantitative PCR

Quantification of endogenous *RPL23aA* and *RPL23aB* transcript level in transgenics carrying the RPL23aA–ihp, RPL23aB–hp and RPL23a–ihp was conducted by qPCR. The Plant Total RNA Extraction Kit (Real Biotech Corporation) was used to extract RNA from 10–18 day-old whole seedlings that were flash frozen in $N_{2(l)}$ and ground to a fine powder. RNA was quantified using a UV spectrophotometer (GeneQuantII, Pfizer, Kirkland, PQ), and 1 µg of RNA was treated with DNase I (Fermentas) following manufacturer's instructions. First strand cDNA was

synthesized using RevertAid M-MuLV RT (Fermentas) as per manufacturer's guidelines with the following exceptions: 400 ng of total RNA was used as template, 10 pmoles of each gene specific reverse primer was used (Table C.1, ACT7_qRT_R, L23aA_qRT_R and L23aB_qRT_R), primer annealing was conducted at 42ºC for 5 min and reverse transcription was conducted at 48ºC for 40 min. In the case of the inducibly lethal RPL23a–ihp transgenic lines (–5 to –7), only 50–100 ng of total RNA was used as template due to very limited amounts of tissue.

Forward primers for qPCR amplification of RPL23aA/B were designed to exploit differences in 5' UTRs and prevent spurious priming, and for all genes, primers were chosen such that amplicon size was ~200 bp, successful amplification required splicing of a spanned intron, and Tm's for primer sets were ~60ºC (Table C.1, ACT7_qRT_F, L23aA_qRT_F and L23aB_qRT_F). PCRs were optimized for template, Mg^{2+} concentrations, and annealing temperatures prior to conducting qPCR analyses. Standard curves were generated for each primer set to verify amplification efficiencies of ~100%. Reactions used EvaGreen (Biotium, Hayward, CA) as the nucleic acid dye, essentially as per manufacturer's instructions except that reactions were scaled back to accommodate a 20 µl volume. qPCR involved 40 cycles of 94ºC for 15 s, 55ºC for 20 s, and 72ºC for 25 s, with fluorescence detection occurring during annealing at 55ºC.

9.2 Supplementary Results for Chapter 4

9.2.1 Properties of nucleoli and cajal bodies in tobacco

Tobacco epidermal cells expressing FIB2–EGFP generally displayed only a single nucleolus, which appeared spherical with a radius of 1–2 µm. Cells with two nucleoli were less common, but notably nucleoli within these cells were nearly always at disparate optical planes, suggesting a spatial separation (see Figure C.1). Accumulation of all chimerics was also observed in the cytoplasm and nucleoplasm, yet no distinct accumulation on the endoplasmic reticulum was detected (see Figure C.2, cf. Figure 1D and 1F Brandizzi et al., 2002b).

Consistent with previous findings, the FIB2–EGFP construct also targeted mobile cajal bodies (Kim et al., 2007; Makimoto et al., 2006), which are nucleolus-associated inclusions that contain snRNPs and snoRNPs, and are involved in the formation of spliceosomal snRNPs and snoRNPs (Beven et al., 1995; Kim et al., 2007). Cajal bodies contain only a small number of nucleolar

proteins (e.g. fibrillarin, dyskerin, Cioce and Lamond, 2005; Kim et al., 2007) and hence it is not unexpected that they were not targeted by RPL23aA- and RPL23aB-fluorescent protein fusions.

9.2.2 RPL23a contributes to ribosome heterogeneity

We observed that both RPL23a isoforms accumulate in the nucleolus when transiently expressed in tobacco (Figure 4.1b–e), albeit possibly with different efficiency. The 'ribosome filter' hypothesis (Mauro and Edelman, 2002) postulates that the ribosome itself may regulate gene expression via heterogeneity in its composition and the resultant differential affinity for specific transcripts and/or binding/targeting/export factors. This heterogeneity can derive from variability in rRNA (sequence, post-transcriptional modifications), r-proteins (isoform incorporation, post-translational modifications), or ribosome associated factors (reviewed in Mauro and Edelman, 2002). That both RPL23aA and RPL23aB accumulate in the nucleolus, presumably indicates that both isoforms are incorporated into the LSU, and although we did not examine whether this occurs by isolating the polysomal fraction, it should be noted that Arabidopsis RPL23aA with a small C-terminal FLAG-HIS tag (~2 kD) has been identified in polysomes (Zanetti et al., 2005). Further, the yeast ortholog to RPL23a, fused C-terminally with GFP, is used as marker for LSU localization in yeast (Hurt et al., 1999). Thus my findings argue against the possibility that one of the RPL23a isoforms has solely an extra-ribosomal function, but instead suggests that both can be incorporated into ribosomal LSUs. The functional consequence of ribosome heterogeneity due to RPL23a is unclear. It is possible that ribosomes with different isoforms of RPL23a could have altered binding affinities for components of the SRP or the protein conducting channel of the endoplasmic reticulum, hence altering the translocation and targeting of translated polypeptides (Menetret et al., 2005; Pool et al., 2002), but this seems unlikely given that all differences between RPL23a isoforms reside in the N-terminal domain, which is absent in the prokaryotic counterparts to RPL23a that remain competent for efficient interaction with cognate docking compounds (e.g. SRP, trigger factor, Gu et al., 2003; Kramer et al., 2002; Rutgers et al., 1990). Nevertheless, that both isoforms of RPL23a appear to be incorporated into the LSU adds to the body of evidence indicating that plant r-protein families contribute to ribosome heterogeneity (Chang et al., 2005; Giavalisco et al., 2005; Szick-Miranda and Bailey-Serres, 2001).

9.3 Supplementary Tables for Chapter 4

Gene	Accession No.	Oligonucleotide Primer	
		Primer ID	Primer Sequence
RPL23aA	At2g39460	L23aA_F_PstI	5'GCGCTGCAGATGTCTCCGGCTAAAG3'
		L23aA_R_EcoRI	5'GCGGAATTCTTAGATGATGCCGATC3'
		L23aA_Sense_F_XhoI	5'GCGCTCGAGTTATAAAGACTATTGTGG3'
		L23aA_Sense_R_HindIII	5'GCGAAGCTTGAACTTGAATTCAACAATAAAC3'
		L23aA_Antisense_F_SpeI	5'GCGACTAGTTTATAAAGACTATTGTGG3'
		L23aA_Antisense_R_PstI	5'GCGCTGCAGGAACTTGAATTCAACAATAAAC3'
		L23a_Sense_F_XhoI	5'GCGCTCGAGAAGATTAGGACCAAGGTC3'
		L23a_Sense_R_HindIII	5'GCGAAGCTTTCTTGTTAGCAACATCC3'
		L23a_Antisense_F_SpeI	5'GCGACTAGTAAGATTAGGACCAAGGTC3'
		L23a_Antisense_R_PstI	5'GCGCTGCAGTCTTGTTAGCAACATCC3'
		L23aA_qRT_F	5'CAGATTTCGTGTGTGAAGAATCAT3'
		L23aA_qRT_R	5'ACCAGTTCTAGGCTTGGTAAGAG3'
RPL23aB	At3g55280	L23aB_F_PstI	5'GCGCTGCAGATGTCTCCAGC3'
		L23aB_R_EcoRI	5'GCGGAATTCTTAGATGATCCCGATTTTG3'
		L23aB_Sense_F_XhoI	5'GCGCTCGAGGGCTAACAAAATCGGG3'
		L23aB_Sense_R_HindIII	5'GCGAAGCTTACACGATCTGAATAGAAAC3'
		L23aB_Antisense_F_SpeI	5'GCGACTAGTGGCTAACAAAATCGGG3'
		L23aB_Antisense_R_PstI	5'GCGCTGCAGACACGATCTGAATAGAAAC3'
		L23aB_qRT_F	5'CGTGAAAAGAATCTATCTTGAGCA3'
		L23aB_qRT_R	5'AGGCTTTCTAGGAACGGTCAATG3'
GST	U13855	GST_F_BamHI	5'GCGGGATCCATGTCCCCTATACTAGG3'
		GST_R_HindIII	5'GCGAAGCTTACGCGGAACCAGATCCG3'
GFP5	U87973	GFP_F_HindIII	5'GCGAAGCTTATGAGTAAAGGAGAAGAAC3'
		GFP_R_SpeI	5'ACTAGTTTATTTGTATAGTTCATC3'
mRFP	AF506027	RFP_F_HindIII	5'GCGAAGCTTATGGCCTCCTCCGAGGACG3'
		RFP_R_SpeI	5'GCGACTAGTTTAGGCGCCGGTGGAGTGGC3'
CaMV 35S	AF234306	35S_F_ApaI	5'GCGGGGCCCCCCAACATGGTGGAGCACG3'
		35S_R_EcoRI	5'GCGGAATTCAGAGATAGATTTGTAGAGAG3'
Nos	AF234306	nos_F_SpeI	5'GCGACTAGTCGTTCAAACATTTGGC3'
terminator		nos_R_NotI	5'GCGGCGGCCGCCCCGATCTAGTAAC3'
Act7	AT5G09810	ACT7_qRT_F	5'GATATTCAGCCACTTGTCTGTGAC3'
		ACT7_qRT_R	5'CATGTTCGATTGGATACTTCAGAG3'

Table C.1 Oligonucleotide primer sequences used in cloning and qRT-PCR.

9.4 Supplementary Figures for Chapter 4

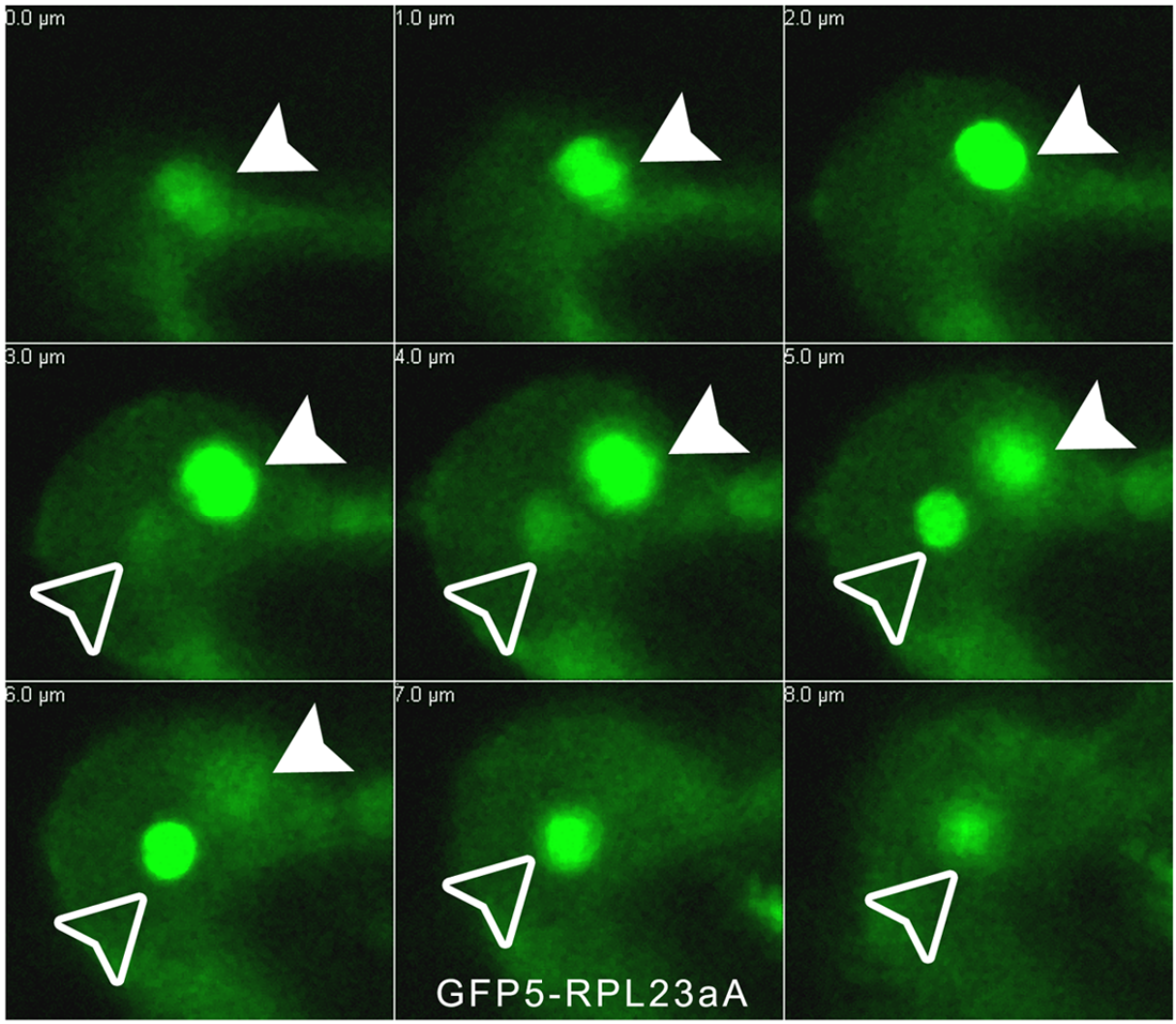

Figure C.1 Nucleoli of tobacco epidermal cells exhibit spatial separation. A z-series gallery of representative CLSM images from tobacco epidermal cells transiently expressing GFP5–RPL23aA. Optical slices begin at the top of the first visible nucleolus (top left frame, solid white arrows) and progress through to the bottom of the second visible nucleolus (bottom right frame, transparent white arrows) at 1 µm intervals. White bars = 10 µm.

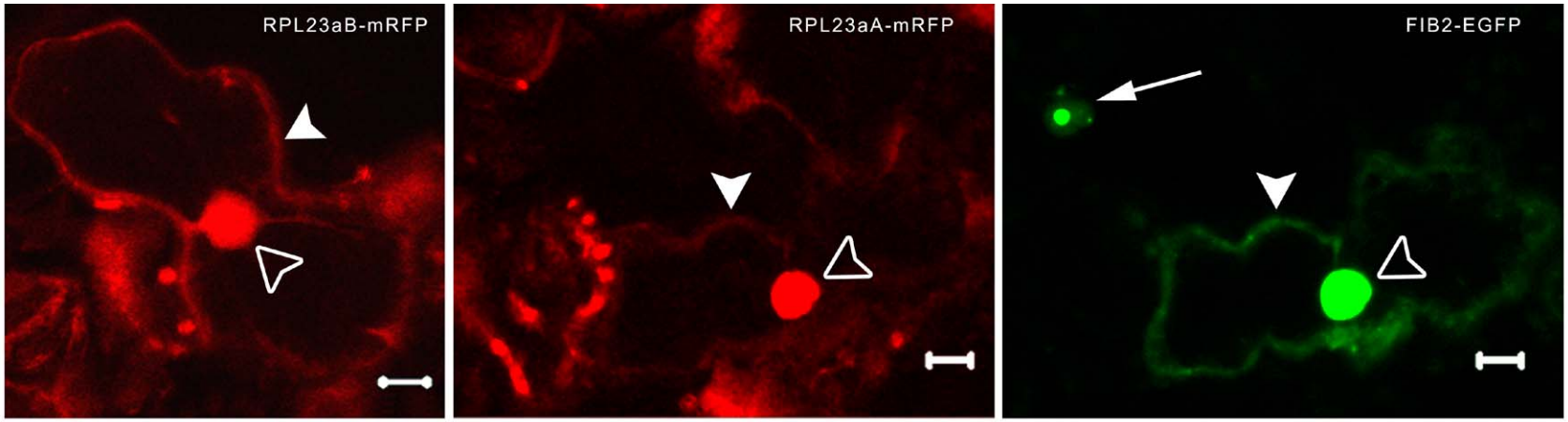

Figure C.2 Fluorescent protein tagged FIB2, RPL23aA and RPL23aB accumulate outside the nucleolus in the cytoplasm and nucleoplasm. Representative CLSM images of tobacco epidermal cells transiently expressing RPL23aB–mRFP, RPL23aA–mRFP and FIB2–EGFP. Cytoplasmic and nucleoplasmic signals are indicated by solid and clear arrowheads, respectively. A more typical nucleoplasmic/nucleolar signal from a different cell expressing FIB2–EGFP is indicated by the narrow arrow. Nucleoplasmic signals are oversaturated due to the buildup of chimeric proteins at the nucleolus. Images of RPL23aA–mRFP and FIB2–EGFP are the same optical slice. White bars = 10 μm.

10 APPENDIX D. EVOLUTIONARY DIVERGENCE OF RIBOSOMAL PROTEIN PARALOGS IN ARABIDOPSIS

A version of this appendix has been published in Plant Signaling & Behavior as an addendum to my manuscript published in Plant Physiology (Chapter 4). I wrote this addendum. Permission to use was obtained from the publisher and is contingent on the following citation.

Degenhardt, R.F. and Bonham-Smith, P.C. (2008) Evolutionary divergence of ribosomal protein paralogs in Arabidopsis. *Plant Signaling & Behavior*, 3, 493-495.

Plant Signaling & Behavior 3:7, 493–495; July 2008; ©2008 Landes Bioscience

As previously discussed, none of the Arabidopsis r-proteins are encoded by single genes, but rather derive from families of 2–7 members that encode nearly-identical isoforms, are independently regulated, dispersed throughout the genome, and largely all transcriptionally active (Barakat et al., 2001). To gain an understanding of why so many plant r-protein paralogs exist, I recently analyzed function and localization of the two-member Arabidopsis *RPL23a* family (RPL23aA and RPL23aB, Degenhardt and Bonham-Smith, 2008a). *RPL23aB* was found to be unnecessary for normal development, while a relatively small decrease in transcript levels of *RPL23aA* resulted in development of a severely abnormal phenotype. Isoforms exhibited differences in nucleolar-targeting, which may result from disparity in putative NLS/NoLS. I postulate a role for ribosome biogenesis in the primary regulation of auxin homeostasis and plant development, and discuss properties of high efficiency NoLSs.

10.1 Plant Ribosomal Proteins Come From Large Gene Families

Whole and partial genome duplication events have played an essential role in the evolution of most angiosperms. Following these events, duplicate genes can undergo purifying selection, become downregulated and removed from the genome, or be subject to modifications that reduce functionality or confer new functionality. All 81 r-proteins of the Arabidopsis cytoplasmic ribosome are encoded by multiple, expressed paralogs (Barakat et al., 2001; Chang et al., 2005; Hulm et al., 2005; McIntosh and Bonham-Smith, 2005). It has been postulated that multiple r-protein gene copies are necessary to meet the translational needs of growing tissues while maintaining the capacity to respond rapidly to development/tissue/stress-specific stimuli (i.e. each family has one or more stimulus-responsive members in addition to one or more

constitutively expressed members, McIntosh and Bonham-Smith, 2006; Van Lijsebettens et al., 1994). This is supported by findings that single paralogs from the Arabidopsis *RPS15a* and *RPL23a* families are up/down regulated in response to hormone and stress treatments, with no corresponding affects on levels of the other expressed paralogs (Hulm et al., 2005; McIntosh and Bonham-Smith, 2005).

10.2 A Link Between Translation and Auxin Homeostasis?

In Arabidopsis, several single r-protein knockdowns/knockouts (*RPS5B, RPS13B*, *RPS18A*, *RPL24B*, *RACK1A*) have been previously described, predominantly resulting in development of the *pfl* phenotype (Chen et al., 2006; Ito et al., 2000; Nishimura et al., 2005; Van Lijsebettens et al., 1994; Weijers et al., 2001). Generally, *pfl* mutants have reduced cell division, retarded growth, late-flowering, atypical/reduced vasculature, and morphological abnormalities including fused leaves and first leaves with a 'pointed' shape. Using an inducible RNAi-mediated gene silencing technique (Guo et al., 2003), I recently reproduced this phenotype via knockdown of *RPL23aA*, but found that no abnormal phenotype developed when the other paralog, *RPL23aB*, was silenced or knocked-out by T-DNA insertion (Degenhardt and Bonham-Smith, 2008a). Arabidopsis RPL23a is part of a universally conserved r-protein family, which bind directly to LSU rRNA, and are essential for ribosome biogenesis and co-translational targeting of nascent peptides (Halic et al., 2004; Rutgers et al., 1991). I showed that the function of RPL23a is essential for survival in Arabidopsis based on the nonviability of transgenics where paralogs were coordinately silenced (Degenhardt and Bonham-Smith, 2008a). To my knowledge, RPL23aB is the only core r-protein paralog that fails to produce an abnormal phenotype following knockdown/knockout. While expression analyses have determined that *RPL23aB* transcripts are less abundant than *RPL23aA* transcripts in all tissues (McIntosh and Bonham-Smith, 2005). a *pfl* phenotype results from a knockout of *RPS18A*, which contributes only ~25% of the total *RPS18* transcript pool (Vanderhaeghen et al., 2006), and from a knockout of *RPS13B*, despite the negligible reduction in total *RPS13* transcript as determined by Northern analysis of the mutant (Ito et al., 2000). I have also determined that an *rpl23ab* knockout shows little to no compensation at the transcript level (Chapter 3), but the possibility remains that compensation occurs post-transcriptionally (i.e. increased polysome loading of *RPL23aA* transcripts) or that RPL23aB is required only under very specific conditions.

A search for additional Arabidopsis mutants with similar growth defects to *RPL23aA*-silencing mutants, suggests that the phenotype results from impaired rRNA maturation and the consequent reduction in ribosome biogenesis (Degenhardt and Bonham-Smith, 2008a). This is supported by the finding that a *pfl* phenotype does not develop following loss-of-function of RACK1A, which is a SSU r-protein that functions in signal transduction and regulating translation, but is not involved in ribosome biogenesis within the nucleolus (Chen et al., 2006; Sengupta et al., 2004). My most intriguing discovery was that both auxin-responsiveness- and microRNA- (miRNA) biogenesis mutants resemble *pfl* mutants, and I postulate a model whereby translational status regulates auxin homeostasis via miRNAs (Figure D.1, Degenhardt and Bonham-Smith, 2008a). miRNAs are a class of small RNAs (~22 nts) that are processed from RNA pol II-derived transcripts and function to direct cleavage or impair translation of mRNAs with near-perfect complementarity (Mallory and Vaucheret, 2006b). My model is based on the finding that a large number of auxin response genes are regulated by miRNAs and that degradation of a subset of miRNA targets in Drosophila requires active translation (Eulalio et al., 2007; Mallory and Vaucheret, 2006b). Under my model, translational inhibition disrupts auxin homeostasis and impairs auxin transport by disrupting the miRNA-mediated regulation of auxin-conjugating enzymes, and auxin-regulated transcription factors (auxin response factors [ARFs], NAC domain proteins, and class III homeodomain leucine zipper proteins, Mallory et al., 2005; Mallory and Vaucheret, 2006b; Zhou et al., 2007). This model provides a tangible link for the observed developmental correlation between translational status and auxin-mediated responses. For example, in young leaves the rate of protein synthesis is high, and this corresponds to a high distribution of auxin-response maxima and rapid cell division (Mattsson et al., 2003); in mature leaves, the rate of protein synthesis is low, auxin response maxima disappear and cell division is minimal (Mattsson et al., 2003).

10.3 Nucleolin Binding May Enhance Nucleolar Targeting

Eukaryotic RPL23a orthologs possess an N-terminal domain that confers nuclear import (Jakel and Gorlich, 1998; Schaap et al., 1991), however the exact NLS/NoLS has not been experimentally determined in plants. I found that RPL23aA was efficiently targeted to the nucleolus when fused with large (~53 kD) C- or N-terminal fluorescent protein tags, while nucleolar targeting of tagged RPL23aB was disrupted by fusion to a more acidic fluorescent protein tag, and eliminated by moving the tag to the N-terminus. I suggest that disparity in

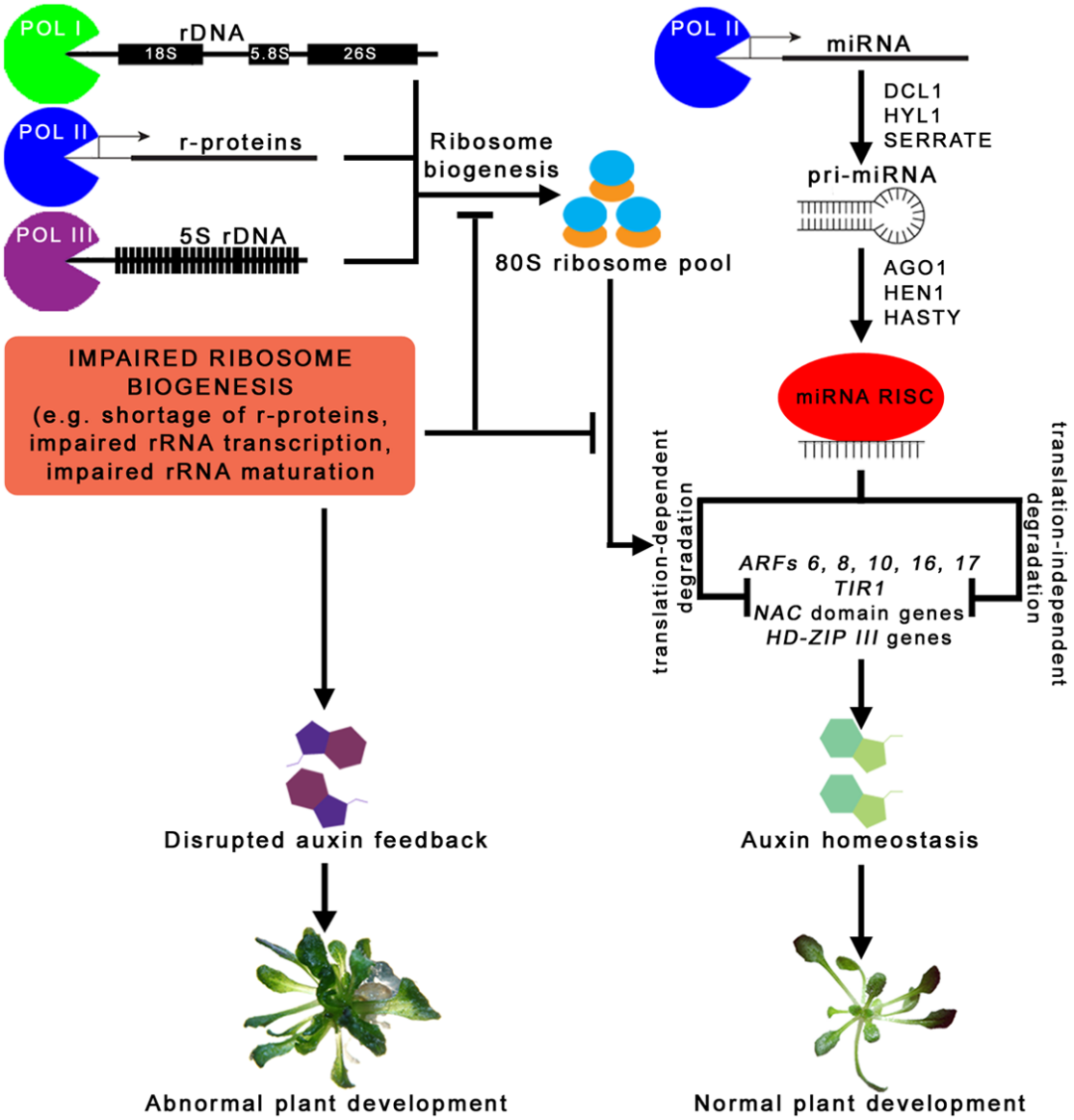

Figure D.1 Schematic representation of a mechanism for the regulation of auxin homeostasis by miRNAs and active translation. RNA pol II-derived primary miRNA precursors (pri-miRNA) mature via a pathway that involves cleavage, methylation, loading onto a RNA-induced silencing complex (RISC), and export. miRNAs downregulate a number of important transcription factors involved in mediating the auxin response and controlling plant development via translation independent and dependent pathways. The latter requires active ribosome biogenesis and a full complement of rRNAs and r-proteins. When ribosome biogenesis is impaired, translation dependent miRNA target degradation is reduced/abolished, disrupting auxin homeostasis and plant development (Degenhardt and Bonham-Smith, 2008a; Eulalio et al., 2007; Mallory et al., 2005; Mallory and Vaucheret, 2006b; Zhou et al., 2007).

targeting results from a non-conservative K^{34} to P^{34} substitution within a putative monopartite, SV40 large T-antigen-like, RPL23aA NLS (^{33}KKDK^{36}) that reportedly confers nucleolar-targeting and nucleolin binding in mammals (Wang et al., 2005a; Xue et al., 1993). Nucleolin is one of the most abundant nucleolar proteins, and functions in rDNA transcription, rRNA processing, nucleocytoplasmic trafficking and maintenance of the nucleolar integrity (Ginisty et al., 1999; Pontvianne et al., 2007). If the putative nucleolin-binding motif of RPL23aA is functional, it would confer a competitive advantage by enabling this paralog to associate with nascent rRNA and assemble rapidly into the LSU. Further, given recent findings in mammals that r-proteins not incorporated into subunits are in constant flux between the nucleolus and nucleoplasm, where they are subject to degradation via the 26 S proteasome (Lam et al., 2007), binding to nucleolin might increase nucleolar retention time and shift the equilibrium in favor of LSU incorporation versus nucleoplasmic degradation. Support for nucleolin binding of an r-protein NoLS comes from the findings that several mammalian r-proteins bind to nucleolin *in vitro* (Bouvet et al., 1998), and that the putative nucleolin binding motif (consensus $[K/R]_2XK$) is found within the delineated NoLSs of a number of animal and yeast r-proteins including RPS6, RPS25, RPL5, RPL7a, RPL22 and RPL23a (Jakel and Gorlich, 1998; Kundu-Michalik et al., 2008). I suggest that this motif functions in a context-specific manner to facilitate both nuclear import and high affinity nucleolus-binding via interaction with nucleolin, resulting in efficient ribosome biogenesis.

11 REFERENCES

Abovich, N., Gritz, L., Tung, L. and Rosbash, M. (1985) Effect of RP51 gene dosage alterations on ribosome synthesis in *Saccharomyces cerevisiae*. *Molecular and Cellular Biology*, **5**, 3429-3435.

Agetsuma, M., Furumoto, T., Yanagisawa, S. and Izui, K. (2005) The ubiquitin-proteasome pathway is involved in rapid degradation of phosphoenolpyruvate carboxylase kinase for C4 photosynthesis. *Plant and Cell Physiology*, **46**, 389-398.

AGI (2000) Analysis of the genome sequence of the flowering plant *Arabidopsis thaliana*. *Nature*, **408**, 796-815.

Agrawal, R.K., Heagle, A.B., Penczek, P., Grassucci, R.A. and Frank, J. (1999) EF-G-dependent GTP hydrolysis induces translocation accompanied by large conformational changes in the 70S ribosome. *Nature Structural Biology*, **6**, 643-647.

Agrawal, R.K., Spahn, C.M.T., Penczek, P., Grassucci, R.A., Nierhaus, K.H., et al. (2000) Visualization of tRNA movements on the *Escherichia coli* 70S ribosome during the elongation cycle. *Journal of Cell Biology*, **150**, 447-459.

Alonso-Peral, M.M., Candela, H., del Pozo, J.C., Martinez-Laborda, A., Ponce, M.R., et al. (2006) The *HVE/CAND1* gene is required for the early patterning of leaf venation in Arabidopsis. *Development*, **133**, 3755-3766.

Alonso, J.M., Stepanova, A.N., Leisse, T.J., Kim, C.J., Chen, H., et al. (2003) Genome-wide insertional mutagenesis of *Arabidopsis thaliana*. *Science*, **301**, 653-657.

Amaldi, F., CamachoVenegas, O., Cardinali, B., Cecconi, F., Crosio, C., et al. (1995) Structure and expression of ribosomal protein genes in *Xenopus laevis*. *Biochemistry and Cell Biology*, **73**, 969-977.

Andersen, J.S., Lam, Y.W., Leung, A.K.L., Ong, S.-E., Lyon, C.E., et al. (2005) Nucleolar proteome dynamics. *Nature*, **433**, 77-83.

Andersen, J.S., Lyon, C.E., Fox, A.H., Leung, A.K.L., Lam, Y.W., et al. (2002) Directed proteomic analysis of the human nucleolus. *Current Biology*, **12**, 1-11.

Arnold, R.J. and Reilly, J.P. (1999) Observation of *Escherichia coli* ribosomal proteins and their posttranslational modifications by mass spectrometry. *Analytical Biochemistry*, **269**, 105-112.

Aro, E.M., Virgin, I. and Andersson, B. (1993) Photoinhibition of photosystem II - Inactivation, protein damage and turnover. *Biochimica Et Biophysica Acta*, **1143**, 113-134.

Bachand, F., Lackner, D.H., Bahler, J. and Silver, P.A. (2006) Autoregulation of ribosome biosynthesis by a translational response in fission yeast. *Molecular and Cellular Biology*, **26**, 1731-1742.

Bailey-Serres, J. (1998) Cytoplasmic ribosomes of higher plants. In *A Look Beyond Transcription: Mechanisms Determining mRNA Stability and Translation in Plants* (Bailey-Serres, J. and Gallie, D.R., eds). Rockville, MD: American Society of Plant Physiologists, pp. 125-144.

Bailey-Serres, J. and Freeling, M. (1990) Hypoxic stress-induced changes in ribosomes of maize seedling roots. *Plant Physiology*, **94**, 1237-1243.

Bailey, S., Horton, P. and Walters, R.G. (2004) Acclimation of *Arabidopsis thaliana* to the light environment: the relationship between photosynthetic function and chloroplast composition. *Planta*, **218**, 793-802.

Bailey, S., Walters, R.G., Jansson, S. and Horton, P. (2001) Acclimation of *Arabidopsis thaliana* to the light environment: the existence of separate low light and high light responses. *Planta*, **213**, 794-801.

Bailey, T.L., Williams, N., Misleh, C. and Li, W.W. (2006) MEME: discovering and analyzing DNA and protein sequence motifs. *Nucleic Acids Research*, **34**, W369-W373.

Ban, N., Nissen, P., Hansen, J., Moore, P.B. and Steitz, T.A. (2000) The complete atomic structure of the large ribosomal subunit at 2.4 Å resolution. *Science*, **289**, 905-920.

Barakat, A., Muller, K.F. and Saenz-De-Miera, L.E. (2007) Molecular evolutionary analyses of the Arabidopsis L7 ribosomal protein gene family. *Gene*, **403**, 143-150.

Barakat, A., Szick-Miranda, K., Chang, I.F., Guyot, R., Blanc, G., et al. (2001) The organization of cytoplasmic ribosomal protein genes in the Arabidopsis genome. *Plant Physiology*, **127**, 398-415.

Bargis-Surgey, P., Lavergne, J.-P., Gonzalo, P., Vard, C., Filhol-Cochet, O., et al. (1999) Interaction of elongation factor eEF-2 with ribosomal P proteins. *European Journal of Biochemistry*, **262**, 606-611.

Barneche, F., Steinmetz, F. and Echeverria, M. (2000) Fibrillarin genes encode both a conserved nucleolar protein and a novel small nucleolar RNA involved in ribosomal RNA methylation in *Arabidopsis thaliana*. *Journal of Biological Chemistry*, **275**, 27212-27220.

Barta, A. and Kuechler, E. (1983) Part of the 23S RNA located in the 13S RNA fragment is a constituent of the ribosomal peptidyltransferase centre. *Febs Letters*, **163**, 319-323.

Barta, A., Steiner, G., Brosius, J., Noller, H.F. and Kuechler, E. (1984) Identification of a site on 23S ribosomal RNA located at the peptidyl transferase center. *Proceedings of the National Academy of Sciences of the United States of America*, **81**, 3607-3611.

Barthelemy, R.M., Chenuil, A., Blanquart, S., Casanova, J.P. and Faure, E. (2007) Translational machinery of the chaetognath *Spadella cephaloptera*: a transcriptomic approach to the analysis of cytosolic ribosomal protein genes and their expression. *Bmc Evolutionary Biology*, **7**.

Bate, N. and Twell, D. (1998) Functional architecture of a late pollen promoter: pollen-specific transcription is developmentally regulated by multiple stage-specific and co-dependent activator elements. *Plant Molecular Biology*, **37**, 859-869.

Batoko, H., Zheng, H.Q., Hawes, C. and Moore, I. (2000) A Rab1 GTPase is required for transport between the endoplasmic reticulum and Golgi apparatus and for normal Golgi movement in plants. *Plant Cell*, **12**, 2201-2217.

Baudin-Baillieu, A., Tollervey, D., Cullin, C. and Lacroute, F. (1997) Functional analysis of RRP7p, an essential yeast protein involved in pre-rRNA processing and ribosome assembly. *Molecular and Cellular Biology*, **17**, 5023-5032.

Beckmann, R., Bubeck, D., Grassucci, R., Penczek, P., Verschoor, A., et al. (1997) Alignment of conduits for the nascent polypeptide chain in the ribosome-Sec61 complex. *Science*, **278**, 2123-2126.

Beltran-Pena, E., Ortiz-Lopez, A. and de Jimenez, E. (1995) Synthesis of ribosomal proteins from stored mRNAs early in seed germination. *Plant Molecular Biology*, **28**, 327-336.

Ben Ali, A., Wuyts, J., De Wachter, R., Meyer, A. and Van de Peer, Y. (1999) Construction of a variability map for eukaryotic large subunit ribosomal RNA. *Nucleic Acids Research*, **27**, 2825-2831.

Bennett, S.R.M., Alvarez, J., Bossinger, G. and Smyth, D.R. (1995) Morphogenesis in Pinoid mutants of *Arabidopsis thaliana*. *Plant Journal*, **8**, 505-520.

Berriman, M., Ghedin, E., Hertz-Fowler, C., Blandin, G., Renauld, H., et al. (2005) The genome of the African trypanosome *Trypanosoma brucei*. *Science*, **309**, 416-422.

Beven, A.F., Simpson, G.G., Brown, J.W.S. and Shaw, P.J. (1995) The organization of spliceosomal components in the nuclei of higher-plants. *Journal of Cell Science*, **108**, 509-518.

Bielka, H. (1982) *The Eukaryotic Ribosome*. Berlin: Springer-Verlag.

Biggiogera, M., Malatesta, M., Abolhassani-Dadras, S., Amalric, F., Rothblum, L.I., et al. (2001) Revealing the unseen: the organizer region of the nucleolus. *Journal of Cell Science*, **114**, 3199-3205.

Bogorad, L. (1975) Evolution of organelles and eukaryotic genomes. *Science*, **188**, 891-898.

Bohmert, K., Camus, I., Bellini, C., Bouchez, D., Caboche, M., et al. (1998) AGO1 defines a novel locus of Arabidopsis controlling leaf development. *The EMBO Journal*, **17**, 170-180.

Bohnsack, M.T., Regener, K., Schwappach, B., Saffrich, R., Paraskeva, E., et al. (2002) Exp5 exports eEF1A via tRNA from nuclei and synergizes with other transport pathways to confine translation to the cytoplasm. *Embo Journal*, **21**, 6205-6215.

Bonham-Smith, P.C., Oancia, T.L. and Moloney, M.M. (1992) Cytoplasmic ribosomal protein S15a from *Brassica napus*: molecular cloning and developmental expression in mitotically active tissues. *Plant Molecular Biology*, **18**, 909-919.

Bonnet, E., Wuyts, J., Rouze, P. and Van de Peer, Y. (2004) Detection of 91 potential in plant conserved plant microRNAs in *Arabidopsis thaliana* and *Oryza sativa* identifies important target genes. *Proceedings of the National Academy of Sciences of the United States of America*, **101**, 11511-11516.

Boublik, M., Mandiyan, V. and Tumminia, S. (1990) Potential of electron microscopic techniques for structural analysis of ribosomes. In *The Ribosome: Structure, Function, and Evolution* (Hill, W.E., Dahlberg, A., Garrett, R.A., Moore, P.B., Schlessinger, D. and Warner, J.R., eds). Washington, D.C.: American Society for Microbiology, pp. 114-122.

Bourdon, V., Harvey, A. and Lonsdale, D.M. (2001) Introns and their positions affect the translational activity of mRNA in plant cells. *Embo Reports*, **2**, 394-398.

Bouvet, P., Diaz, J.J., Kindbeiter, K., Madjar, J.J. and Amalric, F. (1998) Nucleolin interacts with several ribosomal proteins through its RGG domain. *Journal of Biological Chemistry*, **273**, 19025-19029.

Branco-Price, C., Kawaguchi, R., Ferreira, R.B. and Bailey-Serres, J. (2005) Genome-wide analysis of transcript abundance and translation in Arabidopsis seedlings subjected to oxygen deprivation. *Annals of Botany*, **96**, 647-660.

Brandizzi, F., Frangne, N., Marc-Martin, S., Hawes, C., Neuhaus, J.M., et al. (2002a) The destination for single-pass membrane proteins is influenced markedly by the length of the hydrophobic domain. *Plant Cell*, **14**, 1077-1092.

Brandizzi, F., Fricker, M. and Hawes, C. (2002b) A greener world: the revolution in plant bioimaging. *Nature Reviews Molecular Cell Biology*, **3**, 520-530.

Brandizzi, F., Hanton, S., daSilva, L.L.P., Boevink, P., Evans, D., et al. (2003) ER quality control can lead to retrograde transport from the ER lumen to the cytosol and the nucleoplasm in plants. *Plant Journal*, **34**, 269-281.

Brandizzi, F., Snapp, E.L., Roberts, A.G., Lippincott-Schwartz, J. and Hawes, C. (2002c) Membrane protein transport between the endoplasmic reticulum and the golgi in tobacco leaves is energy dependent but cytoskeleton independent: Evidence from selective photobleaching. *Plant Cell*, **14**, 1293-1309.

Brodersen, D.E., Clemons, W.M., Carter, A.P., Wimberly, B.T. and Ramakrishnan, V. (2002) Crystal structure of the 30S ribosomal subunit from *Thermus thermophilus*: structure of the proteins and their interactions with 16 S RNA. *Journal of Molecular Biology*, **316**, 725-768.

Brodersen, D.E. and Nissen, P. (2005) The social life of ribosomal proteins. *FEBS Journal*, **272**, 2098-2108.

Brown, D.D. and Dawid, I.B. (1969) Developmental genetics. *Annual Review of Genetics*, **3**, 127-154.

Brown, J.W.S., Clark, G.P., Leader, D.J., Simpson, C.G. and Lowe, T. (2001) Multiple snoRNA gene clusters from Arabidopsis. *Rna-a Publication of the Rna Society*, **7**, 1817-1832.

Brown, J.W.S., Echeverria, M. and Qu, L.-H. (2003) Plant snoRNAs: functional evolution and new modes of gene expression. *Trends in Plant Science*, **8**, 42-49.

Brown, J.W.S., Shaw, P.J., Shawl, P. and Marshall, D.F. (2005) Arabidopsis nucleolar protein database (AtNoPDB). *Nucleic Acids Research*, **33**, D633-D636.

Buisson, M. and Reboud, A.M. (1982) Carbodiimide-induced protein RNA crosslinking in mammalian ribosomal-subunits. *Febs Letters*, **148**, 247-250.

Busch, M.A., Bomblies, K. and Weigel, D. (1999) Activation of a floral homeotic gene in Arabidopsis. *Science*, **285**, 585-587.

Campbell, R.E., Tour, O., Palmer, A.E., Steinbach, P.A., Baird, G.S., et al. (2002) A monomeric red fluorescent protein. *Proceedings of the National Academy of Sciences of the United States of America*, **99**, 7877-7882.

Campell, B.R., Song, Y.G., Posch, T.E., Cullis, C.A. and Town, C.D. (1992) Sequence and organization of 5S ribosomal RNA-encoding genes of *Arabidopsis thaliana*. *Gene*, **112**, 225-228.

Campisi, L., Yang, Y.Z., Yi, Y., Heilig, E., Herman, B., et al. (1999) Generation of enhancer trap lines in Arabidopsis and characterization of expression patterns in the inflorescence. *Plant Journal*, **17**, 699-707.

Cannon, S.B., Mitra, A., Baumgarten, A., Young, N.D. and May, G. (2004) The roles of segmental and tandem gene duplication in the evolution of large gene families in Arabidopsis thaliana. *BMC Plant Biology*, **4**.

Caparros-Ruiz, D., Lahmy, S., Piersanti, S. and Echeverria, M. (1997) Two ribosomal DNA-binding factors interact with a cluster of motifs on the 5' external transcribed spacer, upstream from the primary pre-rRNA processing site in a higher plant. *European Journal of Biochemistry*, **247**, 981-989.

Cardinali, B., Carissimi, C., Gravina, P. and Pierandrei-Amaldi, P. (2003) La protein is associated with terminal oligopyrimidine mRNAs in actively translating polysomes. *Journal of Biological Chemistry*, **278**, 35145-35151.

Carland, F.M. and McHale, N.A. (1996) *LOP1*: A gene involved in auxin transport and vascular patterning in Arabidopsis. *Development*, **122**, 1811-1819.

Carmo-Fonseca, M., Mendes-Soares, L. and Campos, I. (2000) To be or not to be in the nucleolus. *Nature Cell Biology*, **2**, 107-112.

Carroll, A.J., Heazlewood, J.L., Ito, J. and Millar, A.H. (2008) Analysis of the Arabidopsis cytosolic ribosome proteome provides detailed insights into its components and their post-translational modification. *Molecular Cellular Proteomics*, **7**, 347-369.

Carter, A.P., Clemons, W.M., Brodersen, D.E., Morgan-Warren, R.J., Wimberly, B.T., et al. (2000) Functional insights from the structure of the 30S ribosomal subunit and its interactions with antibiotics. *Nature*, **407**, 340-348.

Cate, J.H., Yusupov, M.M., Yusupova, G.Z., Earnest, T.N. and Noller, H.F. (1999) X-ray crystal structures of 70S ribosome functional complexes. *Science*, **285**, 2095-2104.

Causevic, M., Hislop, R.G., Kernohan, N.M., Carey, F.A., Kay, R.A., et al. (2001) Overexpression and poly-ubiquitylation of the DEAD-box RNA helicase p68 in colorectal tumours. *Oncogene*, **20**, 7734-7743.

Chandramouli, P., Topf, M., Ménétret, J.-F., Eswar, N., Cannone, J.J., et al. (2008) Structure of the mammalian 80S ribosome at 8.7 Å resolution. *Structure*, **16**, 535-548.

Chang, I.-F., Szick-Miranda, K., Pan, S. and Bailey-Serres, J. (2005) Proteomic characterization of evolutionarily conserved and variable proteins of Arabidopsis cytosolic ribosomes. *Plant Physiology*, **137**, 848-862.

Chatfield, S.P., Stirnberg, P., Forde, B.G. and Leyser, O. (2000) The hormonal regulation of axillary bud growth in Arabidopsis. *Plant Journal*, **24**, 159-169.

Chen, C.L., Liang, D., Zhou, H., Zhuo, M., Chen, Y.Q., et al. (2003) The high diversity of snoRNAs in plants: identification and comparative study of 120 snoRNA genes from *Oryza sativa*. *Nucleic Acids Research*, **31**, 2601-2613.

Chen, D.Y. and Huang, S. (2001) Nucleolar components involved in ribosome biogenesis cycle between the nucleolus and nucleoplasm in interphase cells. *Journal of Cell Biology*, **153**, 169-176.

Chen, J.-G., Ullah, H., Temple, B., Liang, J., Guo, J., et al. (2006) RACK1 mediates multiple hormone responsiveness and developmental processes in Arabidopsis. *Journal of Experimental Botany*, **57**, 2697-2708.

Chen, X.M., Liu, J., Cheng, Y.L. and Jia, D.X. (2002) HEN1 functions plelotropically in Arabidopsis development and acts in C function in the flower. *Development*, **129**, 1085-1094.

Cherepneva, G.N., Schmidt, K.H., Kulaeva, O.N., Oelmuller, R. and Kusnetsov, V.V. (2003) Expression of the ribosomal proteins S14, S16, L13a and L30 is regulated by cytokinin and abscisic acid - Implication of the involvement of phytohormones in translational processes. *Plant Science*, **165**, 925-932.

Cherry, S., Doukas, T., Armknecht, S., Whelan, S., Wang, H., et al. (2005) Genome-wide RNAi screen reveals a specific sensitivity of IRES-containing RNA viruses to host translation inhibition. *Genes and Development*, **19**, 445-452.

Childs, K.L., Hamilton, J.P., Zhu, W., Ly, E., Cheung, F., et al. (2007) The TIGR plant transcript assemblies database. *Nucleic Acids Research*, **35**, D846-D851.

Chung, B.Y.W., Simons, C., Firth, A.E., Brown, C.M. and Hellens, R.P. (2006) Effect of 5 ' UTR introns on gene expression in *Arabidopsis thaliana*. *BMC Genomics*, **7**.

Chung, S. and Perry, R.P. (1993) The importance of downstream delta-factor binding elements for the activity of the rpL32 promoter. *Nucleic Acids Research*, **21**, 3301-3308.

Cioce, M. and Lamond, A.I. (2005) Cajal bodies: A long history of discovery. *Annual Review of Cell and Developmental Biology*, **21**, 105-131.

Clancy, M. and Hannah, L.C. (2002) Splicing of the maize Sh1 first intron is essential for enhancement of gene expression, and a T-rich motif increases expression without affecting splicing. *Plant Physiology*, **130**, 918-929.

Clemons, W.M., Jr, May, J.L.C., Wimberly, B.T., McCutcheon, J.P., Capel, M.S., et al. (1999) Structure of a bacterial 30S ribosomal subunit at 5 Å resolution. *Nature*, **400**, 833-840.

Cline, M.G. (1991) Apical dominance. *Botanical Review*, **57**, 318-358.

Clough, R.C. and Vierstra, R.D. (1997) Phytochrome degradation. *Plant Cell and Environment*, **20**, 713-721.

Clough, S.J. and Bent, A.F. (1998) Floral dip: a simplified method for *Agrobacterium*-mediated transformation of *Arabidopsis thaliana*. *Plant Journal*, **16**, 735-743.

Cnops, G., Neyt, P., Raes, J., Petrarulo, M., Nelissen, H., et al. (2006) The *TORNADO1* and *TORNADO2* genes function in several patterning processes during early leaf development in *Arabidopsis thaliana*. *Plant Cell*, **18**, 852-866.

Cnops, G., Wang, X., Linstead, P., Van Montagu, M., Van Lijsebettens, M., et al. (2000) *TORNADO1* and *TORNADO2* are required for the specification of radial and circumferential pattern in the Arabidopsis root. *Development*, **127**, 3385-3394.

Cole, J.R. and Nomura, M. (1986) Translational regulation is responsible for growth rate-dependent and stringent control of the synthesis of ribosomal-proteins L11 and L1 in *Escherichia coli*. *Proceedings of the National Academy of Sciences of the United States of America*, **83**, 4129-4133.

Contento, A.L., Kim, S.J. and Bassham, D.C. (2004) Transcriptome profiling of the response of Arabidopsis suspension culture cells to suc starvation. *Plant Physiology*, **135**, 2330-2347.

Cook, D., Fowler, S., Fiehn, O. and Thomashow, M.F. (2004) A prominent role for the CBF cold response pathway in configuring the low-temperature metabolome of Arabidopsis. *Proceedings of the National Academy of Sciences of the United States of America*, **101**, 15243-15248.

Crawford, B.C.W., Nath, U., Carpenter, R. and Coen, E.S. (2004) *CINCINNATA* controls both cell differentiation and growth in petal lobes and leaves of antirrhinum. *Plant Physiology*, **135**, 244-253.

Crofts, A.J., Leborgne-Castel, N., Hillmer, S., Robinson, D.G., Phillipson, B., et al. (1999) Saturation of the endoplasmic reticulum retention machinery reveals anterograde bulk flow. *Plant Cell*, **11**, 2233-2247.

Crooks, G.E., Hon, G., Chandonia, J.M. and Brenner, S.E. (2004) WebLogo: A sequence logo generator. *Genome Research*, **14**, 1188-1190.

Curie, C., Liboz, T., Bardet, C., Gander, E., Medale, C., et al. (1991) *Cis* and t*rans*-acting elements involved in the activation of *Arabidopsis thaliana* A1 gene encoding the translation elongation factor Ef1α. *Nucleic Acids Research*, **19**, 1305-1310.

Dai, Z.Y., Gao, J.W. and An, G.H. (1995) Regulatory elements controlling developmental and environmental-regulation of a ribosomal-protein gene *L34* in tobacco. *Plant Physiology*, **108**, S27-S27.

Darbinian, N., Gallia, G.L. and Khalili, K. (2001) Helix-destabilizing properties of the human single-stranded DNA- and RNA-binding protein Pur alpha. *Journal of Cellular Biochemistry*, **80**, 589-595.

De Rijk, P., Caers, A., Van de Peer, Y. and De Wachter, R. (1998) Database on the structure of large ribosomal subunit RNA. *Nucleic Acids Research*, **26**, 183-186.

de Souza, D.P., Silva, S.S., Baptista, A.J., Nicola, A.M., Kyaw, C.M., et al. (2005) *Paracoccidioides brasiliensis* translation and protein fate machineries revealed by functional genome analysis. *Genetics and Molecular Research*, **4**, 273-289.

Degenhardt, R.F. and Bonham-Smith, P.C. (2008a) Arabidopsis ribosomal proteins RPL23aA and RPL23aB are differentially targeted to the nucleolus and are disparately required for normal development. *Plant Physiology*, **147**, 128-142.

Degenhardt, R.F. and Bonham-Smith, P.C. (2008b) Evolutionary divergence of ribosomal protein paralogs in Arabidopsis. *Plant Signaling & Behavior*, **3**, 493-495.

Degenhardt, R.F. and Bonham-Smith, P.C. (2008c) Transcript profiling demonstrates absence of dosage compensation in Arabidopsis following loss of a single *RPL23a* paralog. *Planta*, **DOI 10.1007/s00425-008-0765-6**.

del Pozo, J.C., Dharmasiri, S., Hellmann, H., Walker, L., Gray, W.M., et al. (2002) AXR1-ECR1-dependent conjugation of RUB1 to the Arabidopsis cullin AtCUL1 is required for auxin response. *Plant Cell*, **14**, 421-433.

Deprost, D., Yao, L., Sormani, R., Moreau, M., Leterreux, G., et al. (2007) The Arabidopsis TOR kinase links plant growth, yield, stress resistance and mRNA translation. *Embo Reports*, **8**, 864-870.

Desikan, R., Neill, S.J. and Hancock, J.T. (2000) Hydrogen peroxide-induced gene expression in *Arabidopsis thaliana*. *Free Radical Biology and Medicine*, **28**, 773-778.

Deyholos, M.K., Cavaness, G.F., Hall, B., King, E., Punwani, J., et al. (2003) VARICOSE, a WD-domain protein, is required for leaf blade development. *Development*, **130**, 6577-6588.

Deyholos, M.K. and Sieburth, L.E. (2000) Separable whorl-specific expression and negative regulation by enhancer elements within the *AGAMOUS* second intron. *Plant Cell*, **12**, 1799-1810.

Di Cola, A., Frigerio, L., Lord, J.M., Roberts, L.M. and Ceriotti, A. (2005) Endoplasmic reticulum-associated degradation of Ricin A chain has unique and plant-specific features. *Plant Physiology*, **137**, 287-296.

Diaconu, M., Kothe, U., Schlunzen, F., Fischer, N., Harms, J.M., et al. (2005) Structural basis for the function of the ribosomal L7/12 stalk in factor binding and GTPase activation. *Cell*, **121**, 991-1004.

Dingwall, C. and Laskey, R.A. (1991) Nuclear targeting sequences - a consensus. *Trends in Biochemical Sciences*, **16**, 478-481.

Ditt, R.F., Kerr, K.F., de Figueiredo, P., Delrow, J., Comai, L., et al. (2006) The *Arabidopsis thaliana* transcriptome in response to *Agrobacterium tumefaciens*. *Molecular Plant-Microbe Interactions*, **19**, 665-681.

Doelling, J., Gaudino, R. and Pikaard, C. (1993) Functional analysis of *Arabidopsis thaliana* rRNA gene and spacer promoters *in vivo* and by transient expression. *Proceedings of the National Academy of Sciences of the United States of America*, **90**, 7528-7532.

Doelling, J.H. and Pikaard, C.S. (1995) The minimal ribosomal-RNA gene promoter of *Arabidopsis thaliana* includes a critical element at the transcription initiation site. *Plant Journal*, **8**, 683-692.

Dover, G. (1982) Molecular drive: a cohesive mode of species evolution. **299**, 111-117.

Dragon, F., Gallagher, J.E.G., Compagnone-Post, P.A., Mitchell, B.M., Porwancher, K.A., et al. (2002) A large nucleolar U3 ribonucleoprotein required for 18S ribosomal RNA biogenesis. *Nature*, **417**, 967-970.

Dresselhaus, T., Cordts, S., Heuer, S., Sauter, M., Lörz, H., et al. (1999) Novel ribosomal genes from maize are differentially expressed in the zygotic and somatic cell cycles. *Molecular and General Genetics*, **261**, 416-427.

Driessen, H.P.C., Dejong, W.W., Tesser, G.I. and Bloemendal, H. (1985) The mechanism of N-terminal acetylation of proteins. *CRC Critical Reviews in Biochemistry*, **18**, 281-325.

Dundr, M. and Raska, I. (1993) Nonisotopic ultrastructural mapping of transcription sites within the nucleolus. *Experimental Cell Research*, **208**, 275-281.

Eckardt, N.A. (2005) MicroRNAs regulate auxin homeostasis and plant development. *Plant Cell*, **17**, 1335-1338.

Egebjerg, J., Leffers, H., Christensen, A., Andersen, H. and Garrett, R.A. (1987) Structure and accessibility of domain I of *Escherichia coli* 23 S RNA in free RNA, in the L24-RNA complex and in 50 S subunits: Implications for ribosomal assembly. *Journal of Molecular Biology*, **196**, 125-136.

El-Baradi, T., Vandersande, C., Mager, W.H., Raue, H.A. and Planta, R.J. (1986) The cellular-level of yeast ribosomal protein-L25 is controlled principally by rapid degradation of excess protein. *Current Genetics*, **10**, 733-739.

El-Baradi, T.T.A.L., de Regt, V.C.H.F., Planta, R.J., Nierhaus, K.H. and Raue, H.A. (1987) Interaction of ribosomal proteins L25 from yeast and EL23 from *E. coli* with yeast 26S and mouse 28S rRNA. *Biochimie*, **69**, 939-948.

El-Baradi, T.T.A.L., Raue, H.A., de Regt, V.C.H.F. and Planta, R.J. (1984) Stepwise dissociation of yeast 60S ribosomal subunits by LiCl and identification of L25 as a primary 26S rRNA binding protein. *European Journal of Biochemistry*, **144**, 393-400.

El-Baradi, T.T.A.L., Raue, H.A., de Regt, V.C.H.F., Verbree, E.C. and Planta, R.J. (1985) Yeast ribosomal protein L25 binds to an evolutionary conserved site on yeast 26S and *E. coli* 23S rRNA. *EMBO Journal*, **4**, 2101-2107.

Elkon, K.B., Skelly, S., Parnassa, A., Weissbach, H. and Brot, N. (1986) Structural and functional analysis of the ribosomal-P protein antigens. *Clinical Research*, **34**, A616-A616.

Eulalio, A., Rehwinkel, J., Stricker, M., Huntzinger, E., Yang, S.F., et al. (2007) Target-specific requirements for enhancers of decapping in miRNA-mediated gene silencing. *Genes & Development*, **21**, 2558-2570.

Ferbitz, L., Maier, T., Patzelt, H., Bukau, B., Deuerling, E., et al. (2004) Trigger factor in complex with the ribosome forms a molecular cradle for nascent proteins. *Nature*, **431**, 590-596.

Fernandez, P., Di Rienzo, J., Fernandez, L., Hopp, H.E., Paniego, N., et al. (2008) Transcriptomic identification of candidate genes involved in sunflower responses to chilling and salt stresses based on cDNA microarray analysis. *BMC Plant Biology*, **8**.

Fowler, S. and Thomashow, M.F. (2002) Arabidopsis transcriptome profiling indicates that multiple regulatory pathways are activated during cold acclimation in addition to the CBF cold response pathway. *Plant Cell*, **14**, 1675-1690.

Frank, J. and Agrawal, R.K. (2000) A ratchet-like inter-subunit reorganization of the ribosome during translocation. *Nature*, **406**, 318-322.

Fu, H.Y., Kim, S.Y. and Park, W.D. (1995) A potato *SUS3* sucrose synthase gene contains a context-dependent 3' element and a leader intron with both positive and negative tissue-specific effects. *Plant Cell*, **7**, 1395-1403.

Fu, Y.L., Xu, L., Xu, B., Yang, L., Ling, Q.H., et al. (2007) Genetic interactions between leaf polarity-controlling genes and *ASYMMETRIC LEAVES1* and *2* in Arabidopsis leaf patterning. *Plant and Cell Physiology*, **48**, 724-735.

Gabashvili, I.S., Agrawal, R.K., Spahn, C.M.T., Grassucci, R.A., Svergun, D.I., et al. (2000) Solution structure of the *E. coli* 70S ribosome at 11.5 angstrom resolution. *Cell*, **100**, 537-549.

Gantt, J.S. and Key, J.L. (1983) Auxin-induced changes in the level of translatable ribosomal protein messenger ribonucleic acids in soybean hypocotyl. *Biochemistry*, **22**, 4131-4139.

Gantt, J.S. and Key, J.L. (1985) Coordinate expression of ribosomal protein mRNAs following auxin treatment of soybean hypocotyls. *Journal of Biological Chemistry*, **260**, 6175-6181.

Gao, J., Kim, S.R., Chung, Y.Y., Lee, J.M. and An, G. (1994) Developmental and environmental regulation of two ribosomal protein genes in tobacco. *Plant Molecular Biology*, **25**, 761-770.

Garcia-Martinez, J., Gonzalez-Candelas, F. and Perez-Ortin, J.E. (2007) Common gene expression strategies revealed by genome-wide analysis in yeast. *Genome Biology*, **8**, R222.

Geyer, P.K., Meyuhas, O., Perry, R.P. and Johnson, L.F. (1982) Regulation of ribosomal-protein messenger-RNA content and translation in growth-stimulated mouse fibroblasts. *Molecular and Cellular Biology*, **2**, 685-693.

Giannino, D., Grugis, G., Ticconi, C., Florio, S., Mele, G., et al. (2000) Isolation and molecular characterization of the gene encoding the cytoplasmic ribosomal protein S28 in *Prunus persica* (L.) Batsch. *Molecular and General Genetics*, **263**, 201-212.

Giavalisco, P., Wilson, D., Kreitler, T., Lehrach, H., Klose, J., et al. (2005) High heterogeneity within the ribosomal proteins of the *Arabidopsis thaliana* 80S ribosome. *Plant Molecular Biology*, **57**, 577-591.

Gilmour, S.J., Zarka, D.G., Stockinger, E.J., Salazar, M.P., Houghton, J.M., et al. (1998) Low temperature regulation of the Arabidopsis CBF family of AP2 transcriptional activators as an early step in cold-induced COR gene expression. *Plant Journal*, **16**, 433-442.

Ginisty, H., Amalric, F. and Bouvet, P. (1998) Nucleolin functions in the first step of ribosomal RNA processing. *Embo Journal*, **17**, 1476-1486.

Ginisty, H., Sicard, H., Roger, B. and Bouvet, P. (1999) Structure and functions of nucleolin. *Journal of Cell Science*, **112**, 761-772.

Gomez-Lorenzo, M.G., Spahn, C.M.T., Agrawal, R.K., Grassucci, R.A., Penczek, P., et al. (2000) Three-dimensional cryo-electron microscopy localization of EF2 in the Saccharomyces cerevisiae 80S ribosome at 17.5 angstrom resolution. *Embo Journal*, **19**, 2710-2718.

González-Melendi, P., Wells, B., Beven, A.F. and Shaw, P.J. (2001) Single ribosomal transcription units are linear, compacted Christmas trees in plant nucleoli. *Plant Journal*, **27**, 223-233.

Goto, N., Katoh, N. and Kranz, A.R. (1991) Morphogenesis of floral organs in Arabidopsis - predominant carpel formation of the PIN-FORMED mutant. *Japanese Journal of Genetics*, **66**, 551-567.

Grace, M.L., Chandrasekharan, M.B., Hall, T.C. and Crowe, A.J. (2004) Sequence and spacing of TATA box elements are critical for accurate initiation from the β-Phaseolin promoter. *Journal of Biological Chemistry*, **279**, 8102-8110.

Grainger, R.M. and Maizels, N. (1980) *Dictyostelium* ribosomal RNA is processed during transcription. *Cell*, **20**, 619-623.

Granboulan, N. and Granboulan, P. (1965) Cytochimie ultrastructurale du nucleole: II. Etude des sites de synthese du RNA dans le nucleole et le noyau. *Experimental Cell Research*, **38**, 604-619.

Granneman, S. and Baserga, S.J. (2004) Ribosome biogenesis: of knobs and RNA processing. *Experimental Cell Research*, **296**, 43-50.

Gray, G.R., Hope, B.J., Qin, X.Q., Taylor, B.G. and Whitehead, C.L. (2003) The characterization of photoinhibition and recovery during cold acclimation in *Arabidopsis thaliana* using chlorophyll fluorescence imaging. *Physiologia Plantarum*, **119**, 365-375.

Gray, G.R., Savitch, L.V., Ivanov, A.C. and Huner, N.P.A. (1996) Photosystem II excitation pressure and development of resistance to photoinhibition. II. Adjustment of photosynthetic capacity in winter wheat and winter rye. *Plant Physiology*, **110**, 61-71.

Grebenok, R.J., Pierson, E., Lambert, G.M., Gong, F.C., Afonso, C.L., et al. (1997) Green-fluorescent protein fusions for efficient characterization of nuclear targeting. *Plant Journal*, **11**, 573-586.

Gritz, L., Abovich, N., Teem, J.L. and Rosbash, M. (1985) Posttranscriptional regulation and assembly into ribosomes of a *Saccharomyces cerevisiae* ribosomal protein-beta-galactosidase fusion. *Molecular and Cellular Biology*, **5**, 3436-3442.

Grummt, I. (1999) Regulation of mammalian ribosomal gene transcription by RNA polymerase I. *Progress in Nucleic Acid Research and Molecular Biology*, **62**, 109-154.

Gu, S.-Q., Peske, F., Wieden, H.-J., Rodnina, M.V. and Wintermeyer, W. (2003) The signal recognition particle binds to protein L23 at the peptide exit of the *Escherichia coli* ribosome. *RNA*, **9**, 566-573.

Guarinos, E., Santos, C., Sánchez, A., Qiu, D.-Y., Remacha, M., et al. (2003) Tag-mediated fractionation of yeast ribosome populations proves the monomeric organization of the eukaryotic ribosomal stalk structure. *Molecular Microbiology*, **50**, 703-712.

Gudkov, A.T., Khechinashvili, N.N. and Bushev, V.N. (1978) Studies on the structure of protein L7/L12 from *Escherichia coli* ribosomes. *European Journal of Biochemistry*, **90**, 313-318.

Guillier, M., Allemand, F., Raibaud, S., Dardel, F., Springer, M., et al. (2002) Translational feedback regulation of the gene for L35 in *Escherichia coli* requires binding of ribosomal protein L20 to two sites in its leader mRNA: a possible case of ribosomal RNA-messenger RNA molecular mimicry. *RNA*, **8**, 878-889.

Guo, H.S., Fei, J.F., Xie, Q. and Chua, N.H. (2003) A chemical-regulated inducible RNAi system in plants. *Plant Journal*, **34**, 383-392.

Gusmaroli, G., Tonelli, C. and Mantovani, R. (2001) Regulation of the CCAAT-binding NF-Y subunits in *Arabidopsis thaliana*. *Gene*, **264**, 173-185.

Gusmaroli, G., Tonelli, C. and Mantovani, R. (2002) Regulation of novel members of the *Arabidopsis thaliana* CCAAT-binding nuclear factor Y subunits. *Gene*, **283**, 41-48.

Gutierrez, R.A., MacIntosh, G.C. and Green, P.J. (1999) Current perspectives on mRNA stability in plants: multiple levels and mechanisms of control. *Trends in Plant Science*, **4**, 429-438.

Haasen, D., Kohler, C., Neuhaus, G. and Merkle, T. (1999) Nuclear export of proteins in plants: AtXPO1 is the export receptor for leucine-rich nuclear export signals in *Arabidopsis thaliana*. *Plant Journal*, **20**, 695-705.

Hadjiolov, A.A. (1985) *The Nucleolus and Ribosome Biogenesis*. New York, NY: Springer-Verlag.

Halic, M., Becker, T., Pool, M.R., Spahn, C.M.T., Grassucci, R.A., et al. (2004) Structure of the signal recognition particle interacting with the elongation-arrested ribosome. *Nature*, **427**, 808-814.

Hamilton, T.L., Stoneley, M. and Bushell, M. (2006) TOPs and their regulation. *Biochemical Society Transactions*, **34**, 12-16.

Handwerger, K.E. and Gall, J.G. (2006) Subnuclear organelles: new insights into form and function. *Trends in Cell Biology*, **16**, 19-26.

Hannan, K.M., Hannan, R.D. and Rothblum, L.I. (1998) Transcription by RNA polymerase I. *Frontiers in Bioscience*, **3**, 376-398.

Hanson, C.L., Videler, H., Santos, C., Ballesta, J.P.G. and Robinson, C.V. (2004) Mass spectrometry of ribosomes from *Saccharomyces cerevisiae* - Implications for assembly of the stalk complex. *Journal of Biological Chemistry*, **279**, 42750-42757.

Hardin, S.C. and Huber, S.C. (2004) Proteasome activity and the post-translational control of sucrose synthase stability in maize leaves. *Plant Physiology and Biochemistry*, **42**, 197-208.

Haseloff, J., Siemering, K.R., Prasher, D.C. and Hodge, S. (1997) Removal of a cryptic intron and subcellular localization of green fluorescent protein are required to mark transgenic Arabidopsis plants brightly. *Proceedings of the National Academy of Sciences of the United States of America*, **94**, 2122-2127.

Hedges, S.B. and Kumar, S. (2003) Genomic clocks and evolutionary timescales. *Trends in Genetics*, **19**, 200-206.

Held, W.A., Ballou, B., Mizushima, S. and Nomura, M. (1974) Assembly mapping of 30S ribosomal proteins from *Escherichia coli*. Further studies. *Journal of Biological Chemistry*, **249**, 3103-3111.

Helgstrand, M., Mandava, C.S., Mulder, F.A.A., Liljas, A., Sanyal, S., et al. (2007) The ribosomal stalk binds to translation factors IF2, EF-Tu, EF-G and RF3 via a conserved region of the L12 C-terminal domain. *Journal of Molecular Biology*, **365**, 468-479.

Hellens, R.P., Edwards, E.A., Leyland, N.R., Bean, S. and Mullineaux, P.M. (2000) pGreen: a versatile and flexible binary Ti vector for Agrobacterium-mediated plant transformation. *Plant Molecular Biology*, **42**, 819-832.

Hernandez-Verdun, D., Roussel, P. and Gebrane-Younes, J. (2002) Emerging concepts of nucleolar assembly. *Journal of Cell Science*, **115**, 2265-2270.

Higo, K., Ugawa, Y., Iwamoto, M. and Korenaga, T. (1999) Plant *cis*-acting regulatory DNA elements (PLACE) database: 1999. *Nucleic Acids Research*, **27**, 297-300.

Ho, L.H.M., Giraud, E., Lister, R., Thirkettle-Watts, D., Low, J., et al. (2007) Characterization of the regulatory and expression context of an alternative oxidase gene provides insights into cyanide-insensitive respiration during growth and development. *Plant Physiology*, **143**, 1519-1533.

Hoekema, A., Hirsch , P.R., Hooykaas, P.J.J. and Schilperoort, R.A. (1983) A binary plant vector strategy based on separation of *vir*- and T-region of the *Agrobacterium tumefaciens* Ti-plasmid. *Nature*, **303**, 179-180.

Hong, R.L., Hamaguchi, L., Busch, M.A. and Weigel, D. (2003) Regulatory elements of the floral homeotic gene *AGAMOUS* identified by phylogenetic footprinting and shadowing. *Plant Cell*, **15**, 1296-1309.

Hori, K. and Watanabe, Y. (2005) UPF3 suppresses aberrant spliced mRNA in Arabidopsis. *Plant Journal*, **43**, 530-540.

Horke, S., Reumann, K., Schweizer, M., Will, H. and Heise, T. (2004) Nuclear trafficking of La protein depends on a newly identified nucleolar localization signal and the ability to bind RNA. *Journal of Biological Chemistry*, **279**, 26563-26570.

Horvath, B.M., Magyar, Z., Zhang, Y.X., Hamburger, A.W., Bako, L., et al. (2006) EBP1 regulates organ size through cell growth and proliferation in plants. *Embo Journal*, **25**, 4909-4920.

Hoth, S., Morgante, M., Sanchez, J.P., Hanafey, M.K., Tingey, S.V., et al. (2002) Genome-wide gene expression profiling in *Arabidopsis thaliana* reveals new targets of abscisic acid and largely impaired gene regulation in the *abi1-1* mutant. *Journal of Cell Science*, **115**, 4891-4900.

Huang, S. (2002) Building an efficient factory: where is pre-rRNA synthesized in the nucleolus? *Journal of Cell Biology*, **157**, 739-741.

Huang, Z.P., Zhou, H., Liang, D. and Qu, L.H. (2004) Different expression strategy: Multiple intronic gene clusters of box H/ACA snoRNA in *Drosophila melanogaster*. *Journal of Molecular Biology*, **341**, 669-683.

Hulm, J.L., McIntosh, K.B. and Bonham-Smith, P.C. (2005) Variation in transcript abundance among the four members of the *Arabidopsis thaliana* ribosomal protein *S15a* gene family. *Plant Science*, **169**, 267-278.

Humphrey, E.L., Shamji, A.F., Bernstein, B.E. and Schreiber, S.L. (2004) Rpd3p relocation mediates a transcriptional response to rapamycin in yeast. *Chemistry & Biology*, **11**, 295-299.

Huner, N.P.A., Oquist, G., Hurry, V.M., Krol, M., Falk, S., et al. (1993) Photosynthesis, photoinhibition and low-temperature acclimation in cold tolerant plants. *Photosynthesis Research*, **37**, 19-39.

Huner, N.P.A., Oquist, G. and Sarhan, F. (1998) Energy balance and acclimation to light and cold. *Trends in Plant Science*, **3**, 224-230.

Hurt, E., Hannus, S., Schmelzl, B., Lau, D., Tollervey, D., et al. (1999) A novel in vivo assay reveals inhibition of ribosomal nuclear export in Ran-cycle and nucleoporin mutants. *Journal of Cell Biology*, **144**, 389-401.

Hwang, Y.S., Karrer, E.E., Thomas, B.R., Chen, L. and Rodriguez, R.L. (1998) Three cis-elements required for rice alpha-amylase Amy3D expression during sugar starvation. *Plant Molecular Biology*, **36**, 331-341.

Intine, R.V., Dundr, M., Vassilev, A., Schwartz, E., Zhao, Y., et al. (2004) Nonphosphorylated human La antigen interacts with nucleolin at nucleolar sites involved in rRNA biogenesis. *Molecular and Cellular Biology*, **24**, 10894-10904.

Ito, T., Kim, G.T. and Shinozaki, K. (2000) Disruption of an *Arabidopsis* cytoplasmic ribosomal protein S13-homologous gene by transposon-mediated mutagenesis causes aberrant growth and development. *Plant Journal*, **22**, 257-264.

Ivanov, A.V., Malygin, A.A. and Karpova, G.G. (2006) Eukaryotic ribosomal proteins: Interaction with their own pre-mRNAs and involvement in regulation of their splicing. *Molecular Biology*, **40**, 640-649.

Ivens, A.C., Peacock, C.S., Worthey, E.A., Murphy, L., Aggarwal, G., et al. (2005) The genome of the kinetoplastid parasite, *Leishmania major*. *Science*, **309**, 436-442.

Jacob, S.T. (1995) Regulation of ribsomal gene transcription. *Biochemical Journal*, **306**, 617-626.

Jacobsen, S.E., Running, M.P. and Meyerowitz, E.M. (1999) Disruption of an RNA helicase/RNAse III gene in Arabidopsis causes unregulated cell division in floral meristems. *Development*, **126**, 5231-5243.

Jakel, S. and Gorlich, D. (1998) Importin beta , transportin, RanBP5 and RanBP7 mediate nuclear import of ribosomal proteins in mammalian cells. *Embo Journal*, **17**, 4491-4502.

Janaki, C. and Joshi, R.R. (2004) Motif detection in Arabidopsis: Correlation with gene expression data. *In Silico Biology*, **4**, 149-161.

Jeeninga, R.E., Venema, J. and Raue, H.A. (1996) Rat RL23a ribosomal protein efficiently competes with its *Saccharomyces cerevisiae* L25 homologue for assembly into 60 S subunits. *Journal of Molecular Biology*, **263**, 648-656.

Jeong, Y.M., Mun, J.H., Kim, H., Lee, S.Y. and Kim, S.G. (2007) An upstream region in the first intron of petunia actin-depolymerizing factor 1 affects tissue-specific expression in transgenic Arabidopsis (*Arabidopsis thaliana*). *Plant Journal*, **50**, 230-239.

Ji, G.L., Zheng, J.T., Shen, Y.J., Wu, X.H., Jiang, R.H., et al. (2007) Predictive modeling of plant messenger RNA polyadenylation sites. *Bmc Bioinformatics*, **8**, 10.1186/1471-2105-1188-1143.

Jin, Y., Jin, H., Zhou, P. and Bian, T. (2005) Analysis of plant mRNA upstream open reading frames. *Chinese Journal of Agricultural Biotechnology*, **2**, 59-66.

Jordan, E.G. and McGovern, J.H. (1981) The quantitative relationship of the fibrillar centers and other nucleolar components to changes in growth conditions, serum deprivation and low-doses of actinomycin-D in cultured diploid human fibroblasts (strain Mrc-5). *Journal of Cell Science*, **52**, 373-389.

Joyce, G.F. and Orgel, L.E. (1993) Prospects for understanding the origin of the RNA world. In *The RNA World* (Gesteland, R.F. and Atikins, J.F., eds). Cold Spring Harbor, NY: Cold Spring Harbor Laboratory Prss, pp. 1-25.

Jung, S.H., Lee, J.Y. and Lee, D.H. (2003) Use of SAGE technology to reveal changes in gene expression in Arabidopsis leaves undergoing cold stress. *Plant Molecular Biology*, **52**, 553-567.

Kaeberlein, M., Burtner, C.R. and Kennedy, B.K. (2007) Recent developments in yeast aging. *Plos Genetics*, **3**, 655-660.

Kakegawa, T., Ohuchi, N., Hayakawa, A., Hirata, S., Matsuda, M., et al. (2007) Identification of AUF1 as a rapamycin-responsive binding protein to the 5'-terminal oligopyrimidine element of mRNAs. *Archives of Biochemistry and Biophysics*, **465**, 274-281.

Kalderon, D., Roberts, B.L., Richardson, W.D. and Smith, A.E. (1984) A short amino-acid sequence able to specify nuclear location. *Cell*, **39**, 499-509.

Kamath, R.S., Fraser, A.G., Dong, Y., Poulin, G., Durbin, R., et al. (2003) Systematic functional analysis of the *Caenorhabditis elegans* genome using RNAi. *Nature*, **421**, 231-237.

Kavran, J.M. and Steitz, T.A. (2007) Structure of the base of the L7/L12 stalk of the *Haloarcula marismortui* large ribosomal subunit: Analysis of L11 movements. *Journal of Molecular Biology*, **371**, 1047-1059.

Kawaguchi, R. and Bailey-Serres, J. (2005) mRNA sequence features that contribute to translational regulation in Arabidopsis. *Nucleic Acids Research*, **33**, 955-965.

Kawaguchi, R., Girke, T., Bray, E.A. and Bailey-Serres, J. (2004) Differential mRNA translation contributes to gene regulation under non-stress and dehydration stress conditions in *Arabidopsis thaliana*. *Plant Journal*, **38**, 823-839.

Kawaguchi, R., Williams, A.J., Bray, E.A. and Bailey-Serres, J. (2003) Water-deficit-induced translational control in Nicotiana tabacum. *Plant Cell and Environment*, **26**, 221-229.

Kenward, M.G. and Roger, J.H. (1997) Small sample inference for fixed effects from restricted maximum likelihood. *Biometrics*, **53**, 983-997.

Kertesz, S., Kerenyi, Z., Merai, Z., Bartos, I., Palfy, T., et al. (2006) Both introns and long 3 '-UTRs operate as cis-acting elements to trigger nonsense-mediated decay in plants. *Nucleic Acids Research*, **34**, 6147-6157.

Kiba, T., Naitou, T., Koizumi, N., Yamashino, T., Sakakibara, H., et al. (2005) Combinatorial microarray analysis revealing Arabidopsis genes implicated in cytokinin responses through the His->Asp phosphorelay circuitry. *Plant and Cell Physiology*, **46**, 339-355.

Kim, C.H. and Warner, J.R. (1983) Messenger-RNA for ribosomal-proteins in yeast. *Journal of Molecular Biology*, **165**, 79-89.

Kim, J. (2007) Perception, transduction, and networks in cold signaling. *Journal of Plant Biology*, **50**, 139-147.

Kim, K.Y., Park, S.W., Chung, Y.S., Chung, C.H., Kim, J.I., et al. (2004) Molecular cloning of low-temperature-inducible ribosomal proteins from soybean. *Journal of Experimental Botany*, **55**, 1153-1155.

Kim, S.H., Ryabov, E.V., Kalinina, N.O., Rakitina, D.V., Gillespie, T., et al. (2007) Cajal bodies and the nucleolus are required for a plant virus systemic infection. *Embo Journal*, **26**, 2169-2179.

Kimura, M., Yamamoto, Y.Y., Seki, M., Sakurai, T., Sato, M., et al. (2003) Identification of Arabidopsis genes regulated by high light-stress using cDNA microarray. *Photochemistry and Photobiology*, **77**, 226-233.

Kishi, F., Yoshida, T. and Aiso, S. (1996) Location of NRAMP1 molecule on the plasma membrane and its association with microtubules. *Molecular Immunology*, **33**, 1241-1246.

Kiss, T. (2001) Small nucleolar RNA-guided post-transcriptional modification of cellular RNAs. *Embo Journal*, **20**, 3617-3622.

Klein, D.J., Moore, P.B. and Steitz, T.A. (2004) The roles of ribosomal proteins in the structure assembly, and evolution of the large ribosomal subunit. *Journal of Molecular Biology*, **340**, 141-177.

Klein, H.L. and Petes, T.D. (1981) Intrachromosomal gene conversion in yeast. **289**, 144-148.

Klok, E.J., Wilson, I.W., Wilson, D., Chapman, S.C., Ewing, R.M., et al. (2002) Expression profile analysis of the low-oxygen response in Arabidopsis root cultures. *Plant Cell*, **14**, 2481-2494.

Kobayashi, T., Heck, D.J., Nomura, M. and Horiuchi, T. (1998) Expansion and contraction of ribosomal DNA repeats in *Saccharomyces cerevisiae*: requirement of replication fork blocking (Fob1) protein and the role of RNA polymerase I. *Genes and Development*, **12**, 3821-3830.

Kodama, Y., Nagaya, S., Shinmyo, A. and Kato, K. (2007) Mapping and characterization of DNase I hypersensitive sites in Arabidopsis chromatin. *Plant and Cell Physiology*, **48**, 459-470.

Kohrer, C., Mayer, C., Neumair, O., Grobner, P. and Piendl, W. (1998) Interaction of ribosomal L1 proteins from mesophilic and thermophilic Archaea and Bacteria with specific L1-binding sites on 23S rRNA and mRNA. *European Journal of Biochemistry*, **256**, 97-105.

Kojima, H., Suzuki, T., Kato, T., Enomoto, K., Sato, S., et al. (2007) Sugar-inducible expression of the *nucleolin-1* gene of *Arabidopsis thaliana* and its role in ribosome synthesis, growth and development. *Plant Journal*, **49**, 1053-1063.

Komili, S., Famy, N.G., Roth, F.P. and Silver, P.A. (2007) Functional specificity among ribosomal proteins regulates gene expression. *Cell*, **131**, 557-571.

Kooi, E.A., Rutgers, C.A., Kleijmeer, M.J., Vantriet, J., Venema, J., et al. (1994) Mutational analysis of the C-terminal region of *Saccharomyces cerevisiae* ribosomal protein-L25 *in-vitro* and *in-vivo* demonstrates the presence of 2 distinct functional elements. *Journal of Molecular Biology*, **240**, 243-255.

Kopito, R.R. and Sitia, R. (2000) Aggresomes and Russell bodies - Symptoms of cellular indigestion? *Embo Reports*, **1**, 225-231.

Koroleva, O.A., Tomlinson, M.L., Leader, D., Shaw, P. and Doonan, J.H. (2005) High-throughput protein localization in Arabidopsis using *Agrobacterium*-mediated transient expression of GFP-ORF fusions. *Plant Journal*, **41**, 162-174.

Kosugi, S. and Ohashi, Y. (1997) PCF1 and PCF2 specifically bind to *cis* elements in the rice proliferating cell nuclear antigen gene. *Plant Cell*, **9**, 1607-1619.

Kosugi, S. and Ohashi, Y. (2002) DNA binding and dimerization specificity and potential targets for the TCP protein family. *Plant Journal*, **30**, 337-348.

Kozak, M. (1999) Initiation of translation in prokaryotes and eukaryotes. *Gene*, **234**, 187-208.

Kramer, G., Rauch, T., Rist, W., Vorderwulbecke, S., Patzelt, H., et al. (2002) L23 protein functions as a chaperone docking site on the ribosome. *Nature*, **419**, 171-174.

Krieg, J., Hofsteenge, J. and Thomas, G. (1988) Identification of the 40S ribosomal protein S6 phosphorylation sites induced by cycloheximide. *Journal of Biological Chemistry*, **263**, 11473-11477.

Kultz, D. (2005) Molecular and evolutionary basis of the cellular stress response. *Annual Review of Physiology*, **67**, 225-257.

Kundu-Michalik, S., Bisotti, M.-A., Lipsius, E., Bauche, A., Kruppa, A., et al. (2008) Nucleolar binding sequences of the ribosomal protein S6e family reside in evolutionary highly conserved peptide clusters. *Molecular Biology and Evolution*, **25**, 580-590.

Labarga, A., Valentin, F., Anderson, M. and Lopez, R. (2007) Web services at the European bioinformatics institute. *Nucleic Acids Research*, **35**, W6-W11.

Lackner, D.H., Beilharz, T.H., Marguerat, S., Mata, J., Watt, S., et al. (2007) A network of multiple regulatory layers shapes gene expression in fission yeast. *Molecular Cell*, **26**, 145-155.

Laemmli, U.K. (1970) Cleavage of structural proteins during assembly of head of bacteriophage-T4. *Nature*, **227**, 680-685.

Lai, M.D. and Xu, J. (2007) Ribosomal proteins and colorectal cancer. *Current Genomics*, **8**, 43-49.

Lam, Y.W., Lamond, A.I., Mann, M. and Andersen, J.S. (2007) Analysis of nucleolar protein dynamics reveals the nuclear degradation of ribosomal proteins. *Current Biology*, **17**, 749-760.

Larkin, M.A., Blackshields, G., Brown, N.P., Chenna, R., McGettigan, P.A., et al. (2007) Clustal W and Clustal X version 2.0. *Bioinformatics*, **23**, 2947-2948.

Lascaris, R.F., deGroot, E., Hoen, P.B., Mager, W.H. and Planta, R.J. (2000) Different roles for Abf1p and a T-rich promoter element in nucleosome organization of the yeast *RPS28A* gene. *Nucleic Acids Research*, **28**, 1390-1396.

Lawrence, S.D., Dervinis, C., Novak, N. and Davis, J.M. (2006) Wound and insect herbivory responsive genes in poplar. *Biotechnology Letters*, **28**, 1493-1501.

Le Gourrierec, J., Li, Y.F. and Zhou, D.X. (1999) Transcriptional activation by Arabidopsis GT-1 may be through interaction with TFIIA-TBP-TATA complex. *Plant Journal*, **18**, 663-668.

Le Hir, H., Nott, A. and Moore, M.J. (2003) How introns influence and enhance eukaryotic gene expression. *Trends in Biochemical Sciences*, **28**, 215-220.

Lecompte, O., Ripp, R., Thierry, J.-C., Moras, D. and Poch, O. (2002) Comparative analysis of ribosomal proteins in complete genomes: an example of reductive evolution at the domain scale. *Nucleic Acids Research*, **30**, 5382-5390.

Lee, C.-H., Chang, S.C., Chen, C.-J. and Chang, M.-F. (1998) The nucleolin binding activity of hepatitis delta antigen is associated with nucleolus targeting. *Journal of Biological Chemistry*, **273**, 7650-7656.

Lee, S.-W., Berger, S.J., Martinoviæ, S., Pasa-Toliæ, L., Anderson, G.A., et al. (2002a) Direct mass spectrometric analysis of intact proteins of the yeast large ribosomal subunit using capillary LC/FTICR. *Proceedings of the National Academy of Sciences of the United States of America*, **99**, 5942-5947.

Lee, T.I., Rinaldi, N.J., Robert, F., Odom, D.T., Bar-Joseph, Z., et al. (2002b) Transcriptional regulatory networks in *Saccharomyces cerevisiae*. *Science*, **298**, 799-804.

Lee, Y., Tsai, J., Sunkara, S., Karamycheva, S., Pertea, G., et al. (2005) The TIGR Gene Indices: clustering and assembling EST and known genes and integration with eukaryotic genomes. *Nucleic Acids Research*, **33**, D71-D74.

Leffers, H., Egebjerg, J., Andersen, A., Christensen, T. and Garrett, R.A. (1988) Domain VI of *Escherichia coli* 23 S ribosomal RNA: Structure, assembly and function. *Journal of Molecular Biology*, **204**, 507-522.

Li, B., Nierras, C.R. and Warner, J.R. (1999) Transcriptional elements involved in the repression of ribosomal protein synthesis. *Molecular and Cellular Biology*, **19**, 5393-5404.

Li, C.X., Potuschak, T., Colon-Carmona, A., Gutierrez, R.A. and Doerner, P. (2005a) Arabidopsis TCP20 links regulation of growth and cell division control pathways. *Proceedings of the National Academy of Sciences of the United States of America*, **102**, 12978-12983.

Li, H., Xu, L., Wang, H., Yuan, Z., Cao, X.F., et al. (2005b) The putative RNA-dependent RNA polymerase RDR6 acts synergistically with ASYMMETRIC LEAVES1 and 2 to repress *BREVIPEDICELLUS* and *MicroRNA165/166* in Arabidopsis leaf development. *Plant Cell*, **17**, 2157-2171.

Li, Y., Lee, K.K., Walsh, S., Smith, C., Hadingham, S., et al. (2006) Establishing glucose- and ABA-regulated transcription networks in Arabidopsis by microarray analysis and promoter classification using a Relevance Vector Machine. *Genome Research*, **16**, 414-427.

Lieb, J.D., Liu, X.L., Botstein, D. and Brown, P.O. (2001) Promoter-specific binding of Rap1 revealed by genome-wide maps of protein-DNA association. *Nature Genetics*, **28**, 327-334.

Lin, C.T. and Thomashow, M.F. (1992) DNA-sequence analysis of a complementary-DNA for cold-regulated Arabidopsis gene *COR15* and characterization of the COR15 polypeptide. *Plant Physiology*, **99**, 519-525.

Lincoln, C., Britton, J.H. and Estelle, M. (1990) Growth and development of the *axr1* mutants of Arabidopsis. *Plant Cell*, **2**, 1071-1080.

Liu, F.L., VanToai, T., Moy, L.P., Bock, G., Linford, L.D., et al. (2005) Global transcription profiling reveals comprehensive insights into hypoxic response in Arabidopsis. *Plant Physiology*, **137**, 1115-1129.

Livak, K.J. and Schmittgen, T.D. (2001) Analysis of relative gene expression data using real-time quantitative PCR and the 2(T)(-Delta Delta C) method. *Methods*, **25**, 402-408.

Lodmell, J.S. and Dahlberg, A.E. (1997) A conformational switch in *Escherichia coli* 16S ribosomal RNA during decoding of messenger RNA. *Science*, **277**, 1262-1267.

Lohmann, J.U., Hong, R.L., Hobe, M., Busch, M.A., Parcy, F., et al. (2001) A molecular link between stem cell regulation and floral patterning in Arabidopsis. *Cell*, **105**, 793-803.

Loke, J.C., Stahlberg, E.A., Strenski, D.G., Haas, B.J., Wood, P.C., et al. (2005) Compilation of mRNA polyadenylation signals in Arabidopsis revealed a new signal element and potential secondary structures. *Plant Physiology*, **138**, 1457-1468.

Long, E.O. and Dawid, I.B. (1980) Repeated genes in eukaryotes. *Annual Review of Biochemistry*, **49**, 727-764.

Louie, D.F., Resing, K.A., Lewis, T.S. and Ahn, N.G. (1996) Mass spectrometric analysis of 40 S ribosomal proteins from rat-1 fibroblasts. *Journal of Biological Chemistry*, **271**, 28189-28198.

Lu, C. and Fedoroff, N. (2000) A mutation in the Arabidopsis *HYL1* gene encoding a dsRNA binding protein affects responses to abscisic acid, auxin, and cytokinin. *Plant Cell*, **12**, 2351-2366.

Maere, S., De Bodt, S., Raes, J., Casneuf, T., Van Montagu, M., et al. (2005) Modeling gene and genome duplications in eukaryotes. *Proceedings of the National Academy of Sciences of the United States of America*, **102**, 5454-5459.

Mager, W.H. (1988) Control of ribosomal protein gene expression. *Biochimica Et Biophysica Acta*, **949**, 1-15.

Maier, T., Ferbitz, L., Deuerling, E. and Ban, N. (2005) A cradle for new proteins: trigger factor at the ribosome. *Current Opinion in Structural Biology*, **15**, 204-212.

Major, I.T. and Constabel, C.P. (2006) Molecular analysis of poplar defense against herbivory: comparison of wound- and insect elicitor-induced gene expression. *New Phytologist*, **172**, 617-635.

Makarova, K.S., Ponomarev, V.A. and Koonin, E.V. (2001) Two C or not two C: recurrent disruption of Zn-ribbons, gene duplication, lineage-specific gene loss, and horizontal gene transfer in evolution of bacterial ribosomal proteins. *Genome Biology*, **2**, 0033.0031-0033.0014.

Makimoto, Y., Yano, H., Kaneta, T., Sato, Y. and Sato, S. (2006) Molecular cloning and gene expression of a fibrillarin homolog of tobacco BY-2 cells. *Protoplasma*, **229**, 53-62.

Mallory, A.C., Bartel, D.P. and Bartel, B. (2005) MicroRNA-directed regulation of Arabidopsis *AUXIN RESPONSE FACTOR17* is essential for proper development and modulates expression of early auxin response genes. *Plant Cell*, **17**, 1360-1375.

Mallory, A.C. and Vaucheret, H. (2006a) Functions of microRNAs and related small RNAs in plants. *Nature Genetics*, **38**, 850-850.

Mallory, A.C. and Vaucheret, H. (2006b) Functions of microRNAs and related small RNAs in plants. *Nature Genetics*, **38**, S31-S36.

Mandiyan, V., Tumminia, S.J., Wall, J.S., Hainfeld, J.F. and Boublik, M. (1991) Assembly of the *Escherichia coli* 30s ribosomal-subunit reveals protein-dependent folding of the 16S

ribosomal-RNA domains. *Proceedings of the National Academy of Sciences of the United States of America*, **88**, 8174-8178.

Manevski, A., Bardet, C., Tremousaygue, D. and Lescure, B. (1999) Characterization and properties of heteromeric plant protein complexes that interact with *tef cis*-acting elements in both RNA polymerase II-dependent promoters and rDNA spacer sequences. *Molecular and General Genetics*, **261**, 892-900.

Manevski, A., Bertoni, G., Bardet, C., Tremousaygue, D. and Lescure, B. (2000) In synergy with various *cis*-acting elements, plant insterstitial telomere motifs regulate gene expression in Arabidopsis root meristems. *Febs Letters*, **483**, 43-46.

Mankin, S.L. and Thompson, W.F. (2001) New green fluorescent protein genes for plant transformation: Intron-containing, ER-localized, and soluble-modified. *Plant Molecular Biology Reporter*, **19**, 13-26.

Manuell, A.L., Yamaguchi, K., Haynes, P.A., Milligan, R.A. and Mayfield, S.P. (2005) Composition and structure of the 80 S ribosome from the green alga *Chlamydomonas reinhardtii*: 80 S ribosomes are conserved in plants and animals. *Journal of Molecular Biology*, **351**, 266-279.

Maor, R., Jones, A., Nuhse, T.S., Studholme, D.J., Peck, S.C., et al. (2007) Multidimensional protein identification technology (MudPIT) analysis of ubiquitinated proteins in plants. *Molecular & Cellular Proteomics*, **6**, 601-610.

Markham, N.R. and Zuker, M. (2005) DINAMelt web server for nucleic acid melting prediction. *Nucleic Acids Research*, **33**, W577-W581.

Martin, D.E., Soulard, A. and Hall, M.N. (2004) TOR regulates ribosomal protein gene expression via PKA and the forkhead transcription factor FHL1. *Cell*, **119**, 969-979.

Marygold, S.J., Coelho, C.M.A. and Leevers, S.J. (2005) Genetic analysis of RpL38 and RpL5, two minute genes located in the centric heterochromatin of chromosome 2 of *Drosophila melanogaster*. *Genetics*, **169**, 683-695.

Marygold, S.J., Roote, J., Reuter, G., Lambertsson, A., Ashburner, M., et al. (2007) The ribosomal protein genes and Minute loci of *Drosophila melanogaster*. *Genome Biology*, **8**, R216.

Matsumoto, M., Hatakeyama, S., Oyamada, K., Oda, Y., Nishimura, T., et al. (2005a) Large-scale analysis of the human ubiquitin-related proteome. *Proteomics*, **5**, 4145-4151.

Matsumoto, T., Wu, J.Z., Kanamori, H., Katayose, Y., Fujisawa, M., et al. (2005b) The map-based sequence of the rice genome. *Nature*, **436**, 793-800.

Mattsson, J., Ckurshumova, W. and Berleth, T. (2003) Auxin signaling in Arabidopsis leaf vascular development. *Plant Physiology*, **131**, 1327-1339.

Mattsson, J., Sung, Z.R. and Berleth, T. (1999) Responses of plant vascular systems to auxin transport inhibition. *Development*, **126**, 2979-2991.

Mauro, V.P. and Edelman, G.M. (2002) The ribosome filter hypothesis. *Proceedings of the National Academy of Sciences of the United States of America*, **99**, 12031-12036.

Maxwell, E.S. and Fournier, M.J. (1995) The small nucleolar RNAs. *Annual Review of Biochemistry*, **35**, 897-934.

Mayer, C. and Grummt, I. (2006) Ribosome biogenesis and cell growth: mTOR coordinates transcription by all three classes of nuclear RNA polymerases. *Oncogene*, **25**, 6384-6391.

McIntosh, K.B. (2005) Characterization of the two genes encoding cytoplasmic ribosomal protein L23a in *Arabidopsis thaliana*. In *Department of Biology*. Saskatoon, SK: University of Saskatchewan, p. 400.

McIntosh, K.B. and Bonham-Smith, P.C. (2001) Establishment of *Arabidopsis thaliana* ribosomal protein RPL23A-1 as a functional homologue of *Saccharomyces cerevisiae* ribosomal protein L25. *Plant Molecular Biology*, **46**, 673-682.

McIntosh, K.B. and Bonham-Smith, P.C. (2005) The two ribosomal protein *L23A* genes are differentially transcribed in *Arabidopsis thaliana*. *Genome*, **48**, 443-454.

McIntosh, K.B. and Bonham-Smith, P.C. (2006) Ribosomal protein gene regulation: what about plants? *Canadian Journal of Botany*, **84**, 342-362.

Meinhart, A., Kamenski, T., Hoeppner, S., Baumli, S. and Cramer, P. (2005) A structural perspective of CTD function. *Genes & Development*, **19**, 1401-1415.

Menand, B., Desnos, T., Nussaume, L., Berger, F., Bouchez, D., et al. (2002) Expression and disruption of the Arabidopsis *TOR* (target of rapamycin) gene. *Proceedings of the National Academy of Sciences of the United States of America*, **99**, 6422-6427.

Menetret, J.F., Hegde, R.S., Heinrich, S.U., Chandramouli, P., Ludtke, S.J., et al. (2005) Architecture of the ribosome-channel complex derived from native membranes. *Journal of Molecular Biology*, **348**, 445-457.

Merchant, S.S., Prochnik, S.E., Vallon, O., Harris, E.H., Karpowicz, S.J., et al. (2007) The Chlamydomonas genome reveals the evolution of key animal and plant functions. *Science*, **318**, 245-251.

Merkle, T. (2003) Nucleo-cytoplasmic partitioning of proteins in plants: implications for the regulation of environmental and developmental signalling. *Current Genetics*, **44**, 231-260.

Merryman, C., Moazed, D., McWhirter, J. and Noller, H.F. (1999) Nucleotides in 16S rRNA protected by the association of 30S and 50S ribosomal subunits. *Journal of Molecular Biology*, **285**, 97-105.

Meyuhas, O. (2000) Synthesis of the translational apparatus is regulated at the translational level. *European Journal of Biochemistry*, **267**, 6321-6330.

Meyuhas, O. and Klein, A. (1990) The mouse ribosomal protein-L7 gene - Its primary structure and functional-analysis of the promoter region. *Journal of Biological Chemistry*, **265**, 11465-11473.

Miller, O.L. and Beatty, B.R. (1969) Visualization of nucleolar genes. *Science*, **164**, 955-957.

Misteli, T. (2005) Going in GTP cycles in the nucleolus. *Journal of Cell Biology*, **168**, 177-178.

Mitra, K., Schaffitzel, C., Shaikh, T., Tama, F., Jenni, S., et al. (2005) Structure of the *E. coli* protein-conducting channel bound to a translating ribosome. *Nature*, **438**, 318-324.

Moazed, D. and Noller, H.F. (1990) Binding of tRNA to the ribosomal A and P sites protects two distinct sets of nucleotides in 16S rRNA. *Journal of Molecular Biology*, **211**, 135-145.

Mohanty, B., Krishnan, S.P.T., Swarup, S. and Bajic, V.B. (2005) Detection and preliminary analysis of motifs in promoters of anaerobically induced genes of different plant species. *Annals of Botany*, **96**, 669-681.

Molina, C. and Grotewold, E. (2005) Genome wide analysis of Arabidopsis core promoters. *BMC Genomics*, **6**, 1471-2164/1476/1425.

Mongelard, F. and Bouvet, P. (2007) Nucleolin: a multiFACeTed protein. *Trends in Cell Biology*, **17**, 80-86.

Moon, J., Parry, G. and Estelle, M. (2004) The Ubiquitin-Proteasome Pathway and Plant Development. *Plant Cell*, **16**, 3181-3195.

Moore, P.B. and Steitz, T.A. (2002) The involvement of RNA in ribosome function. *Nature*, **418**, 229-235.

Moore, P.B. and Steitz, T.A. (2003) The structural basis of large ribosomal subunit function. *Annual Review of Biochemistry*, **72**, 813-850.

Morgan, D.G., Menetret, J.F., Neuhof, A., Rapoport, T.A. and Akey, C.W. (2002) Structure of the mammalian ribosome-channel complex at 17 angstrom resolution. *Journal of Molecular Biology*, **324**, 871-886.

Mougey, E.B., Pape, L.K. and Sollnerwebb, B. (1993) A U3 small nuclear ribonucleoprotein-requiring processing event in the 5' external transcribed spacer of *Xenopus* precursor ribosomal-RNA. *Molecular and Cellular Biology*, **13**, 5990-5998.

Nakashima, K., Fujita, Y., Katsura, K., Maruyama, K., Narusaka, Y., et al. (2006) Transcriptional regulation of ABI3-and ABA-responsive genes including RD29B and RD29A in seeds, germinating embryos, and seedlings of Arabidopsis. *Plant Molecular Biology*, **60**, 51-68.

Narsai, R., Howell, K.A., Millar, A.H., O'Toole, N., Small, I., et al. (2007) Genome-wide analysis of mRNA decay rates and their determinants in *Arabidopsis thaliana*. *Plant Cell*, **19**, 3418-3436.

Nath, U., Crawford, B.C.W., Carpenter, R. and Coen, E. (2003) Genetic control of surface curvature. *Science*, **299**, 1404-1407.

Nazar, R.N. (2004) Ribosomal RNA processing and ribosome biogenesis in eukaryotes. *Iubmb Life*, **56**, 457-465.

Nemhauser, J.L., Feldman, L.J. and Zambryski, P.C. (2000) Auxin and ETTIN in Arabidopsis gynoecium morphogenesis. *Development*, **127**, 3877-3888.

Nevskaya, N., Tishchenko, S., Gabdoulkhakov, A., Nikonova, E., Nikonov, O., et al. (2005) Ribosomal protein L1 recognizes the same specific structural motif in its target sites on the autoregulatory mRNA and 23S rRNA. *Nucleic Acids Research*, **33**, 478-485.

Ni, M., Dehesh, K., Tepperman, J.M. and Quail, P.H. (1996) GT-2: In vivo transcriptional activation activity and definition of novel twin DNA binding domains with reciprocal target sequence selectivity. *Plant Cell*, **8**, 1041-1059.

Nicolai, M., Roncato, M.A., Canoy, A.S., Rouquie, D., Sarda, X., et al. (2006) Large-scale analysis of mRNA translation states during sucrose starvation in Arabidopsis cells identifies cell proliferation and chromatin structure as targets of translational control. *Plant Physiology*, **141**, 663-673.

Niedhardt, F.C., Ingraham, J.L. and Schaechter, M. (1990) *Physiology of Bacterial Cell: a Molecular Approach*. Sunderland, MA: Sinauer Associates.

Nikulin, A., Eliseikina, I., Tishchenko, S., Nevskaya, N., Davydova, N., et al. (2003) Structure of the L1 protuberance in the ribosome. *Nature Structural Biology*, **10**, 104-108.

Nilsson, J., Sengupta, J., Gursky, R., Nissen, P. and Frank, J. (2007) Comparison of fungal 80 S robosomes by cryo-EM reveals diversity in structure and conformation of rRNA expansion segments. *Journal of Molecular Biology*, **369**, 429-438.

Nishimura, T., Wada, T. and Okada, K. (2004) A key factor of translation reinitiation, ribosomal protein L24, is involved in gynoecium development in Arabidopsis. *Biochemical Society Transactions*, **32**, 611-613.

Nishimura, T., Wada, T., Yamamoto, K.T. and Okada, K. (2005) The Arabidopsis STV1 protein, responsible for translation reinitiation, is required for auxin-mediated gynoecium patterning. *Plant Cell*, **17**, 2940-2953.

Nissan, T.A., Bassler, J., Petfalski, E., Tollervey, D. and Hurt, E. (2002) 60S pre-ribosome formation viewed from assembly in the nucleolus until export to the cytoplasm. *Embo Journal*, **21**, 5539-5547.

Nissen, P., Hansen, J., Ban, N., Moore, P.B. and Steitz, T.A. (2000) The structural basis of ribosome activity in peptide bond synthesis. *Science*, **289**, 920-930.

Noller, H.F. (1993) Peptidyl transferase – protein, ribonucleoprotein, or RNA. *Journal of Bacteriology*, **175**, 5297-5300.

Noller, H.F., Hoffarth, V. and Zimniak, L. (1992) Unusual resistance of peptidyl transferase to protein extraction procedures. *Science*, **256**, 1416-1419.

Nomura, M. (1999) Regulation of ribosome biosynthesis in *Escherichia coli* and *Saccharomyces cerevisiae*: Diversity and common principles. *Journal of Bacteriology*, **181**, 6857-6864.

Nomura, M., Gourse, R. and Baughman, G. (1984) Regulation of the synthesis of ribosomes and ribosomal components. *Annual Review of Biochemistry*, **53**, 75-117.

Nomura, M., Yates, J.L., Dean, D. and Post, L.E. (1980) Feedback regulation of ribosomal protein gene expression in *Escherichia coli*: structural homology of ribosomal RNA and ribosomal protein mRNA. *Proceedings of the National Academy of Sciences of the United States of America*, **77**, 7084-7088.

Nott, A., Le Hir, H. and Moore, M.J. (2004) Splicing enhances translation in mammalian cells: an additional function of the exon junction complex. *Genes & Development*, **18**, 210-222.

Nygard, O. and Nilsson, L. (1990) Translational dynamics. Interactions between the translational factors, tRNA and ribosomes during eukaryotic protein synthesis. *European Journal of Biochemistry*, **191**, 1-17.

Odintsova, T.I., Muller, E.C., Ivanov, A.V., Egorov, T.A., Bienert, R., et al. (2003) Characterization and analysis of posttranslational modifications of the human large cytoplasmic ribosomal subunit proteins by mass spectrometry and Edman sequencing. *Journal of Protein Chemistry*, **22**, 249-258.

Ogle, J.M., Brodersen, D.E., Clemons, W.M., Jr., Tarry, M.J., Carter, A.P., et al. (2001) Recognition of cognate transfer RNA by the 30S ribosomal subunit. *Science*, **292**, 897-902.

Olson, M.O.J. and Dundr, M. (2005) The moving parts of the nucleolus. *Histochemistry and Cell Biology*, **123**, 203-216.

Olson, M.O.J., Hingorani, K. and Szebeni, A. (2002) Conventional and nonconventional roles of the nucleolus. *International Review of Cytology*, **219**, 199-266.

Ookata, K., Hisanaga, S., Bulinski, J.C., Murofushi, H., Aizawa, H., et al. (1995) Cyclin-B interaction with Microtubule-associated protein-4 (Map4) targets P34(Cdc2) kinase to microtubules and is a potential regulator of M-phase microtubule dynamics. *Journal of Cell Biology*, **128**, 849-862.

Oono, Y., Seki, M., Nanjo, T., Narusaka, M., Fujita, M., et al. (2003) Monitoring expression profiles of Arabidopsis gene expression during rehydration process after dehydration using ca. 7000 full-length cDNA microarray. *Plant Journal*, **34**, 868-887.

Oono, Y., Seki, M., Satou, M., Iida, K., Akiyama, K., et al. (2006) Monitoring expression profiles of Arabidopsis genes during cold acclimation and deacclimation using DNA microarrays. *Functional & Integrative Genomics*, **6**, 212-234.

Oquist, G., Chow, W.S. and Anderson, J.M. (1992) Photoinhibition of photosynthesis represents a mechanism for the long-term regulation of photosystem-II. *Planta*, **186**, 450-460.

Ostergaard, P., Phan, H., Johansen, L.B., Egebjerg, J., Ostergaard, L., et al. (1998) Assembly of proteins and 5S rRNA to transcripts of the major structural domains of 23S rRNA. *Journal of Molecular Biology*, **284**, 227-240.

Ouyang, S., Zhu, W., Hamilton, J., Lin, H., Campbell, M., et al. (2007) The TIGR Rice Genome Annotation Resource: improvements and new features. *Nucleic Acids Research*, **35**, D883-887.

Palatnik, J.F., Allen, E., Wu, X.L., Schommer, C., Schwab, R., et al. (2003) Control of leaf morphogenesis by microRNAs. *Nature*, **425**, 257-263.

Pederson, T. (1998) The plurifunctional nucleolus. *Nucleic Acids Research*, **26**, 3871-3876.

Pellizzoni, L., Lotti, F., Maras, B. and PierandreiAmaldi, P. (1997) Cellular nucleic acid binding protein binds a conserved region of the 5' UTR of Xenopus laevis ribosomal protein mRNAs. *Journal of Molecular Biology*, **267**, 264-275.

Pendle, A.F., Clark, G.P., Boon, R., Lewandowska, D., Lam, Y.W., et al. (2005) Proteomic analysis of the Arabidopsis nucleolus suggests novel nucleolar functions. *Molecular Biology of the Cell*, **16**, 260-269.

Perry, R.P. (2005) The architecture of mammalian ribosomal protein promoters. *Bmc Evolutionary Biology*, **5**, 15.

Petes, T.D. (1980) Unequal meiotic recombination within tandem arrays of yeast ribosomal DNA genes. *Cell*, **19**, 765-774.

Petes, T.D. and Hill, C.W. (1988) Recombination between repeated genes in microorganisms. *Annual Review of Genetics*, **22**, 147-168.

Petrasek, J., Mravec, J., Bouchard, R., Blakeslee, J.J., Abas, M., et al. (2006) PIN proteins perform a rate-limiting function in cellular auxin efflux. *Science*, **312**, 914-918.

Petricka, J.J. and Nelson, T.M. (2007) Arabidopsis nucleolin affects plant development and patterning. *Plant Physiology*, **144**, 173-186.

Philippe, C., Eyermann, F., Benard, L., Portier, C., Ehresmann, B., et al. (1993) Ribosomal protein S15 from *Escherichia coli* modulates its own translation by trapping the ribosome on the mRNA initiation loading site. *Proceedings of the National Academy of Sciences of the United States of America*, **90**, 4394-4398.

Philippsen, P., Thomas, M., Kramer, R.A. and Davis, R.W. (1978) Unique arrangement of coding sequences for 5 S, 5.8 S, 18 S and 25 S ribosomal RNA in Saccharomyces cerevisiae as determined by R-loop and hybridization analysis. *Journal of Molecular Biology*, **123**, 387-404.

Pickart, C.M. (2000) Ubiquitin in chains. *Trends in Biochemical Sciences*, **25**, 544-548.

Pierandrei-Amaldi, P., Beccari, E., Bozzoni, I. and Amaldi, F. (1985) Ribosomal-protein production in normal and anucleolate Xenopus embryos - Regulation at the posttranscriptional and translational Levels. *Cell*, **42**, 317-323.

Pikaard, C.S. (2002) Transcription and tyranny in the nucleolus: the organization, activation, dominance and repression of ribosomal RNA genes. In *The Arabidopsis Book* (Somerville, C. and Meyerowitz, E., eds): American Society of Plant Biologists, pp. 1-23.

Pillai, R.S., Bhattacharyya, S.N. and Filipowicz, W. (2007) Repression of protein synthesis by miRNAs: how many mechanisms? *Trends in Cell Biology*, **17**, 118-126.

Pinon, V., Etchells, J.P., Rossignol, P., Collier, S.A., Arroyo, J.M., et al. (2008) Three *PIGGYBACK* genes that specifically influence leaf patterning encode ribosomal proteins. *Development*, **135**, 1315-1324.

Pioletti, M., Schlünzen, F., Harms, J., Zarivach, R., Glühmann, M., et al. (2001) Crystal structures of complexes of the small ribosomal subunit with tetracycline, edeine and IF3. *Embo Journal*, **20**, 1829-1839.

Planta, R.J. (1997) Regulation of ribosome synthesis in yeast. *Yeast*, **13**, 1505-1518.

Planta, R.J., Gonçalves, P.M. and Mager, W.H. (1995) Global regulators of ribosome biosynthesis in yeast. *Biochemistry and Cell Biology*, **73**, 825-834.

Planta, R.J. and Mager, W.H. (1998) The list of cytoplasmic ribosomal proteins of *Saccharomyces cerevisiae*. *Yeast*, **14**, 471-477.

Pnueli, L., Liang, H., Rozenberg, M. and Mittler, R. (2003) Growth suppression, altered stomatal responses, and augmented induction of heat shock proteins in cytosolic ascorbate peroxidase (Apx1)-deficient Arabidopsis plants. *Plant Journal*, **34**, 185-201.

Pontvianne, F., Matia, I., Douet, J., Tourmente, S., Medina, F.J., et al. (2007) Characterization of *AtNUC-L1* reveals a central role of nucleolin in nucleolus organization and silencing of *AtNUC-L2* gene in Arabidopsis. *Molecular Biology of the Cell*, **18**, 369-379.

Pool, M.R., Stumm, J., Fulga, T.A., Sinning, I. and Dobberstein, B. (2002) Distinct modes of signal recognition particle interaction with the ribosome. *Science*, **297**, 1345-1348.

Popescu, S.C. and Tumer, N.E. (2004) Silencing of ribosomal protein L3 genes in *N. tabacum* reveals coordinate expression and significant alterations in plant growth, development and ribosome biogenesis. *Plant Journal*, **39**, 29-44.

Powers, T. and Walter, P. (1999) Regulation of ribosome biogenesis by the rapamycin-sensitive TOR-signaling pathway in *Saccharomyces cerevisiae*. *Molecular Biology of the Cell*, **10**, 987-1000.

Prestridge, D.S. (1991) Signal Scan - a computer program that scans DNA sequences for eukaryotic transcriptional elements. *Computer Applications in the Biosciences*, **7**, 203-206.

Pruitt, R.E. and Meyerowitz, E.M. (1986) Characterization of the genome of *Arabidopsis thaliana*. *Journal of Molecular Biology*, **187**, 169-183.

Przemeck, G.K.H., Mattsson, J., Hardtke, C.S., Sung, Z.R. and Berleth, T. (1996) Studies on the role of the Arabidopsis gene MONOPTEROS in vascular development and plant cell axialization. *Planta*, **200**, 229-237.

Purohit, P. and Stern, S. (1994) Interactions of a small RNA with antibiotic and RNA ligands of the 30S subunit. *Nature*, **370**, 659-662.

Puvion-Dutilleul, F., Puvion, E. and Bachellerie, J.-P. (1997) Early stages of pre-rRNA formation within the nucleolar ultrastructure of mouse cells studied by in situ hybridization with a 5' ETS leader probe. *Chromosoma*, **105**, 496-505.

Pylatuik, J.D., Cross, R.H., Davis, A.R. and Bonham-Smith, P.C. (2003) Elements regulating *AGAMOUS* expression are conserved between *Arabidopsis thaliana*, *Brassica napus*, and *Linum usitatissimum*. *Canadian Journal of Botany*, **81**, 523-530.

Radebaugh, C.A., Gong, X., Bartholomew, B. and Paule, M.R. (1997) Identification of previously unrecognized common elements in eukaryotic promoters. A ribosomal RNA gene initiator element for RNA polymerase I. *Journal of Biological Chemistry*, **272**, 3141-3144.

Radimerski, T., Mini, T., Schneider, U., Wettenhall, R.E.H., Thomas, G., et al. (2000) Identification of insulin-induced sites of ribosomal protein S6 phosphorylation in *Drosophila melanogaster*. *Biochemistry*, **39**, 5766-5774.

Ramakrishnan, V. (2002) Ribosome structure and the mechanism of translation. *Cell*, **108**, 557-572.

Raška, I. (2003) Oldies but goldies: searching for Christmas trees within the nucleolar architecture. *Trends in Cell Biology*, **13**, 517-525.

Raška, I., Shaw, P.J. and Cmarko, D. (2006) Structure and function of the nucleolus in the spotlight. *Current Opinion in Cell Biology*, **18**, 325-334.

Raue, H.A., Klootwijk, J. and Musters, W. (1988) Evolutionary conservation of structure and function of high molecular-weight ribosomal-RNA. *Progress in Biophysics & Molecular Biology*, **51**, 77-129.

Reed, R.C., Brady, S.R. and Muday, G.K. (1998) Inhibition of auxin movement from the shoot into the root inhibits lateral root development in arabidopsis. *Plant Physiology*, **118**, 1369-1378.

Regad, F., Herve, C., Marinx, O., Bergounioux, C., Tremousaygue, D., et al. (1995) The t*ef1* box, a ubiquitous c*is*-acting element involved in the activation of plant genes that are highly expressed in cycling cells. *Molecular and General Genetics*, **248**, 703-711.

Reid, J.L., Iyer, V.R., Brown, P.O. and Struhl, K. (2000) Coordinate regulation of yeast ribosomal protein genes is associated with targeted recruitment of Esa1 histone acetylase. *Molecular Cell*, **6**, 1297-1307.

Reinhardt, D. (2005) Regulation of phyllotaxis. *International Journal of Developmental Biology*, **49**, 539-546.

Revenkova, E., Masson, J., Koncz, C., Afsar, K., Jakovleva, L., et al. (1999) Involvement of *Arabidopsis thaliana* ribosomal protein S27 in mRNA degradation triggered by genotoxic stress. *Embo Journal*, **18**, 490-499.

Rhee, S.Y., Beavis, W., Berardini, T.Z., Chen, G., Dixon, D., et al. (2003) The Arabidopsis Information Resource (TAIR): a model organism database providing a centralized, curated gateway to Arabidopsis biology, research materials and community. *Nucleic Acids Research*, **31**, 224-228.

Rice, P., Longden, I. and Bleasby, A. (2000) EMBOSS: The European molecular biology open software suite. *Trends in Genetics*, **16**, 276-277.

Rockel, T.D., Stuhlmann, D. and von Mikecz, A. (2005) Proteasomes degrade proteins in focal subdomains of the human cell nucleus. *Journal of Cell Science*, **118**, 5231-5242.

Roger, B., Moisand, A., Amalric, F. and Bouvet, P. (2003) Nucleolin provides a link between RNA polymerase I transcription and pre-ribosome assembly. *Chromosoma*, **111**, 399-407.

Rogers, H.J., Bate, N., Combe, J., Sullivan, J., Sweetman, J., et al. (2001) Functional analysis of *cis*-regulatory elements within the promoter of the tobacco late pollen gene *g10*. *Plant Molecular Biology*, **45**, 577-585.

Rohde, J.R. and Cardenas, M.E. (2003) The Tor pathway regulates gene expression by linking nutrient sensing to histone acetylation. *Molecular and Cellular Biology*, **23**, 629-635.

Rohl, R. and Nierhaus, K.H. (1982) Assembly map of the large subunit (50S) of *Escherichia Coli* ribosomes. *Proceedings of the National Academy of Sciences of the United States of America*, **79**, 729-733.

Rose, A.B. (2002) Requirements for intron-mediated enhancement of gene expression in Arabidopsis. *RNA*, **8**, 1444-1453.

Rose, A.B. (2004) The effect of intron location on intron-mediated enhancement of gene expression in Arabidopsis. *Plant Journal*, **40**, 744-751.

Rose, A.B. and Beliakoff, J.A. (2000) Intron-mediated enhancement of gene expression independent of unique intron sequences and splicing. *Plant Physiology*, **122**, 535-542.

Rose, A.B., Elfersi, T., Parra, G. and Korf, I. (2008) Promoter-proximal introns in *Arabidopsis thaliana* are enriched in dispersed signals that elevate gene expression. *Plant Cell*, tpc.107.057190.

Ross, C.L.N., Patel, R.R., Mendelson, T.C. and Ware, V.C. (2007) Functional conservation between structurally diverse ribosomal proteins from *Drosophila melanogaster* and *Saccharomyces cerevisiae*: fly L23a can substitute for yeast L25 in ribosome assembly and function. *Nucleic Acids Research*, **35**, 4503-4514.

Rossel, J.B., Wilson, I.W. and Pogson, B.J. (2002) Global changes in gene expression in response to high light in Arabidopsis. *Plant Physiology*, **130**, 1109-1120.

Rotenberg, M.O., Moritz, M. and Woolford, J.L. (1988) Depletion of *Saccharomyces cerevisiae* ribosomal protein L16 causes a decrease in 60S ribosomal subunits and formation of half-mer polyribosomes. *Genes & Development*, **2**, 160-172.

Rudra, D., Zhao, Y. and Warner, J.R. (2005) Central role of Ifh1p-Fhl1p interaction in the synthesis of yeast ribosomal proteins. *Embo Journal*, **24**, 533-542.

Runions, J., Brach, T., Kuhner, S. and Hawes, C. (2006) Photoactivation of GFP reveals protein dynamics within the endoplasmic reticulum membrane. *Journal of Experimental Botany*, **57**, 43-50.

Russell, J. and Zomerdijk, J. (2005) RNA-polymerase-I-directed rDNA transcription, life and works. *Trends in Biochemical Sciences*, **30**, 87-96.

Rutgers, C.A., Rientjes, J.M.J., van't Riet, J. and Raue, H.A. (1991) rRNA binding domain of yeast ribosomal protein L25: identification of its borders and a key leucine residue. *Journal of Molecular Biology*, **218**, 375-385.

Rutgers, C.A., Schaap, P.J., van't Riet, J., Woldringh, C.L. and Raue, H.A. (1990) In vivo and in vitro analysis of structure-function relationships in ribosomal protein L25 from *Saccharomyces cerevisiae*. *Biochimica Et Biophysica Acta*, **1050**, 74-79.

Sabatini, S., Beis, D., Wolkenfelt, H., Murfett, J., Guilfoyle, T., et al. (1999) An auxin-dependent distal organizer of pattern and polarity in the Arabidopsis root. *Cell*, **99**, 463-472.

Saboe-Larssen, S., Lyamouri, M., Merriam, J., Oksvold, M.P. and Lambertsson, A. (1998) Ribosomal protein insufficiency and the minute syndrome in Drosophila: A dose-response relationship. *Genetics*, **148**, 1215-1224.

Sachs, A.B., Sarnow, P. and Hentze, M.W. (1997) Starting at the beginning, middle, and end: Translation initiation in eukaryotes. *Cell*, **89**, 831-838.

Saez-Vasquez, J., Caparros-Ruiz, D., Barneche, F. and Echeverria, M. (2004) A plant snoRNP complex containing snoRNAs, fibrillarin, and nucleolin-like proteins is competent for both rRNA gene binding and pre-rRNA processing in vitro. *Molecular and Cellular Biology*, **24**, 7284-7297.

Saez-Vasquez, J., Raynal, M., Mezabasso, L. and Delseny, M. (1993) Two related, low-temperature-induced genes from *Brassica napus* are homologous to the human tumor BBC1 (Breast Basic Conserved) gene. *Plant Molecular Biology*, **23**, 1211-1221.

Said, B., Cole, J.R. and Nomura, M. (1988) Mutational analysis of the L1 binding-site of 23S ribosomal-RNA in *Escherichia coli*. *Nucleic Acids Research*, **16**, 10529-10545.

Saint-Jore, C.M., Evins, J., Batoko, H., Brandizzi, F., Moore, I., et al. (2002) Redistribution of membrane proteins between the Golgi apparatus and endoplasmic reticulum in plants is reversible and not dependent on cytoskeletal networks. *Plant Journal*, **29**, 661-678.

Sakakibara, H., Takei, K. and Hirose, N. (2006) Interactions between nitrogen and cytokinin in the regulation of metabolism and development. *Trends in Plant Science*, **11**, 440-448.

Sakuma, Y., Maruyama, K., Osakabe, Y., Qin, F., Seki, M., et al. (2006) Functional analysis of an Arabidopsis transcription factor, DREB2A, involved in drought-responsive gene expression. *Plant Cell*, **18**, 1292-1309.

Sambrook, J., Fritsch, E.F. and Maniatis, T. (1989) *Molecular Cloning: a Laboratory Manual.* 2nd ed. edn. Cold Spring Harbor, NY: Cold Spring Harbor Laboratory Press.

Sanchez-Madrid, F., Vidales, F.J. and Ballesta, J.P.G. (1981) Effect of phosphorylation on the affinity of acidic proteins from *Saccharomyces cerevisiae* for the ribosomes. *European Journal of Biochemistry*, **114**, 609-613.

Scarpeci, T.E. and Valle, E.M. (2008) Rearrangement of carbon metabolism in *Arabidopsis thaliana* subjected to oxidative stress condition: an emergency survival strategy. *Plant Growth Regulation*, **54**, 133-142.

Scarpeci, T.E., Zanor, M.I., Carrillo, N., Mueller-Roeber, B. and Valle, E.M. (2008) Generation of superoxide anion in chloroplasts of *Arabidopsis thaliana* during active photosynthesis: a focus on rapidly induced genes. *Plant Molecular Biology*, **66**, 361-378.

Schaap, P.J., van't Riet, J., Woldringh, C.L. and Raue, H.A. (1991) Identification and functional analysis of the nuclear localization signals of ribosomal protein L25 from *Saccharomyces cerevisiae*. *Journal of Molecular Biology*, **221**, 225-237.

Schaffer, R., Landgraf, J., Accerbi, M., Simon, V., Larson, M., et al. (2001) Microarray analysis of diurnal and circadian-regulated genes in Arabidopsis. *Plant Cell*, **13**, 113-123.

Schafleitner, R. and Wilhelm, E. (2002) Isolation of wound-responsive genes from chestnut (*Castanea sativa*) microstems by mRNA display and their differential expression upon wounding and infection with the chestnut blight fungus (*Chryphonectria parasitica*). *Physiological and Molecular Plant Pathology*, **61**, 339-348.

Scharf, K.D. and Nover, L. (1982) Heat-shock-induced alterations of ribosomal protein phosphorylation in plant cell cultures. *Cell*, **30**, 427-437.

Scheer, U. and Benavente, R. (1990) Functional and dynamic aspects of the mammalian nucleolus. *Bioessays*, **12**, 14-21.

Scheer, U. and Weisenberger, D. (1994) The nucleolus. *Current Opinion in Cell Biology*, **6**, 354-359.

Scherl, A., Coute, Y., Deon, C., Calle, A., Kindbeiter, K., et al. (2002) Functional proteomic analysis of human nucleolus. *Molecular Biology of the Cell*, **13**, 4100-4109.

Schlenstedt, G., Smirnova, E., Deane, R., Solsbacher, J., Kutay, U., et al. (1997) Yrb4p, a yeast Ran-GTP-binding protein involved in import of ribosomal protein L25 into the nucleus. *Embo Journal*, **16**, 6237-6249.

Schnare, M.N., Damberger, S.H., Gray, M.W. and Gutell, R.R. (1996) Comprehensive comparison of structural characteristics in eukaryotic cytoplasmic large subunit (23S-like) ribosomal RNA. *Journal of Molecular Biology*, **256**, 701-719.

Schuwirth, B.S., Borovinskaya, M.A., Hau, C.W., Zhang, W., Vila-Sanjurjo, A., et al. (2005) Structures of the bacterial ribosome at 3.5 A resolution. *Science*, **310**, 827-834.

Seki, M., Narusaka, M., Kamiya, A., Ishida, J., Satou, M., et al. (2002) Functional annotation of a full-length Arabidopsis cDNA collection. *Science*, **296**, 141-145.

Semple, C. and Wolfe, K.H. (1999) Gene duplication and gene conversion in the *Caenorhabditis elegans* genome. *Journal of Molecular Evolution*, **48**, 555-564.

Sengupta, J., Nilsson, J., Gursky, R., Spahn, C.M.T., Nissen, P., et al. (2004) Identification of the versatile scaffold protein RACK1 on the eukaryotic ribosome by cryo-EM. *Nature Structural and Molecular Biology*, **11**, 957-962.

Serganov, A., Polonskaia, A., Ehresmann, B., Ehresmann, C. and Patel, D.J. (2003) Ribosomal protein S15 represses its own translation via adaptation of an rRNA-like fold within its mRNA. *Embo Journal*, **22**, 1898-1908.

Sessions, A., Burke, E., Presting, G., Aux, G., McElver, J., et al. (2002) A high-throughput Arabidopsis reverse genetics system. *Plant Cell*, **14**, 2985-2994.

Sessions, A., Nemhauser, J.L., McColl, A., Roe, J.L., Feldmann, K.A., et al. (1997) ETTIN patterns the Arabidopsis floral meristem and reproductive organs. *Development*, **124**, 4481-4491.

Shahmuradov, I.A., Gammerman, A.J., Hancock, J.M., Bramley, P.M. and Solovyev, V.V. (2003) PlantProm: a database of plant promoter sequences. *Nucleic Acids Research*, **31**, 114-117.

Shama, S. and Meyuhas, O. (1996) The translational cis-regulatory element of mammalian ribosomal protein mRNAs is recognized by the plant translational apparatus. *European Journal of Biochemistry*, **236**, 383-388.

Shaw, P.J., Abranches, R., Paula Santos, A., Beven, A.F., Stoger, E., et al. (2002) The architecture of interphase chromosomes and nucleolar transcription sites in plants. *Journal of Structural Biology*, **140**, 31-38.

Shaw, P.J. and Jordan, E.G. (1995) The nucleolus. *Annual Review of Cell and Developmental Biology*, **11**, 93-121.

Sherman, F., Stewart, J.W. and Tsunasawa, S. (1985) Methionine or not methionine at the beginning of a protein. *Bioessays*, **3**, 27-31.

Shine, J. and Dalgarno, L. (1974) The 3'-terminal sequence of *Escherichia coli* 16S ribosomal RNA: complementarity to nonsense triplets and ribosome binding sites. *Proceedings of the National Academy of Sciences of the United States of America*, **74**, 1342-1346.

Shor, B., Calaycay, J., Rushbrook, J. and McLeod, M. (2003) Cpc2/RACK1 is a ribosome-associated protein that promotes efficient translation in *Schizosaccharomyces pombe*. *Journal of Biological Chemistry*, **278**, 49119-49128.

Sieburth, L.E. (1999) Auxin is required for leaf vein pattern in Arabidopsis. *Plant Physiology*, **121**, 1179-1190.

Sieburth, L.E. and Meyerowitz, E.M. (1997) Molecular dissection of the *AGAMOUS* control region shows that *cis* elements for spatial regulation are located intragenically. *Plant Cell*, **9**, 355-365.

Simillion, C., Vandepoele, K., Van Montagu, M.C.E., Zabeau, M. and Van de Peer, Y. (2002) The hidden duplication past of Arabidopsis thaliana. *Proceedings of the National Academy of Sciences of the United States of America*, **99**, 13627-13632.

Spahn, C.M.T., Beckmann, R., Eswar, N., Penczek, P.A., Sali, A., et al. (2001) Structure of the 80S ribosome from *Saccharomyces cerevisiae* - tRNA-ribosome and subunit-subunit interactions. *Cell*, **107**, 373-386.

Spahn, C.M.T., Jan, E., Mulder, A., Grassucci, R.A., Sarnow, P., et al. (2004) Cryo-EM visualization of a viral internal ribosome entry site bound to human ribosomes: The IRES functions as an RNA-Based translation factor. *Cell*, **118**, 465-475.

Sparkes, I.A., Runions, J., Kearns, A. and Hawes, C. (2006) Rapid, transient expression of fluorescent fusion proteins in tobacco plants and generation of stably transformed plants. *Nature Protocols*, **1**, 2019-2025.

Srivastava, S. and Schlessinger, D. (1990) rRNA processing in *Escherichia coli*. In *The Ribosome: Structure, Function and Evolution* (Hill, W.E., Dahlberg, A., Garrett, R.A., Moore, P.B., Schlessinger, D. and Warner, J.R., eds). Washington, D.C.: American Society for Microbiology, pp. 426-434.

Srivastava, S., Verschoor, A., Radermacher, M., Grassucci, R. and Frank, J. (1995) Three-dimensional reconstruction of mammalian 40 S ribosomal subunit embedded in ice. *Journal of Molecular Biology*, **245**, 461-466.

Stark, H., Mueller, F., Orlova, E.V., Schatz, M., Dube, P., et al. (1995) The 70S *Escherichia coli* ribosome at 23 Å resolution: fitting the ribosomal RNA. *Structure*, **3**, 815-821.

Stark, H., Rodnina, M.V., Wieden, H.J., van Heel, M. and Wintermeyer, W. (2000) Large-scale movement of elongation factor G and extensive conformational change of the ribosome during translocation. *Cell*, **100**, 301-309.

Stark, H., Rodnina, M.V., Wieden, H.J., Zemlin, F., Wintermeyer, W., et al. (2002) Ribosome interactions of aminoacyl-tRNA and elongation factor Tu in the codon-recognition complex. *Nature Structural Biology*, **9**, 849-854.

Steitz, T.A. and Moore, P.B. (2003) RNA, the first macromolecular catalyst: the ribosome is a ribozyme. *Trends in Biochemical Sciences*, **28**, 411-418.

Steponkus, P.L., Uemura, M., Joseph, R.A., Gilmour, S.J. and Thomashow, M.F. (1998) Mode of action of the *COR15a* gene on the freezing tolerance of Arabidopsis thaliana. *Proceedings of the National Academy of Sciences of the United States of America*, **95**, 14570-14575.

Swarbreck, D., Wilks, C., Lamesch, P., Berardini, T.Z., Garcia-Hernandez, M., et al. (2008) The Arabidopsis Information Resource (TAIR): gene structure and function annotation. *Nucleic Acids Research*, **36**, D1009-D1014.

Szick-Miranda, K. and Bailey-Serres, J. (2001) Regulated heterogeneity in 12-kDa P-protein phosphorylation and composition of ribosomes in maize (*Zea mays* L.). *Journal of Biological Chemistry*, **276**, 10921-10928.

Szick, K., Springer, M. and Bailey-Serres, J. (1998) Evolutionary analyses of the 12-kDa acidic ribosomal P-proteins reveal a distinct protein of higher plant ribosomes. *Proceedings of the National Academy of Sciences of the United States of America*, **95**, 2378-2383.

Szostak, J.W. and Wu, R. (1980) Unequal crossing over in the ribosomal DNA of *Saccharomyces cerevisiae*. *Nature*, **284**, 426-430.

Takase, T., Nakazawa, M., Ishikawa, A., Kawashima, M., Ichikawa, T., et al. (2004) y*dk1-D*, an auxin-responsive *GH3* mutant that is involved in hypocotyl and root elongation. *Plant Journal*, **37**, 471-483.

Tartof, K.D. and Perry, R.P. (1970) The 5S RNA genes of *Drosophila melanogaster*. *Journal of Molecular Biology*, **51**, 171-183.

Tatematsu, K., Nakabayashi, K., Kamiya, Y. and Nambara, E. (2008) Transcription factor *AtTCP14* regulates embryonic growth potential during seed germination in Arabidopsis thaliana. *Plant Journal*, **53**, 42-52.

Tatematsu, K., Ward, S., Leyser, O., Kamiya, Y. and Nambara, E. (2005) Identification of *cis*-elements that regulate gene expression during initiation of axillary bud outgrowth in Arabidopsis. *Plant Physiology*, **138**, 757-766.

Thiry, M. and Lafontaine, D.L.J. (2005) Birth of a nucleolus: the evolution of nucleolar compartments. *Trends in Cell Biology*, **15**, 194-199.

Thomashow, M.F. (1999) Plant cold acclimation: Freezing tolerance genes and regulatory mechanisms. *Annual Review of Plant Physiology and Plant Molecular Biology*, **50**, 571-599.

Tollervey, D., Lehtonen, H., Jansen, R., Kern, H. and Hurt, E.C. (1993) Temperature-sensitive mutations demonstrate roles for yeast fibrillarin in pre-ribosomal-RNA processing, pre-ribosomal-RNA methylation, and ribosome assembly. *Cell*, **72**, 443-457.

Tornow, J. and Santangelo, G.M. (1994) *Saccharomyces cerevisiae* ribosomal protein L37 is encoded by duplicate genes that are differentially expressed. *Current Genetics*, **25**, 480-487.

Tremousaygue, D., Garnier, L., Bardet, C., Dabos, P., Herve, C., et al. (2003) Internal telomeric repeats and 'TCP domain' protein-binding sites co-operate to regulate gene expression in *Arabidopsis thaliana* cycling cells. *Plant Journal*, **33**, 957-966.

Tremousaygue, D., Manevski, A., Bardet, C., Lescure, N. and Lescure, B. (1999) Plant interstitial telomere motifs participate in the control of gene expression in root meristems. *Plant Journal*, **20**, 553-561.

Trendelenburg, M.F., Spring, H., Scheer, U. and Franke, W.W. (1974) Morphology of nucleolar cistrons in a plant cell, *Acetabularia mediterranea*. *Proceedings of the National Academy of Sciences of the United States of America*, **71**, 3626-3630.

Tsay, Y.F., Thompson, J.R., Rotenberg, M.O., Larkin, J.C. and Woolford, J.L. (1988) Ribosomal-protein synthesis is not regulated at the translational level in *Saccharomyces-cerevisiae* – balanced accumulation of ribosomal protein L16 and protein Rp59 is mediated by turnover of excess protein. *Genes and Development*, **2**, 664-676.

Tsurugi, K. and Ogata, K. (1985) Evidence for the exchangeability of acidic ribosomal-proteins on cytoplasmic ribosomes in regenerating rat liver. *Journal of Biochemistry*, **98**, 1427-1431.

Uechi, T., Tanaka, T. and Kenmochi, N. (2001) A complete map of the human ribosomal protein genes: assignment of 80 genes to the cytogenetic map and implications for human disorders. *Genomics*, **72**, 223-230.

Ueno, Y., Ishikawa, T., Watanabe, K., Terakura, S., Iwakawa, H., et al. (2007) Histone deacetylases and *ASYMMETRIC LEAVES2* are involved in the establishment of polarity in leaves of Arabidopsis. *Plant Cell*, **19**, 445-457.

Ulmasov, T., Murfett, J., Hagen, G. and Guilfoyle, T.J. (1997) Aux/IAA proteins repress expression of reporter genes containing natural and highly active synthetic auxin response elements. *Plant Cell*, **9**, 1963-1971.

Urade, R. (2007) Cellular response to unfolded proteins in the endoplasmic reticulum of plants. *FEBS Journal*, **274**, 1152-1171.

Valle, M., Zavialov, A., Sengupta, J., Rawat, U., Ehrenberg, M., et al. (2003) Locking and unlocking of ribosomal motions. *Cell*, **114**, 123-134.

van Beekvelt, C.A., de Graaff-Vincent, M., Faber, A.W., van 't Riet, J., Venema, J., et al. (2001) All three functional domains of the large ribosomal subunit protein L25 are required for both early and late pre-rRNA processing steps in *Saccharomyces cerevisiae*. *Nucleic Acids Research*, **29**, 5001-5008.

van Beekvelt, C.A., Kooi, E.A., de Graaff-Vincent, M., van't Riet, J., Venema, J., et al. (2000) Domain III of *Saccharomyces cerevisiae* 25S ribosomal RNA: its role in binding of ribosomal protein L25 and 60S subunit formation. *Journal of Molecular Biology*, **296**, 7-17.

Van de Peer, Y., De Rijk, P., Wuyts, J., Winkelmans, T. and De Wachter, R. (2000) The European small subunit ribosomal RNA database. *Nucleic Acids Research*, **28**, 175-176.

Van de Peer, Y., Jansen, J., De Rijk, P. and De Wachter, R. (1997) Database on the structure of small ribosomal subunit RNA. *Nucleic Acids Research*, **25**, 111-116.

Van Lijsebettens, M., Vanderhaeghen, R., De Block, M., Bauw, G., Villarroel, R., et al. (1994) An S18 ribosomal protein gene copy at the Arabidopsis *PFL* locus affects plant development by its specific expression in meristems. *Embo Journal*, **13**, 3378-3388.

Vandenabeele, S., Van Der Kelen, K., Dat, J., Gadjev, I., Boonefaes, T., et al. (2003) A comprehensive analysis of hydrogen peroxide-induced gene expression in tobacco. *Proceedings of the National Academy of Sciences*, **100**, 16113-16118.

Vanderauwera, S., Zimmermann, P., Rombauts, S., Vandenabeele, S., Langebartels, C., et al. (2005) Genome-wide analysis of hydrogen peroxide-regulated gene expression in Arabidopsis reveals a high light-induced transcriptional cluster involved in anthocyanin biosynthesis. *Plant Physiology*, **139**, 806-821.

Vanderhaeghen, R., De Clercq, R., Karimi, M., Van Montagu, M., Hilson, P., et al. (2006) Leader sequence of a plant ribosomal protein gene with complementarity to the 18S rRNA triggers in vitro cap-independent translation. *Febs Letters*, **580**, 2630-2636.

Vazquez, F., Gasciolli, V., Crete, P. and Vaucheret, H. (2004) The nuclear dsRNA binding protein HYL1 is required for MicroRNA accumulation and plant development, but not posttranscriptional transgene silencing. *Current Biology*, **14**, 346-351.

Venema, J. and Tollervey, D. (1999) Ribosome synthesis in *Saccharomyces cerevisiae*. *Annual Review of Genetics*, **33**, 261-311.

Verschoor, A., Srivastava, S., Grassucci, R. and Frank, J. (1996) Native 3D structure of eukaryotic 80S ribosome: morphological homology with the *E. coli* 70S ribosome. *Journal of Cell Biology*, **133**, 495-505.

Verschoor, A., Warner, J., Srivastava, S., Grassucci, R. and Frank, J. (1998) Three-dimensional structure of the yeast ribosome. *Nucleic Acids Research*, **26**, 655-661.

Vester, B. and Garrett, R.A. (1984) Structure of a protein L23-RNA complex located at the A-site domain of the ribosomal peptidyl transferase center. *Journal of Molecular Biology*, **179**, 431-452.

Vignais, M.L. and Sentenac, A. (1989) Asymmetric DNA bending induced by the yeast multifunctional factor TUF. *Journal of Biological Chemistry*, **264**, 8463-8466.

Villain, P., Mache, R. and Zhou, D.X. (1996) The mechanism of GT element-mediated cell type-specific transcriptional control. *Journal of Biological Chemistry*, **271**, 32593-32598.

Vitale, A., Wu, R.J., Cheng, Z.Q. and Meagher, R.B. (2003) Multiple conserved 5 ' elements are required for high-level pollen expression of the Arabidopsis reproductive actin *ACT1*. *Plant Molecular Biology*, **52**, 1135-1151.

Wade, J.T., Hall, D.B. and Struhl, K. (2004) The transcription factor Ifh1 is a key regulator of yeast ribosomal protein genes. *Nature*, **432**, 1054-1058.

Wahl, M.C. and Moller, W. (2002) Structure and function of the acidic ribosomal stalk proteins. *Current Protein & Peptide Science*, **3**, 93-106.

Wang, B.-B. and Brendel, V. (2006) Genomewide comparative analysis of alternative splicing in plants. *Proceedings of the National Academy of Sciences*, **103**, 7175-7180.

Wang, Y.H., Chen, Y.H., Lu, J.H. and Tsai, H.J. (2005a) A 23-amino acid motif spanning the basic domain targets zebrafish myogenic regulatory factor Myf5 into nucleolus. *DNA and Cell Biology*, **24**, 651-660.

Wang, Z.B., Triezenberg, S.J., Thomashow, M.F. and Stockinger, E.J. (2005b) Multiple hydrophobic motifs in Arabidopsis CBF1COOH-terminus provide functional redundancy in trans-activation. *Plant Molecular Biology*, **58**, 543-559.

Warner, J.R. (1989) Synthesis of ribosomes in *Saccharomyces cerevisiae*. *Microbiological Reviews*, **53**, 256-271.

Warner, J.R. (1999) The economics of ribosome biosynthesis in yeast. *Trends in Biochemical Sciences*, **24**, 437-440.

Warner, J.R., Mitra, G., Schwindinger, W.F., Studeny, M. and Fried, H.M. (1985) *Saccharomyces cerevisiae* coordinates accumulation of yeast ribosomal proteins by modulating messenger-RNA splicing, translational initiation, and protein-turnover. *Molecular and Cellular Biology*, **5**, 1512-1521.

Weber, J.D., Kuo, M.L., Bothner, B., DiGiammarino, E.L., Kriwacki, R.W., et al. (2000) Cooperative signals governing ARF-Mdm2 interaction and nucleolar localization of the complex. *Molecular and Cellular Biology*, **20**, 2517-2528.

Weber, M.J. (2006) Mammalian small nucleolar RNAs are mobile genetic elements. *Plos Genetics*, **2**, 1984-1997.

Weijers, D., Franke-van Dijk, M., Vencken, R.J., Quint, A., Hookaas, P., et al. (2001) An *Arabidopsis* Minute-like phenotype caused by a semi-dominant mutation in a ribosomal protein S5 gene. *Development*, **128**, 4289-4299.

Welchen, E. and Gonzalez, D.H. (2005) Differential expression of the Arabidopsis cytochrome c genes *Cytc-1* and *Cytc-2*. Evidence for the involvement of TCP-domain protein-binding elements in anther- and meristem-specific expression of the *Cytc-1* gene. *Plant Physiology*, **139**, 88-100.

Wilkosz, R. and Schlappi, M. (2000) A gene expression screen identifies EARLI1 as a novel vernalization-responsive gene in *Arabidopsis thaliana*. *Plant Molecular Biology*, **44**, 777-787.

Williams, A.J., Werner-Fraczek, J., Chang, I.-F. and Bailey-Serres, J. (2003) Regulated phosphorylation of 40S ribosomal protein S6 in root tips of maize. *Plant Physiology*, **132**, 2086-2097.

Williams, M.E. and Sussex, I.M. (1995) Developmental regulation of ribosomal protein L16 genes in *Arabidopsis thaliana*. *Plant Journal*, **8**, 65-76.

Wilson, D.N. and Nierhaus, K.H. (2003) The ribosome through the looking glass. *Angewandte Chemie International Edition*, **42**, 3464-3486.

Wimberly, B.T., Brodersen, D.E., Clemons, W.M., Jr, Morgan-Warren, R.J., Carter, A.P., et al. (2000) Structure of the 30S ribosomal subunit. *Nature*, **407**, 327-339.

Wolf, Y.I., Rogozin, I.B., Kondrashov, A.S. and Koonin, E.V. (2001) Genome alignment, evolution of prokaryotic genome organization, and prediction of gene function using genomic context. *Genome Research*, **11**, 356-372.

Wool, I.G. (1996) Extraribosomal functions of ribosomal proteins. *TIBS*, **21**, 164-165.

Wool, I.G., Chan, Y.L. and Gluck, A. (1995) Structure and evolution of mammalian ribosomal proteins. *Biochemistry and Cell Biology*, **73**, 933-947.

Woolhead, C.A., Johnson, A.E. and Bernstein, H.D. (2006) Translation arrest requires two-way communication between a nascent polypeptide and the ribosome. *Molecular Cell*, **22**, 587-598.

Woolhead, C.A., McCormick, P.J. and Johnson, A.E. (2004) Nascent membrane and secretory proteins differ in FRET-detected folding far inside the ribosome and in their exposure to ribosomal proteins. *Cell*, **116**, 725-736.

Wu, H., Jiang, L.H. and Zimmermann, R.A. (1994) The binding site for ribosomal-protein S8 in 16S ribosomal-RNA and s*pc* messenger-RNA from *Escherichia Coli* – minimum structural requirements and the effects of single bulged bases on S8-RNA interaction. *Nucleic Acids Research*, **22**, 1687-1695.

Wu, J.Z., Matsui, E., Yamamoto, K., Nagamura, Y., Kurata, N., et al. (1995) Genomic organization of 57 ribosomal protein genes in rice (*Oryza sativa* L.) through RFLP mapping. *Genome*, **38**, 1189-1200.

Wuyts, J., Van de Peer, Y. and De Wachter, R. (2001) Distribution of substitution rates and location of insertion sites in the tertiary structure of ribosomal RNA. *Nucleic Acids Research*, **29**, 5017-5028.

Xiang, R.H. and Lee, J.C. (1989) Identification of proteins crosslinked to RNA in 40S ribosomal-subunits of *Saccharomyces-cerevisiae*. *Biochimie*, **71**, 1201-1204.

Xie, F.L., Huang, S.Q., Guo, K., Xiang, A.L., Zhu, Y.Y., et al. (2007) Computational identification of novel microRNAs and targets in *Brassica napus*. *Febs Letters*, **581**, 1464-1474.

Xie, Z., Allen, E., Fahlgren, N., Calamar, A., Givan, S.A., et al. (2005) Expression of Arabidopsis *MIRNA* genes. *Plant Physiology*, **138**, 2145-2154.

Xiong, L.M., Lee, B.H., Ishitani, M., Lee, H., Zhang, C.Q., et al. (2001) *FIERY1* encoding an inositol polyphosphate 1-phosphatase is a negative regulator of abscisic acid and stress signaling in Arabidopsis. *Genes & Development*, **15**, 1971-1984.

Xue, Z.X., Shan, X.Y., Lapeyre, B. and Melese, T. (1993) The amino-terminus of mammalian nucleolin specifically recognizes SV40 T-antigen type nuclear-localization sequences. *European Journal of Cell Biology*, **62**, 13-21.

Yamaguchi-Shinozaki, K. and Shinozaki, K. (2006) Transcriptional regulatory networks in cellular responses and tolerance to dehydration and cold stresses. *Annual Review of Plant Biology*, **57**, 781-803.

Yamamoto, Y.Y., Ichida, H., Abe, T., Suzuki, Y., Sugano, S., et al. (2007a) Differentiation of core promoter architecture between plants and mammals revealed by LDSS analysis. *Nucleic Acids Research*, **35**, 6219-6226.

Yamamoto, Y.Y., Ichida, H., Matsui, M., Obokata, J., Sakurai, T., et al. (2007b) Identification of plant promoter constituents by analysis of local distribution of short sequences. *BMC Genomics*, **8**.

Yao, Y., Ling, Q., Wang, H. and Huang, H. (2008) Ribosomal proteins promote leaf adaxial identity. *Development*, **135**, 1325-1334.

Yoo, S.-D., Cho, Y.-H. and Sheen, J. (2007) Arabidopsis mesophyll protoplasts: a versatile cell system for transient gene expression analysis. *Nature Protocols*, **2**, 1565-1572.

Yu, Y., Ji, H., Doudna, J.A. and Leary, J.A. (2005) Mass spectrometric analysis of the human 40S ribosomal subunit: Native and HCV IRES-bound complexes. *Protein Science*, **14**, 1438-1446.

Yusupov, M.M., Yusupova, G.Z., Baucom, A., Lieberman, K., Earnest, T.N., et al. (2001) Crystal structure of the ribosome at 5.5 Å resolution. *Science*, **292**, 883-896.

Zanetti, M.E., Chang, I.F., Gong, F.C., Galbraith, D.W. and Bailey-Serres, J. (2005) Immunopurification of polyribosomal complexes of arabidopsis for global analysis of gene expression. *Plant Physiology*, **138**, 624-635.

Zengel, J.M. and Lindahl, L. (1994) Diverse mechanisms for regulating ribosomal-protein synthesis in *Escherichia coli*. *Progress in Nucleic Acid Research and Molecular Biology*, **47**, 331-370.

Zhang, C.K., Lang, P., Dane, F., Ebel, R.C., Singh, N.K., et al. (2005a) Cold acclimation induced genes of trifoliate orange (*Poncirus trifoliata*). *Plant Cell Reports*, **23**, 764-769.

Zhang, R., Ou, H.-Y. and Zhang, C.-T. (2004) DEG: a database of essential genes. *Nucleic Acids Research*, **32**, D271-272.

Zhang, W., Ruan, J., Ho, T.-h.D., You, Y., Yu, T., et al. (2005b) *Cis*-regulatory element based targeted gene finding: genome-wide identification of abscisic acid- and abiotic stress-responsive genes in *Arabidopsis thaliana*. *Bioinformatics*, **21**, 3074-3081.

Zhang, Z., Harrison, P.M., Liu, Y. and Gerstein, M. (2003) Millions of years of evolution preserved: a comprehensive catalog of the processed pseudogenes in the human genome. *Genome Research*, **13**, 2541-2558.

Zhang, Z.L., Harrison, P. and Gerstein, M. (2002) Identification and analysis of over 2000 ribosomal protein pseudogenes in the human genome. *Genome Research*, **12**, 1466-1482.

Zhou, D.X. (1999) Regulatory mechanism of plant gene transcription by GT-elements and GT-factors. *Trends in Plant Science*, **4**, 210-214.

Zhou, G.-K., Kubo, M., Zhong, R., Demura, T. and Ye, Z.-H. (2007) Overexpression of miR165 affects apical meristem formation, organ polarity establishment and vascular development in Arabidopsis. *Plant and Cell Physiology*, **48**, 391-404.

Zuo, J.R., Niu, Q.W. and Chua, N.H. (2000) An estrogen receptor-based transactivator XVE mediates highly inducible gene expression in transgenic plants. *Plant Journal*, **24**, 265-273.